

Functional MRI Investigation of Complex Sequence Learning

A THESIS SUBMITTED
FOR THE DEGREE OF

Doctor of Philosophy

in

Computer Science

by

Pammi V. S. Chandrasekhar



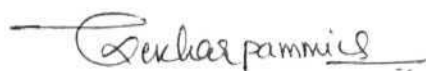
Department of Computer and Information Sciences
School of Mathematics and Computer/Information Sciences
University of Hyderabad
Hyderabad - 500 046
INDIA

JULY 2005

Dedicated to
To My Parents,
Bapi San

DECLARATION

I, Pammi V. S. Chandrasekhar, hereby declare that the work presented in this thesis has been carried out by me under the supervision of **Dr. S. Bapi Raju**, Department of Computer and Information Sciences, University of Hyderabad, Hyderabad, India, as per the PhD ordinances of the University. I declare, to the best of my knowledge, that no part of this thesis has been submitted for the award of a research degree of any other University.



PAMMI V. S. CHANDRASEKHAR
Registration No: 2KMCPC06



Department of Computer and Information Sciences
School of Mathematics and Computer/Information Sciences
University of Hyderabad, Hyderabad, INDIA

CERTIFICATE

This is to certify that the thesis work entitled '**Functional MRI Investigation of Complex Sequence Learning**' being submitted by **Mr. Pammi V. S. Chandrasekhar** (Reg. No. **2KMCPC06**) in partial fulfillment of the requirement for the award of degree of **Doctor of Philosophy (Computer Science)** of the University of Hyderabad, is a record of bona fide work carried out by him under my supervision.

The matter embodied in this thesis has not been submitted for the award of any other research degree.

A handwritten signature in black ink, followed by the date '08/07/2005'.

Dr. S. Bapi Raju
(Supervisor)

Department of Computer and Information Sciences,
University of Hyderabad, Hyderabad, INDIA

A handwritten signature in black ink, followed by the date '8/7/05'.

Prof. Arun Agarwal
(Head)

Department of Computer and
Information Sciences,
University of Hyderabad,
Hyderabad, INDIA

A handwritten signature in black ink.

Prof. Arun K. Pujari
(Dean)

School of Mathematics and
Computer/Information Sciences,
University of Hyderabad,
Hyderabad, INDIA

Abstract

Most of the higher-order and intelligent cognitive behaviours such as reasoning, problem solving, and language involve acquiring and performing complex sequences of activities. Recent advances in neuroimaging techniques, especially the functional MRI, have made it possible to study the brain *in vivo* while subjects are engaged in meaningful behavioural tasks. In this thesis, we used $m \times n$ visuo-motor sequence learning paradigm to investigate the effect of change in complexity of the skill being acquired on various entities such as the nature of internal representation of skills, on the behavioural parameters and on the pattern of brain activation. In the $m \times n$ paradigm the correct order of pressing m keys (set-length) successively for n times (hyperset-length) is learned by trail-and-error process. We vary the complexity of the sequence to be learnt along the two dimensions — m and n , reflecting short-range and long-range prediction loads, respectively. Eighteen subjects were trained and tested on three sequence tasks — 2x6, 2x12 and 4x6. We hypothesized that in the complex sequence learning condition corresponding to increased set-length (i.e., m), the optimization process may be limited to the items within the *set* and may not span across *sets*. In contrast, we expected that in the complex condition corresponding to increased hyperset-length (i.e., n), sequence information may possibly be organized in a hierarchical fashion.

The behavioural results indicate that success rate and key-press response times (RT) revealed the learning related improvements from the early to the consolidation stages in all the sequence learning tasks (2x6, 2x12 and 4x6) and the complexity related effects when 2x6 task was compared to the 2x12 or 4x6 tasks. Although the number of movements and the success rate attained are observed to be similar across the complex tasks (2x12 and 4x6), the RT displayed differential behaviour in the consolidation stages of 2x12 and 4x6. Further, the subjects are observed to be faster in the 2x12 task as compared to the 4x6 task. These differences along with the results from chunking analysis pointed out that the hierarchical organization of complex movement sequences is more likely when the amount of information processed at any point of time is well within the working memory capacity. The results of functional MRI analysis revealed the involvement of cortico-cortical areas in the 4x6 task and the sub-cortical area near the hippocampus has a role in the acquisition stage of the 2x12 task. The posterior lobule of cerebellum, the superior parietal lobule and the Inferior frontal gyrus were found to have a specific role in the chaining across sets and the dorsolateral prefrontal cortex and the caudate nucleus loop may have a specific role in the within-set optimization. Thus the neuroimaging results revealed the recruitment of different, set of brain areas during acquisition and performance stages related to the two dimensions of complexity. Based on the results, we propose a theoretical model consisting of two levels. At one level simple associations are learnt and at the other level higher-order associations are formed.

Acknowledgements

I take this opportunity to thank all those who have directly or indirectly helped me in the successful completion of work leading to this thesis and in making my stay memorable at University of Hyderabad.

First and foremost, I express my gratitude to my supervisor, Dr. S. Bapi Raju for giving me the opportunity to work with him in the exciting field of Computational/Cognitive Neuroscience. In particular, I am thankful for his constant and never tiring guidance. Learning and working with him has been one of the most enriching and fruitful experiences of my life.

I thank Prof. Arun Agarwal, Head, Department of Computer and Information Sciences (DCIS) for making available all the facilities required for this research work. I personally thank him for encouraging me to take up research as a full-time activity.

I am grateful to Prof. Arun K. Pujari, Dean, School of Mathematics and Computer/Information Sciences (MCTS) for providing me the necessary infrastructure to carry out this work. I am indebted for his inspiration and encouragement given from time to time.

I would like to thank the members of doctoral committee Prof. Arun K. Pujari and Dr. Chakravarthy Bhagvati for their useful suggestions and encouragement.

It is indeed a great pleasure to thank Dr. Kenji Doya, Head, Department of Computational Neurobiology, Computational Neuroscience Laboratories, Advanced Telecommunications Research International, Kyoto, Japan for his intellectual guidance and conceiving the idea of the experimental design. I thank Dr. Kazuyuki Samejima for his help in training the subjects and conducting the fMRI experiments. I would like to thank the staff of Brain Activity Imaging Center, ATR Labs, Dr. Shinabu Masaki, Dr. Yasuhiro Shimada and Dr. Ichiro Fujimoto, for smooth running of fMRI experiments. The experimental work was supported by the grants from Kawato Dynamic Brain Project, Exploratory Research for Advanced Technology (ER-ATO) and 'Creating the Brain' Core Research for Evolutional Science and Technology (CREST) Projects of Japan Science and Technology Agency, Japan. I would like to thank Dr. Hiroshi Imamizu and Prof. Mitsuo Kawato for technical advice on data analysis. I also would like to thank Saori Tanaka, Satomi Higuchi, Toshinori Yoshioka, Fredrik Bissmarck, Dr. Tomoe Tamada, Dr. Rieko Osu and Prof. Tomohiro Shibata of ATR Labs for all their help and discussions.

I would like to thank CSIR., New Delhi, India for granting me the senior research fellowship. I also thank our University for giving me scholarship under the 'University with Potential for Excellence'¹ (UPE) programme.

I wish to thank Dr. Atul Negi, Dr. S. Durga Bhavani, Dr. K. Narayana Murthy, Prof. Hrushiksha Mohanty, Dr. P. R. K. Murti, Ms. Shoba Rani and all other faculty members of the department for their encouragement and moral support. I also would like to thank Prof. B. L. Deekshatalu for his encouragement. I would like to specially thank Dr. C. R. Rao for advising on the statistical analysis. I also thank all the supporting staff (both technical and non-technical) for their ready help in TRCT Lab and AI lab.

I also would like to thank the members of 'Centre for Cognitive Science', University of Hyderabad for their encouragement.

My sincere thanks are due to Prof. Karl Friston, University College, London, author of SPM software for his help in validating the image analysis methodology and suggestions on my results. The motivation given by him in Okinawa and the subsequent email correspondence gave me enough confidence to continue in this field of Neuroimaging. I also would like to thank Dr. Russel Poldrack, Dr. Kalina Christoff, Dr. Fatima Hussain, Dr. John Ashburner, Dr. Will Penny for their help (through email correspondence) in clearing my queries in SPM.

It gives me great pleasure to acknowledge Mr. Krishna Prasad Miya-puram and Mr. Ahmed for the collaborative research. I owe Krishna Prasad and Dr. Bapi Raju a lot for spending several long hours discussing the incoming results and pondering over the analysis methodology. My special regards to Shesharao Wanjerkhede for motivating discussions on Reinforcement Learning.

Thanks are due to Dr. Kiranmayi Bapi for extending her moral support and suggestions on behavioural results. Herself, Tejas and Tapa, deserve a whole lot of thanks for sparing a significant amount of their family time for the sake of discussions between me and my supervisor.

My quest towards understanding mystery of higher-order mental functions took a decisive shape after meeting with several eminent neuroscientists from India and Abroad in various meetings. They are Dr. Anthony Bell, Prof. Karl Friston, Dr. Hiroshi Imamizu, Dr. Kenji Doya, Prof. Stefan Schaal, Prof. Peter Dayan, Prof. Seiji Ogawa, Prof. Thomas Albright, Prof. Upinder Bhalla, Prof. Jagnathan, Prof. Jonathan Victor, Dr. Aditya Murthy, Dr. Balaraman Ravindran, Prof. Basabi Bhaumik, Dr. V. S. Chakravarthy, Prof. P. K. Kaira, Dr. Nandini Singh, Dr. Narayanan Srinivasan, Prof. Neeraj Jain, Prof. P. Prakash, Dr. Garimella Ramamurthy, Dr. Rishikesh

Narayanan, Dr. P. K. Roy, Prof. Shobini Rao, Dr. J. Sivaswami, Prof. Subhendu Ghosh, Dr. S. Khushu, Prof. Vijayalaxmi Ravindranath.

My special thanks to Dr. Anthony Bell, Dr. Rajesh Rao, Dr. Konrad Kording, Dr. Uta Noppeney, Dr. Jean-Claude Dreher, and Dr. Jeffery Beck for the exciting discussions in Okinawa which influenced me take the challenges in neuroscience.

There are two important persons Posina Venkata Rayudu and Bala Raju Battu who introduced me to some interesting problems of Science and encouraged me to think differently.

I also would like to thanks organizers of International Conference on Theoretical Neurobiology and International Symposium 'Building the Brain' where awards won by my posters gave me enough confidence to continue this research further.

At this point I would like thanking Dr. M. B. Srinivas for his encouragement and motivation to take up this work.

Good Friends are a rare to find. Thanks due to my friends Naga, Srinivas, Prem Kiran, Mahipal, Varma, Shankar, Pillai, Dr. Challa Sastry, Phani Kumar, Sastry, Trivikram, Syamsundar, Harsha for making my stay at campus memorable. I am delighted to thank the scholars of DCIS, O.B.V. Ramaniah, Satyajit Acharya, C.R.K. Reddy, Myo, Bharadwaj, Murali, Ravindranath, Sanjay, Priti Chandra, Adilaxmi, Harita, Ravi, Chit and Subrat for their constant encouragement and support. Thanks to Shankar Reddy for his affectionate encouragement. I also would like to thank K. Venkateswara: Rao for his encouragement and support.

I am very fortunate to have excellent friends like Bhaskar, Chandrasekhar, Girish, Kalyan, Murali, Narsi, and Ramesh who made my life cheerful and memorable. Eating Bhaskar's Dal and exciting discussions in Usha Enclave and Godavari block are great memories.

Special thanks due to Satyajit Acharya,, Srinivas and Dr. P. S. Srinivasan for their help with the L^AT_EX.

last but not the least, I am, needless to mention, indebted to my parents without whose constant encouragement and support this day of mine would have remained a dream.

July 8, 2005

Pammi V. S. Chandrasekhar

Table of Contents

Abstract	iv
Acknowledgements	v
List of Tables	xii
List of Figures	xiv
1 Introduction	1
1.1 Introduction to Sequence Learning and its Importance	1
1.2 Objective of this Research	2
1.3 Internal Organization of Sequences.	3
1.4 Experimental Methodology.	5
1.5 Questions Addressed in this Thesis.	6
1.6 Hypothesis.	6
1.7 Organization of the Thesis.	7
2 Survey of studies related to Sequence Complexity	10
2.1 Literature Survey.	10
2.1.1 Review of Sequence Complexity Paradigms.	12
2.1.2 Differences between various complexity paradigms reviewed and the paradigm used in this thesis.	24
2.1.3 Summary of our Experimental Paradigm.	25
3 Introduction to fMRI: experimental design and analysis	27
3.1 Introduction to fMRI	27
3.2 Issues related to Experimental design.	28
3.2.1 Block and Event-related Designs.	29
3.2.2 General Taxonomy of Experimental Design.	30
3.3 Analysis of Imaging Data	31
3.3.1 Data Acquisition.	32
3.3.2 Preprocessing.	33
3.3.3 Statistics: Model Setup and Estimation.	35
3.3.4 Statistical Inference.	36
3.3.5 Random Effects Analysis.	36

3.4	Characterizing Learning Related Changes.	37
3.4.1	Using Statistical Parametric Map (SPM).	37
3.4.2	Alternative approaches for characterizing learning induced changes.	38
3.4.3	Summary.	41
4	Experimental Methods	42
4.1	Experimental Subjects.	42
4.2	Details of the Behavioural aspects of the Experiment	43
4.3	Control (Follow) Task.	49
4.4	Possible Cognitive Components.	51
4.5	Details of Functional Imaging Parameters.	51
4.6	Analysis Methodology for Behavioural Parameters.	52
4.7	Statistical Analysis of functional Images	53
5	Behavioural Results	56
5.1	The Behavioural Parameters.	56
5.1.1	Definition of the Parameters.	57
5.2	Demarcating the Learning Stages.	57
5.3	Learning related improvements.	60
5.3.1	Success Rate.	60
5.3.2	Average key-press Response Time (RT).	65
5.3.3	Number of Movements (NM).	70
5.4	Analysis of the Control/Follow Condition.	71
5.4.1	Summary of the Results in the Control Condition.	72
6	Hierarchical organization of Sequential Skills	74
6.1	Introduction	74
6.2	Data analysis.	77
6.3	Results.	78
6.3.1	Repeated-measures ANOVA Results.	78
6.3.2	ANOVA Results across Sequence Conditions.	79
6.3.3	Quantifying the Chunking Phenomenon	79
6.4	Summary and Conclusions.	81
7	Imaging Results	84
7.1	fMRI Results.	85
7.2	Basic comparison results.	86
7.2.1	Detailed description of basic comparison results.	87
7.2.2	Summary of basic comparison results.	88
7.3	Comparisons between the sequence tasks.	89
7.3.1	Detailed description of results from comparison between sequence learning; tasks.	90
7.3.2	Results from direct comparisons of complex conditions	98
7.3.3	Summary of results of comparison between sequence tasks	106

7.4	Brain-Behaviour correlation (BBC) analysis results	107
7.4.1	Summary of BBC Results.	108
8	Modelling of fMRI data to probe effective connectivity	114
8.1	Dynamic Causal Modelling (DCM).	115
8.2	Results.	117
8.2.1	Testing the model of dorsal premotor cortex, primary motor cortex.	117
8.2.2	Testing the model of dorsal premotor cortex, anterior cerebellum	119
8.2.3	Testing the model of caudate, dorsal premotor cortex . . .	120
8.2.4	Testing the model of dorsolateral prefrontal cortex, caudate	121
8.2.5	Testing the model of posterior cerebellum, superior parietal cortex.	121
8.3	Summary and Conclusions.	123
9	Discussion of Results and Conclusions	126
9.1	Interpretation of the fMRI Results.	131
9.1.1	Neural systems underlying the acquisition of long-range sequence.	131
9.1.2	Neural systems underlying the long-range optimization process.	133
9.1.3	Neural systems underlying the short-range prediction process	134
9.1.4	Neural systems underlying the short-range optimization process.	135
9.2	Conclusions.	136
10	Future Work	138
10.1	Future Directions.	138
10.1.1	Experimental Design.	138
10.1.2	Theoretical Framework.	139
	References	143
	Appendices	156
A	Instructions for the Complexity Experiments	156
B	Details of Experimental Procedure and File Formats	158
B.1	Procedure for conducting the experiment	158
B.1.1	Creation of parameter files	158
B.1.2	Running the Program	160
B.1.3	Practice Session.	160
B.2	Subject file.	160
B.2.1	Subject file before the experiment	160

B.2.2	Subject file after the experiment	161
B.3	Result file after the experiment	162
B.4	Post processing of Behavioural Results.	165
C	Hypersets used in the Current Study	166
D	Data Analysis Procedure using SPM99	169
D.1	Preprocessing	170
D.1.1	Setting the origin and reorientation of images.	171
D.1.2	Realignment	173
D.1.3	Coregistration	175
D.1.4	Normalization.	178
D.1.5	Smoothing.	179
D.2	Statistical Analysis.	180
D.2.1	fMRI model setup.	181
D.2.2	Contrasts and Assessment of Results.	185
D.3	Random Effects Analysis (RFX).	189
D.4	Sources and Further Reading	192
E	Imaging Results from Basic Comparisons	194
F	Imaging Results from Comparison of 2x6 with the Complex Sequence Tasks	202

B.2.2	Subject file after the experiment	161
B.3	Result file after the experiment	162
B.4	Post processing of Behavioural Results.	165
C	Hypersets used in the Current Study	166
D	Data Analysis Procedure using SPM99	169
D.1	Preprocessing	170
D.1.1	Setting the origin and reorientation of images.	171
D.1.2	Realignment	173
D.1.3	Coregistration.	175
D.1.4	Normalization.	178
D.1.5	Smoothing	179
D.2	Statistical Analysis.	180
D.2.1	fMRI model setup.	181
D.2.2	Contrasts and Assessment of Results.	185
D.3	Random Effects Analysis (RFX).	189
D.4	Sources and Further Reading	192
E	Imaging Results from Basic Comparisons	194
F	Imaging Results from Comparison of 2x6 with the Complex Sequence Tasks	202

List of Tables

5.1	Demarcation of the early Stage for 2x6, 2x12 and 4x6 tasks. The numbers in the table indicate the session number up to which the early stage is considered	60
5.2	The percentage change of success rate for the four sessions. The standard deviation indicates the variability across each session. . .	62
5.3	The Key-press Response times for the four sessions. The standard deviation indicates the variability across each session.	67
7.1	Location of Stereotaxic Talairach coordinates of peak activations in the Early 4x6>2x6 Regressor and the Early 2x12>2x6 Regressor Contrasts.	92
7.2	Location of Stereotaxic Talairach coordinates of peak activations in the Consolidation 4x6>2x6 Regressor and the Consolidation 2x12 > 2x6 Regressor Contrasts.	95
7.3	Location of Stereotaxic Talairach coordinates of peak activations in the Early 4x6>2x12 Regressor and the Early 2x12>4x6 Regressor Contrasts. Bold faced T-score indicates that the activation survived whole brain correction for multiple comparisons at $p < 0.05$	99
7.4	Location of Stereotaxic Talairach coordinates of peak activations in the Consolidation 4x6>2x12 Regressor and the Consolidation 2x12>4x6 Regressor Contrasts. Bold faced T-score indicates that the activation survived whole brain correction for multiple comparisons at $p < 0.05$	102
E.1	Location of Stereotaxic Talairach coordinates of peak activations in the Early 2x6>Control Regressor and the Early Control>2x6 Regressor Contrasts.	194
E.2	Location of Stereotaxic Talairach coordinates of peak activations in the Early 2x12>Control Regressor and the Early Control>2x12 Regressor Contrasts.	195
E.3	Location of Stereotaxic Talairach coordinates of peak activations in the Early 4x6>Control Regressor and the Early Control>4x6 Regressor Contrasts. Bold faced T-score indicates that the activation survived whole brain correction for multiple comparisons at $V < 0.05$	196

E.4	Location of Stereotaxic Talairach coordinates of peak activations in the Consolidation 2x6 > Control Regressor and the Consolidation Control>2x6 Regressor Contrasts.	198
E.5	Location of Stereotaxic; Talairach coordinates of peak activations in the Consolidation 2x12>Control Regressor and the Consolidation Control>2x12 Regressor Contrasts.	199
E.6	Location of Stereotaxic Talairach coordinates of peak activations in the Consolidation 4x6>Control Regressor and the Consolidation Control>4x6 Regressor Contrasts. Bold faced T-score indicates that the activation survived whole brain correction for multiple comparisons at $p < 0.05$	200
F.1	Location of Stereotaxic Talairach coordinates of peak activations in the Early 2x6>4x6 Regressor and the Early 2x6>2x12 Regressor Contrasts	202
F.2	Location of Stereotaxic Talairach coordinates of peak activations in the Consolidation 2x6>4x6 Regressor and the Consolidation 2x6>2x12 Regressor Contrasts.	203

List of Figures

1.1	Flat versus Hierarchical representation. Schematic diagram depicts a, sequence of seven elements represented in flat (linear) and hierarchical (non-linear) arrangement. In hierarchical organization, nodes a_{123} and a_{4567} represent chunks of elements.	4
3.1	Data Processing Steps in SPM	32
4.1	fMRI Scanner setup for stimulus presentation. Subjects lay supine in the fMRI scanner and learned the visuo-motor sequences. The non-magnetic key-pad in the scanner room is connected to the experimental computer in the control room. A separate functional image acquisition computer was also present in the control room (not shown in this figure). The stimulus generation and the image acquisition timings were synchronized.	44
4.2	(a) Stimulus, Key-pad and Hand arrangements, (b) The 3x3 numeric key-pad with corresponding finger positions.	45
4.3	Procedure for the 2x6 Task.	46
4.4	Procedure for the 2x12 Task.	46
4.5	Procedure for the 4x6 Task.	47
4.6	Dimensions of complexity used in the experiments.	47
4.7	The design of experiments. Each of the Experiments (2x6, 2x12 and 4x6) is divided into sessions (S1, S2, S3 and S4). Sessions consist of alternating Control/Baseline/Follow (lasting for 18 seconds) and Task/Sequence learning (lasting for 36 seconds) Blocks. In each block subjects practiced sequence or follow random visual targets in the form of trials. With the repetition time (TR) set to 6 seconds, a total of 3 whole-brain scans and 6 whole brain-scans could be obtained in the control (C) and sequence task (T) blocks, respectively.	49
4.8	Design of Task (test) and Control Conditions. The process module in part (a) indicates the trial-and-error learning process as in the sequence tasks and part (b) indicates no such component of learning in the control/follow condition.	50

4.9	Modelling the effects of the two dimensions of sequence complexity. (a) set complexity effects (b) hyperset complexity effects. The error bar indicates the variations across subjects. The values corresponding to each subject are entered as regressors in the first level fMR image analysis.	54
5.1	Success rate graph indicating the improvements from session 1 to 4 in the three sequence tasks (2x12, 4x6 and 2x6). The session-wise mean values are plotted for the four sessions. The error-bar indicates the variability across each session. The statistical significance values are also shown [*** is highly significant ($p < 0.001$), * is significant ($p < 0.001$) and NS is non-significant ($p > 0.05$)].	59
5.2	The block-wise graphs containing the success rate separately plotted for the three experiments with the error-bars indicating the standard deviation across the subjects.	61
5.3	Session-wise improvements of success rate across the experiments. S1, S2, S3, and S4 indicate the session number index. The error-bar indicates the standard deviation across sessions. The statistical significance values are also shown [* is significant ($p < 0.001$) and NS is non-significant ($p > 0.05$)].	61
5.4	Stage-wise improvements of success rate across the experiments (2x12, 4x6 and 2x6 experiments) for (a) Early (E) and (b) Consolidation (C) stages separately. The error-bar indicates the variability across the subjects. The statistical significance values are also indicated in the plot [*** is highly significant ($p < 0.001$), ** is more significant ($p < 0.0001$) and NS is non-significant ($p > 0.05$)].	64
5.5	The block-wise graphs containing the average key-press RT separately plotted for the three experiments with the error-bars indicating the standard deviation across the subjects.	65
5.6	Session-wise improvements of Response Time across the experiments for comparison. S1, S2, S3, and S4 indicate the session number index. The error-bar indicates the standard deviation across sessions. The statistical significance values are also shown [*** is more significant ($p < 0.0001$), * is significant ($p < 0.001$) and NS is non-significant ($p > 0.05$)].	66
5.7	Stage-wise improvements of key-press response time across the experiments (2x12, 4x6 and 2x6 experiments) for (a) Early and (b) Consolidation stages separately. The error-bar indicated the variability across the subjects. The statistical significance values are also indicated in the plot [*** is highly significant ($p < 0.001$), ** is more significant ($p < 0.0001$), * is significant ($p < 0.01$), and NS is non-significant ($p > 0.05$)].	69

5.8	The block-wise graphs containing the success rate plotted for the three experiments with the error-bars indicating the standard deviation across the subjects. This plot indicates the similarity of the success rate values in the control condition across experiments.	73
5.9	The block-wise graphs containing the response time plotted for the three experiments with the error-bars indicating the standard deviation across the subjects. This plot indicates the similarity of the key-press response time values in the control condition across experiments.	73
6.1	Learning related improvements observed in the three $m \times n$ tasks for one subject (WY). Number of sets completed (<i>left panel</i>) and average set completion time (<i>right panel</i>) over all the trials across the four sessions (S1 to S4) are shown. Vertical lines in the <i>right panel</i> and the gaps in the <i>left panel</i> corresponds to the session-to-session demarcation. The Early (E), Consolidation (C) and Late (L) stages (in <i>left panel</i>) are also indicated along with the session index (S1, S2, S3 and S4).	80
6.2	Chunking phenomenon observed in three subjects (KU, NS, WY) for the 2x12 and 4x6 tasks. <i>top panel</i> : The cumulative set RTs for successful trials for all the sessions (delineated by vertical lines), <i>middle panel</i> : dendrogram, <i>bottom panel</i> : mean set RTs in the last session. (a) 2x12 Task. Cumulative set RTs show a clear bunching pattern for few sets of 2x12 task. The dendrogram shows the hierarchical structure of the sequence acquired by the subject. (b) 4x6 Task. The cumulative set RTs for successful trials do not show any bunching pattern across sets. The dendrogram shows that subjects require similar amount of time for each set.	83
7.1	The example Design matrix in RFX analysis of Sequence conditions. The contrast images of every subject for the two sequence task conditions were taken to the second level and two-sample t-test was performed.	90
7.2	Early 4x6>2x6 Regressor contrast activations.	93
7.3	Early 2x12>2x6 Regressor contrast activations.	94
7.4	Consolidation 4x6>2x6 Regressor contrast activations.	96
7.5	Consolidation 2x12>2x6 Regressor contrast activations.	97
7.6	Early 4x6>2x12 Regressor contrast activations.	100
7.7	Early 2x12>4x6 Regressor contrast activations.	101
7.8	Consolidation 4x6>2x12 Regressor contrast activations.	103
7.9	Consolidation 2x12>4x6 Regressor contrast activations.	104
7.10	Early 4x6>2x12 (Red colour) and Early 2x12>4x6 (Green colour) Regressor contrast activations.	105

7.11	Consolidation 4x6>2x12 (Red colour) and Consolidation 2x12>4x6 (Green colour) Regressor contrast activations.	106
7.12	The brain-behaviour correlations of 2x6, 4x6 & 2x12 (x-axis: behaviour and y-axis: brain activation) and their time courses at Right Dorsolateral prefrontal cortex (Brodmann area 10/46) obtained from the Early 2x6>Control Regressor contrast. The <i>top panel</i> : The brain-behaviour correlation (BBC) of 2x6 and 4x6 tasks (left and right respectively). <i>bottom panel</i> : The BBC of 2x12 task (left) and the time course of activation in the three tasks (2x12, 4x6 and 2x6 respectively).	109
7.13	The brain-behaviour correlations of 2x6, 4x6 & 2x12 (x-axis: behaviour and y-axis: brain activation) and their time courses at Right Dorsolateral prefrontal cortex (Brodmann area 46) obtained from the Consolidation 4x6>Control Regressor contrast. The <i>top panel</i> : The brain-behaviour correlation (BBC) of 2x6 and 4x6 tasks (left and right respectively). <i>bottom panel</i> : The BBC of 2x12 task (left) and the time course of activation in the three tasks (2x12, 4x6 and 2x6 respectively).	110
7.14	The brain-behaviour correlations of 2x6, 4x6 & 2x12 (x-axis: behaviour and y-axis: brain activation) and their time courses at Left Primary motor area (Brodmann area 4) obtained from the Consolidation 4x6>Control Regressor contrast. The <i>top panel</i> : The brain-behaviour correlation (BBC) of 2x6 and 4x6 tasks (left and right respectively). <i>bottom panel</i> : The BBC of 2x12 task (left) and the time course of activation in the three tasks (2x12, 4x6 and 2x6 respectively).	111
7.15	The brain-behaviour correlations of 2x6, 4x6 & 2x12 (x-axis: behaviour and y-axis: brain activation) and their time courses at Right Lateral Globus Pallidus obtained from the Consolidation 2x12>Control Regressor contrast. The <i>top panel</i> : The brain-behaviour correlation (BBC) of 2x6 and 4x6 tasks (left and right respectively). <i>bottom panel</i> : The BBC of 2x12 task (left) and the time course of activation in the three tasks (2x12, 4x6 and 2x6 respectively).	112
7.16	The brain-behaviour correlations of 2x6, 4x6 & 2x12 (x-axis: behaviour and y-axis: brain activation) and their time courses at Left Precentral gyrus (Brodmann area 3/4) obtained from the Early 4x6>2x6 Regressor contrast. The <i>top panel</i> : The brain-behaviour correlation (BBC) of 2x6 and 4x6 tasks (left and right respectively). <i>bottom panel</i> : The BBC of 2x12 task (left) and the time course of activation in the three tasks (2x12, 4x6 and 2x6 respectively).	113

8.1	The intrinsic connections strengths between ipsilateral dorsal pre-motor and ipsilateral primary motor area	118
8.2	The modulatory connections for (a) Early and (b) Consolidation stages related to the 4x6 task. This graphs shows in the early stage the connections between right dorsal preniotor and right primary motor are strong in the early stage but became weak by the consolidation stage.	118
8.3	The intrinsic connections strengths between ipsilateral dorsal pre-motor and ipsilateral anterior cerebellum.	119
8.4	The modulatory connections for (a) Early and (b) Consolidation stages related to the 4x6 task. This graphs shows in the early stage the connections between right dorsal premotor and right anterior cerebellum arc strong in the early stage but became weak by the consolidation stage.	120
8.5	The intrinsic connections strengths between left caudate and right dorsal premotor cortex.	121
8.6	The modulatory connections for (a) Early and (b) Consolidation stages related to the 4x6 task. This graphs shows in the consolidation stage the connections between left caudate and right dorsal preniotor is strong but found to be non-significant in the early stage.	122
8.7	The intrinsic connections strengths between left dorsolateral pre-frontal cortex and left caudate.	123
8.8	The modulatory connections for (a) Early and (b) Consolidation stages related to the 4x6 task. This graphs shows in the consolidation stage the connections between left dorsolateral prefrontal cortex and left caudate is strong but found to be non-significant in the early stage.	124
8.9	The intrinsic connections strengths between right posterior cerebellum and right superior parietal cortex.	124
8.10	The modulatory connections for (a) Early and (b) Consolidation stages related to the 2x12 task. This graphs shows in the consolidation stage the connections between right posterior cerebellum and right superior parietal cortex is strong but found to be weak in the early stage.	125
10.1	Block Diagram of the Proposed Hybrid Model. Actor-critic based model incorporating Markov model and hierarchical policy as sub-modules in the actor module. The two-levels in the actor module, namely, the Markov model and the hierarchical policy module would enable learning hierarchical sequence decision problems. . .	142
D.1	SPM GUI	170
D.2	EP1 Template Image and Locating the Origin.	171
D.3	Images before and after Reorientation.	172

D.4	Realignment Parameters	175
D.5	Coregistration of functional image with anatomical image	177
D.6	Normalization	179
D.7	Design Matrix	185
D.8	Contrast Manager for selecting or creating contrasts	186
D.9	Results (Glass brain)	188
D.10	Visualising activations overlaid on subject's high resolution image	189
D.11	Design Matrix in RFX for one Sample T-Test	191
D.12	Results from Random Effects (RFX) analysis for one Sample T-Test	192

Chapter 1

Introduction

1.1 Introduction to Sequence Learning and its Importance

Sequencing of information and actions is a fundamental human ability that underlies several intelligent activities and behaviours. We resort to sequencing of information in a variety of day-to-day tasks: from sequencing sounds in order to utter sentences, sequencing movements in order to type or for playing a piano, sequencing actions to be able to drive a car and sequencing moves in the game of chess, etc. (Clegg et al., 1998; Sun, 2000; Sun and Giles, 2001). Sequence learning is very prevalent in humans and animals. It is believed that intelligence is based on the ability to learn a complex sequence of movements, as implicated in the usage of tools and languages (Hikosaka et al., 2000). Karl Lashley, in his classic paper titled *'The Problem of Serial Order in Behavior'* (Lashley, 1951), pointed out the prime importance of investigating serial order or sequentiality in the studies of cognition. We consider serial order or sequence processing as synonymous in this thesis. Learning of sequences is one important aspect of sequence processing.

There are many other areas of application for sequence learning. Research work on sequence learning has been going on in several disciplines such as artificial intelligence, neural networks, cognitive science (sequence learning aspects in skill acquisition), and engineering. How humans learn sequential procedures has been a long-standing research problem in cognitive science and currently is a major topic in neuroscience. In human skill learning [for example, Willingham

(1998); Bapi et al. (2000)], high-level problem solving and reasoning [for example, Anderson (1995)], sequentiality is often the most important aspect. Therefore, when building intelligent systems to emulate human intelligence and cognition, we must pay serious attention to sequences, including learning of sequence (Sun and Giles, 2001).

The aim of this thesis is to investigate how humans learn and execute complex skills. Acquiring complex sequential skill involves chaining a number of primitive actions to make a complete sequence. Sequence learning is a viable experimental paradigm for investigating skill acquisition (Clegg et al., 1998). With the insights gathered from the investigation of human sequential behaviour and understanding the underlying mechanisms, it is hoped that more flexible and robust machines can be designed in the future (Sun, 2000; Sun and Giles, 2001).

Recent advances in medical imaging techniques, especially the functional Magnetic resonance Imaging (fMRI), have made it possible to study the brain *in vivo* while subjects are engaged in meaningful behavioural tasks. The resulting dynamic picture gives more direct insights into the workings of the brain. In this research we would like to study aspects of complexity in sequential skill learning using fMRI as an investigation tool. The current research investigation attempts to further scientific understanding of human sequential behaviour — an interesting research problem, both in the areas of *Cognitive Neuroscience* and *Artificial Intelligence*. Recently Colwell (2005) pointed out that understanding *intelligence* from the neuroscience perspective is becoming important to achieve the goal of *Artificial Intelligence*.

1.2 Objective of this Research

The objective is to investigate the effect of change in complexity of the skill being acquired on various entities such as the nature of internal representation of skills, on the behavioural parameters and on the pattern of brain activation. We used *visuo-motor sequence learning paradigm* to address these questions.

Further, we would like to demonstrate the effective connectivity of some brain areas obtained from the experiments, which gives more insight into the functional circuits of the brain. The modelling exercise may also spawn further predictions to be experimentally verified in future.

1.3 Internal Organization of Sequences

Investigation of the internal organization of sequential skills is one of the important issues in the domain of sequence processing. The other possible issues related to sequence processing are - distributed versus local representation, pre-wired versus adaptive origins of representation, implicit versus explicit learning, fixed/fiat versus hierarchical organization, timing aspects, order information embedded in sequences, primacy versus recency in list learning and aspects of sequence perception such as recognition, recall and generation. Recently Bapi et al. (2005) reviewed these issues separately with examples. It is to be noted that no single experimental paradigm in literature covers all these issues in a unified fashion. In this section we describe in detail about *sequence organization* as this issue is central to the problem discussed in this thesis.

Internal organization of behavioural sequences can be either linear (fiat) or nonlinear (hierarchical) (see figure 1.1). Lashley (1951) argued that the sequential responses that appear to be organized in linear and flat fashion concealed an underlying hierarchical structure. Hierarchical representations of sequences have an edge over linear representations. They allow easier access to common subroutines of sequences, easier to self-repair in the event of failure, and combine efficient local action at low hierarchical levels while maintaining the guidance of an overall structure. A linear (flat) organization of a sequence will be in the form of one long linear string of actions as shown in Figure 1.1. While the representation is simple from the storage point-of-view, there can be potential problems during retrieval. For instance, if the n^{th} element has to be retrieved, all the $n - 1$ preceding elements have to be processed. Further, if there is a break in the chain, subsequent elements will become inaccessible. On the other hand, a hierarchical representation would have multiple levels of representation. Figure 1.1 shows a 2-level hierarchical representation. At the lower level, the representation of the elements of the sequence is flat. At the higher level, control nodes (chunk nodes) are connected among themselves in a linear fashion and also connect to their respective sequence elements forming a hierarchy. A break in the link between lower level nodes does not render any part of the sequence inaccessible, since the control nodes (chunk nodes) would still be able to facilitate access to the lower level nodes. In human behaviour, hierarchical structuring has been argued to be essential for many acquired skills, such as language, problem solving

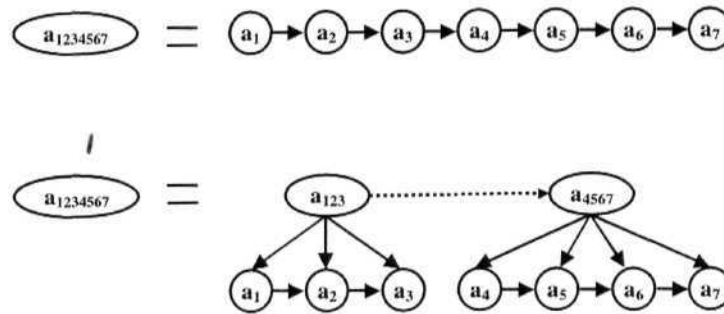


Figure 1.1: Flat versus Hierarchical representation. Schematic diagram depicts a sequence of seven elements represented in flat (linear) and hierarchical (non-linear) arrangement. In hierarchical organization, nodes a_{123} and a_{4567} represent chunks of elements.

and everyday planning (Chomsky, 1957; Newell et al., 1958; Miller et al., 1960; Newell and Simon, 1972; Conway and Christansen, 2001). Further, studies show that representation at the higher level supports grouping of low level units to form what are popularly known as chunks [for example, Wickelgren (1969, 1999); MacKay (1982); Rosenbaum et al. (1983); Koch and Hoffmann (2000); Verwey (2001); Sakai et al. (2003)]. Chunking also enables overcoming the limitations imposed by the limited-capacity working memory, whose limit is proposed to be 7 ± 2 constituents (Miller, 1956). In summary, when the amount of information exceeds the capacity limits of working memory, it is expected that the internal organization of sequences would be hierarchical in nature.

1.4 Experimental Methodology

In order to investigate sequence learning experimentally, we adopted an $m \times n$ finger movement sequence learning paradigm (Hikosaka et al., 1995; Bapi et al., 2000). In these experiments, subjects learned sequences of finger movements of increasing size (complexity).

In the $m \times n$ complexity paradigm the correct order of pressing m keys (Set) successively for n times (Hypcrset) is learned by trial-and-error process. In this paradigm, a visuo-motor sequence is incrementally acquired by learning smaller sub-sequences. The tasks designed in this experimental paradigm are 2x6, 2x12 and 4x6. Subjects responded to visual stimuli on a 3x3 display by pressing corresponding keys on a keypad inside the scanner. We trained eighteen subjects in 1.5 Tesla functional Magnetic Resonance Imaging (fMRI) scanner on sequences where *set* length and *hyperset* lengths were varied independently. Set length was increased from 2 to 4 and hyperset length from 6 to 12. The experiments consisted of four sessions of alternating sequence and base line conditions (called, a box-car design or epoch based). The baseline condition required subjects to follow random visual targets. Complexity of learning in this paradigm is controlled along two dimensions – the size of the sub-sequence (m) and the number of sub-sequences (n). We wish to investigate the effect of independently varying m and n on the acquisition and performance of sequential skill. The major advantage of preferring the $m \times n$ experimental paradigm is that innumerable number of new hypersets can be generated (the number of possible combinations for a hyperset will be of the order of 10^{11}). The other interesting feature of this experimental paradigm is that learning is facilitated by a trial-and-error process. The learning by trial-and-error process used in our experimental paradigm constitutes a very good example of the popular machine learning framework called *Reinforcement Learning* (Sutton and Barto, 1998).

The earlier neuroimaging studies of sequence complexity varied the sequence length linearly (Sadato et al., 1996; Catalan et al, 1998, 1999; Boecker et al., 1998, 2002) or compared between different types of sequence i.e, contrasting between repeated and heterogeneous sequence of finger movements (Wexler et al., 1997; Dassonville et al., 1998; Gordon et al, 1998; Harrington et al., 2000; Hummel et al, 2003; Haaland et al, 2004). The work reported in this thesis differs in methodology from the earlier investigations of sequence complexity. Most of these

studies used well-learned sequences. But, our tasks involve progressively learning the visuo-motor sequence by a trial-and-error process. It was also possible to probe the learning phenomenon of a new sequence (early stage) and mastering that sequence (consolidation for the efficient retrieval of the sequence). Our task also allowed us to probe the progression of learning hierarchical sequences, i.e. acquisition of chunks.

1.5 Questions Addressed in this Thesis

- How do behavioural parameters such as performance accuracy and speed change by increasing the complexity of the visuo-motor sequence?
- How does the brain activity profile change with respect to changes in the complexity of the sequence?
- What is the time course of changes (early-to-late differences) in the brain areas related to aspects of sequence complexity?
- How does brain cope with short-range versus long-range prediction loads in the working memory?
- Can we model mathematically the changes occurring in the coupling of brain modules as the learning progressed?

1.6 Hypothesis

As learning progresses the differences in the behavioural parameters and the brain activity in the initial learning phase might reflect the differential working memory load whereas the differences in the later phase might reflect the sequence buffer load requirements.

In our experiment, the amount of information to be processed at a time is represented by a *set*. Increase in the set-length (increase of m in 2x6 to 4x6 tasks) might increase the short-range prediction load while acquiring the sets. Similarly, increasing the hyperset-length (increase of n in 2x6 to 2x12 tasks) could be related to the increase in the long-range prediction load (acquisition of long hyperset).

We hypothesized that in the complex condition corresponding to increased set-length (i.e., in the 4x6 task), the optimization process may be limited to the items within the *set* and may not span across *sets*. In contrast, we expect that in the complex condition corresponding to increased hyperset-length (i.e., in the 2x12 task), sequence information may possibly be organized in a hierarchical fashion. Further, these differential effects may have implications in the behavioural parameters (such as success rate and response time) and in the brain activity pattern.

1.7 Organization of the Thesis

The organization of the thesis is as follows.

Chapter 2 reviews various neuroimaging studies related to sequence complexity and their main contributions along with their experimental paradigms. A summary of these studies and a comparison of other paradigms with the paradigm used in our study will be made. Lastly, salient points of our experimental paradigm will be highlighted.

Chapter 3 is an introduction to functional imaging and experimental design issues. In this chapter we also describe various analysis methods and approaches for analyzing functional images.

Chapter 4 describes the task procedures of our $m \times n$ complexity experimental paradigm, possible cognitive processes associated with the experimental tasks, methods adopted for the behavioural analysis, fMRI scanner parameters used for our experiments, methods of statistical analysis of functional images, how we modelled the effects of complexity in the analysis and the types of fMRI analysis performed in the current investigation. Thus this chapter describes the materials and experimental methods.

Chapter 5 reports the statistical analysis results on the behavioural parameters while subjects performed complex sequential skill by trial-and-error. Session-wise and stage-wise results for the three experiments for each behavioural parameter (success rate, average key-press response time and number of movements) are reported. The demarcation procedure for marking the learning stages in the behavioural data will be discussed. The repeated-measures (RM) ANOVA results

for each behavioural parameter are also reported. The RM ANOVA results play an important role in understanding the learning related improvements and their differences among the experimental tasks.

Chapter 6 reports an interesting finding on the hierarchical organization of sequential skills. In this chapter behavioural analysis of the response times is presented. The aim is to systematically quantify the hierarchical organization of sequential skills (i.e., the chunking process) and its differential effects when the sequence is arranged in different ways (i.e., as 2x12 or 4x6).

Chapter 7 reports functional Magnetic Resonance (fMRI) results of our complexity experiment obtained using SPM99 package. SPM99 is developed by the Wellcome Department of Imaging Neuroscience, University College London. The results from the random effects analysis (RFX) of comparisons of complex sequence conditions (2x12 and 4x6) with 2x6 in both the stages (*effects of complexity*), RFX analysis of complex sequence learning conditions 2x12 versus 4x6 and 4x6 versus 2x12 in both the stages (*direct comparisons*) for both the stages are reported in this chapter.

Chapter 8 introduces a recent statistical modelling methodology called, *effective connectivity* (Friston et al., 2003). The basic idea of effective connectivity is to construct a reasonable realistic neuronal model of interacting cortical regions using the neuroimaging data. The effective connectivity analysis is realized through *Dynamic Causal Modelling* (DCM) in the SPM2 package (a recent tool developed by the Wellcome Department of Imaging Neuroscience, University College London). In this chapter we utilize the DCM analysis methodology and test a few models relevant to our tasks.

Chapter 9 presents the overall discussion of results obtained from the behavioural, neuroimaging data and the modelling efforts. This chapter will also point out possible interpretation of our results. This chapter also summaries the results of this thesis.

Chapter 10 suggests the future directions of this research.

Appendix A describes the list of instructions given to subjects before they performed the experiment in the fMRI scanner.

Appendix B lists the procedure for conducting empirical experimentation and recording the resulting behavioural parameters from the experiments. Sample

files and their formats are also described in this Appendix.

Appendix C lists the hypersets generated by our experimental program for all the 17 subjects for each of the experimental task.

Appendix D demonstrates a step-by-step procedure for performing fMRI data analysis using the SPM99 package developed by the Wellcome department of imaging neuroscience, University College London.

Appendix E lists the location of stereotaxic Talairach coordinates of peak activations in the early and consolidation stages of $2 \times 6 > \text{Control}$, $2 \times 12 > \text{Control}$ and the $4 \times 6 > \text{Control}$ regressor Contrasts in the form of tables.

Appendix F lists the location of stereotaxic Talairach coordinates of peak activations in the early and consolidation stages of $2 \times 6 > 2 \times 12$ and $2 \times 6 > 4 \times 6$ regressor contrasts.

Chapter 2

Survey of studies related to Sequence Complexity

In this chapter various neuroimaging studies related to the sequence complexity and their main contributions along with their experimental paradigms will be presented. A summary of these studies and differences of their paradigms with our complexity paradigm will be discussed. The salient points of our experimental paradigm will be pointed at the end.

2.1 Literature Survey

Neural basis of motor sequence learning has been extensively studied using various paradigms. Some studies investigated motor sequence learning with trial-and-error [Hikosaka and colleagues: (Sakai et al., 1998; Hikosaka et al., 2000); Passingham and colleagues: (Jenkins et al., 1994; Jueptner et al., 1997b,a; Toni et al., 1998)]. In trial-and-error learning subjects learned a sequence of finger movements by actively exploring sensori cues and evaluating responses based on external feedback. Other studies explored explicit [for example, Kami et al. (1995)] or implicit sequence learning [for example, Grafton et al. (1995, 1998)] or both [for example, Honda et al. (1998)]. In explicit type of learning subjects makes conscious attempt to construct a representation of the task whereas in the implicit learning the task relevant information is acquired automatically and without conscious awareness of what is being learnt. In several of these studies activity was observed in cortical, including the parietal, the primary motor, the premotor, the supplementary motor, the dorsolateral prefrontal, the frontal

pole, the anterior cingulate areas and in the subcortical areas, including the caudate, the putamen, the thalamus, the hippocampus, and the cerebellar areas. In all these studies new learning is either compared with prelearned sequences or pseudo-learning condition or random order sequences. Jenkins et al. (1994) and Jueptner et al. (1997a,b) observed activation in the dorsal prefrontal cortex [Brodmann Areas (BA) 9/46] and in the caudate nucleus during new learning. It has been suggested that these areas participate in one or several component processes involved in trial-and-error learning such as trying various choices, remembering previous choices, evaluating the responses and learning successive movements on the basis of feedback. Sakai et al. (1998) observed transition of activity from frontal areas in the early stages to the parietal areas by the late stages of sequence learning. In an explicitly guided learning paradigm, Kami et al. (1995) observed an enlarged activity in the primary motor cortex due to repeated practice of a motor sequence. In a serial reaction task paradigm [a popular implicit sequence learning paradigm developed originally by Nissen and Bullemer (1987), in which subjects learn sequential finger movements without conscious awareness of task in response to visual cues that appear one after the other and the learning is evidenced by the improvements in response times], Grafton et al. (1998) noticed learning related activity in the inferior parietal area reflecting abstract representation and that in the sensorimotor cortex reflecting effector-specific representation of the motor sequence.

Most of the earlier imaging studies of sequence complexity manipulated sequence length (Sadato et al., 1996; Catalan et al., 1998, 1999; Boecker et al., 1998, 2002) or type of sequence i.e. contrast between repeated and heterogeneous sequence of finger movements [for example, (Wexler et al., 1997; Dassonville et al., 1998; Gordon et al., 1998; Harrington et al., 2000; Hummel et al., 2003; Haaland et al., 2004)]. The current investigation methodologically differs from the earlier investigations of sequence complexity. Most of the previous studies used well learned sequences. But, our task involves progressively learning the visuo-motor sequence by trial and error. It was also possible to probe in our experimental design learning a new sequence (early stage) and mastering that sequence (consolidation for the efficient retrieval of the sequence). Our task also allowed us to probe the progression of learning hierarchical sequences, i.e. acquisition of chunks.

In the next section we review in detail some of the important studies related

to the sequence complexity in chronological order. Summarization of all the paradigms discussed along with the salient points about the current sequence complexity investigation will also be done.

2.1.1 Review of Sequence Complexity Paradigms

Sadato et al. (1996)

In a positron emission tomography (PET) study on 10 right-handed human subjects, Sadato et al. (1996) investigated the effects of sequence complexity during the performance of sequential finger movement tasks. The main contribution of their study was that they showed differences in the brain activation between the performance (execution) of simple and complex finger movements. In this study they used acoustically paced sequential opponent finger movement tasks in which subjects briskly and precisely touched the tip of the thumb with the fingers of right-hand at a frequency of 2Hz. As the index of complexity, they varied the length of unit sequences (number of finger orderings) progressively, namely, 4, 8, 12 & 16 element sequences (the index of complexity: 1, 2, 3, 4 respectively). During these finger movement opposition tasks of varied complexity, even though subjects showed over 90% of correct finger taps in all the tasks for the two trials, the performance declined from task 1 (complexity index: 1, sequence 1,2,3,4) to task 4 (complexity index: 4, sequence 1,2,3,4,1,3,2,4,4,2,3,1,4,3,2,1) indicating the effects of complexity. It means the performance value decreased from the simple sequence condition (task 1) to the complex sequence condition (task 4).

The brain activations in the bilateral primary sensorimotor area [Talairach coordinates: (-34,-24,52) & (28,-14,52)], the ipsilateral (right) anterior cerebellum [Talairach coordinate: (14,-58,-16)], the contralateral (left) ventral premotor cortex [Talairach coordinate: (-48,-8,28)], the posterior supplementary motor area [Talairach coordinate: (-6,-8,56)] and the left putamen [Talairach coordinate: (-30,-6,4)] were observed as common activations in all the sequence conditions. They suggested that these areas could be involved in execution of sequential fingers movements. A linear increase in regional cerebral blood flow (rCBF) in the ipsilateral (right) dorsal premotor cortex [Brodmann area 6, Talairach coordinate: (16,2,56)], the ipsilateral (right) precuneus [Brodmann area 7, Talairach coordinate: (18,-56,48)], the cerebellar vermis [Talairach coordinate: (-4,-56,-12)]

and the left thalamus [Talairach coordinate: (-12,-20,4)] were observed with the increase of complexity index (increased from 1 to 4). Decrease in rCBF in the contralateral (left) inferior parietal lobule [Brodmann area 40, Talairach coordinate: (-48,-56,24)] was observed with increase in complexity. These activation loci observed in this investigation did not reflect any learning related cognitive components, as the subjects were over trained before PET scanning. In this study they suggested functional roles for the right dorsal premotor and the right precuneus. The ipsilateral (right) premotor could be part of the mechanism for storing motor sequences in working memory buffer and the right precuneus might have a role in selecting and monitoring the sequence with on-line reference to a working memory in the ipsilateral premotor cortex.

Catalan et al. (1998) and Catalan et al. (1999)

Catalan et al. (1998) adapted the sequence finger movement paradigm of Sadato et al. (1996). On these experiments, they investigated the effects of changing sequence length in an acoustically paced opponent finger movement task. 13 normal right-handed human subjects performed four sequence conditions (length of unit sequences: 1, 4, 12, 16 denoted as simple, sequence-4, sequence-12, sequence-16 respectively) in a PET scanner. In this study they tried to distinguish neural basis of simple and complex sequential finger movements. They included a simple condition (one finger movement) in this study in order to perform such comparisons possible.

The experimental design is similar to that of Sadato et al. (1996). The subjects performed four conditions in a opponent finger tapping of the thumb paradigm where the length of the movement sequences varied from 1 to 16. Different unit sequence lengths reflected different indices of complexity and one rest condition as control condition. The shortest sequence (simple movement) is just one finger movement, i.e., by tapping right index finger with thumb. The other three sequences (lengths 4, 12 & 16) used all fingers i.e., index, middle & ring. Subjects briskly and precisely touched the tip of the thumb with the right hand fingers at a frequency of 0.5 Hz, paced with a beat of a metronome. Subjects were made to 'overlearn' the sequences before scanning.

Comparing the rest with the simple sequence condition they observed linear significant increase in the contralateral (left) primary sensorimotor area and the

ipsilateral (right) cerebellar cortex. These areas are interpreted to be involved in the executive role in running the sequences. In addition, they observed regional cerebral blood flow (rCBF) increase in the ipsilateral (right) premotor [Brodmann area 6, Talairach coordinate: (28,-8,56)], the bilateral posterior parietal cortex [Brodmann area 7, Talairach coordinates: (-26,-66,44) & (28,-66,44)] and the bilateral precuneus [Brodmann area 7, Talairach coordinates: (-18,-76,44) & (14,-68,40)]. These areas might be more selectively involved in sequence processing rather than just the execution of movement per se and could be involved in the storage of motor sequences in spatial working memory.

In a seminal work with the similar paradigm, Catalan et al. (1999) investigated the effects of performing long sequential movements by comparing normals with patients with parkinson's disease. They observed overactivity in the parietal and the premotor areas while the sequence complexity was increased in comparison to normals. Further, another finding in this study is the extra activation found in the pre-supplementary area (pre-SMA)/anterior cingulate in the parkinson's patients when the complexity of sequence was increased. They concluded by suggesting that the parietal, the premotor and the pre-SMA/anterior cingulate areas 'work harder' in parkinson's patients presumably because of the striatal dysfunction and this overactivity seemed to attempt to compensate for this dysfunction.

Boecker et al. (1998)

The main aim of this study was to investigate the neural bases within the motor related areas (cortical and subcortical) in humans that participated mainly in the 'overlearned' complex sequential finger movements. In a PET scanner, 7 healthy human subjects executed five different key-press sequences (overlearned before scanning) of varying sequence complexity. Repeated measurements of rCBF was done on each subject. Their 12-run PET experiment consisted of two resting conditions and five pairs of key-press sequences involving finger movements arranged in the form of a square design. They used similar experimental methodology of Sadato et al. (1996) but they differed in the arrangement of sequences. Five sequence conditions of varying complexity were given to the subjects which vary from 4 (sequence: 2,3,4,5) to 8 (sequence: 2,2,3,4,4,3,5,3) finger movements. Computer generated sound at one second interval used as guidance for pacing the finger movements. They took care of not assigning numbers to the finger move-

ments (2=index finger, 3=middle finger, 4=ring finger, 5=little finger), there by they could investigate cognitive components related to overlearned complex finger movement sequences. So, there are two main differences between Boecker et al. (1998) and other studies that used the same paradigm. One is that repeated measurements were made to improve the signal-to-noise (SNR) ratio. The other is that with arbitrary assignment of numbers to fingers, they avoided possible confounds because of a routine (direct) mapping being used.

They observed positive correlations of regional cerebral blood flow (rCBF) with the increase of complexity in the brain areas, left rostral supplementary motor area [Brodmann area 6, Talairach coordinate: (-4,2,56)], left thalamus [Talairach coordinate: (-6,-26,8)], bilateral globus pallidus [Talairach coordinates: (-12,-2,8) & (14,2,8)], left supplementary motor area [Brodmann area 6 antero-superior part, Talairach coordinate: (0,0,60)], right precuneus [Brodmann area 7, Talairach coordinate: (12,-68,44)] and right sensorimotor cortex [Brodmann area 4, Talairach coordinate: (48,-16,40)]. Interestingly they observed inverse correlations of rCBF with increasing complexity in left superior frontal gyrus [Brodmann area 10, Talairach coordinate: (-18,58,20)], right dorsal frontal gyrus [Brodmann area 10, Talairach coordinate: (8,58,8)], left anterior cingulate [Brodmann area 32, Talairach coordinate: (-6,36,10)] and right medial temporal gyrus [Brodmann area 39, Talairach coordinate: (46,-64,20)]. Their main conclusion was that the anterior globus pallidus activation suggests a specific role for the basal ganglia role in the process of motor sequence facilitation and control.

Harrington et al. (2000)

Harrington et al. (2000) investigated the effects of different structural properties of sequential actions on 15 right-handed human subjects in functional Magnetic Resonance Imaging (fMRI) scanner. The structural property in this study is measured by two independent factors: the number of fingers (surface structure) and number of finger transitions (abstract or sequence specific structure). These two factors were systematically varied to form measures of complexity. They varied sequence complexity independently in the two factors (varying the surface structure or varying the abstract/sequence specific structure) and investigated neural systems that were functional in these two aspects of structural properties of sequential actions.

In this study subjects performed sequences consisting of five key-press responses in response to a numeric (digit) sequence that was visually presented on a screen. The subjects used their index (left key - "1"), middle (middle key - "2") and ring (right key - "3") fingers of their right-hand and responded on a horizontal key-pad placed near their right-hand in the fMRI scanner. The left, middle and right keys were always pressed using the index, middle and ring fingers and experimenter took care that subjects did not move their left-hand inadvertently when performing sequences with their right-hand. Their experiment consisted of blocks and within each block, one of the three sequences (for example, in condition 1 the sequences are '11111', '22222' and '33333') were randomly presented, which constituted one trial. The conditions 2-8 were heterogeneous sequence forms. They designed these heterogeneous forms of sequences by systematically varying the number of finger transitions (0-4) and the number of fingers used (1-3). The subjects briefly practiced the sequence conditions before scanning.

Their results suggested a network of brain areas common to both the aspects of sequence structure. They observed common areas involve possibly in visual processing in the extrastriate cortex [left inferior occipital gyrus, Brodmann area 18, Talairach coordinate: (-34,-88,-1) and the right superior occipital gyrus, Brodmann area 19, Talairach coordinate: (35,-74,29)] and for preparation of sensory aspects of the movement in the rostral inferior parietal [left supramarginal gyrus, Brodmann area 40, Talairach coordinate: (-45,-3,32)] and the ventral premotor cortex [Brodmann area 6, Talairach coordinate: (-45,-3,32)]. By varying the number of fingers used in sequence execution, they found activations in the cerebellum [left superior anterior lobule, Talairach coordinate: (-26,-41,-19)] and the superior parietal cortex [right rostral lobule, Brodmann area 7, Talairach coordinate: (26,-41,51)], which implicated their involvement in sensorimotor and kinematic representations of the movement respectively. These two areas i.e., the cerebellum and the superior parietal cortex were also positively correlated with the number of fingers used. Changing the number of finger transitions activated the inferior parietal cortex [left angular gyrus, Brodmann area 39, Talairach coordinate: (-49,-60,33); bilateral supramarginal gyrus, Brodmann area 40, Talairach coordinates: (-56,-42,36) & (50,-35,53)] and the dorsal premotor cortex [Brodmann area 6, Talairach coordinates of activations: (-25,-9,49), (-19,18,58) & (-43,3,47)]. They also demonstrated that the dorsal premotor cortex positively correlated with the increase in the number of finger transitions. The correlated activity in

the dorsal premotor with the finger transitions (abstract structure) could be due to its role in the *retrieval or preparation of abstract action plans*. This paper concluded with a suggestion that the surface and the abstract/sequence-specific structure of sequential movements is subserved by distinct distributed systems.

Boecker et al. (2002)

In a PET study, Boecker et al. (2002) investigated complexity effects during mental imagery of movement sequences. Five different sequence conditions ("2,3,4,5"; "2,2,3,4,5"; "2,2,3,4,4,5"; "2,2,3,4,4,3,5"; "2,2,3,4,4,3,5,3") of increasing complexity (i.e., increasing the sequence length, single-finger repetitions and rehearsals) were tested on 6 healthy right-handed human subjects in a PET scanner. The paradigm used in the study is similar to that of their earlier investigation (Boecker et al., 1998). The mental imagery is defined as a state of *mental rehearsal of motor act* (Crammond, 1997). Their 12-run PET experiment consisted of five different activation conditions (two PET scans per condition) and two resting scans, arranged in the form of a square design. The activation condition is defined as the continuous mental rehearsal of a specified, *previously overlearned* key-press sequence. 1Hz sounds generated by PC were used to trigger the individual imagined finger movements. The sequence conditions were similar to that of Boecker et al. (1998) and they also took care that subjects did not mentally assign any numerical value to the individual finger movements. As the aim of this investigation was to probe complexity effects during mental rehearsal rather than execution of finger movements, they instructed subjects to quickly imagine one of the five activation conditions without actually making the movements of the hand or the arm. Subjects imagined each of the five sequence conditions which required all four digits.

They observed activations in the left sensorimotor cortex [Brodmann area 4/3, Talairach coordinate: (-48,-22,58)], the left inferior parietal cortex [Brodmann area 40, Talairach coordinate: (-44,-40,52)], the bilateral dorsal premotor cortex [Brodmann area 6, Talairach coordinates: (-18,-4,54) & (24,0,66)], the left caudal supplementary motor area [Brodmann area, 6, Talairach coordinate: (-2,-4,62)], the bilateral ventral premotor [Brodmann area, 6, Talairach coordinates: (64,4,26) & (-64,6,26)], the right primary motor cortex [Brodmann area 4, Talairach coordinate: (32,-36,52)], the left superior parietal cortex [Brodmann

area 7, Talairach coordinate: (-18,-58,64)], the left putamen [Talairach coordinate: (-20,12,4)] and the right cerebellum [Talairach coordinate: (26,-52,-12)] found in association with the mental rehearsal of movement sequences in comparison with the rest condition. Brain activation positively correlated with the sequence complexity in the left dorsal premotor cortex [Brodmann area 6, Talairach coordinate: (-22,6,50)], the right superior parietal cortex [Brodmann area 7, Talairach coordinate: (26,-68,56)], the right cerebellar vermis [Talairach coordinate: (8,-82,-16)], the left superior parietal cortex [Brodmann area 7, Talairach coordinate: (-16,-78,46)] and the right dorsal premotor cortex [Brodmann area 6, Talairach coordinate: (28,0,46)]. Their main conclusion of the neuroimaging results of varying sequence complexity was that the task-related changes in the parieto-premotor-cerebellar structures indicated their involvement in sequence control.

Hamzei et al. (2002)

In an fMRI study, Hamzei et al. (2002) investigated the differences in neural correlates in visuo-motor control with increasing task complexity. 12 Right-handed human subjects performed their signature under different degrees of visual control in four types of condition in the fMRI scanner. These four tasks differed in their degree of visual control: (i) Internally generated movement, (ii) Internally generated movement with eyes open, (iii) tracing the line of the projected signature forwards and (iv) tracing the line of the projected signature backwards. The main finding of their study was that there is a gradual transition of visuo-motor control with increase in complexity within a distributed parieto-frontal network and also the strength of the activation shifts between different structures depending on the complexity of the visual task.

The activation transits from the superior parietal lobule during visually guided movements to the inferior parietal lobule during internally generated movements with closed eyes. Another observation of this study was that the activation of the rostral cingulate cortex area, the pre-supplementary motor area and the proper supplementary motor area during internally generated movements. Visually guided movements activated the dorsal premotor. These results suggest differential role for the medial and the lateral premotor areas.

Janata and Grafton (2003)

Recently, Janata and Grafton (2003) reviewed various neuroimaging studies related to explicit sequence learning and temporal production. They targeted their review to explain *perception and action cycle* problem pertaining to the field of *Music* (how complex musical sequences are represented and produced). The authors pointed out that understanding the neural basis of sequencing behaviour in music can be achieved through three cognitive processes namely: timing, attention and sequence learning. As their review mainly targeted as a case study of music, they reviewed earlier studies related to the increase in temporal and ordinal complexity. The temporal complexity refers to the number of different durations that are perceived or produced during a task. The ordinal complexity refers to the overall number of elements in the sequence, represented by different spatial locations, that are to be learned and produced, and/or the number of effectors involved in producing a sequence. The sequence with the lowest temporal and ordinal complexity is produced with a single effector, and the timing between elements of sequence are constant throughout.

Their meta-analysis based on a review of 34 neuroimaging studies revealed the following relevant observations to our study. The sensorimotor cortex, the supplementary motor area, the cerebellum and the premotor cortex seem to be involved in a wide range of temporal and ordinal complexity studies. They also showed that the involvement of the cerebellum (CB) and the premotor cortex (PM) is similar across many studies and is possibly related to their involvement in higher levels of complexity. The activations of the sensorimotor cortex and the supplementary motor area showed less complexity related activations compared to CB and PM. They also reported that the activations found in the pre-supplementary motor area, the superior parietal lobule, the occipital cortex, the superior temporal gyrus, the intraparietal sulcus, the thalamus, the inferior parietal lobule, the ventrolateral prefrontal cortex, the basal ganglia, the insula and the anterior cingulate might be related to various complexity patterns (patterns across levels of ordinal and temporal complexity).

Hummel et al. (2003)

Hummel et al. (2003) investigated the effects of complexity on ipsilateral cortical

activation on 15 healthy right-handed subjects using the Electroencephalogram (EEG). Their main finding is the activation increase in ipsilateral sensorimotor areas during complex motor behaviour.

The motor sequences in this paper consisted of 16 consecutive finger movements using four fingers of the right-hand (2=index finger, 3=middle finger, 4=ring finger and 5=little finger) on electronic key-board, the subjects performed three different types of motor sequences (i) Simple: repetitive key-presses of same finger (e.g., 2-2-2-2-2-2-2-2-2-2-2-2-2-2-2-2), (ii) Scale: scale like key-presses in consecutive order arranged as either up or down using 4 fingers (e.g., 2-5-4-3-2-5-4-3-2-5-4-3-2-5-4-3) & Complex: complex non-consecutive order using all the four fingers (e.g., 5-3-2-4-3-4-2-5-4-4-2-3-5-2-4-3). The sequences of *complex* type are randomly generated by a computer algorithm. Subjects practiced one set of sequences on the first day and undergone experimental session on the subsequent day. During *Day 1* subjects attained good performance levels and the sequences which are practiced were labelled as 'MEM' (memorized) condition. During *Day 2* subjects had to perform pre-learned sequences (called as 'MEM' condition) as well as the randomly displayed novel sequences (called as 'NOV condition) of matched complexity (Simple, Scale or Complex). In the 'NOV condition subjects had to perform corresponding to a numbered cue (finger numbers indicated above) displayed on the visual display. The 'NOV condition was designed such that no memory load was involved.

The conclusion of this study is that they found similar dynamics (simple to scale to complex) of cortical activation patterns (positive correlation) across movement sequences during 'MEM' and 'NOV conditions. They interpreted that the increasing ipsilateral activation might primarily reflect processing of increasingly difficult transitions between movements and not the motor memory load.

Haaland et al. (2004)

Stephen Rao and colleagues (Haaland et al., 2004), in a recent study, investigated the effects of complexity during sequential finger movements. Their main focus of the investigation was to demonstrate the left hemisphere dominance during heterogeneous (complex) sequential movements by either the right or the left hand. The concept of complexity used by their earlier study (Harrington et al., 2000)

inspired them to conduct this focussed study. In this investigation complexity is defined in terms of heterogeneous sequences. Simple sequences are repetitive sequences with one of the fingers. Subjects performed key-presses with the digits of their right or left hand in response to computer generated visual stimuli. The indexing scheme used for the fingers, the usage of fingers and the placement of fingers on the horizontal key-pad are the same as in the previous study (Harrington et al., 2000). But in this experiment the key-pad was arranged on the right or the left thigh to perform sequences with their right or left hands. 14 healthy right-handed human subjects performed finger key-presses involving simple or complex sequences with their right or left hand. In this fMRI study they used novel sequences that were not highly practiced or predictable and were cued with a visual stimulus. Unlike most of the earlier studies, in the current study subjects practiced briefly before performing the task in the fMRI scanner. Only two of the eight sequence conditions (simple sequence condition of type: '11111' or '22222' or '33333'; complex sequence condition of type: '12131' or '23231' or '32321') that were used in the current study as compared to the earlier study (Harrington et al., 2000). Additionally, subjects performed these conditions with the digits of both their right and left hands. In a block subjects performed 40 trials randomly presented and a trial consisted of performance of one sequence.

They performed fMRI analysis leading to two types of inferences, 1) activation foci for comparison of right and left hand performance collapsed over sequence complexity (i.e., to study hemispheric dominance) and 2) activation foci for comparison of simple and complex movement sequences collapsed over movement hand (i.e., comparison between simple and complex sequential movements). This kind of analysis methodology enabled two types of comparisons i.e., left versus right dominance and simple versus complex tasks. Their results showed that the overall MR signal was larger in the left than the right sensorimotor cortex, the extent of this asymmetry did not change with the hand or complexity level, the parietal and the premotor cortices activated more in the left than the right hemisphere when complex sequences were compared with simple sequences. The statistical comparisons of activation of complex versus simple conditions (complex > simple) irrespective of the hand used showed a network of brain areas. The left dorsal premotor [Brodmann area 6, Talairach coordinate: (-24,-7,47)], the bilateral superior parietal cortex [Brodmann area 7, Talairach coordinates: (-26,-56,43) & (26,-64,39)], the left posterior cingulate

[Brodmann area 23, Talairach coordinate: (-3,-52,8)], the right extrastriate cortex [Brodmann area 18/19, Talairach coordinate: (33,-80,-2)], the left thalamus [Pulvinar/ventral nucleus, Talairach coordinate: (-13,-24,7)], the bilateral anterior cerebellum [Vermis, coordinates as per Schmahmann et al. (2000): (-9,-57,-27) & (9,-59,-21)] and the right lateral anterior cerebellum [Schmahmann coordinate (Schmahmann et al., 2000): (17,-39,-23)] were activated when complex sequence conditions were compared with simple conditions. Their interpretation was that the left dorsal premotor cortex and the parietal areas might be engaged when advanced planning is required.

In the following an interesting study related to the investigation of implicit and explicit sequence learning in a single experimental paradigm will be reviewed. The reason for reviewing this study is that it has relevance to our current investigation in demarcating the learning stages based on subject specific behaviour.

Honda et al. (1998)

Using PET on 21 healthy right-handed human subjects, Honda et al. (1998) tested the dynamics of brain activations during implicit, explicit and post-learning phases of sequence learning. The objective of this study was to examine the brain regions correlated with implicit and explicit phases of motor sequence learning and their dynamics using a modified SRT task. The dynamics were examined by using a parametric analysis on PET images where brain activity was correlated with the behavioural task.

A variation of the SRT task paradigm was adapted in their investigation. On a four button key-pad subjects performed the task while supine in PET scanner bed while the key-pad was placed near their right-hand. Visual stimuli consisting of a number (1,2, 3 or 4) was presented on a screen in front of the subject. The subjects were instructed to press key-pad buttons as quickly and accurately as possible with a different finger in response to each number in the visual display (1=index finger, 2=middle finger, 3=ring finger and 4=little finger). The feedback information regarding the correctness of key-presses was given. When subjects pressed correct response then the number in the visual stimulus disappeared. Otherwise i.e., when the key-press was incorrect visual stimulus remained on the display until the presentation of the next stimulus and subjects were instructed not to press during that period. Subjects performed three conditions,

namely, random, sequence and visual control in a block design. In the random condition, subjects responded to 100 randomly generated numbers on the visual display. In the sequence condition, all the subjects practiced the same test sequence (4-3-2-1-3-4-2-3-1-2) and after each block subjects were examined as to whether they observed anything in the task. In the visual control condition the 100 numbers were displayed in a random order but no key-press responses were required. The mean reaction time and correctness of recall of sequence were recorded for each block, which formed the behavioural parameters. Based on the performance of each subject, the blocks in the total experiment were divided into three learning phases namely implicit learning, explicit learning and post-learning. The demarcations into learning phases was done as follows, (i) implicit learning phase, blocks before subjects reported awareness of the sequence; (ii) the explicit learning phase, defined by the blocks between explicit awareness of sequence to the blocks where subjects reported the sequence correctly; (iii) post-learning phase, defined by the blocks after subjects reported the sequence correctly to the last block of the experiment. The elegance of this paradigm is that they studied brain responses correlated to behaviour in the three phases of learning with an appropriate behaviour (measure such as, reaction time for implicit learning phase).

During the implicit learning, they observed negative correlation in the contralateral primary sensorimotor area [MNI coordinate: (-32,-34,52)] and positive correlation in the left anterior insula [MNI coordinate: (-30,18,4)] with reaction time.

In the explicit learning phase, they observed that the correct recall positively correlated with the activation in the bilateral posterior parietal cortex [Brodmann area 40, MNI coordinates: (26,-70,32) & (-30,-64,40)], the precunes [Brodmann area 7, MNI coordinate: (-4,-74,36)], the bilateral dorsal premotor [Brodmann area 6, MNI coordinates: (24,4,52) & (-24,-2,48)], the left anterior part of supplementary motor area [Brodmann area 6, MNI coordinate: (-12,2,48)], the left thalamus [MNI coordinate: (-10,-18,0)] and the right dorsolateral prefrontal cortex [Brodmann area 46, MNI coordinate: (36,42,16)]. During this stage, the reaction time was observed to be significantly negatively correlated with the fronto-parietal network i.e., the supplementary motor area [Brodmann area 6, MNI coordinate: (-10,4,52)], the right dorsal premotor cortex [Brodmann area 6, MNI coordinate: (28,4,48)] and the right posterior parietal cortex [Brodmann area 40, MNI co-

ordinate: (26,-70,32)]. During the post-learning phase reaction time negatively correlated with the ipsilateral primary sensorimotor area [Brodmann area 4/3, MNI coordinate: (30,-20,48)] and the posterior part of supplementary motor area [Brodmann area 6, MNI coordinate: (0,-14,44)]. They concluded that different brain areas are dynamically involved in implicit and explicit sequence learning.

2.1.2 Differences between various complexity paradigms reviewed and the paradigm used in this thesis

The earlier neuroimaging studies of sequence complexity varied sequence length linearly (Sadato et al., 1996; Catalan et al., 1998, 1999; Boecker et al., 1998, 2002) or compared between different types of sequence i.e., contrasting between repeated and heterogeneous sequence finger movements (Wexler et al., 1997; Dasonville et al., 1998; Gordon et al., 1998; Harrington et al., 2000; Hummel et al., 2003; Haaland et al., 2004).

The paradigm used in our study is the $m \times n$ sequence complexity paradigm. In the $m \times n$ paradigm the correct order of pressing m keys (set) successively for n times (hyperset) is learned by trial-and-error process. Our complexity paradigm differs methodologically from the earlier investigations of sequence complexity and we increased the complexity of sequence being acquired along two dimensions. We hypothesized that in the complex condition corresponding to increased set-length (i.e., in the 4x6 task), the optimization process may be limited to the items within the *set* and may not span across *sets*. In contrast, we expect that in the complex condition corresponding to increased hyperset-length (i.e., in the 2x12 task), sequence information may possibly be organized in a hierarchical fashion. Though our experimental paradigm does not contain many points on the complexity space but it is an interesting demonstration to show two types of conditions (2x12 versus 2x6 and 4x6 versus 2x6) in a single experimental design. Previous studies could design more points in the complexity scale because they used well learnt sequences whereas our task involved sequence learning in the fMRI scanner.

Most of the earlier studies investigating motor sequence complexity used over-learned sequences (Sadato et al., 1996; Catalan et al., 1998, 1999; Boecker et al., 1998, 2002; Hummel et al., 2003) or briefly practiced sequences (Harrington et al., 2000; Haaland et al., 2004). Our $m \times n$ sequence complexity paradigm differs from

these studies. A novel sequence that was not seen earlier and not practiced earlier was given to each subject for learning in the course of the experiment. Like in Honda et al. (1998), we also marked the learning stages based on the behavioural data. In our $m \times n$ sequence complexity paradigm we divided scanning sessions of every subject into learning stages i.e., the early and the consolidation stage. Subject-specific demarcation of stages in sequence learning is also an important contribution of our study. The earlier studies did not address learning stages in sequential skill learning. Unfortunately because of time slot limitations in fMRI scanner, we could not scan for more than 4 scanning sessions, that is why we could not probe the so-called 'late' stage of learning of the complex sequence conditions.

The earlier studies of complexity used either auditory paced movements (Sadato et al., 1996; Catalan et al., 1998, 1999; Boecker et al., 1998, 2002) or visually triggered movements (Harrington et al., 2000; Hummel et al., 2003; Haaland et al., 2004). The motor movements performed are either finger opposition type (Sadato et al., 1996; Catalan et al., 1998, 1999) or key-press performance tasks (Boecker et al., 1998; Harrington et al., 2000; Boecker et al., 2002; Hummel et al., 2003; Haaland et al., 2004). In the $m \times n$ complexity paradigm, we used a 3x3 grid display for visual stimulus and a 3x3 key-pad to perform motor (finger) movements. In our tasks, the sequences are learned by their spatial grid positions and not explicitly numbered.

The sequences learned in our $r \times n$ complexity paradigm are not performed solely by visual guidance but subjects had to discover the order of the sequence by a trial-and-error process. The other interesting point to mention in our paradigm is that subjects acquired the sequences progressively.

2.1.3 Summary of our Experimental Paradigm

The $r \times n$ visuo-motor sequence learning paradigm we used for probing complexity along two dimensions is the first of its kind designed to demonstrate the effects of complexity in trial-and-error learning. The experimental design allowed us to address the stages of sequential skill learning. Increase of complexity along two dimensions is also an important feature of our study. From the point of view of fMRI analysis methodology, our study is novel. We have modelled the effects of two dimensions of complexity separately (2x12 versus 2x6 and 4x6 versus 2x6

in two design matrices). The usage of response times as explanatory variable to probe into the effects of increase in set size (set completion time is used to model the short-range processes) and increase in hyperset size (hyperset completion time is used to model the long-range processes) is also a novel procedure. The current study is a whole-brain study, so we could image the whole-brain responses, i.e., Blood Oxygen Level Dependant signals (BOLD) related to the task conditions over the entire brain.

Chapter 3

Introduction to fMRI: experimental design and analysis

In this chapter an introduction to functional imaging and the issues related to experimental design will be presented. This chapter also discusses various analysis methods and approaches for analyzing functional magnetic resonance images (fMRI).

3.1 Introduction to fMRI

The functional Magnetic Resonance Imaging (fMRI) is a powerful imaging tool that can be used to perform brain activation studies non-invasively *in vivo* while subjects are engaged in meaningful behavioural tasks. The resulting activation of the brain indirectly depends on blood-oxygen-level-dependent (BOLD) signal (Ogawa et al., 1990). Before the emergence of fMRI, radioisotope based techniques, such as positron emission tomography (PET) which measures regional cerebral blood flow (rCBF), were widely used for mapping the brain function. However, these techniques are invasive and have a low spatial and temporal resolution. Electroencephalography (EEG) which records the electrical activity of nerve cells in the human brain by measuring electrical potential on the scalp is also another widely used experimental technique in neuroscience. Magnetoencephalography (MEG) is another non-invasive technique which is becoming popular now-a-days. MEG measures the weak magnetic fields generated above the scalp by current flow in the brain. This technique directly measures the neuronal activity. EEG and MEG techniques though they probe brain activity at very

finer temporal resolutions, their spatial resolutions are very poor. The fMRI provides a non-invasive method to access indirectly neuronal activity in the brain, by measuring the haemodynamic metabolic signal i.e., blood-oxygen-level-dependant (BOLD) signal. Effects of blood oxygen on the apparent transverse relaxation time (T_2^*) were reported by Ogawa and colleagues (Ogawa et al., 1992). Increased neuronal activity in a brain area leads to an increase in localized cerebral blood flow, blood volume, and blood oxygenation. The BOLD fMRI techniques are designed to measure primarily, changes in the inhomogeneity of the magnetic field that result from changes in blood oxygenation. Deoxyhaemoglobin is paramagnetic and introduces an inhomogeneity into the nearby magnetic field, while oxyhaemoglobin is weakly diamagnetic and has little effect. Hence, a decrease in deoxyhaemoglobin would cause an increase in image intensity [refer to Hornak (2002) for more details of fMRI Physics]. fMRI is well suited to measuring the dynamic changes in brain activity induced by tasks that involve learning (such as tasks investigated in this thesis) as it provides a reasonable spatial and temporal resolution compared to other neuroimaging techniques such as positron emission tomography [refer to Cohen and Bookheimer (1994); Volkow et al. (1997)]. After more than ten years of fMRI research, there is still much to learn about how neuronal activity, haemodynamics and fMRI signals are interrelated (Heeger and Ress, 2002). A recent review of Ugurbil et al. (2003) suggested the possibility of obtaining spatially accurate and quantitative data on brain function from magnetic resonance technologies. Recently Chem and Schneider (2003); Culham (2005) pointed out that there is a growing scientific and clinical community using fMRI and the neuroimaging publications continue to increase exponentially.

3.2 Issues related to Experimental design

Developing successful fMRI experiments requires careful attention to experimental design, data acquisition techniques, and data analysis (Chem and Schneider, 2003). The experimental design is at the heart of any cognitive neuroscience investigation. In this chapter we present a brief review of various issues related to the experimental design [for more details refer to: Chem and Schneider (2003); Culham (2005)].

3.2.1 Block and Event-related Designs

The experimental designs are broadly classified into two classes i.e., blocked (epoch) designs and event-related designs. The properties of haemodynamic response function (i.e., the transfer function mapping neuronal activity onto BOLD signal) play an important role in the design of experiments (Friston, 1998). In a recent investigation by Friston's group (Mechelli et al., 2008), comparison between these two design methodologies was presented taking a case study. Though event-related designs are efficient in capturing transient behaviours, the blocked designs give good signal to noise ratio (SNR) and are very useful in group studies.

The *blocked or epoch designs* are commonly used in neuroimaging literature. Typically the task condition in the blocked designs is performed for an extended period that is more than the haemodynamic response (HR) time. Some of the advantages of blocked designs are that they normally give reasonably significant areas of activation and they are comparatively easy to analyze. On the other hand, the *event-related designs* (sometimes called trial-based or single-trial designs) aim to characterize transient changes in fMRI signal that emanate as the consequence of individual trials either separated in time or spaced closely together in time (Culham, 2005). Some of the advantages of using event-related designs are: (1) allow random intermixing of the trials, (2) they are useful in characterizing the temporal dynamics of brain activation, (3) allow separation of sub-processes within multi-componential trials, (4) may facilitate separation of HR, signals from art if actual events etc. Thus the blocked designs are special case of event-related designs and each has its own advantages and disadvantages.

Selection of experimental design should be based on the particular research question of interest. For example, in this thesis we are interested in the acquisition of sequential motor skill while subjects repeatedly practiced a sequence. The usage of epoch based design in our experimental paradigms is meaningful because our tasks require subjects to perform continuous motor actions and there are no events to be really probed. On the other hand, the event-related designs could be used, for example, when stimulus-action mapping at a particular event is to be investigated.

3.2.2 General Taxonomy of Experimental Design

In the previous section we briefly reviewed types of designs suitable for fMRI experiments. In this section we briefly review taxonomy of experimental designs useful for the cognitive psychology experiments (i.e., behavioural paradigms). Overall, designs can be classified into three types i.e., categorical, factorial or parametric [refer to, Friston (1997)].

The categorical designs assume that the cognitive processes can be dissected into sub-cognitive processes. That is one can remove and add different cognitive processes by the assumption of pure insertion. The categorical designs are further divided into subtraction type or conjunction type. Cognitive subtraction designs are used to test the hypothesis pertaining to activation in one task as compared to that in another task considering the fact that the neural structures supporting cognitive and behavioural processes combine in a simple additive manner. Whereas in the cognitive conjunctions type designs, several hypotheses are tested, asking whether all the activations in a series of task pairs, are jointly significant.

Factorial designs involve combining two or more factors within a task or tasks and looking at the interaction between the different factors, or the effect of one factor on the response to other factor. The simplest example of factorial design is that one can probe into the interaction between motor activation and time that can be interpreted in terms of plasticity and adaptation [for example, Friston et al. (1992)]. Factorial designs are mainly used where the assessment of direct interaction between the task factors is of interest. Thus in factorial designs one can mix two effects in a single design. The effectors could be either categorical or parametric type.

In parametric designs, rather than assuming that the cognitive processes are composed of different cognitive components, they are considered as belonging to different psychological dimensions. The main difference in parametric designs is that the sensorimotor attributes or the cognitive components of interest are treated as dimensions as opposed to categories. The systematic changes in the brain responses according to some performance attributes of task can be investigated in parametric designs. In parametric designs one can also look at the linear and non-linear types of relations.

Thus, one can use factorial approach in a parametric context, i.e. to examine the brain responses to increasing frequency of stimulus presentation in different contexts and look for a differential sensitivity to increasing presentation rate.

3.3 Analysis of Imaging Data

Data analysis mainly consists of motion correction, coregistration, normalization to a template (if required), smoothing, estimation of parameters of a statistical model (statistical modelling), and statistical inference to determine significant areas of brain activation. These steps could be implemented using many softwares available such as AFNI, MEDx, FIASCO, FSL, STIMULATE. In this thesis we have used one such software package called SPM99. SPM99 is designed to analyze functional neuroimaging data. Its primary goal is to produce a statistically meaningful comparison between groups of images. The fMRI images are preprocessed and a General Linear Model (Friston et al., 1994, 1995b,c) would be setup to investigate the candidate brain regions that are activated preferentially by the sequence tasks. This section outlines the analysis procedure used for image analysis (see Figure. 3.1). A step-by-step guide to using SPM99 is given in Appendix D.

The major steps of data analysis include:

- Data Acquisition
- Preprocessing
- Model Setup and Estimation
- Statistical inference (Results assessment)

SPM stands for *Statistical Parametric Mapping*, which is the main output of the software. Statistical Parametric Mapping refers to the construction and assessment, of spatially extended statistical process used to test hypotheses about [neuro] imaging data obtained from PET (Positron Emission Tomography) and fMRI. SPM99 separately examines every voxel (3-dimensional pixel) location across all images, and computes a parametric map containing a parameterized value at each voxel. The parametric map is a form of data, reduction, condensing

information from a number of individual scans into a single image volume that can be more easily viewed and interpreted. The parameterized value is generally some form of Student's t-test estimating the likelihood that a comparison of two image groups matches a given model that explains their possible differences.

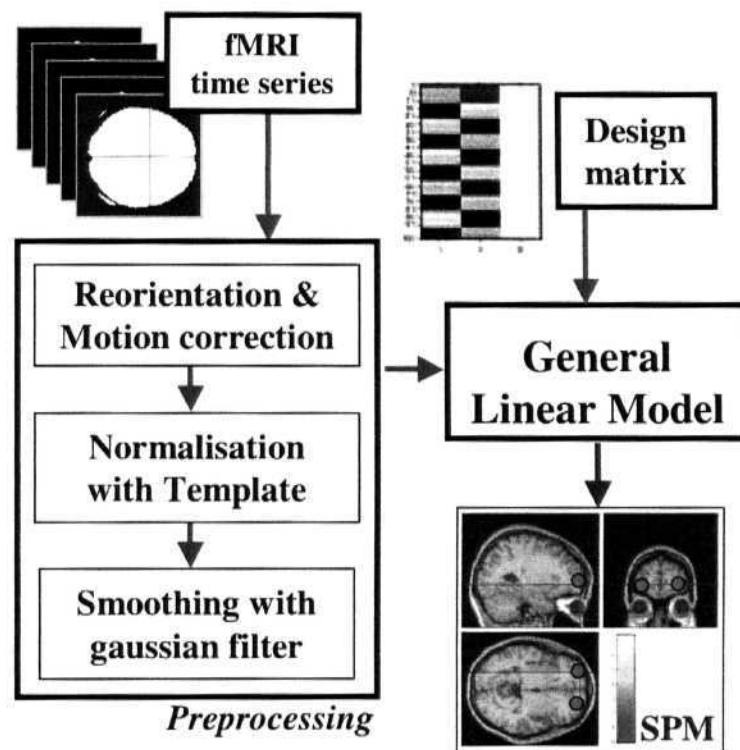


Figure 3.1: Data Processing Steps in SPM

3.3.1 Data Acquisition

Issues of data acquisition are included here because it is crucial that the data are acquired in a way that the experimental hypothesis can be addressed. This includes the experimental design as well as technical questions of modality, acquisition parameters, and reconstruction.

An fMRI experiment to test a given psychological hypothesis must be designed within the constraints of the temporal characteristics of the fMRI BOLD signal and of the various confounding effects to which fMRI signal is susceptible. Typically, two designs are possible 1) Epoch-based design using Blocks of stimulation (boxcar designs with alternating activation and rest) and 2) Event-related design, where data may be recorded to monitor the BOLD response following a marked (pre-determined) event such as a single stimulus or task.

The most important consideration is the actual design of the experiment. In conducting a hypothesis-based experiment, we wish to be able to attribute any observed effects to experimentally manipulated conditions. This can be guaranteed only if conditions are randomly allocated to a presentation order for each subject in a sensible manner. Further, this randomization should be appropriately balanced, both across and within subjects. With such random allocation of conditions, any unexpected effects are randomly scattered between the conditions, and therefore do not affect the designed effects.

The next step after specifying the hypothesis, and designing the experiment is to acquire the data. Most fMRI studies use a, box-car design with alternating epochs of rest and a single activation task of about thirty seconds.

SPM uses the simple header and flat binary image file format of ANALYZE-7. Images need to be converted into 'Analyze' format, by using other utilities such as MRIcro (Rorden, 2004).

3.3.2 Preprocessing

This stage includes several steps, all of which are aimed at massaging the data so that it is suitable to be statistically analyzed by SPM99. In our experiment, the scanner was operated continuously for a session. Two additional scans acquired at the beginning of each session were discarded to account for the transients in the magnetic field of the scanner. Further, one scan at the beginning of every block that corresponded to the block instruction was also discarded from analysis.

Realignment: In functional imaging, the signal changes corresponding to any haemodynamic response can be small compared to the signal changes that can result from subject motion. So, prior to performing the statistical tests, it is

important that the images are as closely aligned as possible. Hence, the functional images were first reoriented to set a common origin for all the images to match with the line joining the anterior and posterior commissures (AC-PC plane). Realignment algorithm is then applied to all the images to account for any head movement during scanning. If not corrected, the head movement gives rise to artifact in the signal intensity variations. A *rigid body transformation* with 6 parameters (3 translations and 3 rotations about orthogonal axes) is computed to minimize the sum of squared differences between each scan to the first scan in the series. Applying this transformation (rigid body transformation) is performed by resampling the data using *sinc* or *trilinear* or *nearest neighbour interpolation* methods.

Coregistration: Coregistration enables the functional images to be overlaid onto the anatomical (structural) image of the subject. This step finds the transformation that maps the anatomical image into the space of the functional images. A further use of registration is that a more precise spatial normalization can be achieved. The first functional image is co-registered to the anatomical image in order to ensure correct anatomical localization of the blood-oxygen-level-dependent (BOLD) activity. This process is not based on minimizing mean squared difference between images but follows a three step process: simultaneous affine registrations (12 parameter affine transformations are used) between each image and template images of same modality, partitioning of images into grey and white matter (*mixture model* cluster analysis used to classify MR image as grey matter, white matter & Cerebrospinal Fluid), and final simultaneous registration of image partitions (rigid body transformation is used for registering grey and white matter partitions).

Normalization: Images need to be normalized to account for variation in brain sizes of different subjects. Normalization would also help standardization of reporting the co-ordinates of the brain space across different studies. The anatomical image was normalized (Friston et al., 1995a) to a template image and the resulting parameters were used for normalizing all the functional images. A 12 parameter affine transformation of image partitions is used in this spatial normalization process (this process is similar to that of the transformation used in coregistration but, also includes zooms and shears). A global nonlinear warping

technique is applied to fit the overall shape and size between the template image and source image.

Smoothing: The normalized functional images are spatially smoothed with a gaussian filter using a suitable full width half maximum (FWHM of 6mm in our case i.e., double the voxel size). The smoothing process not only increases the signal to noise ratio (SNR), but also validates the underlying gaussian assumption for the BOLD activity that is in turn used in the statistical inference step.

3.3.3 Statistics: Model Setup and Estimation

Statistical analysis is performed on the preprocessed image data for each experiment using a general linear model. The general linear model (GLM) is used to specify the covariates of interest, such as the experimental design and the nature of hypothesis testing to be implemented in the form of a design matrix.

The general linear model allows to phrase an analysis of variance with condition or group effects in terms of a multiple regression (Strange, 2000). The GLM is simply an equation that relates what one observes, to what one expected to see, by expressing the observations (response variable Y) as a linear combination of expected components (or explanatory variables x) and some residual error (ϵ), thereby equivalent to linear regression.

$$Y_j = x_{j1}\beta_1 + \dots + x_{jk}\beta_k + \dots + x_{jL}\beta_L + \epsilon_j \quad (3.1)$$

The β_k are unknown parameters to be estimated, corresponding to each of the L explanatory variables (x_{jk}) for the j^{th} observation of Y . This can be expressed in the matrix form as

$$Y = X\beta + \epsilon \quad (3.2)$$

Here, X is called the design matrix that contains the explanatory variables and β is the parameter estimate. Each column in the design matrix corresponds to some effect that one has built into the experiment or effects that may confound the results. The rows of the matrix correspond to the number of observations.

Commonly used parametric models, such as linear regression, t-tests and analysis of variance (ANOVA) are special cases of the general linear model.

Subjects continually adapt to a particular task and both neuronal and cognitive adaptations take place. It can thus be argued that no observation is truly a replicate of the previous one. To model these adaptations, we may partition the overall model into learning stages, and/or include regressors or explanatory variable (for example, behavioural parameters such as success rate and response time) in our experiment that represent time effects.

3.3.4 Statistical Inference

The GLM approach to neuroimaging has been used successfully during the past 10 years. For majority of behavioural studies, the "box-car" design is adopted where the activity of the brain areas correlated with the test blocks is obtained by comparing the average activation in test blocks to that of the control blocks. This approach is called the *cognitive subtraction* approach [refer to Friston (1997) for review of fMRI experimental design]. Brain activity specific to the task is obtained by specifying **linear contrasts**. The activations thus obtained can be overlaid or rendered onto the high-resolution anatomical image of the subject in order to accurately locate the neural activity.

A contrast can be used to compare different conditions. The conditions of interest are given a positive value, such as 1, and conditions that are to be subtracted from these conditions of interest take on a negative value, such as -1. One rule for making a contrast that is applied to conditions is that the sum of all elements of the contrast vector must always be equal to zero.

There are many ways to view the results, both from within SPM99 as well as using other programs. The two major issues are (i) figuring out which voxels are significantly active, and (ii) determining the precise anatomic location of a purported activation.

3.3.5 Random Effects Analysis

A *Random-Effects* (R.FX) analysis is also referred to as a "Mixed Effects" analysis, since it considers both *within*- and *between-subject variance*. In SPM this is

realized through a "second level" analysis. A "first level" or *Fixed Effects* (FFX) analysis is the standard way to set up an analysis design using the GLM explained above. A first level design uses within-subject variance, thus providing for inferences that generalize to the subjects studied. The Fixed effects model (FFX) can be effectively used to find the typical activation of a group of subjects or for comparing between subject groups. This approach is appropriate for qualitative assessment of the results. For example, if among eight subjects, three of them show significant activation then the average activation will also show significant effect. However in order to make broader inferences or conclusions about the general population from which the subjects were drawn and to make quantitative inferences, the **Random Effects** analysis approach should be used. The problem with RFX (Holmes and Friston, 1998) analysis is that it requires a large sample. For a discussion on RFX Analysis and how many subjects constitute a study see Friston et al. (1999). A Random Effects analysis was performed within SPM by the second level of analysis in which contrast images from the first level are analyzed using student's t-test or ANOVA-like methods.

3.4 Characterizing Learning Related Changes

In this section we review some methods and approaches for characterizing learning related changes observed in fMRI data. In this section first we discuss possible methodology for characterizing learning induced changes in the data in the SPM framework. We also reviewed various approaches available for characterizing learning other than the SPM approach.

3.4.1 Using Statistical Parametric Map (SPM)

Partitioning the Model into Learning Stages

Strictly speaking, fixed effects method is not suitable for learning studies as it ignores the fact that the epochs are not replicated and that learning causes differential changes in the early as compared to the late epochs. A simple way to incorporate early versus late differences is to partition the overall average into two parts - one corresponding to the average of early epochs and the other corresponding to the late epochs. The comparison of these two averages gives us

the typical features of the early stages of learning and that of the late stages.

Time effects within a session (Parametric Modulation)

In the approach outlined thus far, we ignored any session specific improvements. These can be accounted by using the "parametric modulation" approach in SPM. Parametric modulation is a special case of the approach of using "user specified regressors" in SPM. Regressors are used to study session specific adaptation in brain activity, general effects of time on brain activity and Brain-Behaviour correlations effectively.

Random Effects Analysis (RFX)

All the above methods use fixed effects model where inter-session variance is ignored. Subjects continually adapt to a particular task and both neuronal and cognitive adaptations take place. It can thus be argued that no observation is truly a replicate of a previous one (Vazquez and Noll, 1998). An approach called random effects analysis (RFX) takes inter-session variance also into account and provides generalizability of results to populations and also to make quantitative inferences (Friston et al., 1999). Problems with RFX are that it requires large sample and is more complex to implement. All these methods offer different ways of adapting the basic SPM framework for studying learning related effects. As such these methods address the problem only partially, but acceptable as they conform to existing framework used in practice. In the next section, we point out alternative approaches.

3.4.2 Alternative approaches for characterizing learning induced changes

Statistical Time Series Approaches

The SPM framework has special limitations when used for studies that investigate learning and similarly for investigating pharmacological effects. Hence there is an immediate need to explore alternative methods that explicitly characterize the effects of time in fMRI data. One alternative is to augment the current methodology with a second-level analysis where statistical time series techniques are

applied on regions selected from the first-level ANOVA based analysis. Explicit modelling of time series can potentially reveal and enable the characterization of learning induced changes in the brain activity.

A series of 228 BOLD intensity values are obtained from the activated brain areas. These intensity values are extracted from the local maxima (of voxels) in the volume of interest as revealed by the SPM fixed effects analysis. We used the standard Auto Regressive Integrated Moving Average (ARIMA) statistical time series model (Box and Jenkins, 1976), as it is well known for uncovering hidden patterns in time series data.

Pammi et al. (2004b) conducted preliminary investigations on fMRI time series data obtained from one of our sequence learning experiments (Pammi et al., 2003a). The coefficients of ARIMA model from different brain regions revealed a pattern of periodicities in the control condition but dissimilar behaviour in the test condition. The time series data of the sequence learning (test condition) fitted optimally in an auto regressive (AR) model reflecting dependencies on previous history. The dependency could possibly be related to the progressive sequence learning accomplished by the subject. The data from the control condition fitted optimally in a moving average (MA) model revealing that there are no history-related dependencies. This is in accordance with the experimental design as there is no learning involved in the control condition. Further investigation needs to be carried out to tease out various components in the AR model related to sequence learning (test condition).

Modelling haemodynamic response function (HRF)

The other possible approach to characterize learning effects is to explicitly model and estimate the haemodynamic response function [for example, Svensen et al. (2000); Marrelec et al. (2002); Friston (2002a); Srikanth et al. (2003); Marrelec et al. (2004)]. The modelling of HRF is recently becoming popular among engineering community. HRF is the theoretical signal that BOLD fMRI would measure in response to a single, very short stimulus of unit intensity. The local change of BOLD is not immediate but usually has a delay of 2–6 seconds from the onset of the stimulus. This change¹ is observed to increase slowly and attains maximum and returns to the baseline. The signal obtained from the fMRI experiments generally consists of noise and BOLD response components. The noise

is due to physiological sources such as breathing, heartbeat and system sources like scanner and noise drift.

Estimation of the HRF is of great interest when analyzing fMRI data, since it can give a deep insight into the underlying dynamics of brain activation and relationship between activated areas. There are broadly two categories of techniques for HRF estimation - parametric approaches and non-parametric approaches. In parametric approach HRF is modelled by functions such as Gaussian, Gamma, Poisson etc. These functions give a parsimonious representation of the underlying HRF. With these models the problem simplifies to estimating the parameters of the above functions. In the non-parametric approach the HRF is modelled by an FIR filter. The coefficients of FIR filter are then estimated from the fMRI time series data.

Independent Component Analysis (ICA)

Another powerful alternative approach is to use model-free methods such as the Independent Component Analysis. ICA is a data-driven method and can potentially reveal the complex spatiotemporal dynamics of a task (Bell and Sejnowski, 1995, 1997). The ICA algorithm is similar to principal component analysis (PCA) in that it decomposes a data set into discrete components. PCA orients the first component in the direction of maximal variance in the data set with subsequent components oriented orthogonally. The ICA algorithm decomposes the data set using the principle of minimizing the mutual information between components. The resultant spatial maps in ICA are independent, but the corresponding time courses are not constrained to be independent. ICA may be better at identifying task-related signals in the brain, wherein the contribution of cognitive effects to the overall variance in functional imaging data is relatively small (Berns et al., 1999). It is particularly useful in paradigms in which the time course of the brain response is unknown. This is a powerful approach, because it allows one to design experiments in the absence of fixed effects, which are necessary for conventional ANOVA-type models.

3.4.3 Summary

In this section, we have presented four different approaches for studying the temporal dynamics of brain activity, especially for learning tasks. The first approach is the traditional analysis using linear methods such as Statistical Parametric Mapping. Fixed effects model together with conjunction analysis in SPM can potentially help in characterizing typical activation in subjects. Random Effects analysis can be used to generalize results to the population. *SPM framework is useful and popular currently* but has serious limitations for characterizing learning effects. The second approach is to use statistical time series methods at the second level on the results obtained from the first level fixed effects analysis.

The other two approaches are explicit modelling of HRF and ICA. Modelling HRF is also of interest because HRFs are increasingly suspected to vary from region to region, from task to task, and from subject to subject. ICA appears to be promising, as it does not make any assumptions about the brain response signals other than their statistical independence.

Learning is an important cognitive function and fMRI studies have not yet started investigating this phenomenon seriously. One possible reason is that there are still many interesting open questions related to the analysis methodology for studying learning induced changes in fMRI data,

Chapter 4

Experimental Methods

This chapter describes the task procedures for the complexity experimental paradigm, possible cognitive processes, methods for behavioural analysis, fMRI scanner parameters, statistical analysis of functional images, modelling the effects of complexity in our experiments and the types of fMRI analyses performed.

4.1 Experimental Subjects

Eighteen right-handed normal volunteers (15 males and 3 females; 21 to 28 years of age with a mean of 23.65 years) participated in this study. Subjects that participated in our study are from similar educational backgrounds. Each subject performed three experiments corresponding to the three sequence tasks (2x6, 2x12 and 4x6 tasks). The complex sequence learning tasks (2x12 and 4x6) were together in the same experimental slot. The order of experiments was counter-balanced across the subjects. Subjects practiced each task (test sequence for two sessions) before proceeding to scanning experiments to become familiar with task procedures and instructions.

Subjects were paid for their participation. Written informed consents were obtained from each subject before the study. The ethics committee of the Brain Activity Imaging Center (BAIC), Advanced Telecommunications Research Institute International (ATR), Kyoto, Japan approved the experimental protocol. A total of 54 fMRI and behavioural data sets were collected from the 18 human subjects. Data from one subject was not included in the analysis as significant improvements in Key-press Response Times were not observed in one of the ex-

perimental tasks.

4.2 Details of the Behavioural aspects of the Experiment

Subjects lay supine in the scanner and visual stimuli were projected on a mirror in front of the subject (as shown in the Figure 4.1). Subjects performed explicit sequence learning paradigm called the *mxn* task (Hikosaka et al., 1995; Bapi et al., 2000). A set of m squares was illuminated simultaneously in white colour on a 3x3 grid display against gray background. The grid measured 3.7 cm x 3.7 cm on the rear screen and the viewing angle was about 5°. Subjects learned by trial-and-error the correct order of pressing corresponding keys on a 3x3 keypad placed near their right hand (Figure 4.2). The 3x3 key-pad is so chosen to make perfect correspondence with the 3x3 visual grid display. In this visuo-motor sequence learning experimental paradigm, a white colour for the grid button is chosen for the elements of interest (i.e., key-press to be performed for the corresponding button in the 3x3 grid display in front of the subject). The gray background for the rest of the grids elements (squares) separated by the dark black line, indicate the stimuli of no-interest (no key-press is required to be performed. If pressed they may yield flash indicating error and a reset to the initial element of the sequence). These colours are chosen for simplicity and to avoid any effects due to colour processing. Subjects were instructed to use their index, middle and ring fingers for the three columns of the keypad — left, middle and right grid columns respectively (as shown in the Figure 4.2). Refer to Appendix B for more details about the file formats and a step-by-step procedure for conducting the experiment.

In our *mxn* experimental task, the complete sequence of *mxn* key-presses is accomplished by incrementally acquiring sub-goals (called, sets). The sequence to be learned is composed of n sets of m key-presses each set. The correct order of pressing m keys (called a set) is to be learnt, by trial-and-error. On successful completion of a set, subjects are presented the next set and so on. Subjects learn to complete n such sets (called a hyperset). In the current study, subjects performed three tasks namely, 2xG, 2x12 and 4x6 (the task procedure shown in the Figures 4.3, 4.4, 4.5). If subjects are not able to complete a set within a specific

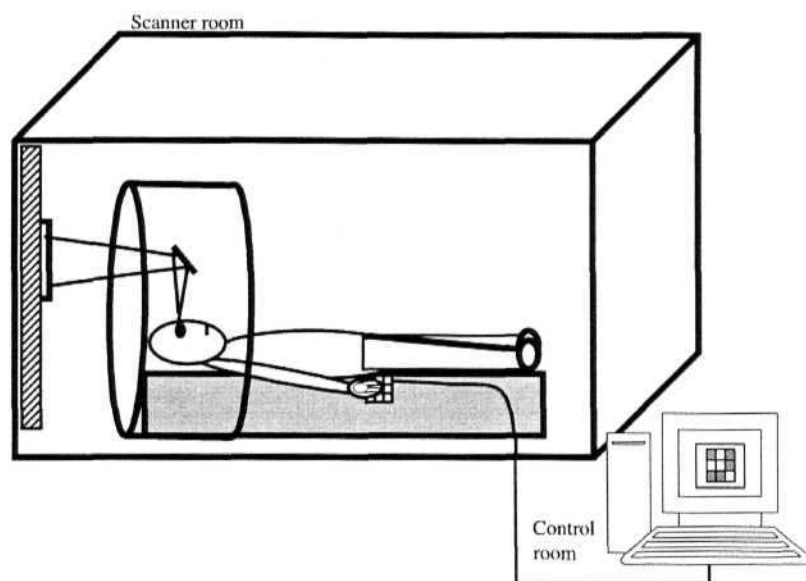


Figure 4.1: fMRI Scanner setup for stimulus presentation. Subjects lay supine in the fMRI scanner and learned the visuo-motor sequences. The non-magnetic key-pad in the scanner room is connected to the experimental computer in the control room. A separate functional image acquisition computer was also present in the control room (not shown in this figure). The stimulus generation and the image acquisition timings were synchronized.

time period (a. maximum of 0.8 sec per key-press) or if they press an incorrect key, a screen-flash appears and the sequence is reset to beginning of the hyper-set. In our paradigm the screen-flash acts like a feed-back signal for enabling learning the elements of a *set*. As the method of learning in our paradigm is based on trial-and-error, this screen flash acts like a *punishment signal* rather than as a reward signal. Typical reward signals such as money or some form of rewards were not given after successful completion of every *set* or *hyperset* in our experimental design. Thus the learning by trial-and-error used in our experimental paradigm constitutes a. very good example of the popular machine learning framework called *Reinforcement learning* (Sutton and Barto, 1998). Thus reinforcement learning in our experiments is facilitated by the punishment signal.

Rote memorisation of finger movements is not possible for the subjects as they need to learn the sequence by trial-and-error. In our experiments, *sets* were not presented at an even pace but to encourage speedier execution subjects were

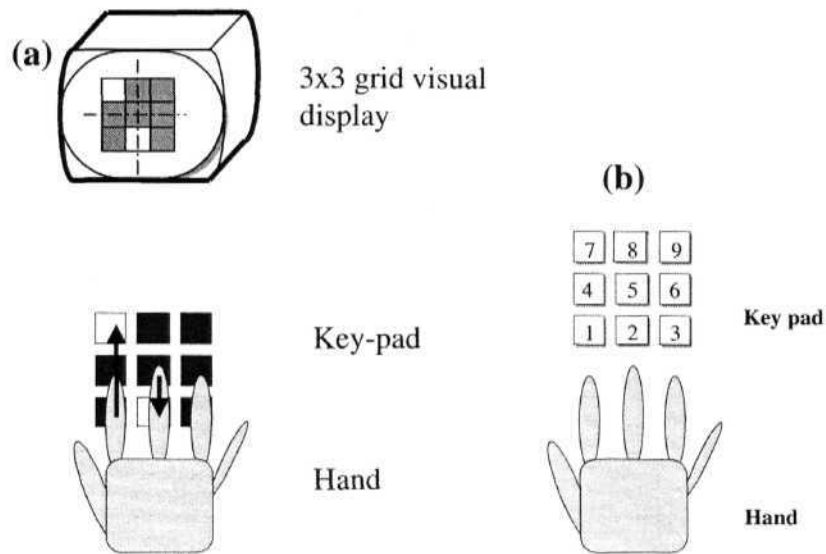


Figure 4.2: (a) Stimulus, Key-pad and Hand arrangements, (b) The 3x3 numeric key-pad with corresponding finger positions.

allowed to proceed to the next *set* as fast as they could.

We investigated the effect of increasing the number of movements to be learned from 12 (in the 2x6 task) to 24 (in the 4x6 and 2x12 tasks). Thus, we manipulated the sequence complexity along two dimensions— m (2 to 4) and n (6 to 12), reflecting the amount of information to be processed in the short-range and long-ranges respectively (shown in Figure 4.6).

Subjects performed three experiments (2x6, 2x12 and 4x6) while lying supine in the fMRI scanner. Each experiment consisted of alternating control (C) and test (T) conditions in a box-car manner (Figure 4.7). The order of the experimental tasks was counterbalanced across subjects. In the control condition (C), the subjects were asked to press one key at a time *following* randomly generated visual targets and thus there was no learning involved. In test or sequence learning condition (T), they continuously practiced one of the $m \times n$ sequence tasks. Subjects were given 0.8 seconds on an average per key-press (1.6 seconds for set completion in 2x12 & 2x6 tasks and 3.2 seconds for set completion in 4x6 task). However, they were allowed to proceed immediately to the next set as soon as they completed one set. The presentation was reset to the beginning

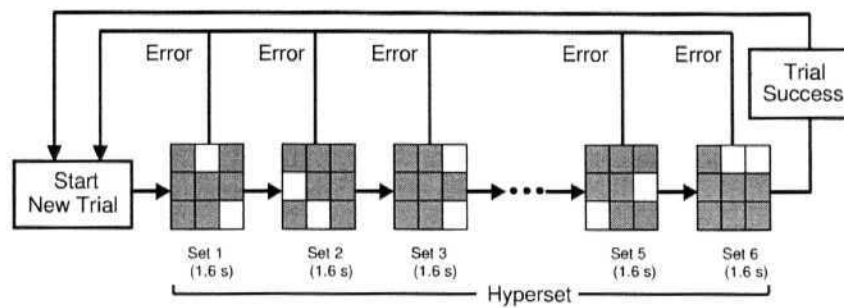


Figure 4.3: Procedure for the 2x6 Task

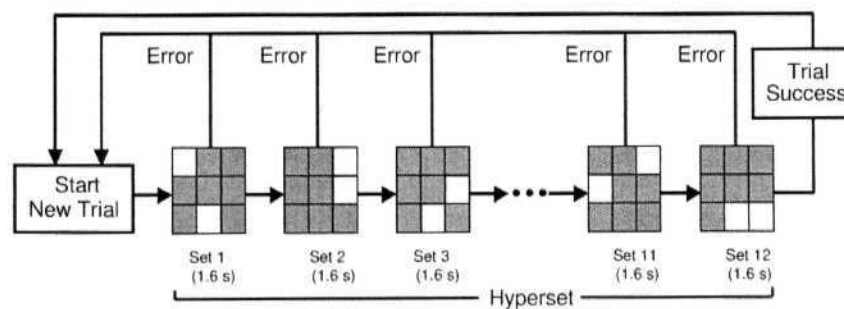


Figure 4.4: Procedure for the 2x12 Task

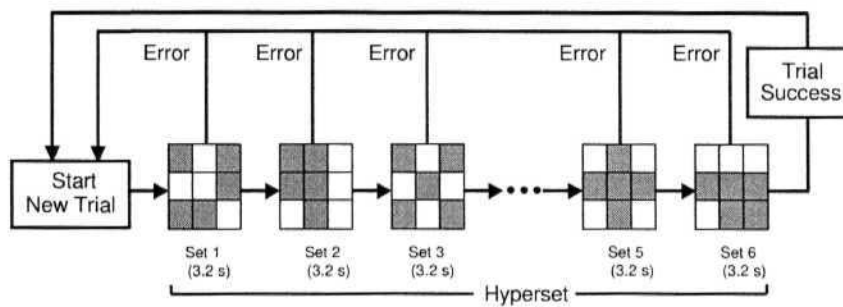


Figure 4.5: Procedure for the 4x6 Task

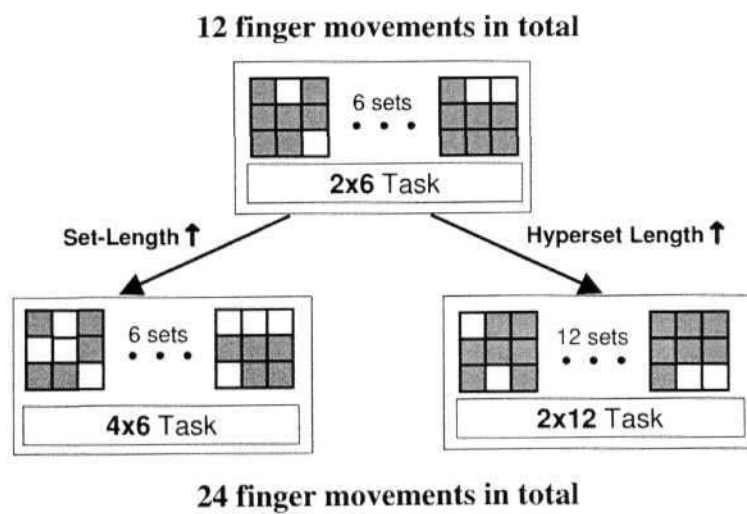


Figure 4.6: Dimensions of complexity used in the experiments.

of the hyperset upon time-out or a hitting error (refer to Figures 4.3, 4.4, 4.5). The successful completion of hyperset (completing the sequence) also resets the program pointer to the beginning of the sequence. This reset to the beginning of hyperset, allowed subjects to repeatedly practice the sequence. The generation of sequences, presentation of visual stimuli and recording of subjects' key-press responses was carried out with custom-built software running on Macintosh computer. A hyperset was generated randomly for each experiment that remained fixed for the entire duration of the experiment. Actual instructions given to the subjects are listed in the Appendix A. Details of experimental procedure are given in Appendix B. The list of hypersets generated for 2x6, 2x12 and 4x6 experiments for all the subjects shown in Appendix C.

To reduce the possibility of any explicit structure or pattern in the sequence, the hyperset was generated such that any repetition or transposition of sets did not occur. To enable smooth performance of the movements, subjects were encouraged to respond as quickly as they could throughout the experiment. All subjects were trained about half an hour before the scanning session using a different hyperset to become familiar with the task procedures.

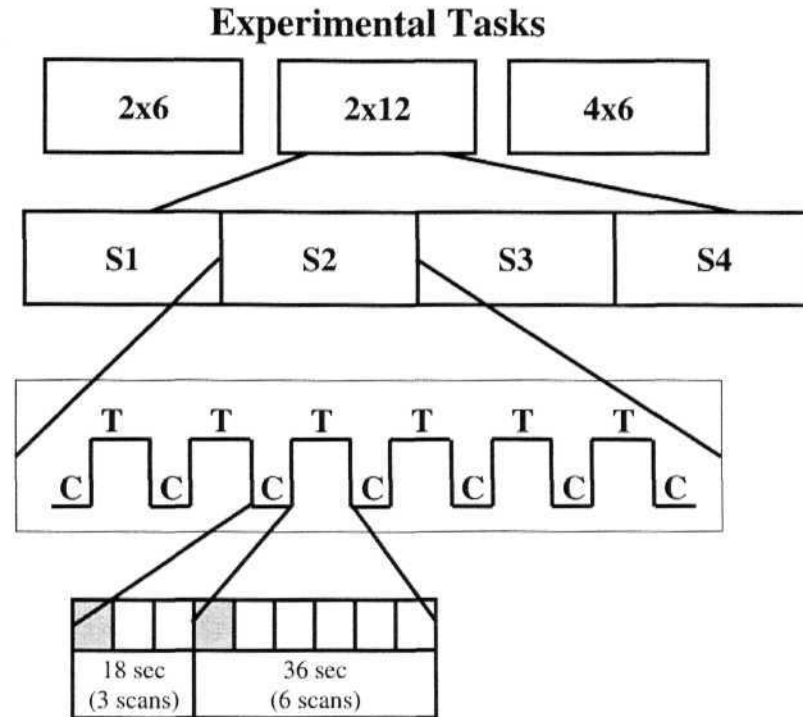


Figure 4.7: The design of experiments. Each of the Experiments (2x6, 2x12 and 4x6) is divided into sessions (S1, S2, S3 and S4). Sessions consist of alternating Control/Baseline/Follow (lasting for 18 seconds) and Task/Sequence learning (lasting for 36 seconds) Blocks. In each block subjects practiced sequence or follow random visual targets in the form of trials. With the repetition time (TR) set to 6 seconds, a total of 3 whole-brain scans and 6 whole brain-scans could be obtained in the control (C) and sequence task (T) blocks, respectively.

4.3 Control (Follow) Task

As fMRI does not measure absolute neural activity, neuroimaging studies must be designed to quantify relative changes of activity. Further, the brain is constantly engaged in several controlling tasks such as respiration, heart-beat etc. Hence, to measure specific task related activity, we need to scan subjects while at rest or while performing a simple baseline task (Gusnard and Raichle, 2001).

Assuming that the brain activity scales in a linear fashion and that cognitive processes are additive, we can test for the brain activations pertaining to certain cognitive processes (Berns, 1999). In our experiments, we adopted a simple

design for the baseline called the *Follow task (Control task)*, in which subjects looked at a random visual stimulus and simply performed finger movements but there was no learning involved. The visuo-motor mapping and the generation of finger movement are common processes in the control and test conditions. Figure 4.8 indicate the process diagrams of test and control conditions.

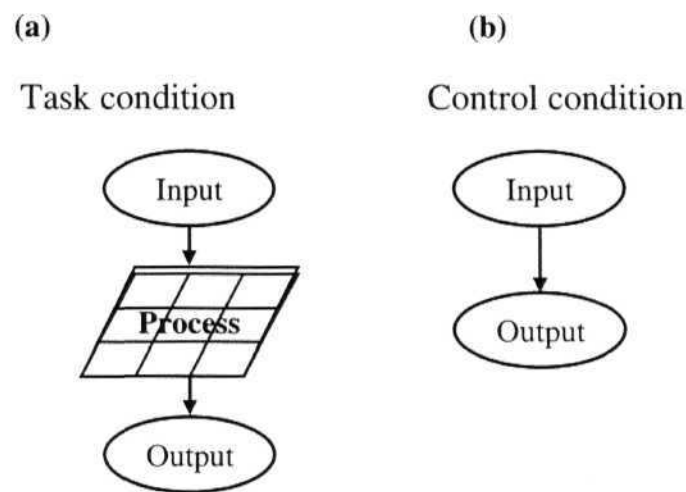


Figure 4.8: Design of Task (test) and Control Conditions. The process module in part (a) indicates the trial-and-error learning process as in the sequence tasks and part (b) indicates no such component of learning in the control/follow condition.

Thus cognitive subtraction of baseline brain activity maps from those corresponding to the sequence tasks would reveal activations related to trial-and-error processes (exploration of visual cues and evaluation of motor response based on visual feedback i.e., flash when subjects pressed a wrong key), visual-spatial processing, working memory for sequence structure, learning sequential dependencies across sets, attentional and executive processes. These cognitive processes depend upon the type of sequence learning task (i.e., 2x6 versus 2x12 or 2x6 versus 4x6) and the stage of learning (Early versus Consolidation, the demarcation of learning stages into Early and Consolidation is demonstrated in the Chapter 5, Section 5.2).

4.4 Possible Cognitive Components

In this section we suggest the possible cognitive components related to our experimental paradigm. As the main focus of this thesis is to find behaviour related neural correlates of the two dimensions of complexity (increase of set size and increase of hyperset size), the comparisons between 2x6 & 4x6 and 2x6 & 2x12 are of interest. Direct comparisons between 4x6 & 2x12 supplement the findings. Broadly, the increase in set-length (increase of m in 2x6 to 4x6 tasks) might increase the short-range prediction load while acquiring the sets. Similarly, increasing the hyperset-length (increase of n in 2x6 to 2x12 tasks) could be related to the increase in the long-range prediction load (acquisition of long hyperset). In this complexity experimental paradigm we are also interested in the acquisition (Early stage) and performance (Consolidation/Late stage) stages of the sequential skill. The cognitive components related to the early stage comparisons of 4x6 and 2x6 could reveal trial-and-error process, increase in the short-term working memory (short-range prediction process i.e., working memory for single-set/processing of limited sets). The consolidation stage differences between 4x6 versus 2x6 could be related to retrieval processes that may have been optimized within a set. As the working memory requirements reach near to the buffer capacity, subjects may try to optimize their performance within a set. As in 4x6 comparisons, the early stage comparisons of 2x12 and 2x6 could be related to trial-and-error set learning process and acquisition component of long-range sequence. The consolidation stage differences between 2x12 and 2x6 could be related to chaining across sets. One way subjects can perform the sequence in a smooth, speedy and skillful way is to chain or chunk across sets.

4.5 Details of Functional Imaging Parameters

Functional images were acquired in a 1.5 Tesla whole-body scanner (Shimadzu-Markoni Magnex Eclipse). Each experiment consisted of four sessions of scanning and each session comprised 13 blocks of alternating control (C) and test (T) conditions, each lasting 18 seconds 36 seconds, respectively (Figure 4.7). Each block began with a relevant instruction screen lasting for six seconds (i.e., instructing either "FOLLOW RANDOM" or "LEARN SEQUENCE"). A time series of 228 whole-brain scans separated by 6 seconds was obtained for each experiment. In

each whole-brain scan, a set of 50 axial T_2^* weighted gradient-echo echo-planar images [repetition time (TR) 6000 ms, echo time (TE) 55 ms, flip angle (FA) 90°, matrix 64 x 64, field of view (FOV) 192 x 192 mm and slice thickness of 3 mm] covering the whole brain were collected parallel to the anterior commissure-posterior commissure (AC-PC) line. In addition, a high-resolution T1-weighted sagittal anatomical brain images consisting of 191 slices (TR 12 ms, TE 4.5 ms, FA 20°, matrix 256 x 256, FOV 256 x 256 mm and slice thickness of 1 mm) was collected for each subject.

4.6 Analysis Methodology for Behavioural Parameters

Performance improvement of subjects was determined by two parameters, namely Success Rate (SR) and average key-press Response Time (RT). We also designed another behavioural measure called the total number of finger movements (NM). success rate was computed as the ratio of the number of successful hypersets or part thereof completed to the total number of hypersets attempted (expressed as percentage) and the average time required to complete a key-press in a successfully completed set was considered as the average key-press response time. The total number of finger movements (key-presses attempted) performed per block is termed as NM. For the control (follow) blocks, the success rate was measured as the ratio of total number of sets completed to the number of sets attempted (expressed as percentage), as there is no sequence to be learned in the follow task. The average key-press RT was measured in a similar way as that of sequence blocks i.e. the average time required to complete a key-press in a successfully completed set. Repeated-measures analysis of variance (RM ANOVA) was performed on the behavioural data from all the experiments to assess the learning related improvements. To account for the difference in the learning performance between subjects, we classified each subject's performance in the complex conditions into two stages — Early and Consolidation stages. For the complex sequence tasks (4x6 and 2x12), we divided the four sessions into one of the two learning stages based on the performance of individual subjects (which showed considerable variation due to learning) using the following criteria: Early stage, sessions in which the subject could not complete a hyperset for more than half of the blocks in that session (limited to minimum of first session); Consolidation stage:

the sessions that were not included in the early stage. For the 2x6 task, there was little variability across subjects and hence the first session was marked as early, and the 2nd and 3rd sessions as consolidation stage for all the subjects. The 2x6 task, being a less complex task, the fourth session in this task would correspond to over-learned stage of performance of sequences.

4.7 Statistical Analysis of functional Images

It has long been established that the brain undergoes learning related changes - both short and long term [for example, Karni et al. (1995)]. Although “*learning*” is an important cognitive function that the brain is constantly engaged in, most of the current fMRT studies do not explicitly investigate this phenomenon. Bapi et al. (2003) have reviewed possible approaches for characterizing learning related fMRI activity.

The imaging data were analyzed using SPM99 (Wellcome Department of Imaging Neuroscience, University College London) using fMRI option (Friston et al., 1995c). The functional images were reoriented to set the origin near the intersection of the coronal plane through AC and the AC-PC line and then motion correction was performed. Anatomical image for each subject was first co-registered with the first functional image and then normalized to the MNI template from the International Consortium for Brain Mapping (ICBM) Project. The resulting parameters were used for normalizing all the functional images (Friston et al., 1995a). This method of normalization was adopted to ensure correct anatomical localization of the blood oxygen level-dependent (BOLD) activity. The normalized functional images were spatially smoothed with an isotropic 6mm full width half maximum gaussian filter. We followed a two stage analysis. Single subjects' data were analyzed with a fixed effects model (Friston et al., 1994, 1995b) and group data were analyzed with a random effects model (Holmes and Friston, 1998; Friston et al., 1999). In the first level of analysis, separate design matrices were constructed by concatenating images from all the sessions of 2x6 and one of the complex tasks (4x6 or 2x12). We designed performance related variable that uses response time as the user specified regressor. The regressor took on the value of set completion times for the sequence blocks in the 2x6—4x6 design matrix and the liyperset completion times for the sequence blocks in the

2x6–2x12 design matrix. Regressors used to model the effects of two dimensions of the complexity are shown in the Figure 4.9. The main idea behind designing the regressor was to explicate the effects of sequence complexity of the task that would also correspond to the psychophysical behaviour of the subjects as learning progressed in the sequence tasks.

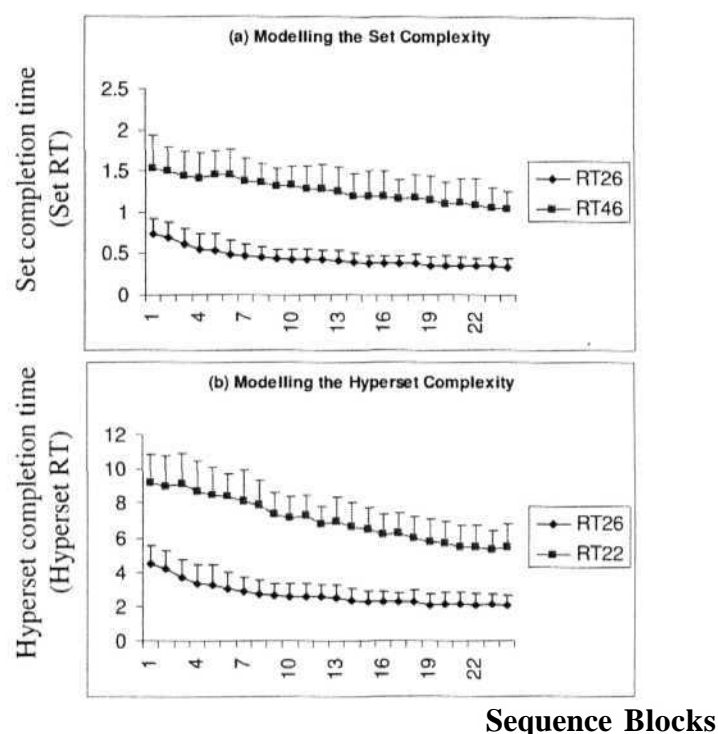


Figure 4.9: Modelling the effects of the two dimensions of sequence complexity. (a) set complexity effects (b) hyperset complexity effects. The error bar indicates the variations across subjects. The values corresponding to each subject are entered as regressors in the first level fMR image analysis.

The follow blocks were given a value of zero to model the ON–OFF design and the regressor would take approximately twice the value in the complex sequence task (4x6 or 2x12) as compared to the value given in the 2x6 task, thus modelling the experimental hypothesis of increasing the complexity of sequence to be learned. Regressor would also model subject specific variations in behaviour. The regressors were convolved with canonical hemodynamic response function to account for hemodynamic delays. A temporal cut-off of 84 seconds was applied to

filter subject-specific low-frequency drifts. Linear contrasts were specified to extract behaviour-related brain activations and deactivations. In the second level analysis, the contrast images of 17 subjects taken from the first level analysis were analyzed using a one sample T-test (for example, Early 2x6 regressor contrast) or two sample T-test (for example, Early 2x12 > 2x6). This corresponds to the random effects analysis as implemented in the SPM99 package. All the contrasts were calculated using a height threshold of $p < 0.001$, uncorrected for multiple comparisons across the volume and extent threshold of zero voxels. We also performed a *small volume correction* (SVC) analysis to make our interpretations more acceptable. We applied SVC to the cluster centered at the coordinates over marginal spherical region of interest of size 5 mm [refer to a recent reference Schendan et al. (2003) for reporting of SVCs]. All the coordinates of voxels of local maxima reported here were transformed from the Montreal Neurological Institute (MNI) template [International Consortium for Brain Mapping's (ICBM) template of average of 152 normal MR1 scans] space to the Talairach space (Talairach and Tournoux, 1988) using the Brett et al. (2001) MATLAB script. This transformation enables us to localise the activation foci and report the Brodmann area names & the anatomical labels using the Talairach atlas. At selected functional regions of interest, voxel data were extracted from a 3 mm spherical volume of interest (VOI) and entered into an *brain-behaviour correlation* (BBC) analysis. Average blood oxygen-level dependent (BOLD) signal was calculated for each of the learning blocks at the designated VOI for each subject in the specified experiment (2x6 or 2x12 or 4x6). Similarly, mean performance measure (response time) were calculated for each of the learning blocks for each subject in the specified experiment. The resultant BOLD signal values and the corresponding behavioural measure were then entered into a correlation analysis. Pearson correlation coefficient (R) and its two-tailed significance level (p) were computed. We developed SPM99 add-on scripts to perform brain-behaviour correlation (BBC) analysis over a specified VOL. The time course of activation over a VOI was also obtained during the BBC analysis. The step-by-step procedure followed in order to implement various fMRI analysis steps in the SPM99 package is given in Appendix D.

Chapter 5

Behavioural Results

The objective of the analysis of behavioural results is to quantify statistically the demarcation of learning stages and the learning related improvements in the behaviour. We present these results separately for each of the behavioural parameters computed. These results will be useful in the neuroimaging analysis for fixing the subject specific learning stages and to model performance related effects for each experiment. These results also useful to understand the behaviour related differences among the task conditions.

This chapter reports the statistical analysis results of the behavioural parameters while subjects performed the complex sequential skill tasks by trial and error procedure. The session-wise, stage-wise results for the three experiments for each behavioural parameters are reported. The repeated-measures ANOVA results for the each behavioural parameter are also reported.

5.1 The Behavioural Parameters

Two behavioural measures of performance (success rate and key-press response time) are designed to measure subjects' performance. We also computed the total number of finger movements as another behavioural measure. The success rate indicates the correctness of attempts made while performing the task and the key-press response times indicate the quickness in acquiring and performance of the movements. The number of movements indicate the total number of finger movements (key-presses attempted) performed. The behavioural parameters computed are averaged to the block level (total of 52 blocks, in which the learn-

ing blocks are 24 and the control/follow blocks are 28). Results from the success rate and key-press RT are reported for the sequence and control/follow blocks, followed by a discussion in the subsequent sections.

5.1.1 Definition of the Parameters

Three behavioural parameters are computed using the following formulae.

1. Success rate (SR): Ratio of the number of successful hypersets or part there of completed to the total number of hypersets attempted (expressed as percentage)
2. Average key-press response time (RT): The average time required to complete a key-press in a successfully completed set.
3. Number of movements (NM): The total number of finger movements (key-press attempts) performed per block.

Eighteen right handed subjects participated in the current study. Simple AN OVA for each subject and for each experiment from session 1 to 4 was performed to look for subject specific improvements. One of the subjects did not show significant improvements on the 2x6 task [Key-press RT: $F_{(1,10)} = 0.14$; $p = 0.71$ and Success Rate: $F_{(1,10)} = 2.42$; $p = 0.14$] and hence was excluded from further analysis.

5.2 Demarcating the Learning Stages

Inspection revealed that learning speeds differed among the subjects. To account for these differences in the learning performance among subjects, we classified each subject's performance in the complex conditions (2x12 and 4x6) into two stages - Early and Consolidation stages.

We divided the four sessions into one of the two learning stages based on the performance of individual subjects (which showed considerable variation during learning) using the following criteria:

Early stage: the sessions in which the subject completed the hyperset or could not complete a hyperset for more than half of the blocks in that session (limited to a minimum of the first session)

Consolidation stage: the sessions that were not included in the early stage.

We adopted a different procedure for demarcating the learning stages in the 2x6 task. Since 2x6 is a simpler task, subjects showed greater amount of learning in this task. It has been observed that subjects went beyond the "consolidation" performance exhibited in the complex tasks (2x12 and 4x6). For the 2x6 task, the first session was marked as early, and the 2nd and 3rd sessions as consolidation stage for all the subjects. This classification for the 2x6 task is justified (refer to Figure 5.1) because the behavioural response of subjects was not significantly different in the 2nd and 3rd sessions [repeated-measures analysis of variance on Success Rate: $F_{(1,96)} = 0.702$, $p = 0.404$]. On the other hand, such saturation was observed only between the 3rd and 4th sessions (Figure 5.1) for the complex conditions [repeated-measures ANOVA on Success Rate for 2x12: $F_{(1,96)} = 0.362$, $p = 0.549$ and for 4x6: $F_{(1,96)} = 2.22$, $p = 0.14$]. Furthermore, it was observed that all the subjects had completed one hyperset in the first session itself in the 2x6 task (block number ranging from a minimum of 2 to a maximum 6 in the first session).

Table 5.1 shows the early stage sessions for all the seventeen subjects. The consolidation stage for the complex sequence learning conditions (2x12 and 4x6) constitutes the early stage sessions subtracted from the total number of sessions. For the 2x6 sequence condition, the 2nd and 3rd sessions were considered as the consolidation stage (as discussed above). We thus demarcated the early and consolidation stages for all the subjects and for all the experiments based on the criteria discussed above. These subject-specific learning stages (i.e., early and consolidation) are used in the fMRI analysis also to model subject-specific stages. The learning phenomenon is modelled within the stages using subject-specific: regressors (as described in Chapter 4).

The performance measures collected repeatedly from each of the subjects, potentially reflect learning and adaptation effects. Hence, statistical tests such as Analysis of Variance (ANOVA) also need to take into account this fact. In these situations where multiple measurements are obtained from a subject, appropriate statistical measure to test difference of means is the repeated-measures

(RM) ANOVA [for a tutorial refer to Hopkins (1997)]. An RM-AN **O**VA was performed on the *success rate*, the *average*, *key-press response times* and the *number of movements* by entering two factors, namely, Experiments (3), Stages (2) for sequence/test and control/follow blocks. The analysis was carried out separately for the three measures and also separately for follow and sequence data. We also performed session-wise RM-ANOVA for the session-wise data for SR, RT and NM measures.

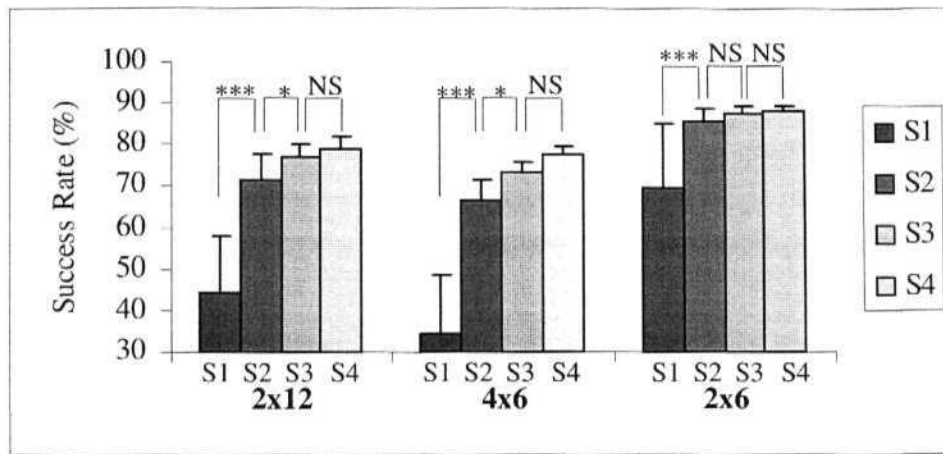


Figure 5.1: Success rate graph indicating the improvements from session 1 to 4 in the three sequence tasks (2x12, 4x6 and 2x6). The session-wise mean values are plotted for the four sessions. The error-bar indicates the variability across each session. The statistical significance values are also shown [*** is highly significant ($p < 0.001$), * is significant ($p < 0.001$) and NS is non-significant ($p > 0.05$)].

Table 5.1: Demarcation of the early Stage for 2x6, 2x12 and 4x6 tasks. The numbers in the table indicate the session number up to which the early stage is considered.

Subject's Name	Early 2x6	Early 2x12	Early 4x6
FB	1	1	3
HU	1	1	3
KU	1	1	1
ST	1	1	2
TF	1	1	1
TG	1	1	2
WY	1	1	1
AS	1	1	2
BN	1	2	2
CH	1	1	2
EC	1	1	2
JC	1	3	3
NS	1	1	1
PV	1	1	1
RC	1	1	1
WP	1	1	2
YU	1	1	1

5.3 Learning related improvements

5.3.1 Success Rate

The learning related improvements in all the tasks and the effect of increasing complexity based on success rate are described with the behavioural measure in Figure 5.2. This plot shows that in the complex conditions (4x6 and 2x12 tasks in Figure 5.2b & c) learning was slower depicted by slower success rate improvements as compared to the simpler condition (2x6 task in Figure 5.2a).

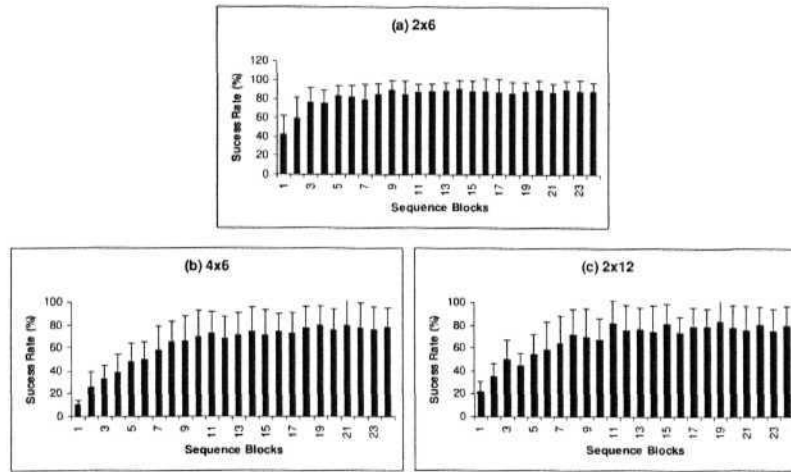


Figure 5.2: The block-wise graphs containing the success rate separately plotted for the three experiments with the error-bars indicating the standard deviation across the subjects.

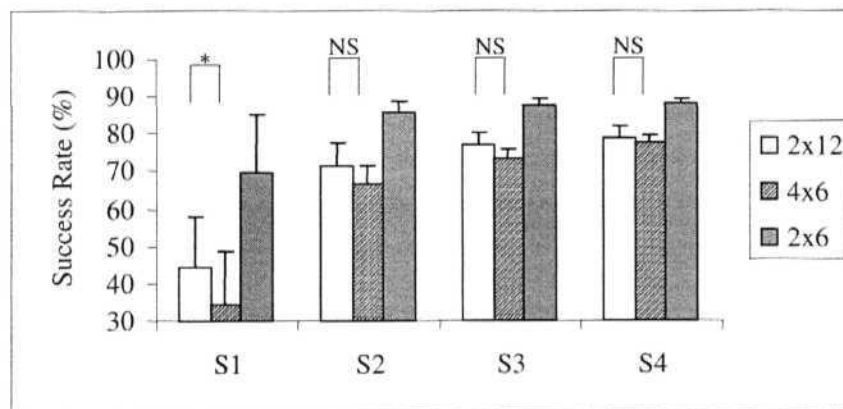


Figure 5.3: Session-wise improvements of success rate across the experiments. S1, S2, S3, and S4 indicate the session number index. The error-bar indicates the standard deviation across sessions. The statistical significance values are also shown [* is significant ($p < 0.001$) and NS is non-significant ($p > 0.05$)].

Session-wise Results of Repeated-measures ANOVA

Repeated-measures ANOVA was performed by entering the number of experiments (3: 2x12, 4x6 and 2x6), the number of sessions (4) and the number of blocks (6) as within subject factors.

A significant main effect was observed for experiment $F_{(2,32)} = 37.01$, $p \ll 0.0001$, sessions $F_{(3,48)} = 159.21$, $p \ll 0.0001$ and blocks $F_{(5,80)} = 21.19$, $p \ll 0.0001$. The Experiment x Session interaction term was significant $F_{(6,96)} = 8.36$, $p \ll 0.0001$. The *post hoc* means comparison analysis on the factor 'experiment' revealed significant differences between 2x6 and 2x12 [$F_{(1,32)} = 37.98$, $p \ll 0.0001$], 2x6 and 4x6 [$F_{(1,32)} = 68.57$, $p \ll 0.0001$] tasks. There was also a marginally significant difference between the 2x12 and 4x6 tasks [$F_{(1,32)} = 4.49$, $p = 0.042$].

Session-wise *post hoc* means comparison was performed to further probe the above mentioned differences across the three experimental tasks. For each of the four sessions (S1, S2, S3, S4) there was significant difference between the 2x6 and 2x12 tasks and between 2x6 and 4x6 tasks ($p < 0.0005$). Interestingly the two complex tasks 2x12 and 4x6 were different in the first session [$F_{(1,96)} = 13.77$, $p < 0.0005$] but were similar in the 2nd session [$F_{(1,96)} = 3.687$, $p = 0.0577$], the 3rd session [$F_{(1,96)} = 1.794$, $p = 0.183$] and the 4th session [$F_{(1,96)} = 0.203$, $p = 0.653$]. The percentage success rates obtained for the three experiments in each of the sessions is tabulated in Table 5.2 and the block and session-wise improvements are presented in Figures 5.2 and 5.3, respectively. It is apparent from the Table 5.2 that success rate attained almost similar values in 2x12 and 4x6 tasks by the last session.

Table 5.2: The percentage change of success rate for the four sessions. The standard deviation indicates the variability across each session.

Session Index	2x12	4x6	2x6
Session 1	44.19±13.68	34.03±14.66	69.51±15.91
Session 2	71.64±6.26	66.38±5.14	85.57±3.56
Session 3	77.19±3.01	73.52±2.29	87.86±1.75
Session 4	78.84±3.21	77.61±1.92	88.09±1.08

Stage-wise Results of Repeated-measures ANOVA

Repeated-measures ANOVA was performed by entering the number of experiments (3: 2x12, 4x6 and 2x6) and the number of Stages (2: Early and Consolidation) as within subject factors.

Repeated-measures ANOVA for the sequence condition revealed a significant main effect for experiment [$F_{(2,32)} = 39.513$, $p << 0.0001$] and Stages [$F_{(1,16)} = 277.151$, $p << 0.0001$]. The Experiment x Stage interaction term was also significant [$F_{(2,32)} = 12.806$, $p < 0.0001$]. The *Post hoc* means comparison analysis on the factor 'experiment' has revealed significant differences between 2x6 and 2x12 tasks [$F_{(1,32)} = 56.07$, $p < 0.0001$], 2x6 and 4x6 tasks [$F_{(1,32)} = 62.358$, $p < 0.0001$]. Whereas, there was a non-significant difference between 2x12 and 4x6 tasks [$F_{(1,32)} = 0.1669$, $p = 0.686$]. We further probed into this non-significant effect to see the differences between 2x12 and 4x6 tasks in the Early and the Consolidation stages separately.

Learning was observed in all the three sequence conditions from the early to the consolidation stages. There was a significant improvement in success rate from $69.5 \pm 10.6\%$ in the early to $86.7 \pm 6.4\%$ in the consolidation stages of the 2x6 task [$F_{(1,32)} = 49.81$, $p << 0.0001$]. In the 4x6 task, the improvement was from $43.7 \pm 7.1\%$ to $76.7 \pm 11.7\%$ [$F_{(1,32)} = 182.71$, $p < 0.0001$]. The improvement in the 2x12 task was from $45.4 \pm 11.6\%$ to $76.9 \pm 9.9\%$ [$F_{(1,32)} = 167.91$, $p < 0.0001$]. For both the learning stages (Early and Consolidation) there was significant difference between the 2x6 and 2x12 tasks and between 2x6 and 4x6 tasks ($p < 0.0001$). Interestingly, success rate (SR) attained similar levels in the complex conditions [Early: $F_{(1,32)} = 0.435$, $p = 0.51$; Consolidation: $F_{(1,32)} = 0.01$, $p = 0.92$]. Figure 5.4 describes the success rate differences with their statistical significance values in the Early and the Consolidation stages separately for the three experiments.

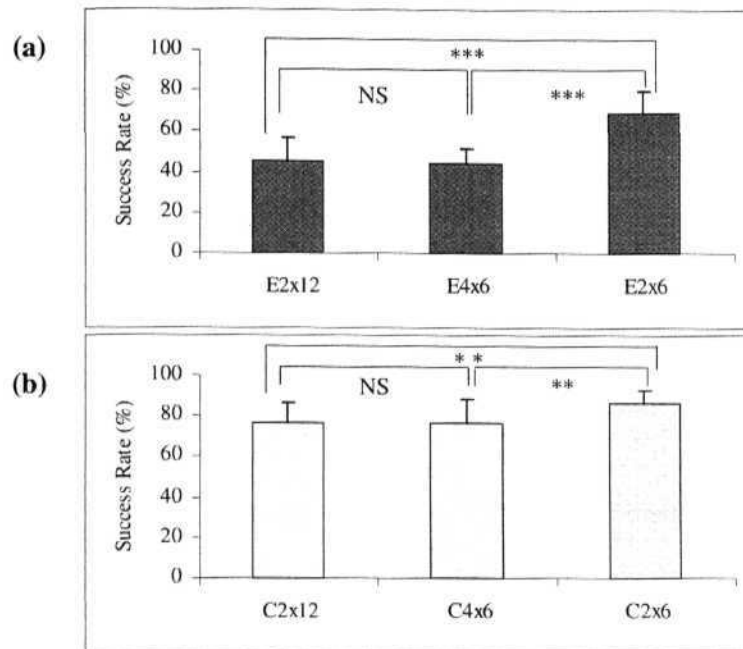


Figure 5.4: Stage-wise improvements of success rate across the experiments (2x12, 4x6 and 2x6 experiments) for (a) Early (E) and (b) Consolidation (C) stages separately. The error-bar indicates the variability across the subjects. The statistical significance values are also indicated in the plot [*** is highly significant ($p < 0.001$), ** is more significant ($p < 0.0001$) and NS is non-significant ($p > 0.05$)].

Summary of Success Rate Analysis Results

The block-wise success rate graphs (Figure 5.2) visually demonstrated a trend of improvements in the three sequence learning tasks. The block-wise trend plot demonstrates that the simpler sequence condition (2x6) attained saturation performance by the last block. Whereas the complex sequence conditions (2x12 and 4x6) depicted slower improvements as compared to 2x6.

The session-wise and stage-wise repeated-measures ANOVA results on success rate revealed learning related improvements in all the sequence learning tasks (2x12, 4x6 and 2x6) as evidenced by the significant main effects. The complexity related effects (i.e., 12 movements in 2x6 task being increased to 24 movements in 2x12 and 4x6 tasks) are revealed from the significant differences in session-wise and stage-wise *post hoc* analyses. Interestingly, in the stage-wise analysis (Figure

5.4) the success rate was observed to be similar across the complex sequence conditions (2x12 and 4x6) in both the stages.

This result clearly demonstrates that the subjects attained similar levels of accuracy in both the complex tasks. Thus the success rate as a behavioural measure is justified and it mainly demonstrated (quantified) the similar difficulty levels across the complex sequence learning conditions.

5.3.2 Average key-press Response Time (RT)

The learning related improvements in all the tasks and the effect of increasing the complexity on RTs are shown in Figure 5.5. This plot shows that in the complex conditions (4x6 and 2x12 tasks in Figure 5.5b&c) learning was slower depicted by slower RT improvements as compared to the simpler condition (2x6 task in Figure 5.5a).

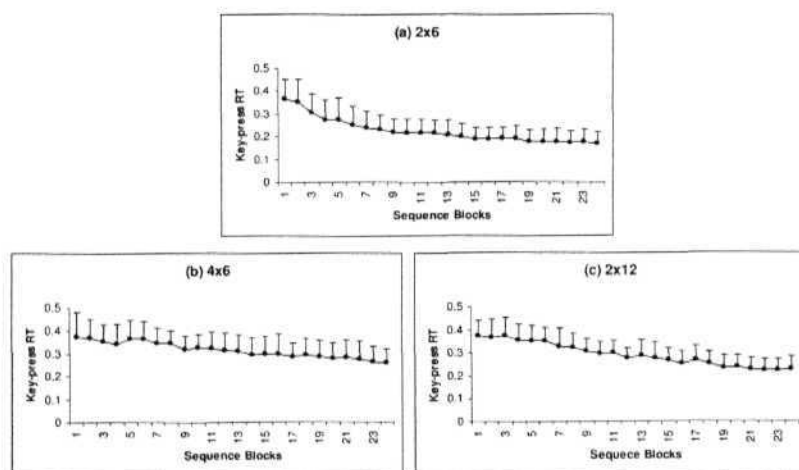


Figure 5.5: The block-wise graphs containing the average key-press RT separately plotted for the three experiments with the error-bars indicating the standard deviation across the subjects.

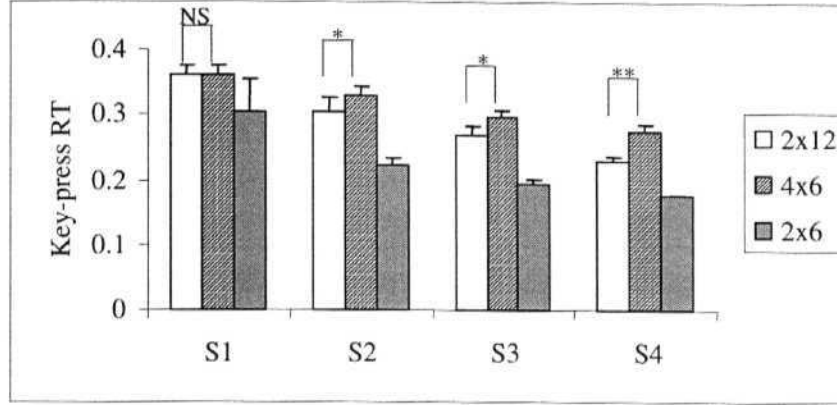


Figure 5.6: Session-wise improvements of Response Time across the experiments for comparison. S1, S2, S3, and S4 indicate the session number index. The error-bar indicates the standard deviation across sessions. The statistical significance values are also shown [** is more significant ($p < 0.0001$), * is significant ($p < 0.001$) and NS is non-significant ($p > 0.05$)].

Session-wise Results of Repeated-measures ANOVA

Repeated-measures ANOVA was performed on key-press response time data by entering the number of experiments (3: 2x12, 4x6 and 2x6), the number of sessions (4) and the number of blocks (6) as within subject factors.

A significant main effect was observed for experiment $F_{(2,32)} = 41.68$, $p \ll 0.0001$, sessions $F_{(3,48)} = 152.47$, $p \ll 0.0001$ and blocks $F_{(5,80)} = 28.34$, $p \ll 0.0001$. The Experiment x Session interaction term was significant $F_{(6,96)} = 4.67$, $p = 0.0003$.

The *post hoc* means comparison analysis on the factor 'experiment' has revealed significant differences between 2x6 and 2x12 [$F_{(1,32)} = 41.662$, $p \ll 0.0001$], 2x6 and 4x6 tasks [$F_{(1,32)} = 77.783$, $p \ll 0.0001$]. On the other hand, there was a marginally significant difference between the 2x12 and 4x6 tasks [$F_{(1,32)} = 5.592$, $p = 0.024$].

The Session-wise *post hoc* means comparison was done to further probe the above mentioned differences across the three experimental tasks. For each of

the four sessions (S1, S2, S3, S4) there was significant difference between the 2x6 and 2x12 tasks and between 2x6 and 4x6 tasks ($p < 0.0001$). Interestingly, the two complex tasks 2x12 and 4x6 were similar in the first session [$F_{(1,96)} = 0.000535$, $p = 0.982$] but were different in the 2nd sessions [$F_{(1,96)} = 7.19$, $p < 0.01$], the 3rd session [$F_{(1,96)} = 11.567$, $p < 0.001$] and the 4th session [$F_{(1,96)} = 28.360$, $p \ll 0.0001$].

The average key-press response time (RT) obtained for the three experiments in each of the sessions is tabulated in Table 5.3 and the block and the session-wise improvements are presented in Figures 5.5 and 5.6, respectively. It is evident from Table 5.3 that response times (RT) became dissimilar between 2x12 and 4x6 tasks by the last session. The RT value in 2x12 is also observed to be lesser compared to the RTs of 4x6 task.

Table 5.3: The Key-press Response times for the four sessions. The standard deviation indicates the variability across each session.

Session Index	2x12	4x6	2x6
Session 1	0.362±0.011	0.362±0.011	0.304±0.047
Session 2	0.306±0.018	0.329±0.013	0.224±0.009
Session 3	0.268±0.013	0.297±0.008	0.195±0.007
Session 4	0.228±0.007	0.274±0.010	0.175±0.003

Stage-wise Results of Repeated-measures ANOVA

Repeated-measures ANOVA was performed on key-press response time data entering the number of experiments (3: 2x12, 4x6 and 2x6) and the number of Stages (2: Early and Consolidation) as within subject factors.

RM ANOVA for sequence condition revealed a significant main effect for experiment [$F_{(2,32)} = 19.307$, $p \ll 0.0001$] and Stages [$F_{(1,16)} = 173.449$, $p \ll 0.0001$]. The Experiment, x Stage interaction term was also significant, [$F_{(2,32)} = 3.603$, $p = 0.038$]. The *post hoc* means comparison analysis on the 'experiment' factor has revealed significant differences between 2x6 and 2x12 [$F_{(1,32)} = 24.162$, $p \ll 0.0001$], 2x6 and 4x6 tasks [$F_{(1,32)} = 33.052$, $p \ll 0.0001$] tasks. On the other hand, the difference was non-significant between the 2x12 and 4x6 tasks [$F_{(1,32)} = 0.694$, $p = 0.4107$]. We further probed into this non-significant

effect to see the differences between 2x12 and 4x6 in the Early and the Consolidation stages separately.

Learning was observed in all the three sequence conditions from the early to the consolidation stages. A significant improvement (decreasing profile) in RT was observed from 0.305 ± 0.08 sec to 0.21 ± 0.05 sec in 2x6 [$F_{(1,32)} = 121.6$, $p \ll 0.0001$], from 0.354 ± 0.06 sec to 0.289 ± 0.06 sec in 4x6 [$F_{(1,32)} = 57.75$, $p \ll 0.0001$] and from 0.359 ± 0.06 sec to 0.266 ± 0.05 sec in 2x12 [$F_{(1,32)} = 115.1$, $p \ll 0.0001$] tasks. For both the learning stages (Early and Consolidation) there was significant difference between the 2x6 and 2x12 tasks and between 2x6 and 4x6 tasks ($p < 0.0001$). Interestingly, key-press response times (RT) showed a differential behaviour. RTs were similar [$F_{(1,32)} = 0.232$, $p = 0.633$] in the Early period. On the other hand in the consolidation stage, RTs were significantly [$F_{(1,32)} = 6.99$, $p = 0.01$] faster in 2x12 compared to the 4x6 task. Figure 5.7 describes the response time differences with their statistical significance in the early and the consolidation separately for the three experiments.

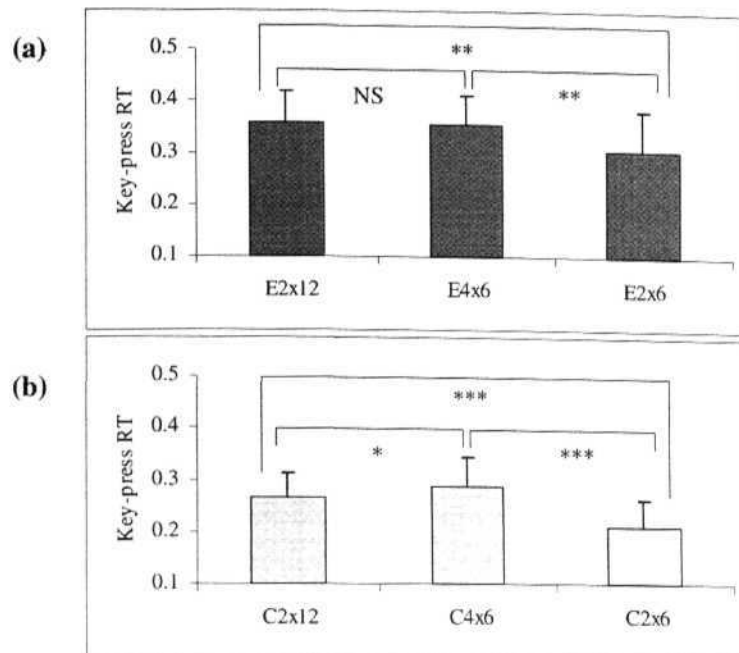


Figure 5.7: Stage-wise improvements of key-press response time across the experiments (2x12, 4x6 and 2x6 experiments) for (a) Early and (b) Consolidation stages separately. The error-bar indicated the variability across the subjects. The statistical significance values are also indicated in the plot [*** is highly significant ($p < 0.001$), ** is more significant ($p < 0.0001$), * is significant ($p < 0.01$), and NS is non-significant ($p > 0.05$)].

Summary of the Analysis of Average Key-press RT Results

The block-wise average key-press RT graphs (Figure 5.5) visually pointed out the trend of improvement in the three sequence learning tasks. The block-wise trend plot demonstrates that the key-press RT decreased rapidly in the simpler sequence condition (2x6). Whereas the complex sequence task conditions (2x12 and 4x6) depicted slower improvements as compared to 2x6 task.

The session-wise and stage-wise repeated-measures ANOVA results on key-press response times revealed learning related improvements in all the sequence learning tasks (2x12, 4x6 and 2x6) as evidenced by the significant main effects. The complexity related effect (i.e., the effect of increasing the number of movements from 12 in 2x6 task to 24 movements in 2x12 & 4x6 tasks) is revealed from the significant differences in session-wise and stage-wise *post hoc* analyses.

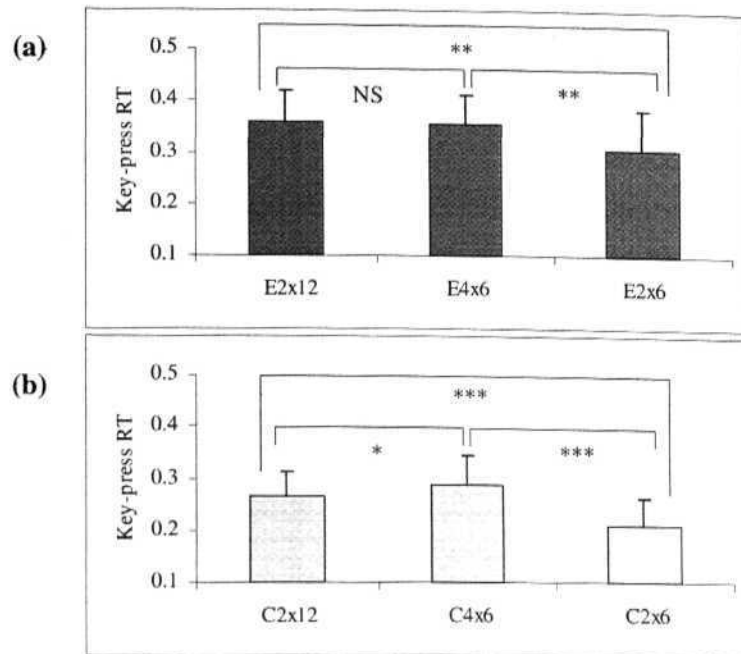


Figure 5.7: Stage-wise improvements of key-press response time across the experiments (2x12, 4x6 and 2x6 experiments) for (a) Early and (b) Consolidation stages separately. The error-bar indicated the variability across the subjects. The statistical significance values are also indicated in the plot [*** is highly significant ($p < 0.001$), ** is more significant ($p < 0.0001$), * is significant ($p < 0.01$), and NS is non-significant ($p > 0.05$)].

Summary of the Analysis of Average Key-press RT Results

The block-wise average key-press RT graphs (Figure 5.5) visually pointed out the trend of improvement in the three sequence learning tasks. The block-wise trend plot demonstrates that the key-press RT decreased rapidly in the simpler sequence condition (2x6). Whereas the complex sequence task conditions (2x12 and 4x6) depicted slower improvements as compared to 2x6 task.

The session-wise and stage-wise repeated-measures ANOVA results on key-press response times revealed learning related improvements in all the sequence learning tasks (2x12, 4x6 and 2x6) as evidenced by the significant, main effects. The complexity related effect (i.e., the effect of increasing the number of movements from 12 in 2x6 task to 24 movements in 2x12 & 4x6 tasks) is revealed from the significant differences in session-wise and stage-wise *post hoc* analyses.

Interestingly, in the stage-wise analysis (Figure 5.7) the average key-press RT revealed a differential behaviour across complex sequence conditions (2x12 & 4x6 tasks) from the early to the consolidation stages. In the early stage the key-press RT was observed to be similar across 2x12 and 4x6. Whereas in the consolidation stage key-press RT became dissimilar. In addition the consolidation stage RT value of 2x12 task was observed to be significantly lesser than that of the consolidation stage RT value of 4x6. Similar differential effects across 2x12 and 4x6 were observed for the session-wise analysis on key-press RTs.

So when 24 movements are arranged as 2x12, the single-key-press RTs were shorter compared to when they are arranged as 4x6. These differences may have potential implication in organizational differences across 2x12 and 4x6 tasks. These issues will be taken up further in the Chapter 6. Thus the key-press RT as a behavioural measure is justified and it mainly demonstrated (quantified) the organizational differences across complex sequence learning conditions.

5.3.3 Number of Movements (NM)

In addition, we computed the total number of finger movements (key-press attempts) performed per block. This measure is an additional one to address questions such as whether the total number of movements differed between the complex sequence tasks (2x12 versus 4x6). We performed repeated-measures ANOVA for the session and stage-wise data.

Session-wise Results of Repeated-measures ANOVA

Repeated-measures ANOVA was performed on the number of movements data by entering the number of experiments (3: 2x12, 4x6 and 2x6), number of sessions (4) and number of blocks (6) as within subject factors.

A significant main effect was observed for experiment $F_{(2,32)} = 17.214$, $p < 0.0001$, Sessions $F_{(3,48)} = 163.68$, $p < 0.0001$ and blocks $F_{(5,80)} = 102.588$, $p < 0.0001$. The Experiment x Session interaction term was observed to be non-significant $F_{(6,96)} = 1.0573$, $p = 0.394$. The non-significant difference in number of movements in the Experiments and the Session interaction term indicates that the time-courses (Session 1 to 4) of the three experimental tasks are similar. Further, the *post hoc* means comparison has revealed a non-significant difference

between the 2x12 and 4x6 tasks with the experiment as main effect [$F_{(1,32)} = 0.357$, $p = 0.544$]. This verifies that the total number of movements across the complex tasks are statistically similar.

Stage-wise Results of Repeated-measures ANOVA

Repeated Measures ANOVA was performed on NM data entering the number of experiments (3: 2x12, 4x6 and 2x6) and number of Stages (2: Early and Consolidation) as within subject factors. A significant, main effect was observed for experiment $F_{(2,32)} = 9.27$, $p = 0.0007$ and Stages $F_{(1,16)} = 201.8$, $p \ll 0.0001$. The Experiment x Stage interaction term was non-significant $F_{(2,32)} = 1.468$, $p = 0.245$. This result is similar to that of session-wise experiment x session interaction obtained earlier.

The *post hoc* means comparison on the factor 'experiment' have revealed a non-significant difference between the 2x12 and 4x6 tasks [$F_{(1,32)} = 2.8257$, $p = 0.103$]. This further reinforces the fact that number of movements across complex tasks was similar.

Summary of the Analysis of Number of Movements Results

The repeated-measures ANOVA results on number of movements revealed that the total key-press attempts increased from the session 1 to the session 4 in session-wise analysis and early to the consolidation stage in the stage-wise analysis. The important finding is that the number of movements remained balanced across the complex sequence learning tasks. This result is evidenced by the results of the *post hoc* analysis of Experiments both in the session-wise and the stage-wise analyses.

5.4 Analysis of the Control/Follow Condition

In the control condition, subjects were asked to press one key at a time, following randomly generated visual targets and thus there was no learning involved. For the control (follow) blocks, *Success Rate* (SR) was measured as the ratio of the total number of sets completed to the number of sets attempted (expressed as %) as there is no concept of a sequence in the Follow task. This measure reflects

the accuracy with which subjects are following the random visual target,. The *average key-press Response Time* (RT) was measured in a similar way to that of sequence blocks i.e., the average time required to complete a key-press in a successfully completed set (here set is a single key-press).

Repeated-measures ANOVA was performed on SR and RT data entering the number of experiments (3: 2x12, 4x6 and 2xG), the number of sessions (4) and the number of blocks (7) as within subject factors. The repeated-measures ANOVA performed on the two behavioural parameters for the control condition yielded no significant difference across the three experiments [Success Rate: $F_{(2,32)} = 0.64$, $p = 0.5318$; key-press RT: $F_{(2,32)} = 0.932$, $p = 0.404$], thereby indicating a steady performance in the control task across the experiments (refer to Figures 5.8 and 5.9).

Repeated-measures ANOVA was also performed on the SR and RT data entering the number of experiments (3: 2x12, 4x6 and 2x6) and the number of Stages (2: Early and Consolidation) as within subject factors. The control/Follow blocks corresponding to the sequence blocks of the Early and the Consolidation are considered here. This analysis also yielded no significant difference across the three experiments by the lack of experimental main effect [SR: $F_{(2,32)} = 0.34$, $p = 0.7158$; RT: $F_{(2,32)} = 0.346$, $p = 0.7101$].

5.4.1 Summary of the Results in the Control Condition

The repeated-measures ANOVA results from the session-wise and stage-wise analysis revealed non-significant experimental main effect for both the behavioural measures computed (success rate and average key-press response time). The results demonstrate that in the control condition, the behavioural parameters were statistically similar across the three tasks.

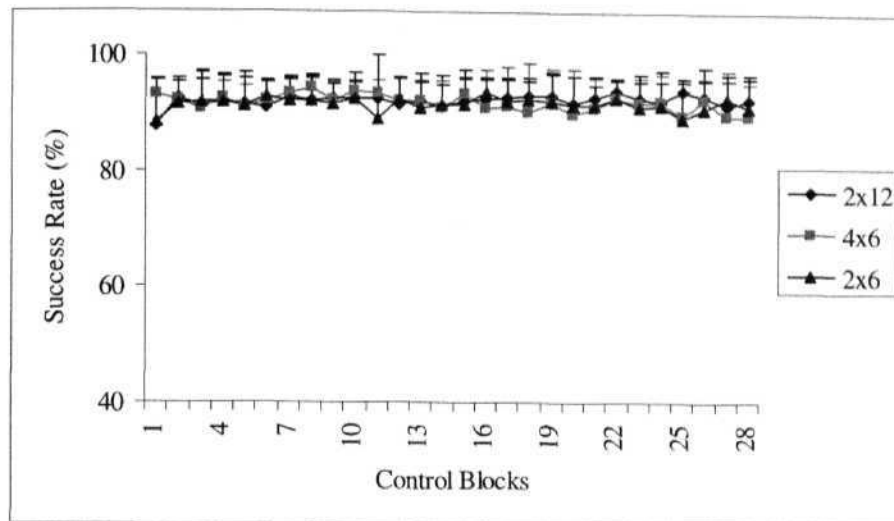


Figure 5.8: The block-wise graphs containing the success rate plotted for the three experiments with the error-bars indicating the standard deviation across the subjects. This plot indicates the similarity of the success rate values in the control condition across experiments.

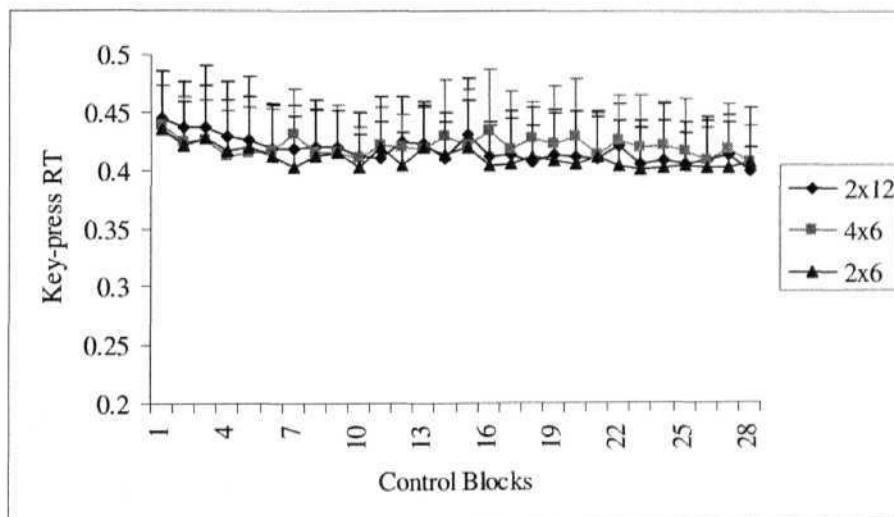


Figure 5.9: The block-wise graphs containing the response time plotted for the three experiments with the error-bars indicating the standard deviation across the subjects. This plot indicates the similarity of the key-press response time values in the control condition across experiments.

Chapter 6

Hierarchical organization of Sequential Skills

This chapter presents a systematic behavioural analysis for quantifying the hierarchical nature of organization of sequential skills (i.e., chunking process) and its differential effects when the sequence was arranged in different ways. We present behavioural analysis results on response times as subjects learned finger movement sequences of length 24 arranged in two ways - 12 sets of two movements each (2x12 task) and 6 sets of four movements each (4x6 task).

This investigation is aimed at studying hierarchical organization of skills that may have an impact in understanding higher cognitive functions such as language, speech, etc., all of which involve sequence processing. In this chapter we first review important studies, report the results obtained on chunking analysis and discuss the findings.

6.1 Introduction

Most of the higher-order intelligent behaviours such as problem solving, reasoning and language involve acquiring and performing complex sequence of activities (Sun, 2000). It is known that acquiring a complex sequential skill involves chaining a number of primitive actions to make the complete sequence. The notion of chunking in the context of limited capacity of short term working memory was introduced by Miller way back in 1956. Miller (1956) suggested the reorganization of unrelated list items into chunks in order to overcome the limitation of immediate memory buffer. In the current terminology it is called as short-term

or working memory (Baddeley, 1986, 1992). Miller suggested that the capacity of short-term memory or working memory (STM or WM) is 7 ± 2 chunks and argued that the amount of information that is retained in STM/WM is independent of the information contained in each chunk. The hierarchical organization of movement sequences has been suggested by several researchers [for example: (Rosenbaum et al, 1983)]. Rosenbaum et al. (1983) first demonstrated the evidence of the hierarchical control of the execution of movement sequences. A sequence might consist of several sub-sequences and these sub-sequences in turn can contain sub-sub-sequences. In their experiment, subjects were required to perform a previously memorized finger-tapping sequence of responses as quickly and accurately as possible. Their latency and error data of the movement sequences suggested a hierarchical model which resembles a tree-traversal-process. Though Karl Lashley, way back in 1951, in his classic paper on serial order (Lashley, 1951) also argued that the sequential responses that appear to be organized in linear and flat fashion concealed an underlying hierarchical structure, Rosenbaum et al. (1983) made notable contributions by actually demonstrating hierarchical control of the execution of movement sequences. In a review, Conway and Christensen (2001) argued that the humans outperform non-human primates on more complex sequential learning tasks — in particular the learning and processing of hierarchically organized temporal sequences.

The concept of chunking in sequential behaviour has been previously studied in animals [see Terrace (2001), for a review] and in humans [for example: see Koch and Hoffmann (2000); Verwey (2001); Sakai et al. (2003)]. Terrace (2001) reviewed mainly the chunking phenomenon in list learning by pigeons, monkeys and humans. He also argued for an operational definition of chunks. He suggested a distinction between the notions of input and output chunks from the ideas of short-term and long-term memory. Input chunks reflect the limitation of working memory during the encoding of new information i.e., how new information is stored in long-term memory, and how it is retrieved during subsequent recall. Output chunks reflect the organization of over-learned motor programs that are generated on-line in working memory. He also suggested that during the sequence performance stage (already learnt stage), subjects download list items as chunks during pauses and that chunk size for order information is approximately 3 items. Koch and Hoffmann (2000) examined the influence of relational structures in the stimulus and in the response sequences on sequence learning using serial reaction

task paradigm. In three experiments, they separately studied patterns, chunks and the higher-order relations (i.e., hierarchical structures). Verwey (2001), using two highly practiced sequences, investigated the robustness of motor chunks (motor representations) in different situations. He suggested a model consisting of dual-processors i.e., cognitive and motor may be involved in the execution of sequences. The familiar sequences are carried out by a dedicated motor processor and the forthcoming sequence predictions are done by cognitive processor. Based on the earlier studies they advised that the dorsal prefrontal cortex and anterior cingulate may have a role in cognitive processor and the motor processor comprises of supplementary motor area, the basal ganglia and the lateral cerebellum. Using a 2x10 sequence task, in a recent study Sakai et al. (2003) have demonstrated that different subjects chunked the same sequence of movements differently. They have also shown that performance on a shuffled sequence after learning was less accurate and slower when the chunk patterns were disrupted than when they were preserved. This clearly suggests an operational role for the chunks as a single memory unit that facilitates efficient performance of the sequence. Most of the studies reviewed in this section suggest that the shorter response time (RT) between successive responses/actions during the sequence performance stage could possibly be due to the spontaneous reorganization (in the form of chunks) across the elements of sequence.

Now, one practical question is to see how a chunk can be identified from behavioural observations. Most of the studies reviewed in this chapter suggest that shorter Response Time (RT) between successive responses/actions during the sequence performance stage could possibly be due to the spontaneous reorganization (in the form of chunks) across the elements of sequence. So identifying places where RTs slow-down is a way of marking the chunk location. Terrace (2001) also suggested that during the sequence performance stage (already learnt stage), subjects download list items as chunks during pauses and that chunk size for order information is approximately 3 items.

The current experiment in this chapter specifically addresses the differences in chunk formation when the same amount of information is organized in two different ways. The amount of information to be processed at a time forms a *set*. We hypothesized that a smaller set-size would enable spontaneous chunking across several sets, while increasing the set-size will limit the chunk formation to single sets. Using the $m \times n$ visuo-motor sequence task (Hikosaka et al., 1995;

Bapi et al., 2000), we set out to investigate the phenomenon of chunking during learning of a complex sequential skill. In this chapter we mainly concentrate on the chunking results of two complex sequence tasks: 2x12 and 4x6.

6.2 Data analysis

Subjects performed several trials in a block and a trial was terminated upon error. We measured the response times for each successful set in a trial and named these the 'set completion times'. In this experimental paradigm we have only resolution of response times up to the set level rather than up to each key-press level. The response time (RT) is defined as the time taken from the presentation of visual cues to the completion of the set (pressing all corresponding keys in the correct order). In addition to these trial-wise behavioural measures, the repeated measures ANOVA results reported in the Chapter 5, Section 5.3.2 were used to support some of the results on chunking. The focus of the current chapter is to examine the hierarchical organization of sequences by controlling the total number of movements to be learnt.

To study the chunk formation, we employed two strategies. Firstly, we plotted the stacked graph of cumulative set completion times for successfully completed trials. Next, we performed cluster analysis on the cumulative set response times (RT) to identify the pattern of chunking (clusters across the sets). We used a bottom-up hierarchical cluster analysis [refer to, Duda et al. (2001)] to identify the hierarchical sequence structure possibly employed by the subjects. Hierarchical clustering methodology is suitable to address the problem of investigating the chunking processes in sequence learning as sequences can consist of sub-sequences, which in turn could be hierarchically organized.

A graphical representation of the hierarchical organization thus found is depicted as a dendrogram. A dendrogram is essentially a tree structure consisting of many upside-down U shaped lines connecting nodes in a hierarchical tree. For constructing the dendrogram, single-linkage analysis was performed in which the distance between two clusters is taken as the minimum between all pairs of patterns from the two clusters [refer to Jain et al. (1999) for a review of clustering methods]. Single-linkage analysis of cumulative set-completion times would result in the distances shown on the y-axis of dendrogram reflecting the actual set

RTs. The clusters corresponding to the chunks were identified by performing a one-way analysis of variance (ANOVA) on the set completion times between successive sets. A significant pause between sets is identified as the beginning of a new chunk.

6.3 Results

6.3.1 Repeated-measures ANOVA Results

In this section we will substantiate the behavioural results from repeated-measures ANOVA [reported in Chapter 5, Section 5.3.2] to point out spontaneous reorganization in 2x12 compared to 4x6. The smaller value of RT in the 2x12 task compared to the 4x6 in the consolidation stage [refer to Figures 5.6 and 5.7] could possibly point out the benefits of long-range optimization process by chaining (spontaneous reorganization) a number of sets in the form of chunks (Rosenbaum et al., 1983; Sakai et al., 2003).

The repeated measures ANOVA results reported in Chapter 5, Section: 5.3.2 are used in this section. The *post hoc* means comparison for each session across experiments in the repeated measures ANOVA on key-press response times (RT) revealed that the two complex tasks 2x12 and 4x6 were similar in the first session [$F_{(1,96)} = 0.000535$, $p = 0.982$] but were different in session 2 [$F_{(1,96)} = 7.19$, $p < 0.01$], session 3 [$F_{(1,96)} = 11.567$, $p < 0.001$] and became more significantly different by the 4th session [$F_{(1,96)} = 28.360$, $p \ll 0.0001$]. It is interesting to note that the RTs in 2x12 and 4x6 were similar in the first session and became dissimilar by the last session. The RT value in 2x12 was observed to be lesser compared to the RTs of 4x6 task (as reported in the Table 5.3 from the Chapter 5). As the number of sets to be internalized (12) is larger than the short-term memory capacity, it appears that subjects compressed the information into a number of chunks. As the average set RT indicates the time taken to complete a single logical unit (set), the lesser value in RT (compared to the RT values in 4x6 task) by the performance (consolidation) stage may indicate that subjects may be improving the performance by chunking across sets. Similar result (lesser values of RT in 2x12 compared to 4x6 in the consolidation stage) was obtained in the RT values in the consolidation stage (reported in the stage-wise analysis of Chapter 5 and Section 5.3.2).

6.3.2 ANOVA Results across Sequence Conditions

To test for differences in the chunking phenomenon across different sequence conditions, we performed ANOVA on Set RTs taking only data corresponding to successfully completed hypersets from the last session. We assumed that the chunking patterns would have stabilized by the fourth session. ANOVA was performed for each experiment separately with 'set' as main effect. Analysis of variance of set completion times (across subjects) revealed significant main effects for *set* in the 2x6 [$F_{(5,96)} = 7.93, p < 0.0001$] and 2x12 [$F_{(11,192)} = 2.32, p = 0.01$] experiments but not for the 4x6 experiment [$F_{(5,96)} = 0.23, p = 0.95$]. This indicates that chunking phenomenon across sets is less likely to happen in the 4x6 task. The visualisation of this behaviour and more formal quantification of these observations are described in the next section.

6.3.3 Quantifying the Chunking Phenomenon

Subjects showed learning related improvements by successfully acquiring the hyperset. This was also reported in Chapter 5, but here we present the trial-wise data of the behavioural parameters, namely, number of sets completed and set response time. Figure 6.1 shows the number of sets completed and the average set completion time for all the trials of one subject (WY) for the 2x6, 4x6 and 2x12 tasks (note that the resolution of measurement of learning is at the trial level).

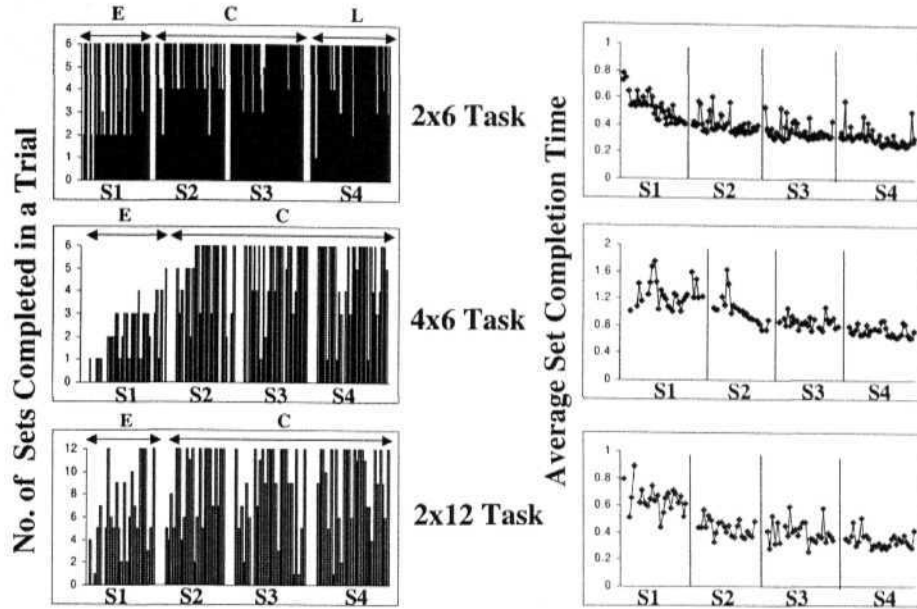


Figure 6.1: Learning related improvements observed in the three raxrc tasks for one subject (WY). Number of sets completed (*left panel*) and average set completion time (*right panel*) over all the trials across the four sessions (S1 to S4) are shown. Vertical lines in the *right panel* and the gaps in the *left panel* corresponds to the session-to-session demarcation. The Early (E), Consolidation (C) and Late (L) stages (in *left panel*) are also indicated along with the session index (S1, S2, S3 and S4).

Out of the 18 subjects that participated in our experiments, we report in detail the results from three representative subjects (KU, NS and WY) for analyzing the chunking phenomenon. These subjects have more number of successful trials in the last session. Other subjects have fewer number of trials in the last session for 2x12 and 4x6 tasks. For better demonstration of chunking phenomenon and statistics we selected these three subjects. The stacked graphs shown in Figure 6.2a reveal a clear bunching pattern evolving as training progressed in the 2x12 task. Each bunch represents a chunk. The data of set RTs from the last session was used for identifying chunking patterns. ANOVA between successive set RTs revealed significant ($p < 0.05$) pauses for several sets representing the beginning of an ensuing chunk. For example, KU: set 3, 8; NS: sets 3, 6, 8, 12; WY: set 7. The

dendrogram plots (2nd row of Figure 6.2a&b) show the hierarchical structuring of the sequence and thus reveal sub-sequences within the cluster identified from the ANOVA. Although ANOVA revealed main cluster patterns, it is interesting that the complete hierarchical sequence structure can be identified by the dendrogram. For example, the nested sequential structure for KU is (1 2) 3 (4 (5 (6 7)) 8 (9 10) (11 12)) and for WY is ((1 2) 3 (4 (5 6)) (7 (8 9)) ((10 11) 12).

Figure 6.2b shows the chunking phenomenon for the 4x6 task for the same three subjects. The cumulative set RTs (Figure 6.2b) did not show any bunching pattern across sets. The dendrogram shows that subjects require similar amount of time for completion of each set. The ANOVA results revealed non-significant p values for all pairs of successive set RTs, thus possibly indicating the absence of any significant pauses during sequence acquisition. Most of the other 14 subjects also displayed chunking phenomenon in the 2x12 task and less in the 4x6 task. Across all the subjects for each task the chunk size varied from 1 to 3 in the 2x6 task, 2 to 4 in the 2x12 task and 0 to 3 in the 4x6 task. Thus across set reorganization of the sequential information is likely in the 2x12 and 2x6 tasks but less likely in the 4x6 task.

6.4 Summary and Conclusions

Chunking offers a flexible way of learning. We have demonstrated that subjects employed different reorganization patterns when the same number of finger movements was arranged in two different ways. Our results suggested that when the *set-size* was larger as in the 4x6 task, there was less reorganization across sets. Subjects had to process more amount of information in each set and because of the increased short-term cognitive load, it appears that performance optimization might possibly have occurred more within the sets but less across the sets. This is consistent with the theory of limited capacity of working memory of Miller (1956). Recent fMRI investigations by Owen (2004) and Todd and Marois (2004) also support the effects of limit on working memory capacity we pointed out in our results. On the other hand, when the *set-size* was kept smaller but the number of sets to be processed was increased as in the 2x12 task, we observed remarkable reorganization across sets. As the number of sets to be internalized (12) is larger than the short-term memory capacity, it appears that subjects compressed the

information into a number of chunks.

The results from the current behavioural study have implications for the cognitive models of hierarchical sequence learning. The results also point out that a *neural network model* that learns sequences using a limited capacity working memory (WM) would need to optimize in two different ways depending on the amount of information to be processed at any instance of time. If the amount stretches beyond the limit of WM then optimization process needs to operate within the logical unit (set). If the amount is well within the WM capacity, optimization across the logical units (sets) would facilitate efficient performance. Some of these findings have been reported in Pammi et al. (2003), 2004a,c, 2005). Neural bases for the chunking phenomenon have been suggested to be located in various brain areas including the pre-supplementary motor area, (Kennereley et al., 2004), lateral prefrontal cortex (Bor et al., 2004) and the basal ganglia (Graybiel, 1998). Our aim in the subsequent chapters is to analyze the fMRI results with a view to identifying brain areas participating in the process of coping with complexity and also in the chunking process.

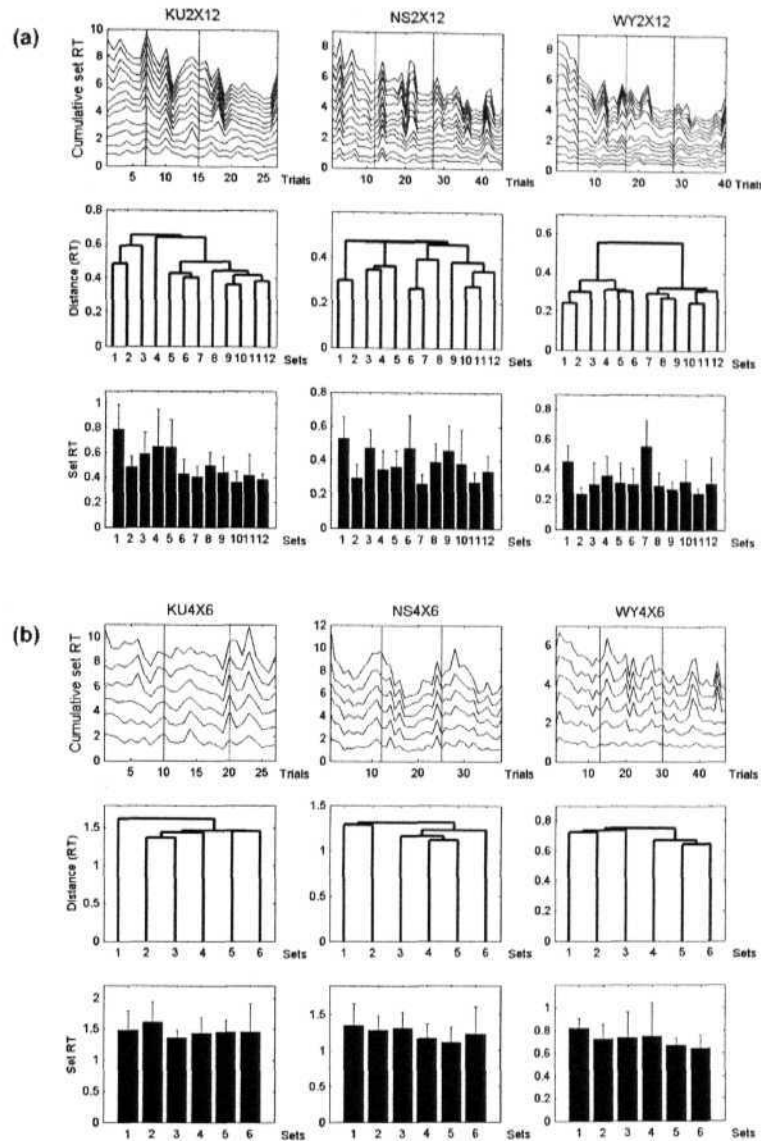


Figure 6.2: Chunking phenomenon observed in three subjects (KU, NS, WY) for the 2x12 and 4x6 tasks. *top panel:* The cumulative set RTs for successful trials for all the sessions (delineated by vertical lines), *middle panel:* dendrogram, *bottom panel:* mean set RTs in the last session. (a) 2x12 Task. Cumulative set RTs show a clear bunching pattern for few sets of 2x12 task. The dendrogram shows the hierarchical structure of the sequence acquired by the subject. (b) 4x6 Task. The cumulative set RTs for successful trials do not show any bunching pattern across sets. The dendrogram shows that subjects require similar amount of time for each set.

Chapter 7

Imaging Results

This chapter reports results of analysis of functional Magnetic Resonance images (fMRI) collected in the complexity experiment. The image analysis was performed in SPM99 (refer to Appendix D for details of Statistical Parametric Mapping framework SPM99), developed by the Wellcome Department of Imaging Neuroscience, University College London.

In this thesis, the objective is to investigate the effects of increasing sequence complexity while human subjects acquired and performed complex sequential skill. The current study is the first- of its kind investigating two dimensions of complexity using trial-and-error sequence learning in a single experimental design. The behavioural results described in Chapter: 5 revealed that the subject-specific demarcation into learning stages is justified based on the statistical results performed on the behavioural parameters (success rate and key-press response time). In addition to the results of learning related improvements observed in each of the sequence learning tasks, the behavioural results also point to the reorganizational differences among complex conditions (2x12 and 4x6). As the main aim of this thesis is to investigate the effects of complexity (i.e., comparison of complex sequence learning conditions with the simple sequence learning condition), the imaging results from these comparisons (i.e., 2x12 and 4x6 with respect to 2x6) are primarily used for major conclusions.

The results from Random Effects Analysis (RFX) analysis of comparisons of complex sequence learning conditions (2x12 and 4x6) with 2x6 in both the stages (*effects of sequence complexity* and the RFX analysis of *direct comparisons* of complex sequence learning conditions (2x12 versus 4x6 and 4x6 versus 2x12 in

both the stages) for both the learning stages are reported in this chapter. The results from Random Effects Analysis (RFX) of comparisons of sequence learning conditions with Control/Follow condition (*basic comparisons*) in both the early & consolidation stages are reported and highlighted separately in Appendix E. The imaging results from the comparison of 2x6 task with complex sequence tasks in both the stages are reported in Appendix F. The general description of various fMRI imaging methodologies, including the RFX analysis, is given in Chapter: 3. The step-by-step procedure used in SPM99 is described in Appendix D.

7.1 fMRI Results

In this thesis we wished to explicitly model the *behaviour related brain activation* in all the sequence tasks in both the stages of learning and performance (i.e., Early and Consolidation) while analyzing the fMRI images. This *behaviour or learning related brain activation* is modelled with the help of *set* and *hyperset* response times (RTs). These RTs are entered into the design matrix of SPM99 as 'user specified regressors'. These regressors would model variations within the sessions and also between sessions (i.e., stages) in an experiment.

We used the following methodology to come up with a meaningful summary of our neuroimaging results. First, we compared all the sequence learning tasks to the control or baseline condition. Activations are listed in Tables E.1, E.2, E.3, E.4, E.5, E.6 in Appendix E (these are listed in the Appendix to avoid clutter in the reporting of results) to identify any area, that was engaged by the three conditions (2x6 or 2x12 or 4x6). We used this to constrain the search for differences among the three conditions. As the aim of this investigation is to probe the neural correlates of the effects of complexity (4x6 versus 2x6 & 2x12 versus 2x6) during learning (Early) and performance (Consolidation) stages, we confined our summary primarily to the findings from Early 4x6>2x6, Early 2x12>2x6, Consolidation 4x6>2x6 and Consolidation 2x12>2x6 regressor contrasts (refer to Tables 7.1, 7.2 and Figures 7.2, 7.3, 7.4, and 7.5). These findings are further supplemented by the difference between 4x6 and 2x12 directly (listed in Tables 7.3 & 7.4, Figures 7.6, 7.7, 7.8, and 7.9 and the brain renderings shown in Figures 7.10 & 7.11). This method of summarization of results enabled us to make inferences about the selective recruitment of the systems involved in the two

forms of complexity.

The results from the random effects analysis for 17 subjects from the two design matrices (i.e, 2x6-4x6 and 2x6-2x12) are summarized in the form of tables listing *stereotaxic Talairach coordinates* of all the peak activations obtained at a threshold of $T > 3.69$ ($p < 0.001$ uncorrected for multiple comparisons). The common method of locating brain activations is by using the Talairach atlas labels (Talairach and Tournoux, 1988), which has Brodmann areas labelled along with the area names (with gyri or sulci labels). SPM99 uses the standard brains from the Montreal Neurological Institute (MNI) space. Using this template SPM99 reports results in MNI coordinates. The corresponding Talairach coordinates were obtained by using the non-linear transformation (Brett et al., 2001) to convert MNI coordinates into Talairach coordinates. The anatomical labels for these coordinates were obtained using the Talairach daemon software (Lancaster et al., 2001), MRIcro (Rorden, 2004) AAL & brodmann templates and manually checking with the talairach atlas (Talairach and Tournoux, 1988).

The first three columns of each table list the categorized Brain area label, hemisphere in which activation is found (Right or Left) and the Brodmann area (BA). X, Y, Z indicate coordinates in *mm* as referenced in the atlas by Talairach and Tournoux (1988). The T-Score is the statistic score computed by SPM, which signifies the strength of activation.

The brain images shown in Figures 7.2-7.9 are the activity maps along with their statistical significance (measured with the help of T-Score). The activations obtained from the respective RFX contrasts are overlaid onto one of the subjects' normalized (to MNI space) high-resolution brain using a modified MATLAB script (Christoff, 2001).

7.2 Basic comparison results

The basic comparison results are obtained from the contrast images of every subject by taking them to the second level and performing one-sample t-test. For every sequence condition with respect to the baseline/follow, we obtained activations and deactivations corresponding to the contrasts of interest. For example, activation: Early 2x6>Control and deactivation: Early Control>2x6. The Talairach coordinates listed in Tables E.1, E.2, E.3, E.4, E.5, E.6, are the local

maxima of activations and deactivations of sequence/task related (2x(i, 2x12, 4x6) regressor contrasts with respect to the Control/Follow condition in both the Early and Consolidation stages.

These activations tabulated in basic comparisons only guided us to have an idea about the brain activity specific to the sequence learning tasks. Further probing into the comparisons gave us more informative or focussed picture, which allowed us to compare the tasks.

7.2.1 Detailed description of basic comparison results

In this section we will point out interesting findings from the basic comparison results (i.e., comparison of sequence learning tasks with the control/follow condition). The brain areas obtained in these comparisons could be related to their role in the sequential skill learning as demanded by the tasks. Though we observed several brain area activations in all the three tasks in both the learning stages, we will highlight some interesting findings.

The cerebellar activations (anterior and posterior) showed differential effects in the 2x12 task. In the early stage activity in these areas was absent, whereas in the consolidation stage both the anterior and the posterior lobules of cerebellum are active.

Another interesting finding is the differential activation of the various areas of striatum during the early and the consolidation phases. We observed selective activation of the right putamen/globus pallidus in the 2x6 and 2x12 tasks in the consolidation stage but not in the early stage. Interestingly, the activity (dorsal) in this area was not seen in the consolidation stage of 4x6. Another notable observation is the bilateral ventral striatum activation in both the early and consolidation stages of 4x6 and 2x12 tasks but not in the 2x6 task. We also observed activation of caudate head in the dorsal striatum in both the early and consolidation stages of 4x6 task but not in 2x12 task.

The Hippocampus is found to be active exclusively in the early stage of 2x12. However, this area got suppressed (control/follow>sequence/test comparison) more in the early stage of 2x6 and 4x6 tasks.

We noticed the activation of contralateral (left) primary motor cortex [Brodmann's area 4]

mann area (BA 4] in the consolidation stages of 2x6 and 4x6 tasks. The activation was not observed in both the stages of 2x12 task and in the early stage of 2x6 and 4x6 tasks.

In the frontal cortex, an exclusive activation of the right dorsolateral prefrontal cortex (BA 46/9) was found in the consolidation stage of 4x6 and in the early stage of 2x6.

We observed the pre-supplementary motor area (BA 6), the bilateral dorsal premotor (BA 6) and the bilateral precuneus (BA 7) activations in all the sequence learning tasks in both the stages. The bilateral precuneus and the right dorsal premotor in the early stage of 4x6 also survived whole brain correction for multiple comparisons ($p < 0.05$). In addition, the left middle occipital gyrus (BA 18/19), the left precuneus and the right dorsal premotor areas in the consolidation stage of 4x6 are also survived the correction (indicated by *bold* T-values in the tables) for multiple comparisons ($p < 0.05$). The supplementary motor area was observed to be activated only in the consolidation stages of 2x6 and 2x12 tasks but not in the 4x6 task. Another interesting observation is the activation of the rostral cingulate motor area only in the consolidation stage of complex sequence learning tasks (2x12 and 4x6) but not in the early stages.

7.2.2 Summary of basic comparison results

The basic comparison analysis resulted in some notable differences in the whole brain activations. The cerebellar activations were found to be more specific to the consolidation stage of 2x12 task than the earlier stage. This may point out, its role in the retrieval processes associated with long-range sequences. The striatal activations revealed possible functional specializations. The ventral striatum is associated more with the complex tasks than simple ones, the right dorsal putamen/globus pallidus is specific to the consolidation stages of 2x6 & 2x12 tasks and the right dorsal caudate is related to the consolidation stage of 4x6 task. The results on differential roles of striatum are also reported in Pammi et al. (2004d). Interestingly, the hippocampus activated exclusively in the early stage of 2x12 task and this may be related to long-range sequence learning. The primary motor activation was observed to be more specific to the consolidation stages of 2x6 and 4x6. The activations in the parietal and related motor areas suggest that the precuneus and the right dorsal premotor areas are more associated with the

4x6 task, the supplementary motor area involved specifically in the retrieval process of short-set sequences, the rostral cingulate motor area more specific to the retrieval process in complex tasks.

7.3 Comparisons between the sequence tasks

Comparisons between the sequence conditions are obtained by taking the contrast images of every subject to the second level and performing two-sample t-test (for example, refer to Figure 7.1). The comparisons could be between 2x12 with 2x6 (from the 2x6-2x12 design matrix) or with 4x6 with 2x6 (from the 2x6-4x6 design matrix) or 2x12 with 4x6 (the respective contrasts obtained from the 2x6—2x12 and 2x6—4x6 design matrices). These comparisons between the sequence tasks allowed us to probe into the effects of the two dimensions of complexity, namely, set related and hyperset related complexity. The talairach coordinates listed in Tables 7.1, 7.2, 7.3 and 7.4, are the local maxima, activations of comparison between the tasks in both the early and consolidation stages. The brain activations for comparisons between the tasks in both the learning stages are shown in the Figures 7.2—7.5. Direct comparison results are shown in Figures 7.6—7.9 and the 3-dimensional surface rendered (on one of the subject's extracted brain) activations for the early and consolidation stages for complex sequence conditions (2x12 versus 4x6) are shown in Figures 7.10 and 7.11, respectively. The comparisons of 2x6 task with the complex sequence tasks are reported separately in Appendix F (tables F.1, F.2).

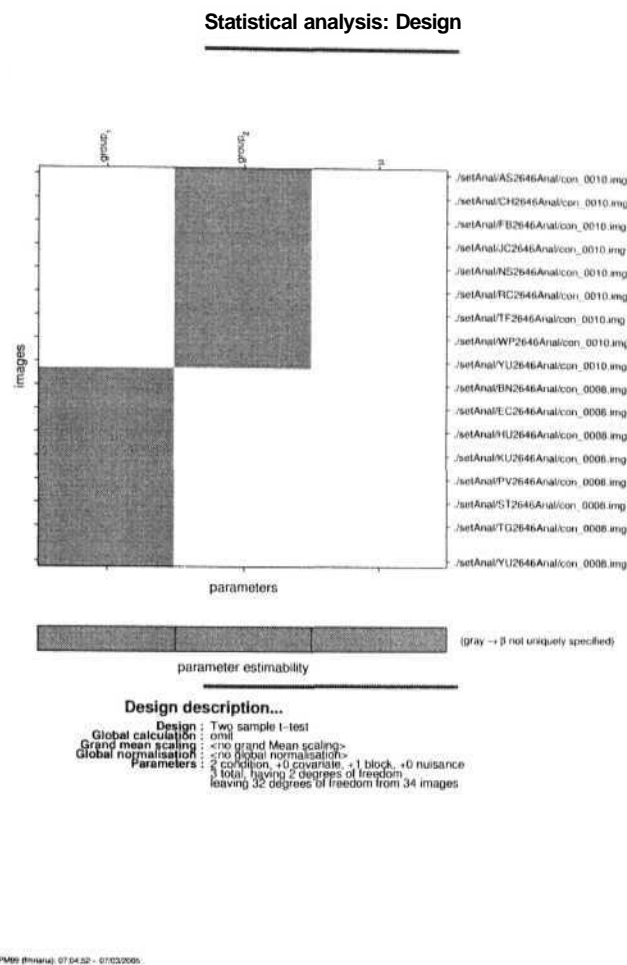


Figure 7.1: The example Design matrix in RFX analysis of Sequence conditions. The contrast images of every subject for the two sequence task conditions were taken to the second level and two-sample t-test was performed.

7.3.1 Detailed description of results from comparison between sequence learning tasks

As the objective of this research is to investigate the effect of change in complexity of the skill being acquired on the pattern of brain activation, we based our findings on the activations obtained from the behaviour related comparisons of Early 4x6>2x6 (refer to the Table 7.1 and Figure 7.2), Early 2x12>2x6 (refer to the Table 7.1 and Figure 7.3), Consolidation 4x6>2x6 (refer to the Table 7.2 and Figure 7.4) and Consolidation 2x12>2x6 (refer to the Table 7.2 and Figure 7.5). The results reported in the tables meet the following criteria: consistency of

activation, a reasonably high T-score, and a minimum of area of activation of greater than or equal to 5 voxels. Thus the results reported in the tables are taken as important set of areas and the brain slice pictures show the location and extent of activation.

Detailed description of brain activations obtained from the learning related comparisons between complex sequence conditions with the simple sequence condition i.e., 2x6 are as follows. We observed activations in ipsilateral (right) primary motor area [brodmann area (BA) 4], ipsilateral post, central gyrus (BA 2/5), contralateral (left) insula, ipsilateral dorsal premotor (BA 6), ipsilateral anterior cerebellum, medial superior frontal gyrus (BA 9), contralateral caudate body, contralateral sensorimotor cortex (BA 3/4), lingual gyrus (BA 18) and left, orbitofrontal cortex (BA 11) in the early stage comparisons of 4xi with 2x0.

The early stage comparison of 2x12 task with 2x6 revealed activations in the right supramarginal gyrus (BA 39/40), medial posterior cingulate gyrus (BA 23/31), left hippocampus, left ventral middle temporal gyrus (BA 21), left cuneus (BA 23/18) near parieto-occipital sulcus, medial superior frontal gyrus (BA 8), bilateral inferior parietal cortex (BA 40), left middle temporal gyrus (BA 39), left orbitofrontal cortex, right fusiform gyrus (BA 39) and the left insula.

The consolidation stage results between 4x6 compared with 2x6 activations revealed activations in the contralateral (left) caudate body (anterior striatum), right fusiform gyrus (BA 37), contralateral (left) primary motor cortex (BA 4), contralateral sensori cortex (BA 2/3) and contralateral dorsolateral prefrontal cortex (BA 9/46).

The consolidation stage results of 2x12 task compared with 2x6 task, revealed activations in the ipsilateral inferior frontal cortex (BA 45/47), right cuneus (BA 18/19) near parieto-occipital sulcus, right superior parietal cortex (BA 7), ipsilateral posterior cerebellum, ipsilateral postcentral gyrus (BA 5/2) and the contralateral middle occipital gyrus (BA 19).

As the results reported are uncorrected p values for multiple comparisons, we also performed *small volume correction (SVC)* to make our interpretations more acceptable. We applied SVC to the cluster centered at the coordinates over marginal spherical region of interest of size 5 mm [refer to a. recent reference Schendan et al. (2003) for the reporting of SVCs]. All the coordinates reported

from regressor contrasts early 4x6>2x6, early 2x12>2x6, consolidation 4x6>2x6, consolidation 2x12>2x6 survived the SVC and their adjusted p values obtained were reliable at $p \leq 0.05$.

Table 7.1: Location of Stereotaxic Talairach coordinates of peak activations in the Early 4x6>2x6 Regressor and the Early 2x12>2x6 Regressor Contrasts

Brain Area	R/L	BA	Early 4x6>2x6 R				Early 2x12>2x6 R			
			Coordinates			T-Score	Coordinates			T-Score
			X	Y	Z		X	Y	Z	
Cerebellum										
Anterior lobule (Culmen)	R		26	-54	-28	4.22				
Basal ganglia										
Caudate body	L		-20	18	14	3.95				
Hippocampus	L						-34	-22	-16	4.64
Occipital areas										
Lingual gyrus	L	18	-6	-72	-5	3.95				
Temporal areas										
Middle Temporal gyrus	L	21					-57	-5	-22	4.62
	L	39					-46	-61	27	3.59
Fusiform gyrus	R	37					32	-49	-13	3.87
Parietal areas										
Supramarginal gyrus	R	39/40					46	-53	32	5.34
Inferior Parietal cortex	L	39/40					-48	-34	22	3.79
	R	40					42	-41	28	3.7
Cuneus	L	23/18					-4	-67	25	4.28
Sensory and Motor areas										
Precentral gyrus	R	4	30	-19	53	5.1				
Postcentral gyrus	L	3/4	-42	-17	51	3.85				
	R	2/5	22	-36	57	4.39				
Premotor (dorsal)	R	6	22	4	48	4.28				
Cingulate gyrus (posterior, medial)	L	23/31					-2	-45	32	5.04
Frontal areas										
Superior frontal gyrus (medial)	L	8					-8	43	46	4.07
	L	9	-6	50	29	4.06				
Insula	L	47	-26	27	6	4.31				
	L	47					-26	27	6	4.13
Orbitofrontal cortex	L	11					-18	40	-12	3.97
	L	11	-20	38	-12	3.49				

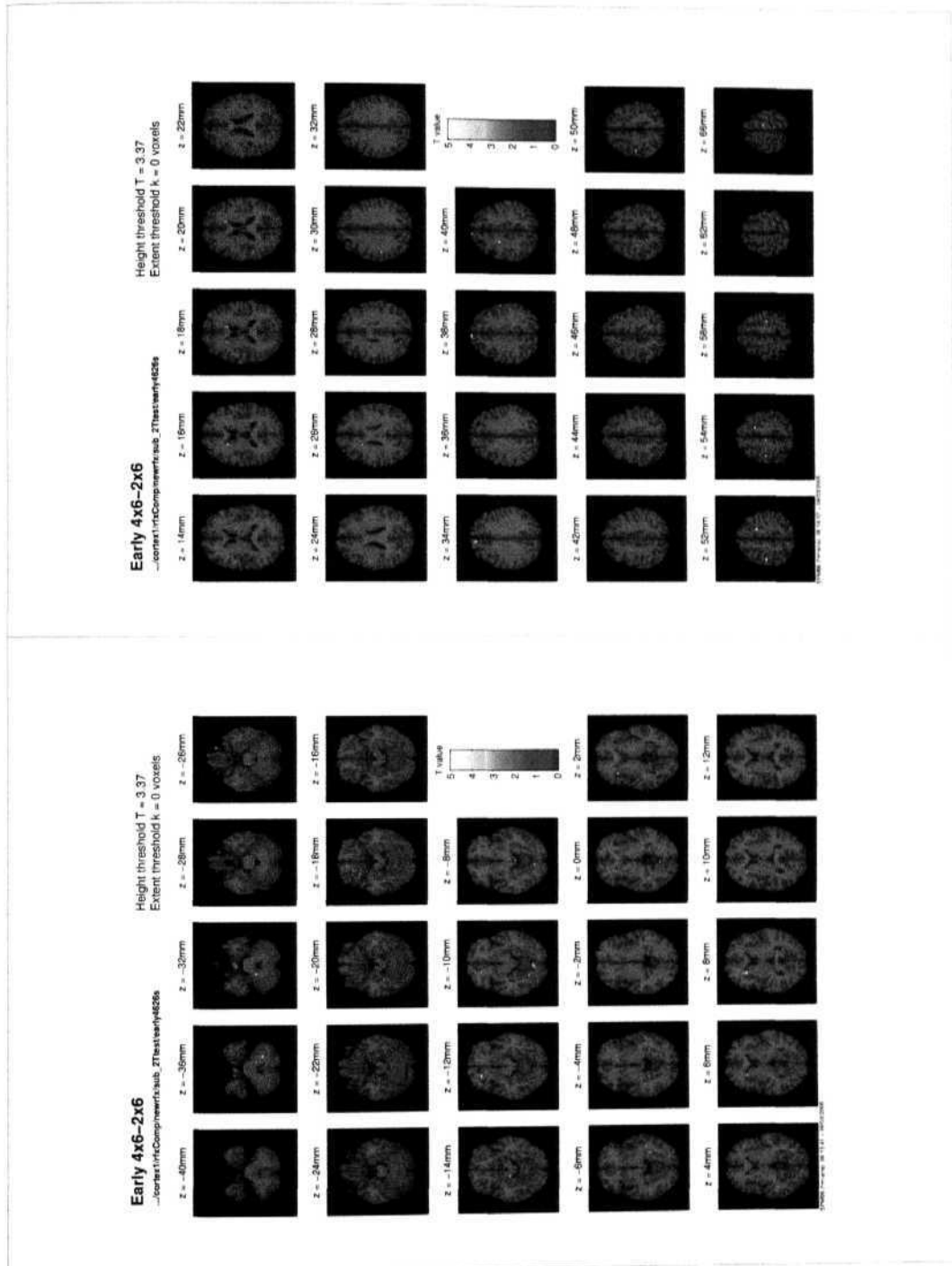


Figure 7.2: Early 4x6>2x6 Regressor contrast activations

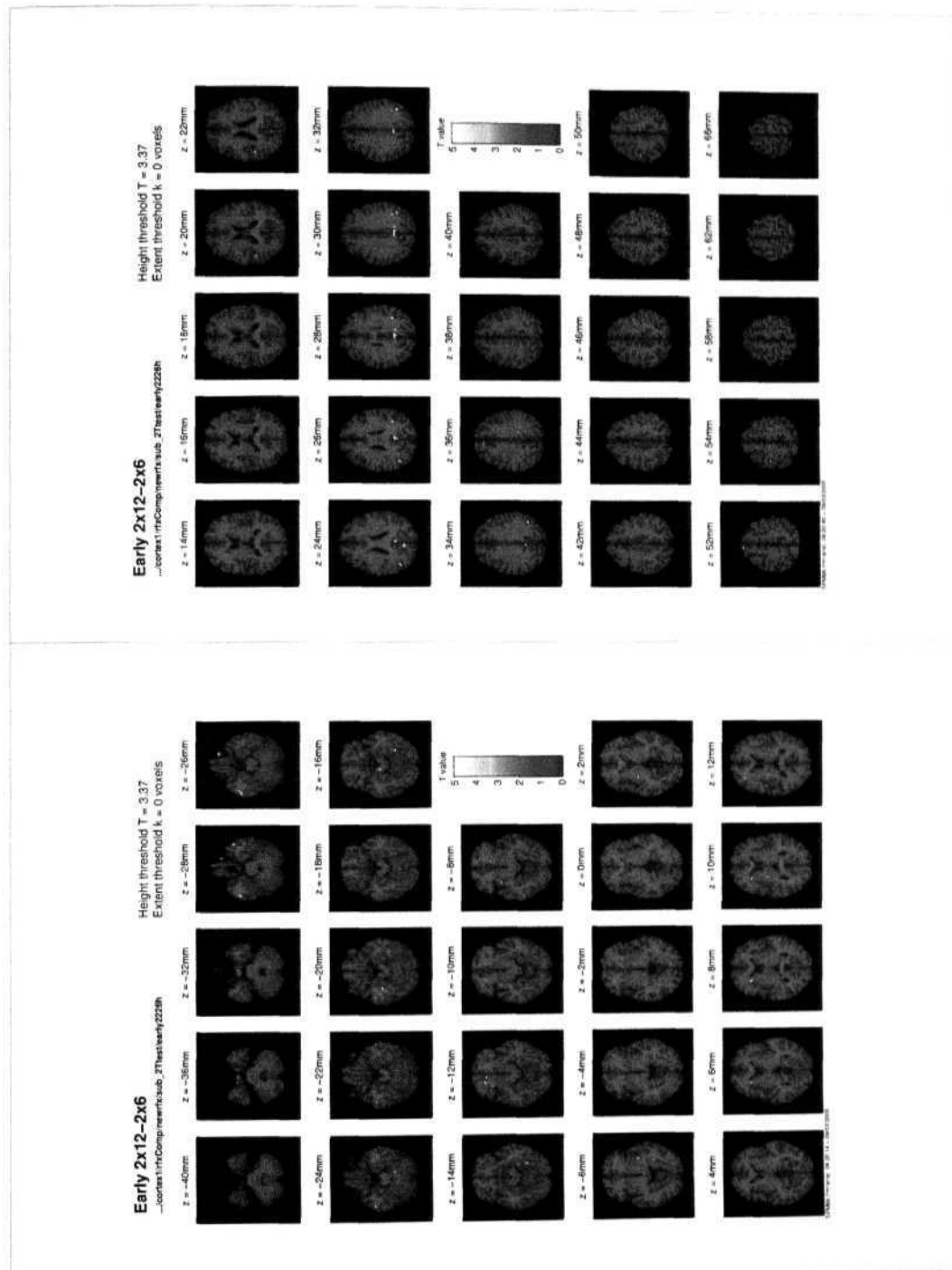


Figure 7.3: Early 2x12>2x6 Regressor contrast activations

Table 7.2: Location of Stereotaxic Talairach coordinates of peak activations in the Consolidation 4x6 > 2x6 Regressor and the Consolidation 2x12 > 2x6 Regressor Contrasts

Brain Area	R/L	BA	Consolidation 4x6>2x6 R				Consolidation 2x12>2x6 R			
			Coordinates			T-Score	Coordinates			T-Score
			X	Y	Z		X	Y	Z	
Cerebellum										
Posterior lobule (Uvula)	R						18	-79	-23	3.81
Basal ganglia										
Caudate body	L		-14	14	7	5.29				
Occipital areas										
Middle Occipital gyrus	L	19					-34	-72	4	3.98
Temporal areas										
Fusiform gyrus	R	37/20	44	-32	-10	4.52				
Parietal areas										
Cuneus	R	18/19					20	-72	28	4.09
Superior Parietal cortex	R	7					30	-47	61	3.61
Sensory and Motor areas										
Precentral gyrus	L	4	-38	-13	50	3.88				
Postcentral gyrus	L	2/3	-55	-23	45	4.19				
	R	5/2					20	-45	67	3.57
Frontal areas										
Inferior frontal gyrus	R	45/47					32	29	6	4.15
Dorsolateral prefrontal cortex	L	9/46	-24	35	30	3.75				

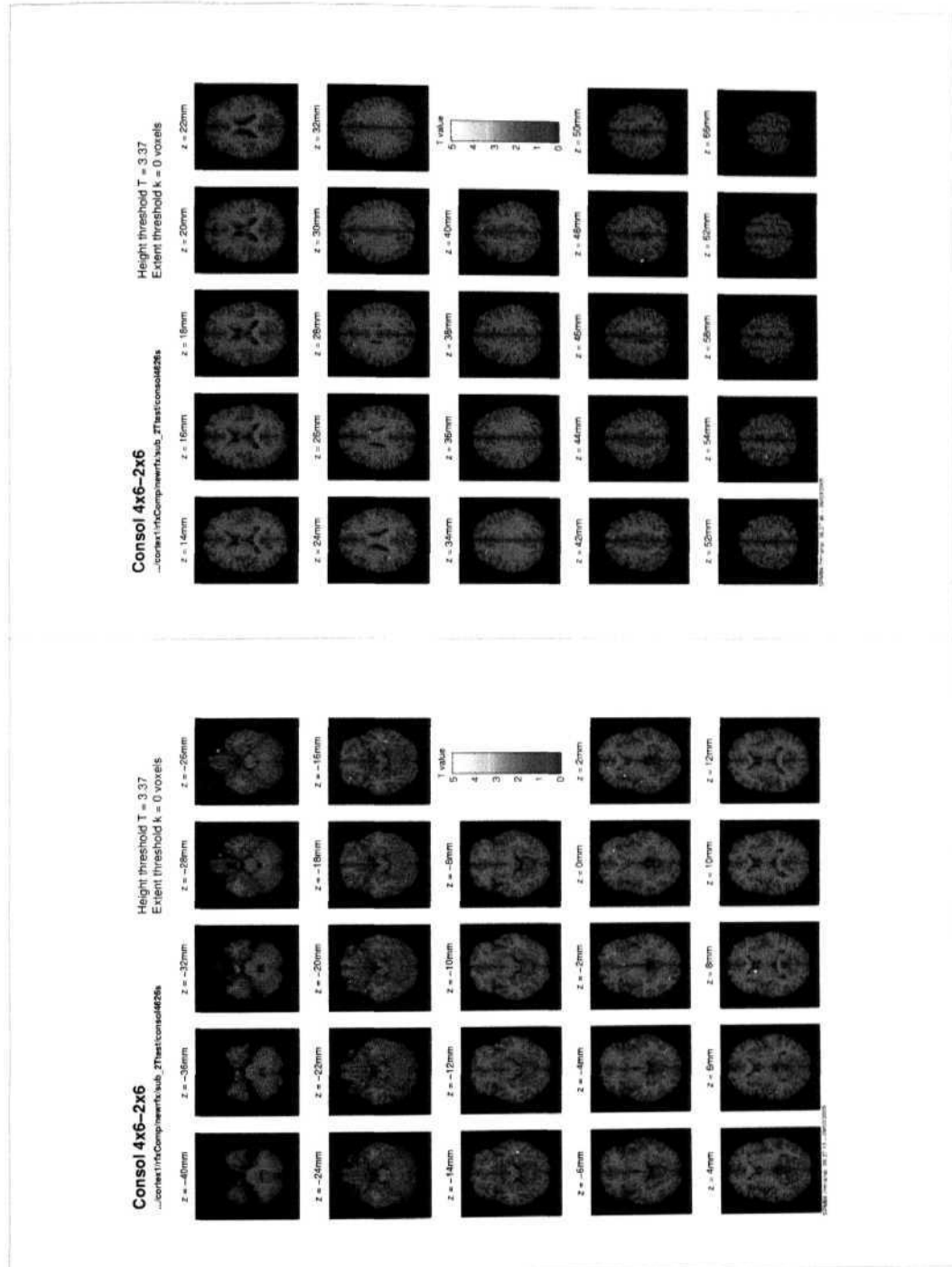


Figure 7.4: Consolidation 4x6>2x6 Regressor contrast activations

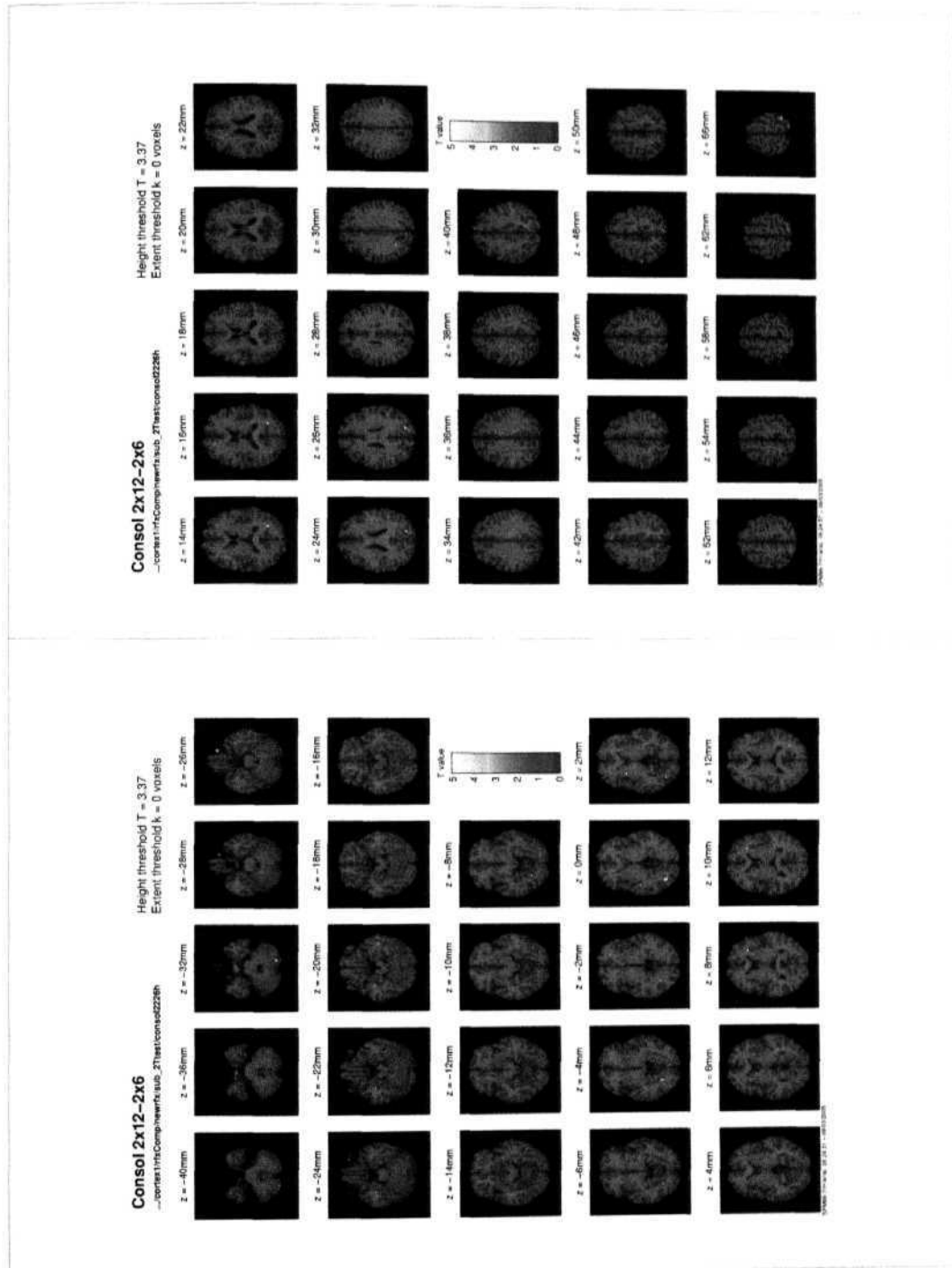


Figure 7.5: Consolidation 2x12>2x6 Regressor contrast activations

7.3.2 Results from direct comparisons of complex conditions

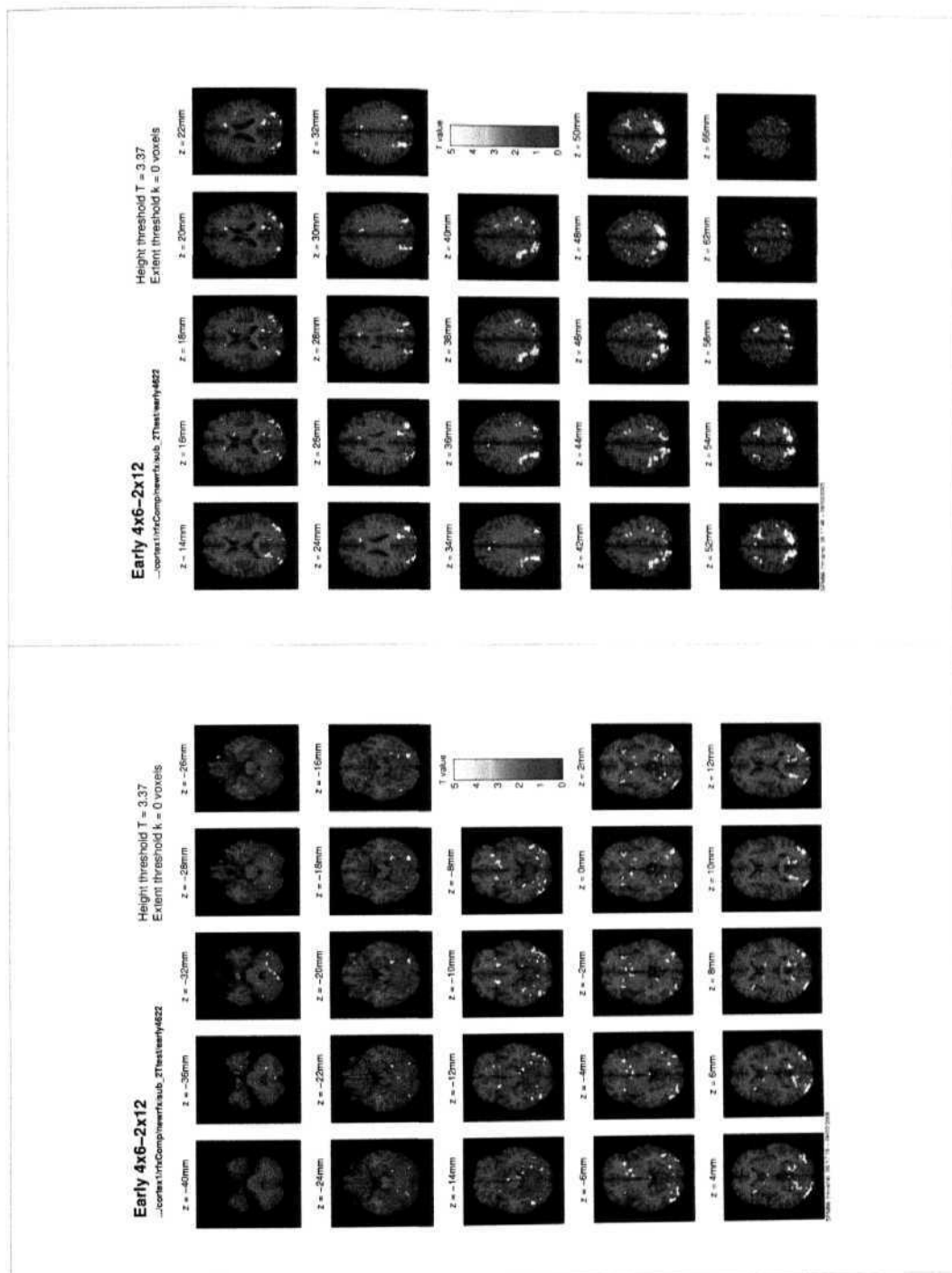
The direct subtraction of complex sequence learning conditions revealed distinct set of brain areas related to 4x6 and 2x12 in both the stages of learning. The results from these comparisons are reported in the Tables 7.3 and 7.4. The brain activations on the transverse slices shown in the Figures 7.6 and 7.9. The 3-D renderings of activations for the early and the consolidation stages separately shown in the Figures 7.10 and 7.11. Interestingly, though we compared 2x6 task with 2x12 and 4x6 (complex sequence learning tasks in two design matrices), the brain activations obtained in the 2x6 tasks in (both stages of learning) in both the design matrices are the *same*. This result enabled the cross comparison of 2x12 versus 4x6 to be meaningful.

The early stage results of 4x6 compared with the 2x12 task revealed activations in the ipsilateral cerebellum, contralateral ventral striatum, contralateral caudate, bilateral middle occipital gyrus [brodmann area (BA) 19], bilateral precuneus (BA 7), bilateral superior parietal cortex (BA 7), ipsilateral dorsal premotor (BA 6), right lateral orbitofrontal cortex (BA 47) and left lateral superior frontal cortex (BA 8/6). It is interesting to note that the activations in left ventral striatum, right middle occipital gyrus, bilateral precuneus, bilateral superior parietal cortex, right dorsal premotor and the left superior frontal cortex (near premotor area) also survived whole brain correction for multiple comparisons ($p < 0.05$). The early stage results of 2x12 compared with the 4x6 task revealed activations in the left caudate tail, left hippocampus, left superior temporal gyrus (BA 22), left middle temporal gyrus (BA 21), right inferior temporal gyrus (BA 20/21), bilateral inferior parietal cortex (BA 40), bilateral supramarginal gyrus (BA 39/40), medial posterior cingulate gyrus (BA 31), left lateral orbitofrontal cortex (BA 11), bilateral superior frontal cortex (BA 9/8). It is interesting to note that the activations in left hippocampus, left caudate tail and left inferior parietal cortex survived whole brain correction for multiple comparisons ($p < 0.05$).

The consolidation stage results of 4x6 compared with the 2x12 task revealed activations in ipsilateral lateral anterior cerebellum, bilateral caudate head, bilateral occipital gyrus (BA 18/19), bilateral thalamus (pulvinar), bilateral precuneus (BA 7), bilateral superior parietal cortex (BA 7), anterior cingulate (BA 32) and ipsilateral dorsal premotor (BA 6), contralateral primary motor cortex (BA 4), pre-supplementary motor area and right orbitofrontal cortex (BA 47). Activation in the right dorsal premotor (BA 6) area and left occipital gyrus (BA 18) survived whole brain correction for multiple comparisons ($p < 0.05$). The consolidation stage results of 2x12 compared with the 4x6 task revealed activations in bilateral middle temporal gyrus (BA 21/20), left superior temporal gyrus (BA 22), left supramarginal gyrus (BA 40/39), bilateral inferior parietal cortex (BA 40), right middle frontal gyrus (BA 8) and left inferior frontal gyrus (BA 45).

Table 7.3: Location of Stereotaxic Talairach coordinates of peak activations in the Early 4x6>2x12 Regressor and the Early 2x12>4x6 Regressor Contrasts. Bold faced T-score indicates that the activation survived whole brain correction for multiple comparisons at $p < 0.05$.

Brain Area	R/L	BA	Early 4x6>2x12 R				Early 2x12>4x6 R			
			Coordinates			T-Score	Coordinates			T-Score
			X	Y	Z		X	Y	Z	
Cerebellum										
Anterior lobule (Culmen)	R		26	-58	-24	6.17				
Basal ganglia										
Putamen	L		-18	11	-11	7.79				
Caudate tail	L						-16	-28	22	6.79
Caudate Head	L		-8	6	0	5.5				
Hippocampus	L						-28	-7	-16	8.01
Occipital areas										
Middle Occipital gyrus	R	19	36	-85	15	7.39				
	L	19	-36	-87	8	5.84				
Temporal areas										
Superior Temporal gyrus	L	22					-50	-56	14	5.52
Middle Temporal gyrus	L	21					-57	-28	-9	5.67
Inferior Temporal gyrus	R	20/21					57	-3	-28	4.06
Parietal areas										
Precuneus	R	7	14	-66	49	8.63				
	L	7	-8	-66	46	7.96				
Superior Parietal cortex	L	7	-18	-61	53	6.74				
	R	7	10	-61	53	6.51				
Inferior Parietal cortex	L	40					-57	-51	38	7.85
	R	40					53	-58	40	5.01
Supramarginal gyrus	L	40/39					-57	-49	26	5.33
	R	39/40					50	-53	25	4.77
Sensory and Motor areas										
Premotor (dorsal)	R	6	26	6	51	8.85				
Cingulate gyrus (posterior, medial)	L	31					-8	-49	28	6.11
Frontal areas										
Orbitofrontal cortex	R	47	34	25	-6	5.46				
	L	11					-44	42	-14	4.58
Superior frontal gyrus	L	8/6	-24	16	49	7.32				
	L	9/8					-22	46	36	5.53
	R	8/9					18	41	40	4.36



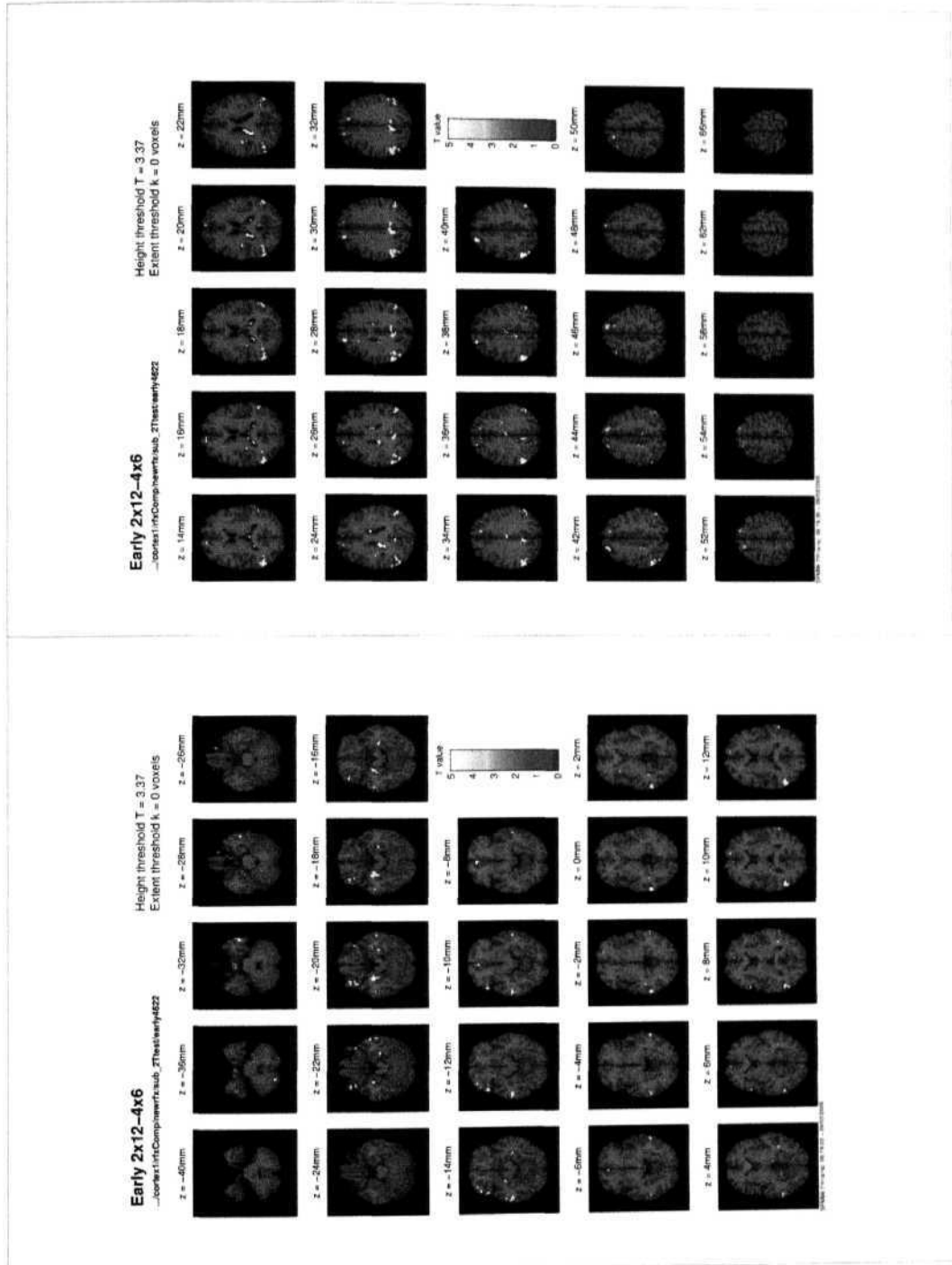


Figure 7.7: Early 2x12>4x6 Regressor contrast activations

Table 7.4: Location of Stereotaxic Talairach coordinates of peak activations in the Consolidation 4x6>2x12 Regressor and the Consolidation 2x12>4x6 Regressor Contrasts. Bold faced T-score indicates that the activation survived whole brain correction for multiple comparisons at $p < 0.05$.

Brain Area	R/L	BA	Consolidation 4x6>2x12 R				Consolidation 2x12>4x6 R			
			Coordinates			T-Score	Coordinates			T-Score
			X	Y	Z		X	Y	Z	
Cerebellum										
Lateral Anterior lobule	R		40	-59	-24	6.00				
Basal ganglia										
Caudate Head	R		4	14	1	4.83				
	L		-6	12	-2	4.02				
Occipital areas										
Middle Occipital gyrus	L	18	-30	-93	12	6.86				
	R	19	30	-86	19	5.01				
Thalamus (Pulvinar)	L		-20	-26	16	5.56				
	R		24	-26	16	5.37				
Temporal areas										
Middle Temporal gyrus	R	21/20					48	-1	-29	7.11
	L	21					-59	-37	-2	5.59
Superior Temporal gyrus	L	22					-55	-57	16	5.89
Parietal areas										
Precuneus	L	7	-26	-68	38	6.17				
	R	7	12	-68	46	6.1				
Superior Parietal cortex	R	7	12	-61	55	5.09				
	L	7	-16	-65	55	4.58				
Supramarginal gyrus	L	40/39					-46	-49	36	5.03
Inferior Parietal cortex	L	40					-53	-58	40	4.78
	R	40					50	-60	40	4.53
Sensory and Motor areas										
Anterior Cingulate	L	32/24	-2	18	41	6.01				
Premotor cortex (dorsal, anterior)	R	6/32	20	8	47	7.01				
	R	6	30	4	48	3.87				
Precentral gyrus	L	4	-40	-20	60	4.41				
Pre-SMA	R	6	10	11	58	4.84				
Frontal areas										
Orbitofrontal cortex	R	47	20	17	-9	6.34				
Middle frontal gyrus	R	8					36	29	41	4.49
Inferior frontal gyrus	L	45					-53	18	10	3.99

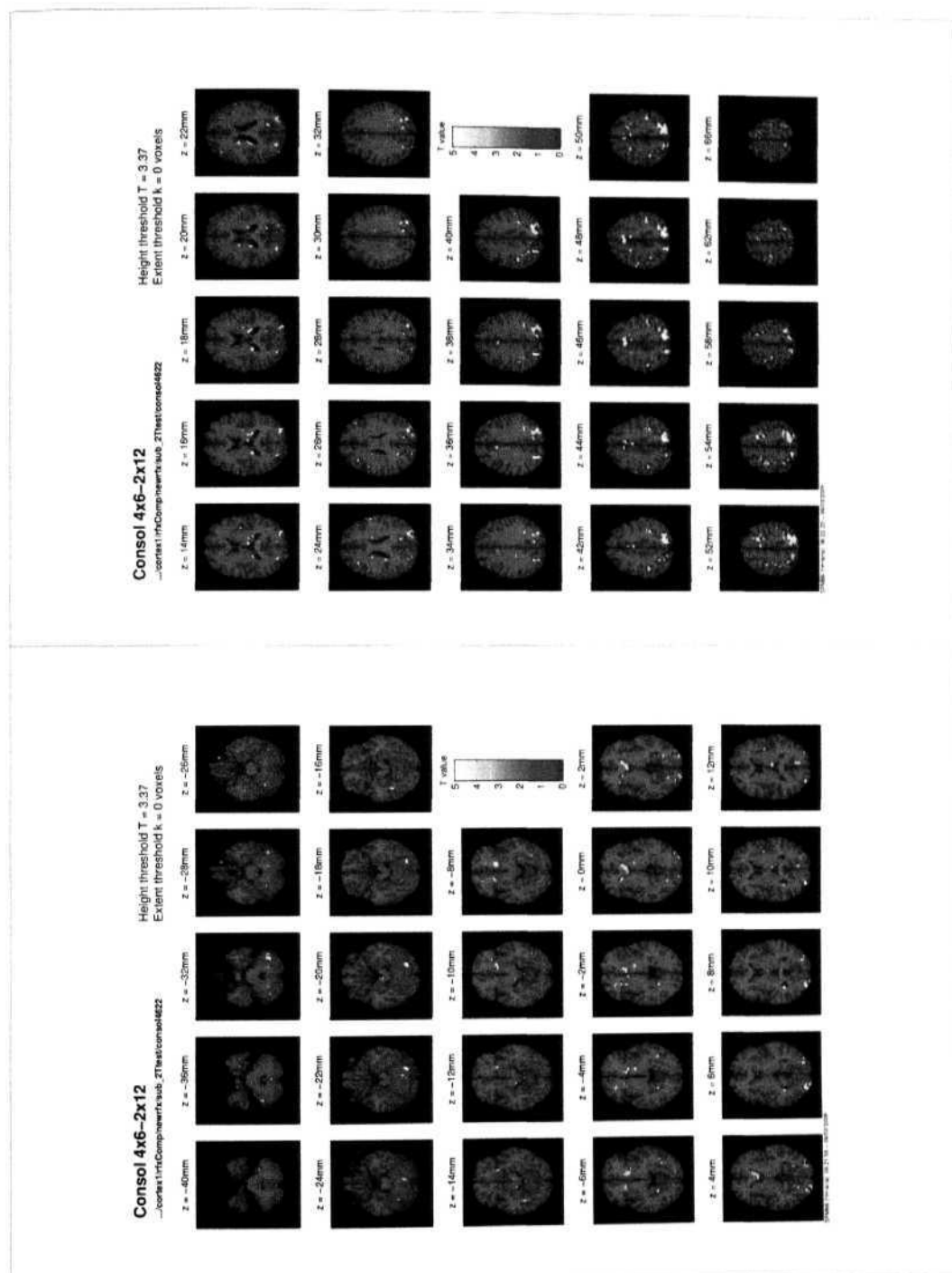


Figure 7.8: Consolidation 4x6>2x12 Regressor contrast activations

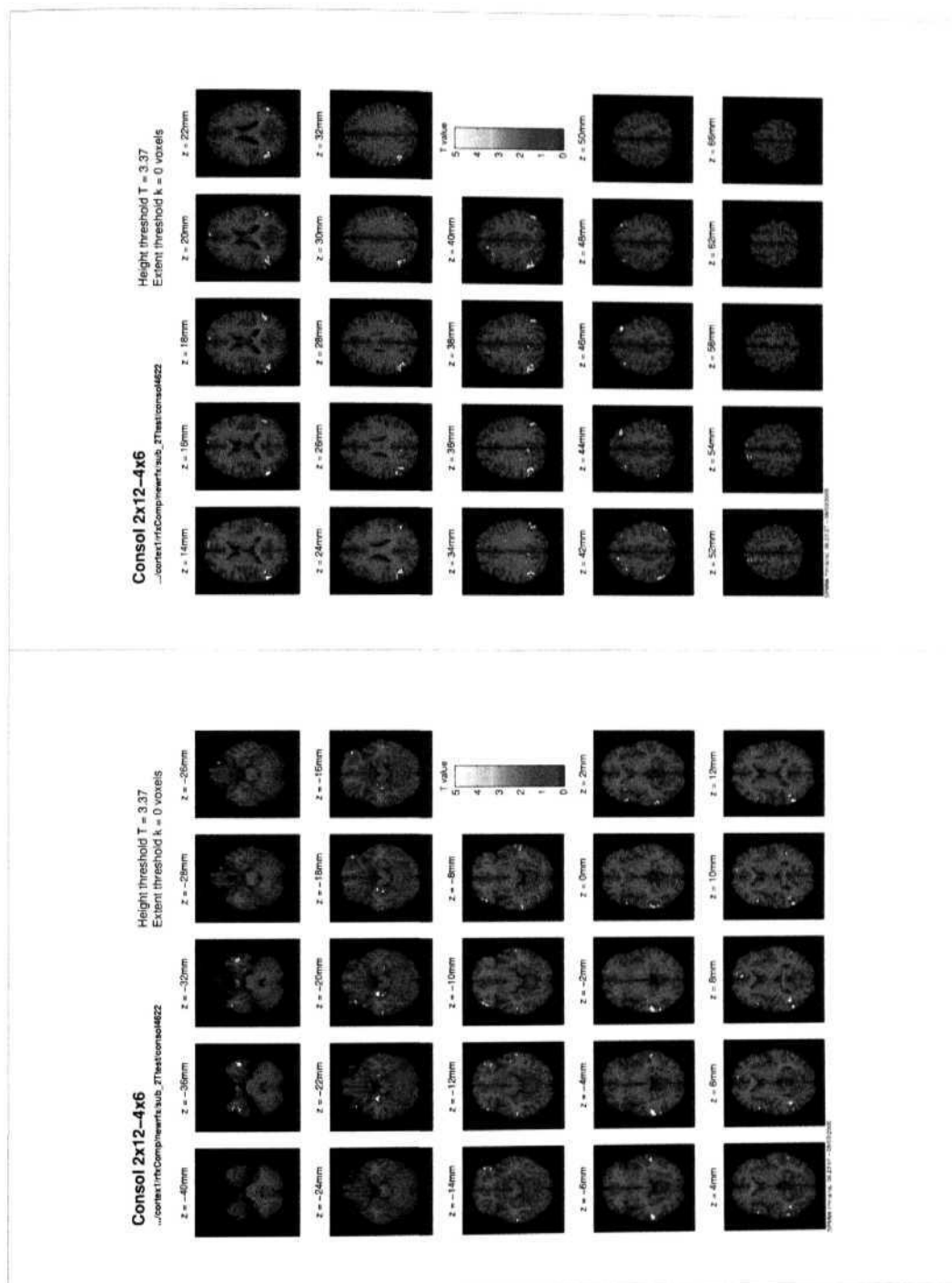


Figure 7.9: Consolidation 2x12>4x6 Regressor contrast activations

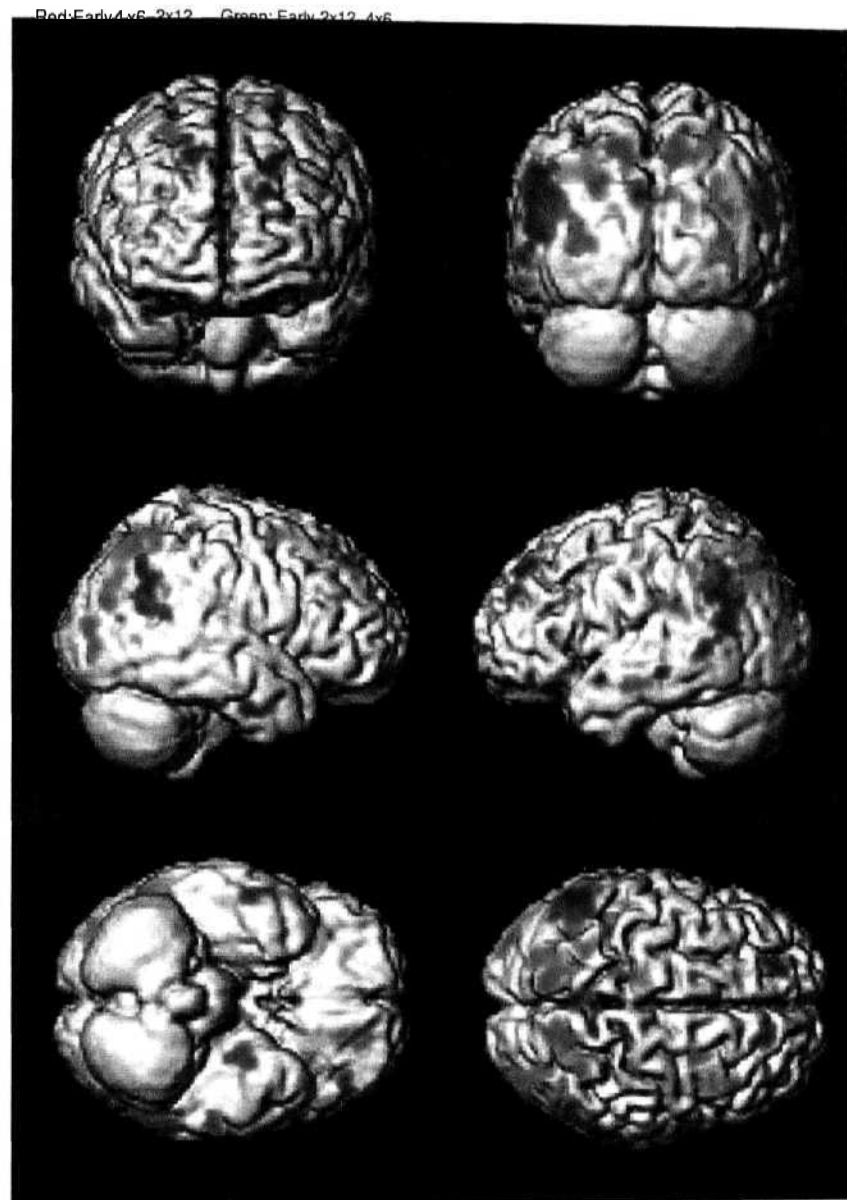


Figure 7.10: Early 4x6 > 2x12 (Red colour) and Early 2x12 > 4x6 (Green colour) Regressor contrast activations

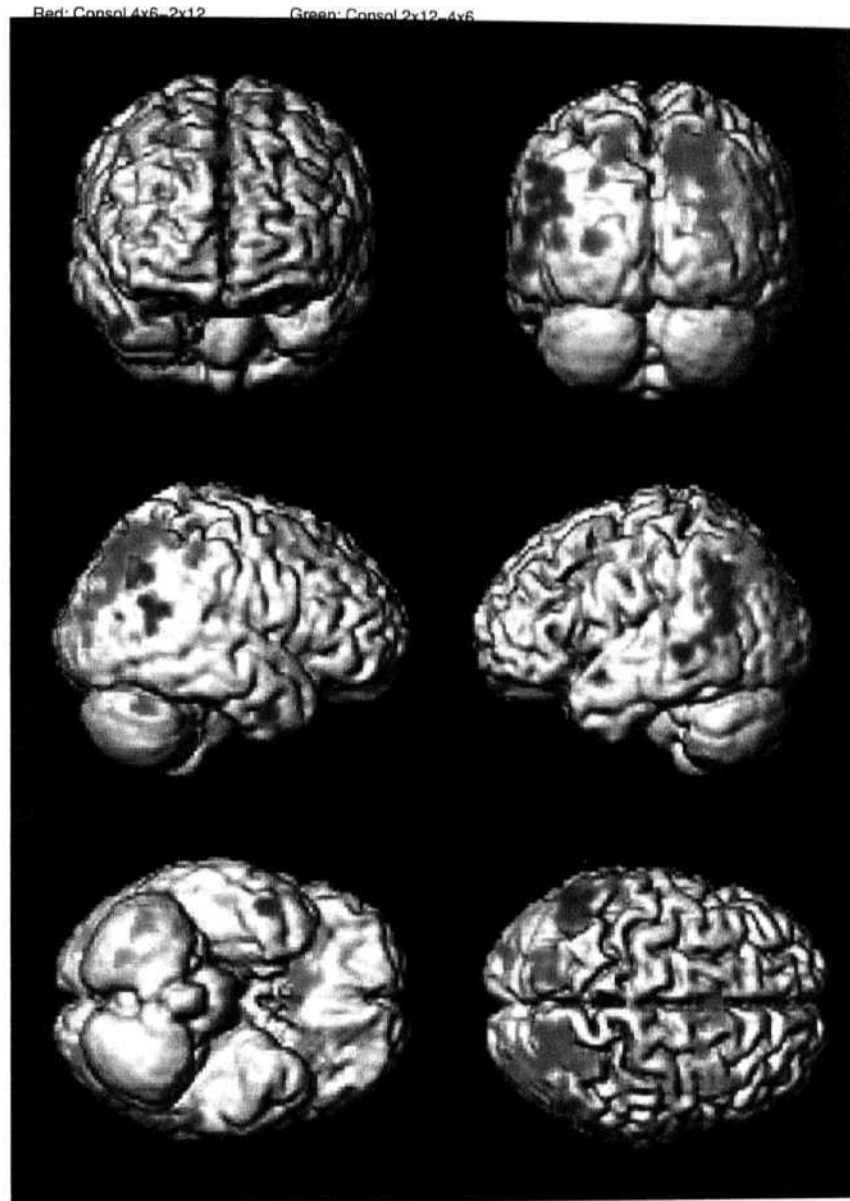


Figure 7.11: Consolidation $4 \times 6 > 2 \times 12$ (Red colour) and Consolidation $2 \times 12 > 4 \times 6$ (Green colour) Regressor contrast activations

7.3.3 Summary of results of comparison between sequence tasks

The interesting findings of comparisons of the complex sequence conditions with the 2×6 task in both the learning stages are that the striatum and that the motor-areas are more specific to the 4×6 task and the hippocampus is more specific to

the early stage of 2x12 task. Further, the activity in the right dorsal premotor (Brodmann area 6) is very interesting in 4x6 task, because its activity is seen strongly in the Early 4x6>Control regressor contrast and it even survived the correction for multiple comparisons ($p < 0.05$). We also observed differential role for cerebellar activations i.e., the ipsilateral anterior cerebellar lobule in the early stage of 4x6 and ipsilateral posterior cerebellar lobule in the consolidation stage of 2x12 task. In the comparisons with the 2x6, the parietal areas were observed to be more specific to the 2x12 task i.e., left inferior parietal lobule in early 2x12>2x6 and right superior parietal cortex in consolidation 2x12>2x6 contrasts. Another interesting observation is the activation of medial posterior cingulate cortex specific to the early 2x12 task. The early stage comparisons of 2x12>2x6 and 4x6>2x6 yielded common activation in the left orbitofrontal cortex and insula. This common activation could be related to the additional trial-and-error processing load imposed by the complex conditions.

In addition, the direct comparison between complex sequence conditions revealed the involvement of the medial parietal areas, occipital areas, lateral frontal areas and areas of striatum specific to the early stage processing of 4x6 task. The activation in the hippocampus, temporal areas, lateral parietal areas and posterior cingulate cortex revealed their specific involvement in the early stage of 2x12 task. These results also suggest specializations within the parietal areas i.e., medial parietal areas for 4x6 and lateral parietal areas for the 2x12 task.

7.4 Brain-Behaviour correlation (BBC) analysis results

At selected regions of interest, voxel data were extracted from a 5 mm spherical volume of interest (VOI) and entered into a *brain-behaviour correlation analysis*. Average blood oxygen-level dependent (BOLD) signal was calculated for each of the learning blocks (24 blocks i.e., 6 learning blocks in each session multiplied by four learning episodes i.e., sessions) at the designated VOI for each subject in the specified experiment (2x6 or 2x12 or 4x6). Similarly, mean performance measure (response time) was calculated for each of the learning blocks for each subject in the specified experiment. The resultant twenty-four values of BOLD signal and the corresponding behavioural measure were then entered into a correlation analysis. Pearson correlation coefficient (R) and its two-tailed significance level (p) were computed. We developed a SPM99 add-on script to automatically perform brain-behaviour correlation analysis over a specified VOI. We performed the brain-behaviour correlation (BBC) analysis from the basic comparison results on the selected VOIs.

Figures 7.12 and 7.13 show the BBCs of right dorsolateral prefrontal cortex (DLPFC) for the two VOIs picked from the coordinates of Early 2x6 Regressor

and Consolidation 4x6 regressor contrasts. In these two VOIs the activity in the 4x6 displayed a very high and significant positive correlation ($R > 0.7651$, $p \ll 0.001$) with the behaviour. The activity in the 2x6 task also displayed significant positive correlation with the behaviour ($R > 0.5595$, $p < 0.004$). But in the 2x12 task, the BBC did not show consistent positive correlations in both the VOIs. The interesting finding from this analysis is the very high correlation of Right DLPFC in the 4x6 sequence learning task with the learning related (indicated by the response times) behaviour. The decrease in activity as indicated by this analysis suggests a role of right dorsolateral prefrontal in working memory.

Figure 7.14 shows the BBCs of left primary motor area (Brodmann area 4) for the VOI picked from the coordinate of consolidation 4x6 regressor contrast. The interesting finding from this BBCs analysis is the significant negative correlation of left primary motor in the 4x6 sequence task with the behaviour ($R = -0.6157$, $p = 0.001$).

Figure 7.15 shows the BBCs of the right lateral globus pallidus (GP) for the VOI picked from the Consolidation 2x12 regressor contrast. The interesting finding from this BBC analysis is the reasonably good negative correlation ($R = -0.4563$, $p = 0.02$) with the behaviour in the 2x12 sequence task and the time course of activation in 2x12 task builds nicely by the last session. The high activity in the last session 2x12 sequence task (refer to the bottom right panel of Figure 7.15) in the right lateral GP brain area may point out its role in the long-range optimization process as demanded by the 2x12 task.

Figure 7.16 shows the BBCs of Left Precentral gyrus i.e., primary sensory motor area (Brodmann area 3/4) for the VOI picked from the coordinate of Early 4x6 > 2x6 regressor contrast. The interesting finding from this BBCs analysis is the significant negative correlation of Left Primary sensory motor in the 4x6 sequence task with the behaviour ($R = -0.677$, $V = 0.00027$).

7.4.1 Summary of BBC Results

The brain-behaviour correlations (BBCs) on the few areas which showed interesting relationship with response time are presented in this section. In summary, the right dorsolateral prefrontal cortex displayed significant positive correlation in the 4x6 & 2x6 tasks, the contralateral primary motor displayed significant negative correlation in the 4x6 task, the right lateral globus pallidus displayed significant negative correlation in the 2x12 task and contralateral sensorimotor cortex displayed significant negative correlation in the 4x6 task.

The interpretations and implications of the findings summarized in Section 7.3 are discussed in Chapter: 9.

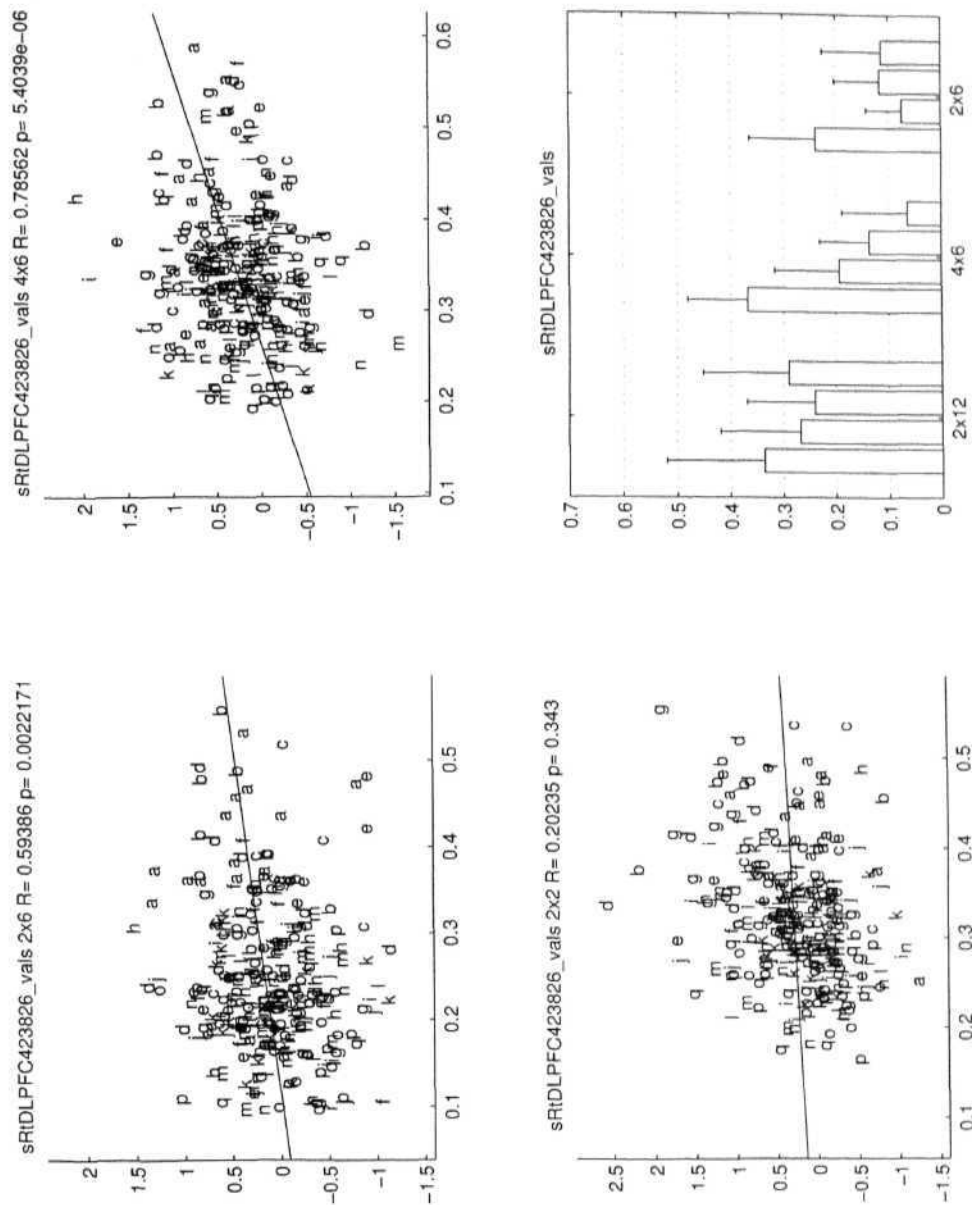


Figure 7.12: The brain-behaviour correlations of 2x6, 4x6 & 2x12 (x-axis: behaviour and y-axis: brain activation) and their time courses at Right Dorsolateral prefrontal cortex (Brodmann area 10/46) obtained from the Early 2x6>Control Regressor contrast. The *top panel*: The brain-behaviour correlation (BBC) of 2x6 and 4x6 tasks (left and right respectively). *bottom panel*: The BBC of 2x12 task (left) and the time course of activation in the three tasks (2x12, 4x6 and 2x6 respectively).

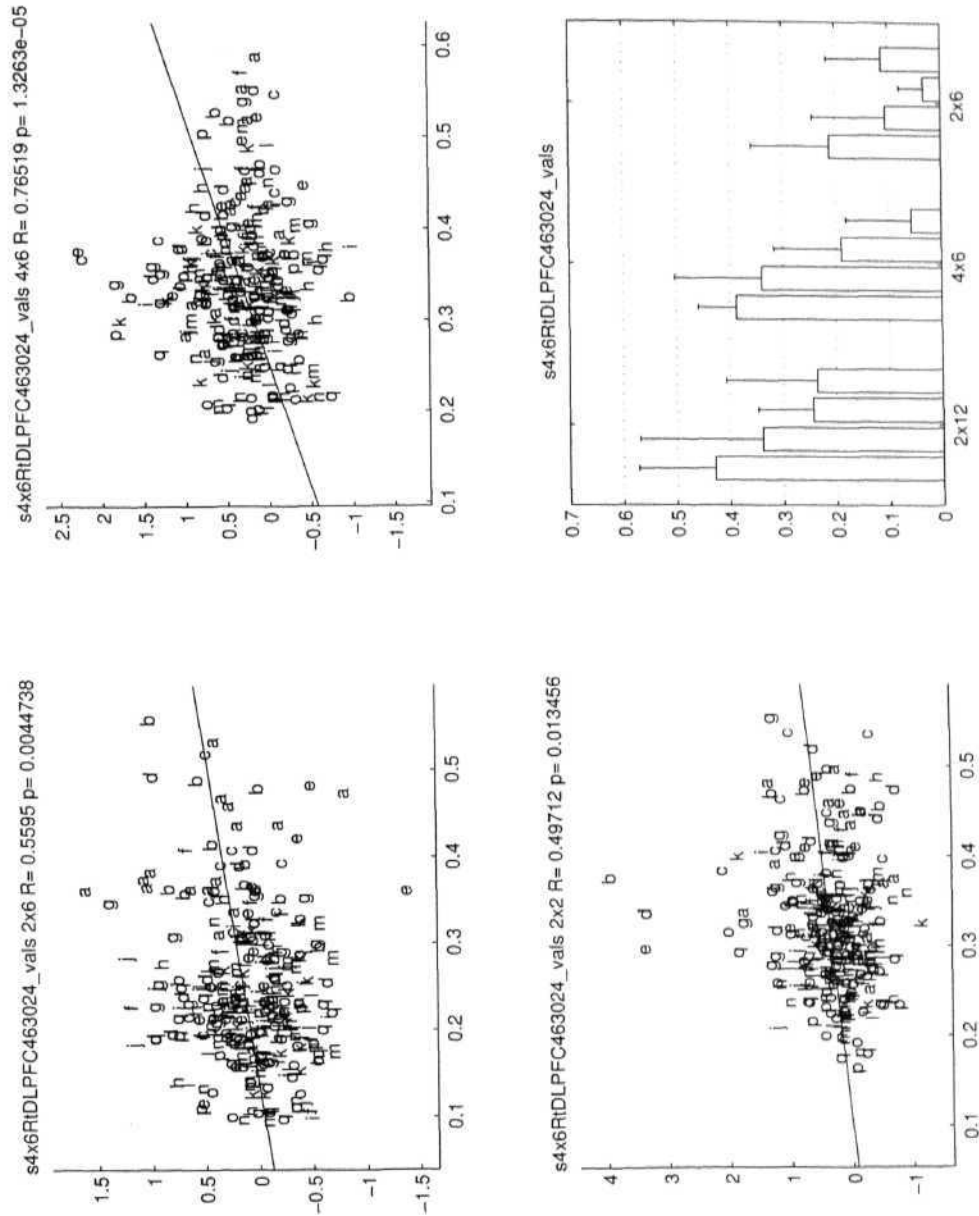


Figure 7.13: The brain-behaviour correlations of 2x6, 4x6 & 2x12 (x-axis: behaviour and y-axis: brain activation) and their time courses at Right Dorsolateral prefrontal cortex (Brodmann area 46) obtained from the Consolidation $4x6 > \text{Control}$ Regressor contrast. The *top panel*: The brain-behaviour correlation (BBC) of 2x6 and 4x6 tasks (left and right respectively). *bottom panel*: The BBC of 2x12 task (left) and the time course of activation in the three tasks (2x12, 4x6 and 2x6 respectively).

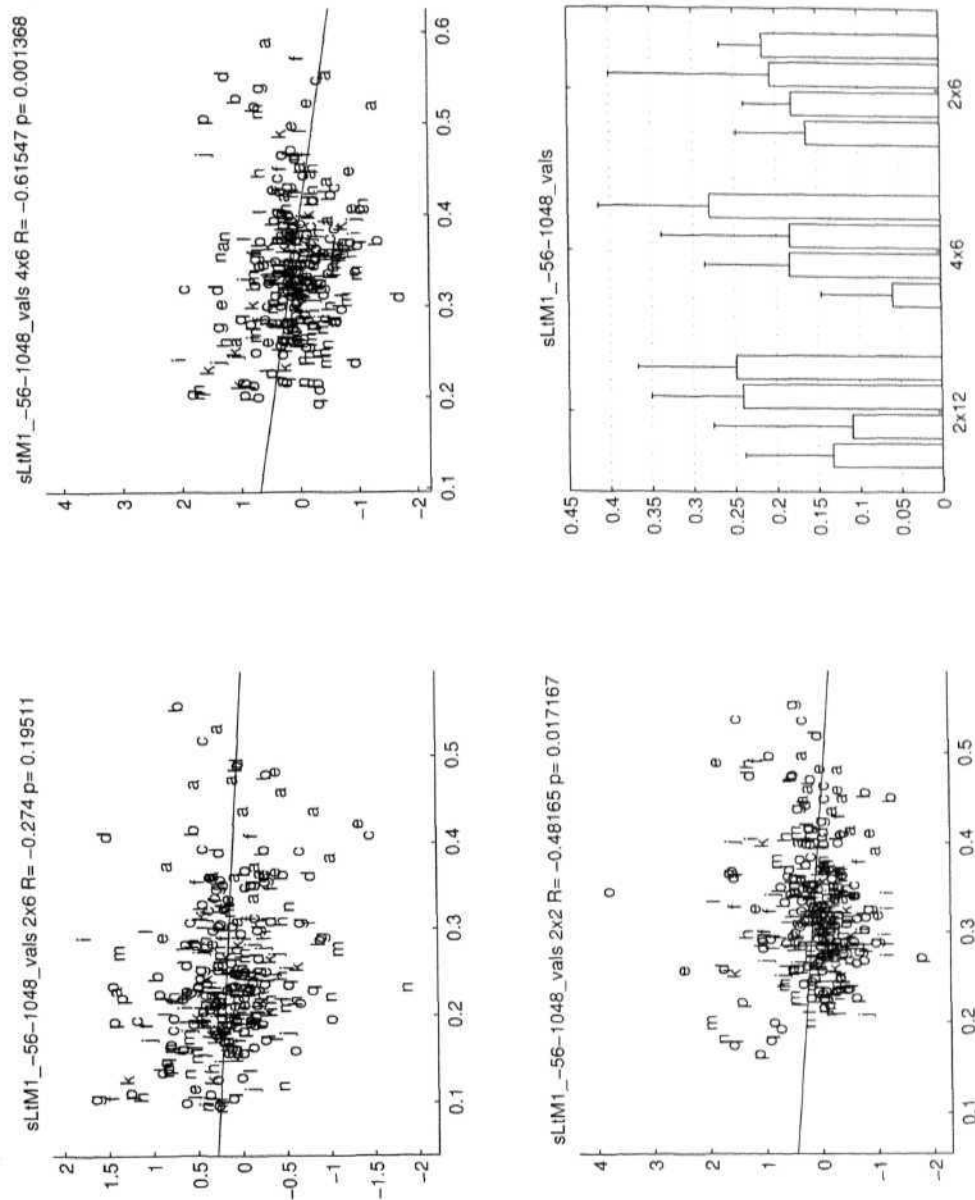


Figure 7.14: The brain-behaviour correlations of 2x6, 4x6 & 2x12 (x-axis: behaviour and y-axis: brain activation) and their time courses at Left Primary motor area (Brodmann area 4) obtained from the Consolidation 4x6>Control Regressor contrast. The *top panel*: The brain-behaviour correlation (BBC) of 2x6 and 4x6 tasks (left and right respectively). *bottom panel*: The BBC of 2x12 task (left) and the time course of activation in the three tasks (2x12, 4x6 and 2x6 respectively).

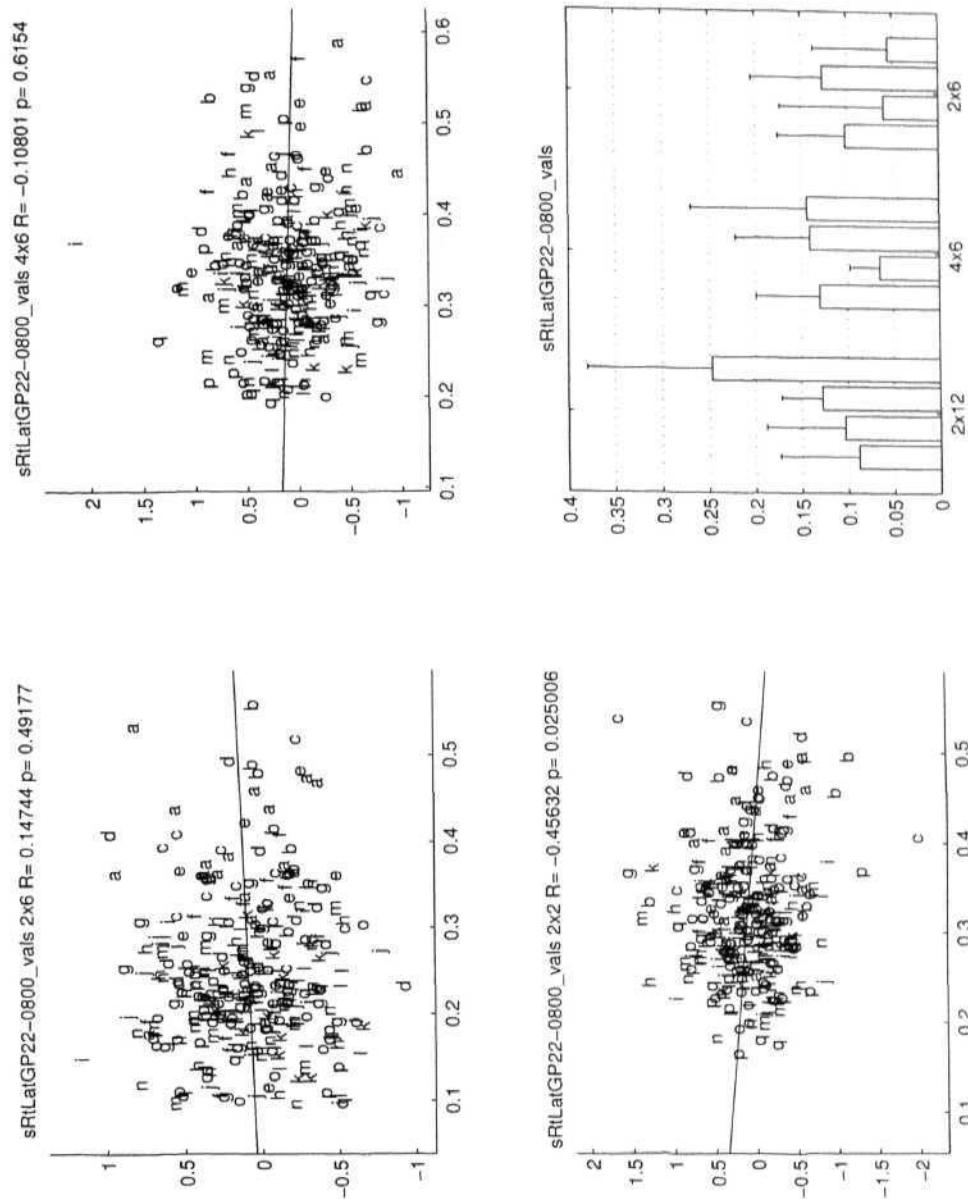


Figure 7.15: The brain-behaviour correlations of 2x6, 4x6 & 2x12 (x-axis: behaviour and y-axis: brain activation) and their time courses at Right Lateral Globus Pallidus obtained from the Consolidation 2x12>Control Regressor contrast. The *top panel*: The brain-behaviour correlation (BBC) of 2x6 and 4x6 tasks (left and right respectively). *bottom panel*: The BBC of 2x12 task (left) and the time course of activation in the three tasks (2x12, 4x6 and 2x6 respectively).

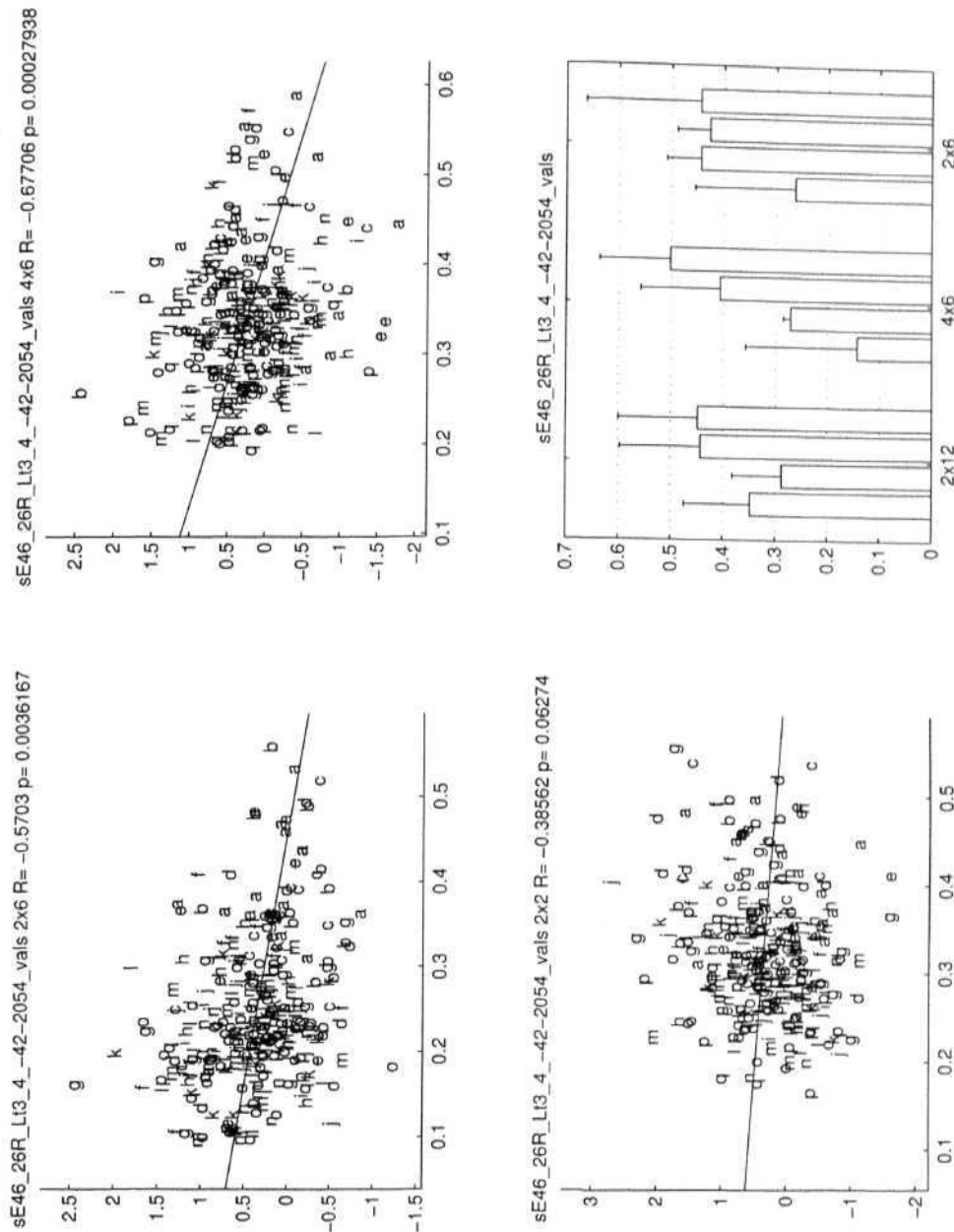


Figure 7.16: The brain-behaviour correlations of 2x6, 4x6 & 2x12 (x-axis: behaviour and y-axis: brain activation) and their time courses at, Left Precentral gyrus (Brodmann area 3/4) obtained from the Early 4x6>2x6 Regressor contrast. The *top panel*: The brain-behaviour correlation (BBC) of 2x6 and 4x6 tasks (left and right respectively). *bottom panel*: The BBC of 2x12 task (left) and the time course of activation in the three tasks (2x12, 4x6 and 2x6 respectively).

Chapter 8

Modelling of fMRI data to probe effective connectivity

In this chapter, we introduce a recent analysis methodology called 'effective connectivity'. The effective connectivity analysis is realized through *Dynamic Causal Modelling* (DCM) option in the SPM2 package. DCM is a recent option in SPM developed by the Wellcome Department of Imaging Neuroscience, University College London. In this chapter we demonstrate the analysis methodology of effective connectivity on a few models.

Historically, neuroimaging has been concerned predominantly with the localization of brain function, i.e. *where* in the brain certain types of cognitive processes is being implemented. The questions are addressed by the 'General Linear Model' for example implemented in SPM (Friston et al., 1995c). In addition, rather than just looking at the localization of areas involved in certain cognitive processes, one can ask the question of *how* this neural implementation works in terms of functional principles of the system i.e., through functional integration. One way to address this question of functional integration is through temporal correlation between spatially segregated remote neurophysiological events. This is called functional connectivity. The nature of functional coupling such as modulation are not dealt in these kind of models. The other way is to use the models of effective connectivity, where one can model the influence one neuronal system exerts over another system through causal statements (Friston et. al., 2003). The basic idea of effective connectivity is to construct a reasonably realistic neuronal model of interacting cortical regions using neuroimaging data. The effective connectivity for the fMRI data is introduced recently by Karl Friston through the

concept of dynamic causal modelling (Friston et al., 2003; Stephan et al., 2004).

8.1 Dynamic Causal Modelling (DCM)

DCM treats the brain as a deterministic nonlinear dynamical system that is subjected to inputs and produces outputs (Friston et al., 2003). The effective connectivity is parameterized in terms of coupling among unobserved brain states i.e., neuronal activity in different regions. The general idea behind DCM is to construct a neuronal model of interacting cortical regions with neurophysiologically meaningful parameters. These parameters are estimated such that the predicted BOLD series, which results from converting the neural dynamics into haemodynamics, corresponds as closely as possible to the observed BOLD series. In DCM, neural dynamics in several regions represented by a neuronal state vector z with one state per region are driven by experimental inputs. These inputs enter into the model in two ways: (1) by eliciting responses through direct influences on specific anatomical nodes, (2) by modulating the coupling among nodes. DCM models the change in neural states as non-linear function of states z , the inputs u and neural parameters θ^n :

$$\dot{z} = F(z, u, \theta^n) \quad (8.1)$$

where F is some non-linear function describing the neurophysiological influences. θ^n are the parameters of the model whose posterior density we require for inference. The parameters are the connectivity matrices ($\theta^n = A, B, C$) that define the functional architecture among brain regions at the neuronal level. The bilinear approximation of the Equation. 8.1 suggested by Friston et al. (2003) is as follows:

$$\begin{aligned} \dot{z} &\approx Az + \sum u_j B^j z + Cu \\ &= (A + \sum u_j B^j) z + Cu \end{aligned} \quad (8.2)$$

in which the coupling parameters correspond to partial derivatives of F :

$$\begin{aligned}
A &= \frac{\partial F}{\partial z} = \frac{\partial \dot{z}}{\partial z} \\
B^j &= \frac{\partial^2 F}{\partial z \partial u_j} = \frac{\partial}{\partial u_j} \frac{\partial \dot{z}}{\partial z} \\
C &= \frac{\partial F}{\partial u}
\end{aligned} \tag{8.3}$$

The Jacobian or effective connectivity matrix A represents the first-order connectivity among the regions in the absence of modulatory input. The matrix B^j encodes the change in effective connectivity induced by the j^{th} input u_j . The C matrix embodies the extrinsic influences of inputs on neural activity. DCM combines this neural model with the biophysical forward model of Friston (20021)) which describes how neuronal activity translates into a BOLD response. This enables the parameters and time constants of the neuronal model to be estimated from the measured data, using a fully Bayesian approach with empirical priors for the biophysical parameters and conservative shrinkage priors for the coupling parameters. The posterior distributions of the parameter estimates can then be used to test hypotheses about the size and nature of modelled effects. Usually, these hypotheses concern context-dependent changes in coupling which are represented by the bilinear terms of the model. Thus dynamic causal modelling is way of modelling the effect one hypothesizes. The nature of effect, is represented in terms of parameters θ^n .

The important points to be noted while designing DCM-compatible fMRI studies are as follows. The experiment should be designed in a multi-factorial fashion with at least one factor being effected by sensori input, while others vary with contextual inputs. The slice time TR of the scanner should be as short, as possible (typically it should be less than 15–2 seconds) to estimate the DCM parameters perfectly. In general it can also works with higher TR.s but one should localize the anatomical hypothesis over nearby brain regions. The specification of a priori hypothesis is also an important point while working with DCM. To make inference over a group, one should evaluate DCM models for each subject/experiment/session and the parameters obtained are taken to the second level to perform statistical tests like t-test.

Though our experimental paradigm does not satisfy all the prerequisites for DCM analysis, in this chapter we try to bring out some results based on the

brain areas we obtained from the SPM analysis of the complexity experiment. The results will be presented on one representative subject to demonstrate the procedure. The procedure for the DCM analysis is adopted from the SPM website (<http://www.fil.ion.ucl.ac.uk/spm/>).

8.2 Results

The idea of doing the DCM analysis is to study the effective connectivity among some of the areas that were activated in the comparisons of complex sequence conditions with the 2x6 task. As the current study investigates motor sequence learning, we selected few motor circuits such as dorsal premotor (PMd)–primary motor (MI), PMd–anterior cerebellum, caudate–PMd, dorsolateral prefrontal cortex (DLPFC)–caudate and posterior cerebellum–superior parietal cortex for investigating effective connectivity between them during the task. Anatomical connections between most of these areas is well known (Alexander et al., 1986; Middleton and Strick, 1998b,a; Picard and Strick, 2001)

8.2.1 Testing the model of dorsal premotor cortex, primary motor cortex

We tested a model consisting of ipsilateral (right) dorsal premotor and ipsilateral (right) primary motor cortex on one representative subject. For the early and the consolidation stages we performed DCM analysis for these; two areas, which were found to be active in the RFX analysis of Early 4x6 > 2x6 contrast. In the absence of modulatory inputs the intrinsic connections (matrix A and its probability values shown in the brackets of Figure 8.1) showed significant connection strength from right dorsal premotor to the right primary motor cortex. Figure 8.2 shows the modulatory effects (matrix B and its posterior probability values) of the early and the consolidation conditions on the reciprocal connections between the these two areas. The results suggest that, in the early stage of 4x6 the connection between right dorsal premotor and right primary motor cortex is significant in strength and displayed high probability value.

Intrinsic connections
 $P(|\text{connection}| > 0.00)$
 Connection strength

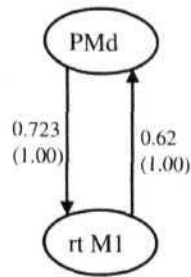


Figure 8.1: The intrinsic connections strengths between ipsilateral dorsal premo- tor and ipsilateral primary motor area.

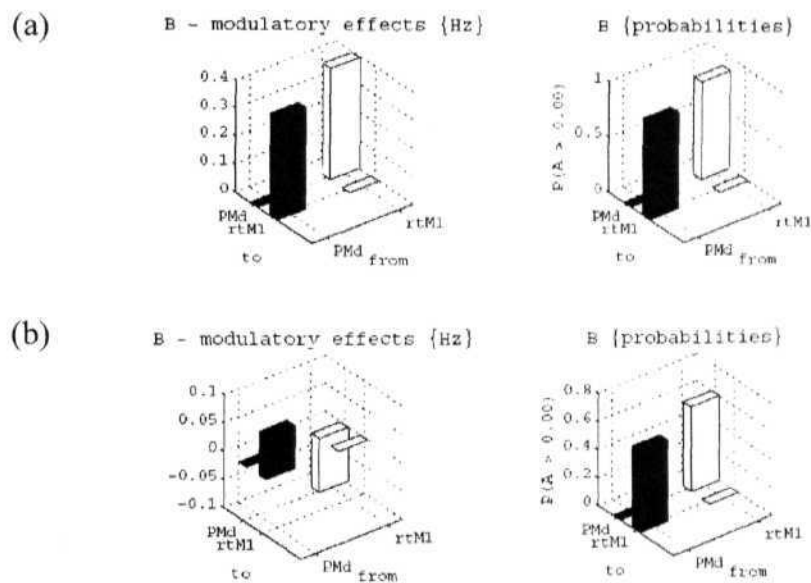


Figure 8.2: The modulatory connections for (a) Early and (b) Consolidation stages related to the 4x6 task. This graphs shows in the early stage the connections between right dorsal premotor and right primary motor are strong in the early stage but became weak by the consolidation stage.

Note that the intrinsic and extrinsic connection strength units are generally defined in Hz. Hence, the strength of a coupling can be thought of as a rate constant or the reciprocal of the time constant (the speed with which one area can affect another one). The modulatory parameters quantify how experimental manipulations change the values of intrinsic connections.

8.2.2 Testing the model of dorsal premotor cortex, anterior cerebellum

We tested another model consisting of ipsilateral (right) dorsal premotor cortex and ipsilateral anterior cerebellum on one representative subject. We performed DCM analysis separately for the early and the consolidation stages on those areas which got activated in the 4x6>2xG contrasts. In the absence of modulatory inputs the intrinsic connection showed significant connection strength from right dorsal premotor to the right anterior cerebellum (Figure 8.3). Figure 8.4 shows the modulatory effects of the early and the consolidation conditions on the reciprocal connections between these two areas. This suggests that, in the early stage of 4x6 the connection between right dorsal premotor and right, anterior cerebellum is more in strength and showed significant probability value.

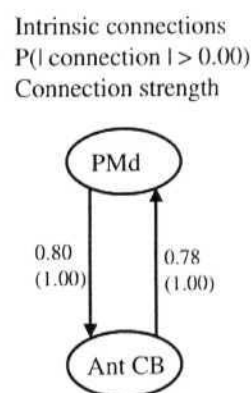


Figure 8.3: The intrinsic connections strengths between ipsilateral dorsal premotor and ipsilateral anterior cerebellum.

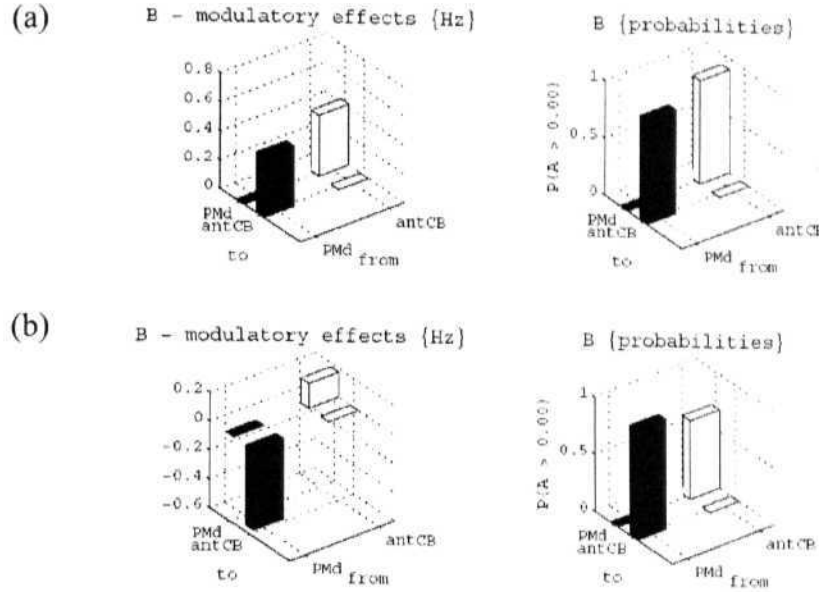


Figure 8.4: The modulatory connections for (a) Early and (b) Consolidation stages related to the 4x6 task. This graphs shows in the early stage the connections between right dorsal premotor and right anterior cerebellum are strong in the early stage but became weak by the consolidation stage.

8.2.3 Testing the model of caudate, dorsal premotor cortex

We tested another model consisting of contralateral caudate and ipsilateral (right) dorsal premotor cortex on one representative subject. We performed DCM analysis separately for the early and the consolidation stages on those areas which got activated in the 4x6>2x6 contrasts. In the absence of modulatory inputs the intrinsic connection showed significant connection strength from left caudate to the right dorsal premotor (Figure 8.5). Figure 8.6 shows the modulatory effects of the early and the consolidation conditions on the reciprocal connections between the these two areas. This demonstrates that in the consolidation stage of 4x6 the connection between left caudate and right dorsal premotor is significant in the strength and displayed more confidence value (greater than 92% as evidenced by the posterior probability value).

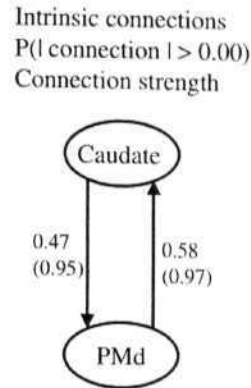


Figure 8.5: The intrinsic connections strengths between left caudate and right dorsal premotor cortex.

8.2.4 Testing the model of dorsolateral prefrontal cortex, caudate

We tested another model consisting of contralateral (left) dorsolateral prefrontal cortex (DLPFC) and contralateral caudate on one representative subject. We performed DCM analysis separately for the early and the consolidation stages on those areas which got activated in the consolidation 4x6>2x6 contrast. In the absence of modulatory inputs the intrinsic connection showed significant connection strength from left dorsolateral prefrontal cortex to the left caudate (Figure 8.7). Figure 8.8 shows the modulatory effects of the early and the consolidation conditions on the reciprocal connections between these two areas. This demonstrates that in the consolidation stage of 4x6 the connection between left DLPFC and left caudate is significant in the strength and displayed more than confidence value (greater than 95% as evidenced by the posterior probability value).

8.2.5 Testing the model of posterior cerebellum, superior parietal cortex

We tested another model consisting of ipsilateral (right) posterior cerebellum and ipsilateral (right) superior parietal cortex on one representative subject. We

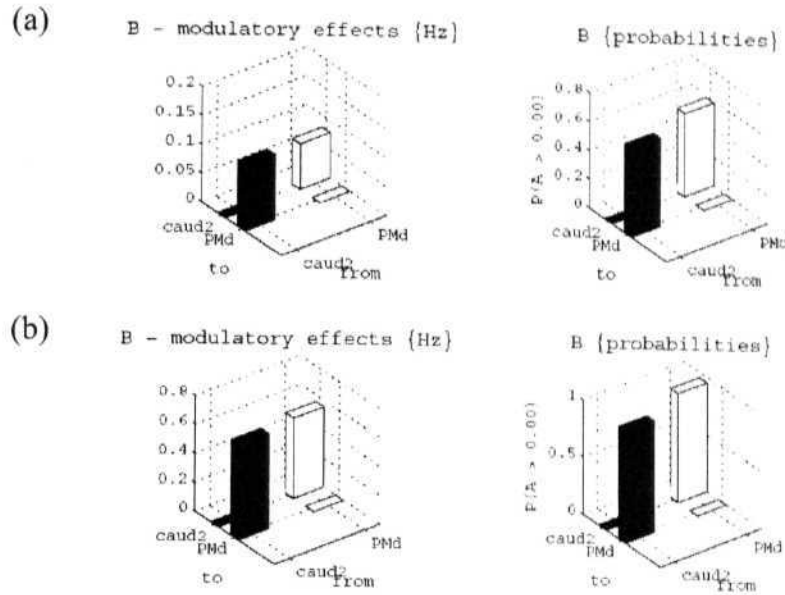


Figure 8.6: The modulatory connections for (a) Early and (b) Consolidation stages related to the 4x6 task. This graphs shows in the consolidation stage the connections between left caudate and right dorsal premotor is strong but found to be non-significant in the early stage.

performed DCM analysis separately for the early and the consolidation stages on those areas which got activated in the consolidation 2x12>2x6 contrast. In the absence of modulatory inputs the intrinsic connection showed significant connection but negative valued strength from right posterior cerebellum to right superior parietal cortex (Figure 8.9). Figure 8.10 shows the modulatory effects of the early and the consolidation conditions on the reciprocal connections between the these two areas. This demonstrates that in the consolidation stage of 2x12 the connection between posterior cerebellum and posterior superior parietal cortex is significant in the strength and displayed more probability value.

The modulatory connections (matrix B and their corresponding probability values) for 2x6 task on all the five models did not yield any significant connections either in the early or the consolidation stages. This further validates the complexity related effects (i.e., areas of activation in the complex tasks and their

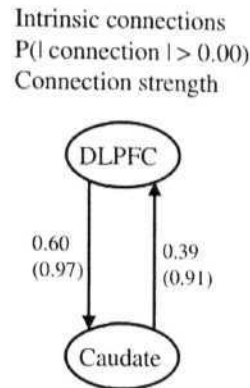


Figure 8.7: The intrinsic connections strengths between left dorsolateral prefrontal cortex and left caudate.

context sensitive connectivity) and significant connections for 4x0 task or 2x12 task.

8.3 Summary and Conclusions

In this chapter we presented results from DCM analysis to demonstrate the effect of learning on some connections. The results suggest that in the 4x0 task the modulatory connections from right dorsal premotor to right primary motor and from the right dorsal premotor to the right anterior cerebellum are significantly high as compared to their connections in the consolidation stage. The modulatory connections from left caudate to right dorsal premotor and left dorsolateral prefrontal cortex and left caudate displayed significant connections in the consolidation stage of the 4x6 task. In the 2x12 task we probed in the modulatory connection between right posterior cerebellum and right superior parietal cortex. The DCM analysis yielded their connectivity was strong in the consolidation stage. The results also point out the importance of DCM analysis to probe into the effective connectivity as effected by the experimental/modulatory inputs.

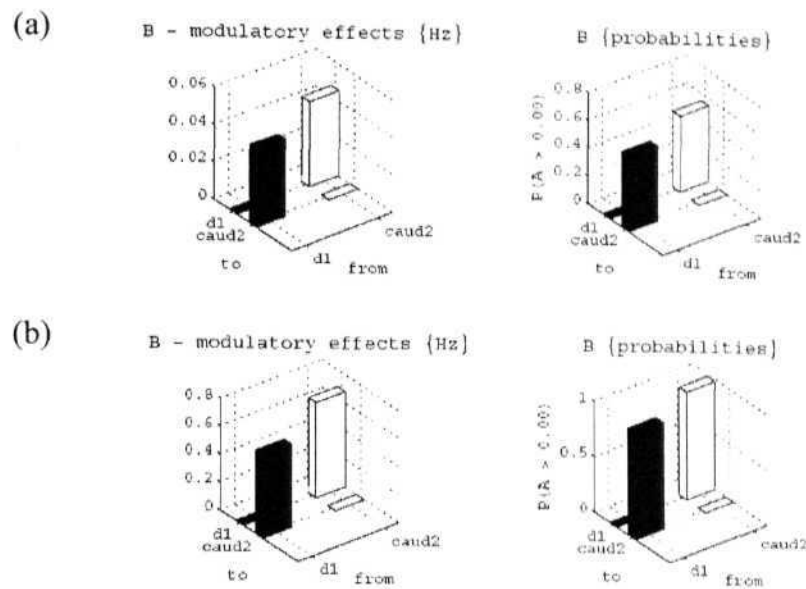


Figure 8.8: The modulatory connections for (a) Early and (b) Consolidation stages related to the 4x6 task. This graphs shows in the consolidation stage the connections between left dorsolateral prefrontal cortex and left caudate is strong but found to be non-significant in the early stage.

Intrinsic connections
 $P(|\text{connection}| > 0.00)$
 Connection strength

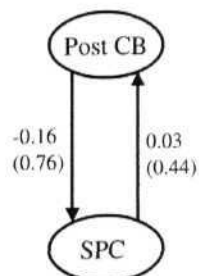


Figure 8.9: The intrinsic connections strengths between right posterior cerebellum and right superior parietal cortex.

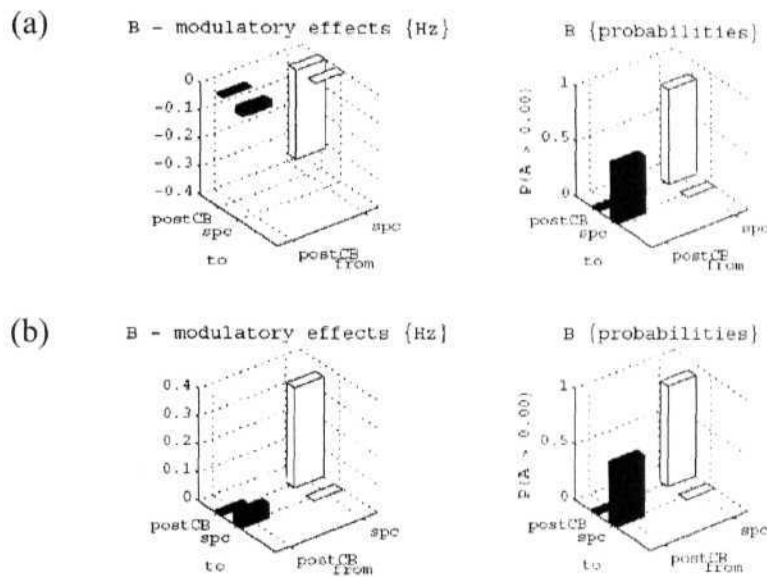


Figure 8.10: The modulatory connections for (a) Early and (b) Consolidation stages related to the 2x12 task. This graphs shows in the consolidation stage the connections between right posterior cerebellum and right superior parietal cortex is strong but found to be weak in the early stage.

Chapter 9

Discussion of Results and Conclusions

This chapter describes the overall discussion of results obtained from the behavioural, neuroimaging data and modelling efforts. This chapter will also point out possible interpretation of our results and major conclusions of this thesis.

We process sequences of stimuli or engage in sequences of actions in a variety of everyday tasks: from sequencing sounds in speech, to sequencing movements in typing or playing instruments, to sequencing actions in driving an automobile (Clegg et al., 1998). Thus sequencing is an essential aspect of animal and human behaviour. The ease with which movements are combined into skilled actions depends on many factors, including the factor of how complex the movement sequences are (Harrington et al., 2000). Most of the higher-order and intelligent cognitive behaviours such as reasoning, problem solving, and language involve acquiring and performing complex sequences of activities. Thus investigating the aspects of sequencing is important to not only understand human behaviour but also in designing intelligent systems (Sun, 2000). In the current work we examined one aspect of sequence processing i.e., sequence complexity, which encompasses organization of sequences.

In this thesis we investigated the effects of change in complexity while human subjects acquired and performed the sequential skill. We used $m \times n$ visuo-motor sequence learning paradigm where subjects learned a complete sequence of $m \times n$ key-presses by successively acquiring sub-goals (called, sets). The sequence learned in our paradigm is composed of n sets of m key-presses in each set. The correct order of pressing m keys (called a set) is learned by a trial-and-

error process by actively exploring visual cues and evaluating motor responses based on visual feedback i.e., flash when subjects pressed the wrong key. On successful completion of a set, subjects are allowed to proceed to the next set and so on. Subjects learn to complete n such sets (called a hyperset). Eighteen human subjects participated in the current study and they performed the three sequence learning tasks (2x6, 2x12 and 4x6) while supine in the 1.5 Tesla fMRI scanner. Each experimental task consisted of four sessions and a session comprised 13 epochs of alternating control (seven) and test (six) conditions. In control condition, subjects followed randomly generated visual targets and thus no learning was involved. In the test condition they learned a sequence.

In the current study, subjects performed three sequence tasks namely, 2x*i*, 2x12 and 4x6 where the number of finger movements varied from 12 (in the 2x6 task) to 24 (in the 4x6 and 2x12 tasks). We thus manipulated the sequence complexity along two dimensions — m (2 to 4 i.e., by holding the number of sets to be learned the same, the number of elements in each set is doubled) and n (6 to 12 i.e., by keeping the amount of information per unit time the same, the number of sets is doubled). m and n reflect the amount of information to be processed in the short-range and long-ranges, respectively. In addition to investigating the general effects of complexity, we also probed into the behavioural and brain activation patterns related to the learning stages. Our aim was to investigate the differences among the sequence conditions in various learning stages. The current investigation is the first of its kind in demonstrating the effects of increasing complexity in two dimensions in the $m \times n$ visuo-motor sequence learning paradigm that uses trial-and-error learning process.

Earlier imaging studies of sequence complexity manipulated sequence length (Sadato et al., 1996; Catalan et al., 1998, 1999; Boecker et al., 1998, 2002) or type of sequence i.e. contrast between repeated and heterogeneous sequence of finger movements [for example, (Harrington et al., 2000; Hummel et al., 2003; Haaland et al., 2004)]. Our study methodologically differs from the earlier investigations of sequence complexity. Most of the previous studies used well learned sequences. But, our tasks involved progressively learning the visuo-motor sequence by trial-and-error process. It was also possible to probe in our experimental design learning a new sequence (early stage) and mastering that sequence (consolidation for the efficient retrieval of the sequence). Our task also allowed us to probe the progression of learning hierarchical sequences, i.e. acquisition of chunks. We hy-

pothesized that in the complex condition corresponding to increased set-length (i.e., in the 4x6 task), the optimization process may be limited to the items within the *set* and may not span across *sets*. In contrast, we expect that in the complex condition corresponding to increased hyperset-length (i.e., in the 2x12 task), sequence information may possibly be organized in a hierarchical fashion. Further, these differential effects may have implications in the behavioural parameters (such as success rate and response time) and in the brain activity pattern.

While subjects performed the sequence learning tasks inside the scanner, our experimental software recorded behaviour related variables (as indicated in Appendix B). The result file is post-processed, wherein we computed two behavioural parameters namely, the success rate and the average key-press response time to characterize the performance improvements of the subjects for each experimental task. In addition, we also computed the total number of finger movements. These parameters are carefully designed to tease out behaviour related changes in the sequence tasks and also allowed us to compare the sequence tasks. Based on these behavioural measures we demarcated the learning episodes mainly into the early and consolidation stages.

In the imaging analysis, we designed a performance related parameter that uses response time as the regressor to model the complexity related learning effects in the imaging data. These regressor values take approximately twice the value in the complex sequence tasks (2x12 or 4x6) as compared to the values obtained for the 2x6 task. As the main aim of this thesis is to investigate the neural correlates of the effects of complexity (4x6 versus 2x6 & 2x12 versus 2x6) during learning (Early) and performance (Consolidation) stages, we constructed two separate design matrices for every subject corresponding to 2x6-4x6 and 2x6-2x12. We used appropriate regressor values i.e., set completion time to model set increase and hyperset completion time for hyperset increase; in order to model the effects of sequence complexity. The behavioural parameters would correspond to the psychophysical behaviour of the subjects as learning progressed in sequence tasks.

The behavioural results demonstrate that the success rate and the average key-press response times (RT) revealed learning related improvements in all the sequence learning tasks (2x6, 2x12 and 4x6). The complexity related effects (i.e., the effect of increasing from 12 movements in 2x6 task to 24 movements in 2x12

and 4x6 tasks) are observed to be significant. The results from the success rate analysis revealed that the subjects attained similar levels of accuracy in both the complex tasks. Thus the success rate as a behavioural measure is meaningful and it could quantify the similarity of difficulty levels across complex sequence learning conditions.

Interestingly, results from the average key-press RT analysis revealed a differential behaviour across complex sequence conditions (2x12 and 4x6 tasks) from early to consolidation stage. In the early stage the key-press RT was observed to be similar across 2x12 and 4x6 tasks. Whereas in the consolidation stage key-press RT became dissimilar. In addition, the consolidation stage RT value of 2x12 task was observed to be significantly lesser as compared to the consolidation stage RT value of 4x6. So when 24 movements are arranged as 2x12, the key-press RTs were shorter compared to when they are arranged as 4x6. These results may have potential implication in organizational differences across 2x12 and 4x6 tasks. Thus the key-press RT as a behavioural measure is justified and it mainly demonstrated (quantified) the organizational differences across complex sequence learning conditions. The results from the number of movements analysis revealed that the total number of movements remained balanced across the complex sequence learning tasks. The behavioural parameters separately computed for the control/follow task revealed a steady state performance across all the sequence tasks, thus justifying the nature of the task design.

The results from the chunking analysis, suggested that when the *set-size* was kept smaller but the number of sets to be processed was increased (as in the 2x12 task), we observed notable reorganization across sets. As the number of sets to be internalized (12) is larger than the short-term memory capacity, it appears that subjects compressed the information into a number of chunks. On the other hand, when the *set-size* was larger (as in the 4x6 task), there is less reorganization across sets. Subjects have to process more amount of information in each set and because of the increased short-term cognitive load, it appears that performance optimization may possibly have been more within the sets and less across the sets. These results have consequence for the cognitive model of hierarchical sequence learning. A model that learns sequences using a limited capacity working memory (WM) would need to optimize in two different ways depending on the amount of information to be processed at any instance of time. If the amount stretches beyond the limit of WM then optimization process needs to operate within the

logical unit (set). If the amount is well within the WM capacity, optimization across the logical units (sets) would facilitate efficient performance.

The findings from the fMRI analysis comparing the complex sequence conditions with the simple sequence condition (2x6 task) in both the learning stages suggest that the motor areas (dorsal premotor and primary motor) are more specific to the 4x6 task and the hippocampus is more specific to the early stage of 2x12 task. Further, the activity in the right dorsal premotor (Brodmann area. 6) is very interesting in 4x6 task, because its activity is seen strongly in the Early 4x6>Control regressor contrast and it even survived the correction for multiple comparisons ($p < 0.05$). We also observed differential role for cerebellar activations i.e., the ipsilateral anterior cerebellar lobule in the early stage of 1x6 and ipsilateral posterior cerebellar lobule in the consolidation stage of 2x12 task. In the comparisons with the 2x6, the parietal areas are observed to be more specific to the 2x12 tasks i.e., left inferior parietal lobule in early 2x12>2x6 and right, superior parietal cortex in the consolidation 2x12>2x6 contrasts. Another interesting observation is the activation of medial posterior cingulate cortex specific to the early 2x12 task. In addition, the direct comparisons between complex sequence conditions revealed the involvement of the medial parietal areas, occipital areas, lateral frontal areas and areas of striatum specific to the early stage processing in the 4x6 task. The activations in hippocampus, temporal areas, lateral parietal areas and posterior cingulate cortex revealed their specific involvement in the early stage of 2x12 task. These results also suggest specializations within the parietal areas i.e., medial parietal areas for 4x6 and lateral parietal areas for the 2x12 task.

The 4x6 task can be termed an on-line processing task as the information to be processed at a time within a *set* is quite large. 2x12 task can be viewed as an off-line task where the information to be processed is available over time across the sets. From the neuroimaging findings, we can say that the cortico-cortical areas may have a role in the 4x6 like tasks and sub-cortical area near the hippocampus may have a role in the acquisition stage of 2x12 like tasks. The posterior lobule of cerebellum, superior parietal lobule and Inferior frontal gyrus may have a specific role in the chaining across the sets and the dorsolateral prefrontal cortex and caudate nucleus loop may have a specific role in within-set optimization and linking across sets.

The effective connectivity Dynamic causal modelling (DCM) analysis suggested the following findings. In the 4x6 task the modulatory connections from right dorsal premotor to right primary motor and from the right dorsal premotor to the right anterior cerebellum are significantly high as compared to their connections in the consolidation stage as well as when compared to both the stages of 2x6 task. The modulatory effects from left caudate to right dorsal premotor and left dorsolateral prefrontal cortex and left caudate displayed significant strength in the consolidation stage of the 4x6 task. In the 2x12 task the modulatory connection between right posterior cerebellum and right superior parietal cortex yielded strong connectivity in the consolidation stage. Interestingly, these modulatory connections tested above did not depict any significant strength in both the stages of 2x6 task. This will enable us to say that these areas and their connections are more relevant to the complex tasks compared to the simple task.

9.1 Interpretation of the fMRI Results

In the following sub-sections some of the important results will be discussed area-wise with respect to their involvement in effects of complexity in the early and the consolidation stages. As discussed earlier, 4x6 task can be viewed as an on-line task where the sequence optimization works within the set and hence the acquisition and performance depend on short-range window spanning the length of the set i.e., 4 items. On the other hand, the 2x12 task has been termed off-line as the set size is smaller (2 items) but the number of sets to be learned is larger (12 sets). Hence in the 2x12 task, the sequence acquisition, performance and optimization process need to operate across sets, i.e., they need to span a long-range sequence horizon.

9.1.1 Neural systems underlying the acquisition of long-range sequence

Increasing the number of sets from 6 to 12 by keeping the amount of information Per unit time the same as in the 2x12 task, we observed some distinct set of brain areas in the early and consolidation stages. The areas activated in the early stage of the 2x12 task would participate in the acquisition of long sequences.

The left hippocampus activation seems to be interesting and that, may be involved in the learning of long-range sequences where the amount of information in local load is minimum. This activation is consistent with the recent studies of animals indicating a role for the hippocampus in sequence learning (Agster et al., 2002; Fortin et al., 2002). Schendan et al. (2003) demonstrated that the learning-related activity in the medial temporal lobe (near hippocampus) is related to the acquisition of the higher-order associations in both explicit and implicit sequence learning tasks. In a recent study Fletcher et al. (2005) showed learning related decrease in the left hippocampus. Sequence learning, of a probabilistic sort, usually engages the hippocampus (Strange et al., 2005). In our study the activation of hippocampus in the early stage is in line with the above mentioned studies. Thus, the hippocampus may be necessary for learning long-range sequences, especially those that go beyond the capacity of working memory capacity.

The inferior parietal cortex is said to be involved in the building (encoding) of an abstract representation of complex sequences (Harrington et al., 2000). In our task, the inferior parietal cortex may have a similar function in the abstract representation of 2x12 like tasks. This may be related to the process of learning to group consecutive sets in order to efficiently learn the long-range sequences.

The activation in the medial posterior cingulate cortex may be related to the attentional cognitive processes (Barbas, 2000). Recently Tracy et al. (2003) suggested that the posterior medial regions of cingulate gyrus may have a role in long-term storage for a newly learned motor skill. Thus the activation of this area, in the early stage may reflect its role in acquisition processes of long-range sequences.

The activation in the right supramarginal gyrus (SMG) is said to be involved in the spatial encoding processes (Smith et al., 1996). The activation of this area in our study may relate to the encoding processes that are involved in the chunking across sets. This area together with the inferior parietal cortex may be involved in building abstract representations needed for the long-range sequences.

The activation in the left orbitofrontal cortex and left insula found to be common in the early stages of 2x12>2x6 and 4x6>2x6 comparisons may reflect uncommon cognitive processes such as the extra, trial-and-error processes operating in complex tasks. The interpretation of orbitofrontal cortex involved in the trial-and-error learning is in line with our earlier study Pammi et al. (2003a) and also

in accordance with its role in the punishment based learning (Doherty et al., 2001).

9.1.2 Neural systems underlying the long-range optimization process

Areas found to be active in the consolidation stage of the 2x12 task might be participating in the optimization processes operating in this stage to consolidate and internalize the sequence. Three important areas were observed to be activated in the consolidation stage of 2x12>2x6 stage. They are ipsilateral (right) posterior cerebellum (near Uvula), ipsilateral (right) superior parietal cortex (more towards dorsal at $z=61$) and ipsilateral inferior frontal cortex (brodmann area 45/47).

Superior parietal cortex is known to translate a plan into an action/goal (Harrington et al., 2000). In line with this result the observed activation in our study during the consolidation stage could be related to the retrieval process of long-range plan/predictions. For example, if a mobile number 9440746882 is being processed by a subject into three chunks, say, 94407, 463 & 82. The superior parietal cortex would be involved in predicting what comes next after 94407 and so on. Whereas the inferior parietal cortex may create an abstract representation of the sequence by partitioning into three chunks. As mentioned already, Harrington et al. (2000) postulated that the inferior parietal cortex helps building abstract representation of complex sequences. Thus it appears that while inferior parietal cortex builds representations, the superior parietal cortex helps in retrieving them.

It is known that posterior cerebellum is involved in the timing adjustment i.e., the difference between predicted timing and actual timing (Sakai et al., 2000). The posterior cerebellum also attributed a role in supporting abstract representation of sequences in the early stage (Nakahara et al., 2001) and has contribution in the error-based learning of sequence of visuo-spatial cues (Doya, 2000). From these earlier findings, we can speculate that the posterior cerebellum together with the superior parietal cortex participate in long-range prediction processes.

The prefrontal cortex is the only area that can simultaneously represent cues, responses and outcomes (Passingham et al., 2000). The right inferior frontal

cortex is known for its role in executive functions and damage to this area crucially affects performance in paradigms like task-set switching and response inhibition, apparently by disrupting the inhibition process (Aron et al., 2004). Thus the activation obtained in the consolidation stage of 2x12>2x6 may indicate its role in enabling smooth transition from one chunk to another chunk by inhibiting irrelevant chunks.

9.1.3 Neural systems underlying the short-range prediction process

Increasing the number of elements in each set from 2 to 4 by holding the number of sets to be learned the same as in the 4x6 task, we observed some distinct set of brain areas in the early and consolidation stages. Brain activations observed in the early stage of the 4x6 task could be attributed to the short-range prediction processes operating when sequences are learned.

The dorsal premotor cortex is activated very significantly in the early stage of 4x6 and may have a role in the learning of short-range predictions. The term *pre-motor cortex* originally used to label the lateral portion of frontal angular cortex rostral to the primary motor cortex, was considered to be the center of complex skilled movements (Dum and Strick, 1991). Sadato et al. (1996) suggested that the right dorsal premotor could be part of mechanisms for storing motor sequences in a working memory buffer and Harrington et al. (2000) suggested a role for it in the retrieval or preparation of abstract action plans. The ipsilateral activation we found in this area may possibly indicate its role as buffer for storing short-range sequence predictions that help in the acquisition of individual sets in the 4x6 task.

The ipsilateral primary motor activation in our study was specifically observed when the set-size was increased as in the 4x6 task. Activation of ipsilateral primary motor (M1) during complex sequential tasks is supported by earlier studies (Boecker et al., 1998; Hummel et al., 2003).

The anterior cerebellum activation is said to be related to the execution of motor tasks driven by external stimuli or internal cues i.e., spatial working memory (Sadato et al., 1996) and various processes related to motor and non-motor Processes (Boecker et al., 2002). The result in our study could be attributed to

the non-motor spatial working memory for the sets.

9.1.4 Neural systems underlying the short-range optimization process

In the consolidation stage of 4x6 task, we envisage optimization processes to be working to internalize short-range sequences. Three important areas were observed to be activated in the consolidation stage of 4x6>2x6 stage. They are contralateral (left) striatum (caudate body), left dorsolateral prefrontal cortex (Brodmann area 9/46) and contralateral primary motor area (Brodmann area 4).

Hikosaka et al. (1996, 2000) investigated learning of visuomotor sequences by trial and error and suggested functional differences between anterior and posterior striatum in that the former is associated with new learning and the latter with retrieval of learned sequences. Boecker et al. (1998, 2002) suggested basal ganglia involvement in the process of facilitation and optimization of performance of sequential movements. In line with this result, the activation we found in the striatum in the consolidation stage of 4x6>2x6 could be related to the facilitation process of set-level optimization.

The dorsolateral prefrontal cortex (DLPFC) is well known for its role in executive and working memory functions (Jenkins et al., 1994; Jueptner et al., 1997b; Sakai et al., 1998). Together with the striatum, DLPFC may be participating in the retrieval process in the consolidation stage.

In a recent investigation, Pasupathy and Miller (2005) demonstrated that the learning related activity in dorsolateral prefrontal cortex and the striatum showed different time courses during associative learning. Their results on monkeys suggested that the striatum generates quick predictions about the behavioural choice and the prefrontal cortex reveals the slower accumulation of the correct answer. Thus in our study the role of striatum may be involved in the generation of quick predictions within a set and dorsolateral prefrontal cortex may accumulate these predictions to reach the goal of completing the hyperset.

The primary motor cortex is known for participating in execution of individual finger movements during sequence performance and direct production of movements (Boecker et al., 1998). In an fMRI study, Khushu et al. (2001) suggested

an increase in primary motor cortex BOLD signal in response to the increase in functional demands. In line with these results, we suggest that the primary motor area might be involved in the production of movements while the functional demands are more i.e., the amount of information at a given time is more as in the 4x6 task.

The effective connectivity analysis using dynamic causal modelling on a representative subject demonstrated the relevance of the neuronal circuits such as dorsal premotor (PMd)-primary motor (M1), PMd-anterior cerebellum, caudate-PMd, dorsolateral prefrontal cortex (DLPFC)-caudate and posterior cerebellum-superior parietal cortex during the complex sequence conditions. Thus the relevance of certain neuronal circuits of interest can be verified using this recent, fMRI modelling exercise.

9.2 Conclusions

In this thesis we set out to investigate sequence complexity in three ways i.e., through behavioural analysis, imaging analysis and modelling the fMRI data to probe effective connectivity. The behavioural analysis on performance measures not only demonstrated the effects of two dimensions of complexity but also demonstrated differences in temporal reorganization. These reorganizational differences are quantified by using statistical analysis and clustering analysis. The neuroimaging analysis brought out the brain responses correlated with the behaviour. As the main aim of this thesis is to investigate¹ the neural correlates of the effects of complexity (4x6 versus 2x6 *k* 2x12 versus 2x6) during learning (the early) and performance (the consolidation) stages, we modelled these effects of complexity suitably. The imaging results point out distinct set of brain areas responsible for each stage and for different complexity effects. The neuroimaging findings suggest that the eortico-cortical areas may have a role in the 4x6 like tasks and the sub-cortical area near the hippocampus may have a role in the acquisition stage of 2x12 like tasks. The posterior lobule of cerebellum, the superior parietal lobule and the inferior frontal gyrus may have a specific role in the chaining across the sets and the dorsolateral prefrontal cortex and caudate nucleus loop may have a specific role in the within-set optimization and linking across sets. We demonstrated few simple models of effective connectivity among

selected brain areas and their importance in the specific stage and task. The effects of complexity are shown for five models on a single representative subject. Thus the results support our hypothesis that in the complex sequence learning condition corresponding to increased set-length, the optimization process may be limited to the items within the *set*. In contrast, in the complex sequence learning condition corresponding to increased hyperset-length, sequence information may possibly be organized in a hierarchical fashion.

Chapter 10

Future Work

In this chapter we point out the future directions in this research. The future research also contains hypothesis for a possible computational framework.

10.1 Future Directions

10.1.1 Experimental Design

The strength of the current investigation lies in demonstrating the sequence complexity effects across learning stages in a single experimental design. This research work can be extended further by refining the experimental design to address more focussed questions such as chunking. One of the limitations of the current study is that there are only a few points sampling the complexity space. One possibility is to design tasks such as 2x6, 3x6, 4x6, 5x6 for studying the *sat* increase effect and 2x6, 2x9, 2x12 and 2x15 tasks for studying the effect of *hyperset* increase. In this case though the dimensions of increase in both the cases are not similarly varying but the finger movements across corresponding tasks, for example, 5x6 and 2x15 have 30 equal finger movements. This kind of study will be a large study with 7 experimental tasks to be performed by each subject.

The current investigation indirectly examined the chunking process and provided empirical evidence from the behavioural analysis. More focussed experiments can be designed in future to address this phenomenon. The current study has only resolution up to the set level response times. By recording the single key-press level response times along with the demarcation of the choice and the

movement times, one can address and explain more precisely the nature of chunk evolution and performance optimization processes. Another possibility could be to design an event-related experiment. If the repetition time (TR) of the scanner is comparable to the chunking process times, this kind of experimental design may be useful in revealing these fast varying events. By modelling each scan as an event and marking the specific events related to the chunking process, one may address the issues related to chunking. No such study has been done so far.

In the current research we presented different hypotheses for every subject. The main idea behind designing this kind of procedure is to probe into the general effects related to the learning or complexity. In future, one can use the same hypersets (for the 2x6, 2x12 and 4xG tasks) for all the subjects. This kind of design may reveal the common/different strategies employed by subjects during learning/complexity. Measuring choice and movement times in this kind of design may bring out more microscopic details of learning related behaviour.

Most of the earlier studies on complexity utilized well-learned sequences. But no study was performed on well-learned $m \times n$ sequences. This kind of design will allow to investigate the effects of complexity in the automatic stage of sequential skill performance. The elimination of visual stimuli during the performance of well-learned sequences in the scanner will enable probing specifically the motor related brain activations. Using well-learned sequences, it is easier to manipulate many points in the complexity space.

10.1.2 Theoretical Framework

In this section we suggest a possible theoretical framework. In the literature, several researchers described computational models for serial learning. These models can be broadly classified into three categories – biologically inspired models, Connectionist models, and hybrid models. In biologically inspired computational models some aspects of anatomical organization and function are mimicked [for example, Dominey et al. (1995); Berns and Sejnowski (1998)]. In Connectionist models, the aim is to mimic the overall behaviour of the biological system rather than replicating the internal organizational details [for example, Servan-Schreiber et al. (1994)]. In hybrid models, engineering principles enable the construction of models that illuminate biological function. These models usually do not attempt an explicit replication of anatomical organization [for example, Suri and Schultz

(1998); Bapi and Doya (2001)].

We present here a theoretical framework for modelling sequence processing focusing on the organisational aspects especially based on our results on chunking (described in chapter 6). The framework we propose comes under the third category i.e. hybrid computational model. If we interpret our imaging results broadly, we can summarize that while for learning short-range information cortico-cortical connections may be sufficient, for learning predictions across sets, i.e. for learning long-range associations, cortico-subcortical connections may be necessary. This suggests a two-level model wherein at one level simple associations are acquired and at the other level higher-order associations are formed. Based on this we propose a two-level model where Markov models and reinforcement learning (RL) are combined to specifically address how biological systems learn to organize sequential information in a hierarchical fashion. In this framework of two-level model where at the lower level, first order sequential dependencies are extracted and at the higher level, hierarchical structure corresponding to the entire sequence is captured using reinforcement learning as shown in the Figure 10.1.

First-order Markov Model: Markov model is a well-formulated mathematical framework for capturing first and higher order sequential dependencies among random variables describing the behaviour of a system [for review Rabiner (1989)]. The main assumption (also called Markov-Assumption) is that prediction of the next state depends only on a portion of the previous history of state transitions. In the case of first-order Markov models, the probability that, q_t (state at time t) is equal to i is completely predictable by knowing q_{t-1} and ignoring the rest of the previous state history (a second-order Markov model would require q_{t-1} and q_{t-2} to predict q_t). A formal definition of the first-order Markov model is given below.

$$P(q_t = i \mid q_{t-1} = j, q_{t-2} = k, \dots) = P(q_t = i \mid \mathbf{fc-i} = j) \quad (10.1)$$

Reinforcement Learning (RL): Reinforcement learning has been proposed as a biologically realistic framework for learning sequential decisions in animals and humans (Sutton and Barto, 1998). In this paradigm, the sequential decision problem involves assuming a policy (a mapping from the states to possible actions) and learning a value function over the state space so that the sequence of actions maximizes the expected future reward. The most popular method for

learning the value function is the method of temporal difference (TD). A formal definition is given below.

$$V(t) = E[r(t+1) + r(t+2) + \dots] \quad (10.2)$$

$$\delta(t) = r(t) + V(t) - V(t-1) \quad (10.3)$$

Where, $V(t)$ represents the value of a state, $r(t)$ is the reward and $\delta(t)$ is the temporal difference signal all at time t . $E[\]$ represents the expectation or averaging operator. Value of a state, $V(t)$, is set to be the average future reward that is likely to be obtained in the current state. Temporal difference signal, $\delta(t)$, tracks the difference between the expected reward and actual reward and serves as the reinforcement learning (internal feedback) signal.

The first-order Markov models alone would capture a flat organization of the sequence and do not incorporate learning. Although RL models incorporate learning, the policies that are learned would still have a flat organization. We propose that by combining these two models and utilizing the TD error signal, hierarchical policies could be learned. Computer modelling (simulation) of the two-level architecture (see Figure 10.1) combining Markov models and reinforcement learning is expected to reveal whether models based on this framework can really solve the hierarchical sequence decision problems. Such models would mimic the hierarchical nature of organization of sequences as observed in biological systems. The simulation and verification of this theoretical model is left for future investigation.

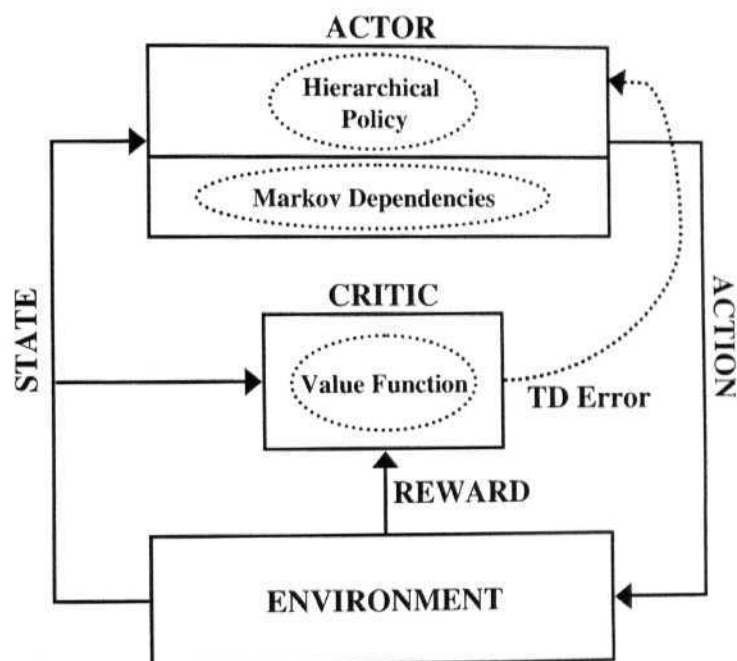


Figure 10.1: Block Diagram of the Proposed Hybrid Model. Actor-critic based model incorporating Markov model and hierarchical policy as sub-modules in the actor module. The two-levels in the actor module, namely, the Markov model and the hierarchical policy module would enable learning hierarchical sequence decision problems.

References

- Agster, K. L., Fortin, N. J., and Eichenbaum, H. B. (2002). The hippocampus and disambiguation of overlapping sequences. *Journal of Neuroscience*, 22:5760-5768.
- Alexander, G. E., DeLong, M. R., and Strick, P. L. (1986). Functionally segregated circuits linking basal ganglia and cortex. *Annual Review of Neuroscience*, 2:357-381.
- Anderson, J. (1995). *Learning and Memory*. John Wiley and Sons, New York.
- Aron, A. R., Robbins, T. W., and Poldrack, R. A. (2004). Inhibition and the right inferior frontal gyrus. *Trends in Cognitive Science*, 8:170-177.
- Baddeley, A. (1986). *Working Memory*. Oxford University Press, New York.
- Baddeley, A. (1992). Is working memory working? *The fifteenth, Bartlett lecture, Quarterly Journal of Experimental Psychology*, 44.
- Bapi, R. S. and Doya, K. (2001). Multiple forward model architecture for sequence processing. In Sun, R. and Giles, L., editors, *Sequence Learning: Paradigms, Algorithms, and Applications*, pages 309-320. Springer Verlag, Germany.
- Bapi, R. S., Doya, K., and Harner, A. M. (2000). Evidence for effector dependent and independent representations and their differential time course of acquisition during motor sequence learning. *Experimental Brain Research*, 132:149-162.
- Bapi, R. S., Pammi, V. S. C., and Miyapuram, K. P. (2003). Methods and approaches for characterizing learning related changes observed in functional MRI data - a review. In Singh, N., editor, *Proceedings of the International Conference on Theoretical Neurobiology*, pages 221-229. India.

References

144

- Bapi, R. S., Pammi, V. S. C, Miyapuram, K. P., and Ahmed (2005). Investigation of sequence learning: A cognitive and computational neuroscience perspective. *Accepted in Current Science Journal*.
- Barbas, H. (2000). Connections underlying the synthesis of cognition, memory, and emotion in primate prefrontal cortex. *Bruin Research Bulletin*, 5:319–330.
- Bell, A. J. and Sejnowski, T. J. (1995). An information maximisation approach to blind separation and blind deconvolution. *Neural Computation*, 7:1129–1159.
- Bell, A. J. and Sejnowski, T. J. (1997). The independent components of natural scenes are edge filters. *Vision Research*, 37:3327–3338.
- Berns, G. and Sejnowski, T. J. (1998). A computational model of how the basal ganglia produce sequences. *Journal of Cognitive Neuroscience*, 10:108–121.
- Berns, G. S. (1999). Functional neuroimaging. *Life Sciences*, 65(24):2531–2540.
- Berns, G. S., Song, A. W., and Mao, H. (1999). Continuous functional magnetic resonance imaging reveals dynamic nonlinearities of dose-response curves for finger opposition. *Journal of Neuroscience*, 19:RC17:1–6.
- Boecker, H., Ceballos-Baumann, A. O., Bartenstein, P., Dagher, A., Forster, K., Haslinger, B., Brooks, D. J., Schwaiger, M., , and Conrad, B. (2002). A $H_2^{15}O$ positron emission tomography study on mental imagery of movement sequences - the effect of modulating sequence length and direction. *NeuroImage*, 17:999–1009.
- Boecker, H., Dagher, A., Ceballos-Baumann, A. ()., Passingham, R. E., Samuel, M., Friston, K. .J., Poline, J. B., Dettmers, C, Conrad, B., and Brooks, I). .1. (1998). Role of the human rostral supplementary motor area and the basal ganglia in motor sequence control: Investigations with $H_2^{15}O$ PET. *Journal of Neurophysiology*, 79:1070–1080.
- Bor, D., Gunning, N, Scott, C. E. L., and Owen, A. M. (2004). Prefrontal cortical involvement in verbal encoding strategies. *European Journal of Neuroscience*, 19:3365-3370.
- Box, G. E. P. and Jenkins, G. (1976). *Time series analysis: Forecasting and control* Holden Day Inc., San Francisco.

References

145

- Brett, M, Christoff, K., Cusack, R., and Lancaster, J. (2001). Using the talairach atlas with the mni template. *Neuroimage*, 13:S85.
- Catalan, M. J., Honda, M., Weeks, R. A., Cohen, L. G., and Hallett. M. (1998). The functional neuroanatomy of simple and complex sequential finger movements: a PET study. *Brain*, 121:253–264.
- Catalan, M. J., Ishii, K., Honda, M., Samii, A., and Hallett, M. (1999). A PET study of sequential finger movements of varying length in patients with parkinson's disease. *Brain*, 122:483-495.
- Chein, J. M. and Schneider, W. (2003). Designing effective fVIRI experiments. In Grafman, J. and Robertson, I., editors, *Handbook of Neuropsychology*. tltsevier Science B.V., Amsterdam.
- Chomsky, N. (1957). *Syntactic Structures*. Mouton & Co., The Hague.
- Christoff, K. (2001). *Displaying activation on multiple slices*. Web resource available at: http://www-psych.stanford.edu/~kalina/SPM99/Tools/m_slice.html, Psychology Department, Stanford University.
- Clegg, B. A., DiGirolamo, G. J., and Keele, S. W. (1998). Sequence learning. *Trends in Cognitive Sciences*, 2(8):275-281.
- Cohen, M. S. and Bookheimer, S. Y. (1994). Functional magnetic resonance imaging. *Trends in N euro sciences*, 17:268-277.
- Colwell, B. (2005). Machine intelligence meets neuroscience. *IEEE Computer*, 38:12-15.
- Conway, C. M. and Christansen, M. H. (2001). Sequential learning in non-human primates. *Trends in Cognitive Science*, 5:539-546.
- Crammond, D. J. (1997). Motor imagery: Never in your wildest dream. *Trends in Neuroscience*, 20:54-57.
- Culham, J. C. (2005). Functional neuroimaging: Experimental design and analysis. In Cabeza, R. and Kingstone, A., editors, *Handbook of Functional Neuroimaging of Cognition*, 2nd edition. MIT Press, Cambridge MA.

- Dassonville, P., Lewis, S., Zhu, X., Ugurbil, K., Kim, S., and Ashe, J. (1998). Effects of movement predictability on cortical motor activation. *Neuroscience Research*, 32:65-74.
- Doherty, J. O., Kringelbach, M. L., Rolls, E. T., Hornak, J., and Andrews, C. (2001). Abstract reward and punishment representations in the human orbitofrontal cortex. *Nature Neuroscience*, 4:95-102.
- Dominey, P. F., Arbib, M. A., and Joseph, J. P. (1995). A model of corticostriatal plasticity for learning oculomotor associations and sequences. *Journal of Cognitive Neuroscience*, 7:311-336.
- Doya, K. (2000). Complementary roles of basal ganglia and cerebellum in learning and motor control. *Current Opinion in Neurobiology*, 10:732-739.
- Duda, R. O., Hart, P. E., and Stork, I. G. (2001). *Pattern Classification (2nd ed.)*. John Wiley and Sons.
- Dum, R. P. and Strick, P. L. (1991). The origin of corticospinal projections from the premotor areas in the frontal lobe. *Journal of Neuroscience*, 11:667-689.
- Fletcher, P. C., Zafiris, O., Frith, C. D., Honey, R. A. E., Corlett, P. R., Zillies, K., and Fink, G. R. (2005). On the benefits of not trying: Brain activity and connectivity reflecting the interactions of explicit and implicit sequence learning. *Cerebral Cortex*, 15:1002-1015.
- Fortin, N. J., Agster, K. L., and Eichenbaum, H. B. (2002). Critical role of the hippocampus in memory for sequences of events. *Nature Neuroscience*, 5:458-462.
- Friston, K. (1998). Imaging neuroscience: principles or maps? *Proc. Natl. Acad. Sci. USA*, 95:796-802.
- Friston, K., Frith, C., Passingham, R., Liddle, P., and Frackowiak, R. (1992). Motor practice and neurophysiological adaptation in the cerebellum: a positron tomography study. *Proceedings of Royal Society of London, Series B*, 248:223-228.
- Friston, K. J. (1997). Imaging cognitive anatomy. *Trends in Cognitive Sciences*, 1:21-27.

- Friston, K. J. (2002a). Bayesian estimation of dynamical systems: an application to fMRI. *NeuroImage*, 16:513–530.
- Friston, K. J. (2002b). Bayesian estimation of dynamical systems: an application to fMRI. *NeuroImage*, 16:513–530.
- Friston, K. J., Ashburner, J., Frith, C. D., Poline, J. B., Heather, J. L., and Frackowiak, R. S. J. (1995a). Spatial registration and normalisation of images. *Human Brain Mapping*, 2:165–189.
- Friston, K. J., Harrison, L., and Penny, W. (2003). Dynamic causal modelling. *NeuroImage*, 19:1273–1302.
- Friston, K. J., Holmes, A. P., Poline, J.-B., Grasby, P., Williams, S., Frackowiak, R., and Turner, R. (1995b). Analysis of fMRI time-series revisited. *Neuroimage*, 2:45–53.
- Friston, K. J., Holmes, A. P., and Worsley, K. J. (1999). How many subjects constitute a study? *Neuroimage*, 10:1–5.
- Friston, K. J., Holmes, A. P., Worsley, K. J., Poline, J. B., Frith, C. D., and Frackowiak, R. S. J. (1995c). Statistical parametric maps in functional imaging: A general linear approach. *Human Brain Mapping*, 2:189–210.
- Friston, K. J., Jezzard, P., and Turner, R. (1991). Analysis of functional MRI time series. *Human Brain Mapping*, 1:153–171.
- Gordon, A. M., Lee, J. H., Flament, D., and Ugurbil, K. (1998). Functional magnetic resonance imaging of motor, sensory, and posterior parietal cortical areas during performance of sequential typing movements. *Experimental Brain Research*, 121:153–166.
- Grafton, S. T., Hazeltine, E., and Ivry, R. (1995). Functional mapping of sequence learning in normal humans. *Journal of Cognitive Neuroscience*, 7:497–510.
- Grafton, S. T., Hazeltine, E., and Ivry, R. (1998). Abstract and effector-specific representations of motor sequences identified with PET. *Journal of Neuroscience*, 18:9420–9428.
- Graybiel, A. M. (1998). The basal ganglia and chunking of action repertoires. *Neurobiology of Learning and Memory*, 70:119–136.

References

148

- Gusnard, D. A. and Raichle, M. E. (2001). Searching for a baseline: Functional imaging and the resting human brain. *Nature Reviews Neuroscience*, 2:085–694.
- Haaland, K. Y., Elsinger, C. L., Mayer, A. R., Durgerian, S., and Rao, S. M. (2004). Motor sequence complexity and performing hand produce differential patterns of hemispheric lateralization. *Journal of Cognitive Neuroscience*, 16:621–636.
- Hamzei, F., Dettmers, C., Rijntjes, M., Glauche, V., Kiebel, S., Weber, B., and Weiller, C. (2002). Visuomotor control within a distributed parieto-frontal network. *Experimental Brain Research*, 146:273–281.
- Harrington, D. L., Rao, S., Haaland, K. Y., Bobholz, J. A., Mayer, A. R., Binder, J. R., and Cox, R. W. (2000). Specialized neural systems underlying representations of sequential movements. *Journal of Cognitive Neuroscience*, 12:56–77.
- Heeger, D. J. and Ress, D. (2002). What does fMRI tell us about neural activity? *Nature Reviews*, 3:142–150.
- Hikosaka, O., Miyachi, S., Miyashita, K., and Rand, M. K. (1990). Learning of sequential procedures in monkeys. In Bloedel, J. R., Ebner, T. J., and Wise, S. P., editors, *The acquisition of motor behaviour in vertebrates*, pages 303–317. Cambridge: MIT Press.
- Hikosaka, O., Rand, M. K., Miyachi, S., and Miyashita, K. (1995). Learning of sequential movements in the monkey: Process of learning and retention of memory. *Journal of Neurophysiology*, 74:1652–1661.
- Hikosaka, O., Sakai, K., Nakahara, H., Lu, X., Miyachi, K., Nakamura, K., and Rand, M. K. (2000). Neural mechanisms for learning of sequential procedures. In Gazzaniga, M., editor, *The New Cognitive Neurosciences*, pages 553–572. MIT press.
- Holmes, A. and Friston, K. (1998). Generalisability, random effects and population inference. In *NeuroImage*, volume 7, page S754.
- Honda, M., Deiber, M.-P., Ibanez, V., Pascual-Leone, A., Zhuang, P., and Hallett, M. (1998). Dynamic cortical involvement in implicit and explicit motor sequence learning: A PET study. *Brain*, 121:2159–2173.

References

149

- Hopkins, W. G. (1997). *HyperStat Online Textbook*. Available at: <http://davidmlane.com/hyperstat/within-subjects.html>, University of Otago.
- Hornak, J. P. (2002). *The Basics of MRL* Online book at: <http://www.cis.rit.edu/htbooks/mri/>, Rochester, NY.
- Hummel, F., Kirsammer, R., and Gerloff, C. (2003). Ipsilateral cortical activation during finger sequences of increasing complexity: representation of movement difficulty or memory load? *Clinical Neurophysiology*, 114:605–613.
- Jain, A. K., Murty, M. N., and Flynn, P. J. (1999). Data clustering: A review. *ACM Computing Surveys*, 31:264–323.
- Janata, P. and Grafton, S. T. (2003). Swinging in the brain: shared neural substrates for behaviors related to sequencing and music. *Nature Neuroscience Review*, 6:682–687.
- Jenkins, I. H., Brooks, D. J., Nixon, P. D., Frackowiak, R. S., and Passingham, R. E. (1994). Motor sequence learning: A study with positron emission tomography. *Journal of Neuroscience*, 14:3775–3790.
- Jueptner, M., Frith, C. D., Brooks, D. J., Frackowiak, R. S. J., and Passingham, R. E. (1997a). Anatomy of motor learning. II. subcortical structures and learning by trial and error. *Journal of Neurophysiology*, 77:1325–1337.
- Jueptner, M., Stephan, K. M., Frith, C. D., Brooks, D. J., Frackowiak, R. S. J., and Passingham, R. E. (1997b). Anatomy of motor learning. 1. frontal cortex and attention to action. *Journal of Neurophysiology*, 77:1313–1324.
- Kami, A., Meyer, G., Jezzard, P., Adams, M. M., Turner, R., and Ungerleider, L. G. (1995). Functional MRI evidence for adult motor cortex plasticity during motor skill learning. *Nature*, 377:155–158.
- Kennerley, S. W., Sakai, K., and Rushworth, M. F. S. (2004). Organization of action sequences and role of the pre-sma. *Journal of Neurophysiology*, 91:978–993.
- Khushu, S., Kumaran, S. S., Tripathi, R. P., Gupta, A., Jain, P. C., and Jain, V. (2001). Functional magnetic resonance imaging of primary motor cortex in humans: response to increased functional demands. *Journal of Biosciences*, 2:205–215.

- Koch, I. and Hoffmann, J. (2000). Patterns, chunks, and hierarchies in serial reaction-time tasks. *Psychological Research*, 63:22-35.
- Lancaster, J. L., Fox, P. T., Mikiten, S., and Rainey, L. (2001). *Talairach Daemon Client Software*. Web resource available at: <http://ric.uthscsa.edu/projects/talairachdaemon.html>, University of Texas Health Science Center, San Antonio.
- Lashley, K. S. (1951). The problem of serial order in behavior. In Jeffress, L. A., editor, *Cerebral Mechanisms in Behavior*. Wiley, New York.
- MacKay, D. G. (1982). The problem of flexibility, fluency, and speed-accuracy trade-off in skilled behavior. *Psychological Review*, 89:483-506.
- Marrelec, G., Benali, H., Chitin, P., and Poline, J. B. (2002). Bayesian estimation of the haemodynamic response function in functional MRL In Fry, R., editor, *Bayesian Inference and Maximum Entropy Methods*, pages 229-247, AIP, Melville. 21st International Workshop.
- Marrelec, G., Ciuciu, P., Plgrini-Issac, M., and Benali, H. (2004). Estimation of the hemodynamic response in event-related functional MR I: Bayesian networks as a framework for efficient bayesian modeling and inference. *IEEE Transactions Medical Imaging*, 23:959-967.
- Mechelli, A., Henson, R. N. A., Price, C. J., and Friston, K..]. (2003). Comparing event-related and epoch analysis in blocked design fMRI. *N euro Image*, 18:806-810.
- Middleton, F. A. and Strick, P. L. (1998a). Cerebellar output: Motor and cognitive channels. *Trends in Cognitive Sciences*, 2:348-354.
- Middleton, F. A. and Strick, P. L. (1998b). The cerebellum: an overview. *Trends in NeuroScienc.es*, 21:367-369.
- Miller, G. A. (1956). The magical number seven, plus or minus two: Some limits on our capacity for processing information. *Psychological Review*, 63:81-97.
- Miller, G. A., Galanter, E., and Pribram, K. H. (1960). *Plans and the Structure of Behaviour*. Holt, Rinehart and Winston, Inc., New York.

References

151

- Nakahara, H., Doya, K., and Hikosaka, O. (2001). Parallel cortico basal ganglia mechanisms for acquisition and execution of visuomotor sequences: a computational approach. *Journal of Cognitive Neuroscience*, 13:626–647.
- Newell, A., Shaw, J. C, and Simon, H. A. (1958). Elements of a theory of human problem solving. *Psychological Review*, 05:151–166.
- Newell, A. and Simon, H. (1972). *Human Problem Solving*. Prentice Hall, Englewood Cliffs NJ.
- Nissen, M. J. and Bullemer, P. (1987). Attentional requirements of learning: Evidence from performance measures. *Cognitive Psychology*, 19:1–32.
- Ogawa, S., Lee, T. M., Kay, A. R., and Tank, D. W. (1990). Brain magnetic resonance imaging with contrast dependent on blood oxygenation. *Proceedings of the National Academy of Sciences, USA*, 87:9868–9872.
- Ogawa, S., Tank, D. W., Menon, R., Ellermann, J. M., Kim, S., Merkle, H., and Ugurbil, K. (1992). Intrinsic signal changes accompanying sensory stimulation: Functional brain mapping with magnetic resonance imaging. *Proceedings of the National Academy of Sciences, USA*, 89:5951–5955.
- Owen, A. M. (2004). Working memory: Imaging the magic number four. *Current Biology*, 14:R573–R574.
- Pammi, V. S. C., Bapi, R. S., Ahmed, Miyapuram, K. P., and Doya, K. (2005). Hierarchical organization of complex visuo-motor sequences. In Press.
- Pammi, V. S. C., Bapi, R. S., Miyapuram, K. P., Ahmed, and Doya, K. (2004a). Differential spontaneous reorganization of sequences during performance of complex visuo-motor skills. In *Proceedings of the International Conference on Cognitive Science 2004*, pages 211–215, Allahabad, India,
- Pammi, V. S. C., Bapi, R. S., Miyapuram, K. P., Samejima, K., and Doya, K. (2003a). The activation of orbitofrontal cortex reflects trial and error processes in a visuomotor sequence learning task. In *Networks and Behavior, NCBS International Neurobiology Symposium*, Bangalore, India.
- Pammi, V. S. C., Miyapuram, K. P., Bapi, R. S., Bhagavati, C., Brahmaiah, T., and Rao, C. C. S. (2004b). Investigation of time series modelling to explicate

- the learning related activity observed in fMRI data. In *Proceedings of the International Conference on Systemics, Cybernetics and Informatics (I CSI 2004)*, pages 667-672, Hyderabad, India.
- Pammi, V. S. C, Miyapuram, K. P., Bapi, R. S., and Doya, K. (2004c). Chunking phenomenon in complex sequential skill learning in humans. In Pal, N. R., Kasabov, N., Mudi, R. K., Pal, S., and Parui, S. K., editors, *Neural Information Processing*, volume 3316, pages 294-299. Springer-Verlag Heidelberg LNCS.
- Pammi, V. S. C, Miyapuram, K. P., Bapi, R. S., Samejima, K., and Doya, K. (2003b). Acquisition of complex sequential skills: Behavioral and fMRI investigation. In *Building the Brain, Proceedings of the NBRC International Symposium*, Manesar, India.
- Pammi, V. S. C., Miyapuram, K. P., Bapi, R. S., Samejima, K., and Doya, K. (2004d). Differential roles of areas of striatum in complex sequential skill learning. In *Proceedings of the International Neuro science Conference (IAN-SNCI)*, pages 67-68, Hyderabad, India.
- Passingham, R. E., Toni, I., and Rushworth, M. P. S. (2000). Specialisation within the prefrontal cortex: the ventral prefrontal cortex and associative learning. *Experimental Brain Research*, 133:103-113.
- Pasupathy, A. and Miller, E. K. (2005). Different timecourses of learning-related activity in the prefrontal cortex and striatum. *Nature*, 433:873-876.
- Picard, N. and Strick, P. L. (2001). Imaging the premotor areas. *Current Opinion in Neurobiology*, 11:663-72.
- Rabiner, L. (1989). A tutorial on hidden markov models and selected applications in speech recognition. *Proceedings of the IEEE*, 77:257-286.
- Rorden, C. (2004). *MRICro Software*. Version 1.38, Built 5.
- Rosenbaum, D. A., Kenny, S. B., and Derr, M. A. (1983). Hierarchical control of rapid movement sequences. *Journal of Experimental Psychology: Human Perception and Performance*, 9:86-102.
- Sadato, N., Campbell, G., Ibanez, V., Deiber, M., and Hallett, M. (1996). Complexity affects regional cerebral blood flow change during sequential finger movements. *Journal of Neuro science*, 16:2693-2700.

- Sakai, K., Hikosaka, O., Miyauchi, S., Takino, R., Sasaki, Y., and Putz, B. (1998). Transition of brain activation from frontal to parietal areas in visuomotor sequence learning. *Journal of Neuroscience*, 18:1827-1840.
- Sakai, K., Hikosaka, O., Takino, R., Miyauchi, S., Nielsen, M., and Tamada, T. (2000). What and when parallel and convergent processing in motor control. *Journal of Neuroscience*, 20:2691-2700.
- Sakai, K., Kitaguchi, K., and Hikosaka, O. (2003). Chunking during human visuomotor sequence learning. *Experimental Brain Research*, 152:229-242.
- Schendan, H. E., Searl, M. M., Melrose, R. J., and Stern, C. E. (2003). An fMRI study of the role of the medial temporal lobe in implicit and explicit sequence learning. *Neuron*, 37:1013-1025.
- Schmahmann, J. D., Doyon, J., Toga, A. W., and Petrides, M. (2000). *MRI atlas of the human cerebellum*. Academic Press, San Diego.
- Servan-Schreiber, D., Cleeremans, A., and McClelland, J. L. (1991). Graded state machines: The representation of temporal contingencies in simple recurrent networks. In Honavar, V. and Uhr, L., editors, *Artificial Intelligence and Neural Networks: Steps toward principled integration*, pages 241-268. Academic Press, San Diego CA.
- Smith, E. E., Jonides, J., and Koeppe, R. A. (1996). Dissociating verbal and spatial working memory using PET. *Cerebral Cortex*, 6:11-20.
- Srikanth, R., P.N.Jayakumar, and Ramakrishna, A. (J. (2003). Signal subspace enhancement and map parameter estimation of fMRI signals. *Proceedings of IEEE TENCON*.
- Stephan, K. E., Harrison, L. M., Penny, W. D., and Friston, K. J. (2004). Dynamic causal models of brain responses. *Okinawa, Computational Neuroscience Course Lecture Notes*.
- Strange, B. A. (2000). *Imaging the Functions of Human Hippocampus*. PhD Thesis, University College London.
- Strange, B. A., Duggins, A., Penny, W., Dolan, R. J., and Friston, K. J. (2005). Information theory, novelty and hippocampus responses: unpredicted or unpredictable? *Neural Networks*, 18:225-230.

-
- Sun, R. (2000). Introduction to sequence learning. In Sun, R. and Giles, C. L., editors, *Sequence Learning Paradigms, Applications and Algorithms*, volume 1828, pages 1–10. Springer-Verlag LNAI.
- Sun, R. and Giles, L. (2001). Sequence learning: from prediction and recognition to sequential decision making. *IEEE Intelligent Systems*, 16(4):67–70.
- Suri, R. E. and Schultz, W. (1998). Dopamine-like reinforcement signal improves learning of sequential movements by neural network. *Experimental Brain Research*, 121:350–354.
- Sutton, R. S. and Barto, A. G. (1998). *Reinforcement Learning: An Introduction*. MIT Press, Cambridge, MA.
- Svensen, M., Kruggel, F., and von Cramon, D. Y. (2000). Probabilistic modeling of single-trial fMRI data. *IEEE Transactions on Medical Imaging*, 19:25–35.
- Talairach, J. and Tournoux, P. (1988). *Co-planar Stereotaxic Atlas of the Human Brain*. Thieme, New York.
- Terrace, H. (2001). Chunking and serially organized behavior in pigeons, monkeys and humans. In Cook, R. G., editor, *Avian visual cognition*. Comparative Cognition Press, Medford, MA.
- Todd, J. J. and Marois, R. (2004). Capacity limit of visual short-term memory in human posterior parietal cortex. *Nature*, 428:751–754.
- Toni, I., Krams, M., Turner, R., and Passingham, R. E. (1998). The time course of changes during motor sequence learning: a whole-brain fMRI study. *Neuro Image*, 8:50–61.
- Tracy, J., Flanders, A., Madi, S., Laskas, J., Stoddard, E., Pyrros, A., Natale, P., and DelVecchio, N. (2003). Regional brain activation associated with different performance patterns during learning of complex motor skill. *Cerebral Cortex*, 13:904–910.
- Ugurbil, K., Toth, L., and Kim, D. S. (2003). How accurate is magnetic resonance imaging of brain function? *Trends in Neuroscience*, 26:108–114.
- Vazquez, A. L. and Noll, D. C. (1998). Nonlinear aspects of the bold response in functional MRI. *NeuroImage*, 7:108–118.

References

155

- Verwey, W. B. (2001). Concatenating familiar movement sequences: the versatile cognitive processor. *Acta Psychologica*, 10(i):69–95.
- Volkow, N. D., Rosen, B., and Farde, L. (1997). Imaging the living human brain: Magnetic resonance imaging and positron emission tomography. *Proceedings of National Academy of Sciences, USA*, 94:2787–2788.
- Wexler, B. E., Fulbright, R. K., Lacadie, C. M., Skudlarski, P., Kelz, M. B., Constable, R. T., and Gore, J. C. (1997). An fMRI study of human cortical motor system response to increasing functional demands. *Magnetic Resonance Imaging*, 15:385–396.
- Wickelgren, W. A. (1969). Context sensitive coding, associative memory, and serial order in (speech) behavior. *Psychological Review*, 7(i):1–15.
- Wickelgren, W. A. (1999). Webs, cell assemblies, and chunking in neural nets: Introduction. *Canadian Journal of Experimental Psychology*, 53:118–131.
- Willingham, D. B. (1998). A neuropsychological theory of motor skill learning. *Psychological Review*, 105:558–584.

Appendix A

Instructions for the Complexity Experiments

The following list of instructions was given to subjects before the experiment. After ensuring that subjects understood these instructions, a brief practice session (on a test sequence) outside the scanner was given before proceeding to the actual experiment in the scanner.

1. In this experiment, you will see a small "stimulus window" which displays a grid of 3x3 squares.
2. You have to perform two types of blocks in this experiment: FOLLOW RANDOM and LEARN SEQUENCE.
3. During the "FOLLOW RANDOM" blocks, one square is illuminated. Please press as fast as possible the corresponding key on the keypad. The sequence of lights is randomly generated and so do not try to memorize them.
4. During the "LEARN SEQUENCE" blocks, some of the squares in the 3x3 grid are illuminated. Please clear each target by pressing the corresponding keys on the keypad. You have to figure out the correct order of key presses in each set by trial and error.

If you make a mistake in key presses, the program will start, you over from the beginning of the entire sequence. The sequence remains unaltered throughout the experiment. As you practice, please try to memorize the sequence.

5. Before you start a new block you will be shown instructions on the screen such as "FOLLOW RANDOM" and "LEARN SEQUENCE". Please pay attention to these instructions so as to perform the appropriate actions.

FOLLOW RANDOM: Clear the targets by pressing the corresponding keys on the keypad. The sequence of lights is randomly generated and so do not try to memorize them.

LEARN SEQUENCE: You have to figure out the correct order of key-presses in each set by trial and error. The sequence remains unaltered throughout the experiment. As you practice, please try to memorize the sequence!!

Do not forget to press the keys as fast as you can throughout the experiment!

Appendix B

Details of Experimental Procedure and File Formats

This appendix lists the procedure for conducting empirical experimentation and recording the resulting behavioral parameters from experiments. Sample files and their formats are described here.

B.1 Procedure for conducting the experiment

Parameters used in an experiment are stored in subject files (*.sub) and the results of an experiment are stored in result files (*.res). Subject files need to be created for practice and main sessions.

B.1.1 Creation of parameter files

Create subject files in the same directory as the executable file Exp. Enter the following Subject information:

Subject data — first name
 — last name
Results file — file name O.res)

The following notations are used in the Subject file:

- "Block" indicates the Block number. Each experiment consists of 52 blocks arranged in *four* sessions. Each session contains *13* alternating control and

test condition blocks. Every block begins with an instruction screen lasts for 6 seconds.

- "Label" indicates the type of block – "TrainN" (2x0 or 2x12 or 4x6, test or sequence learning conditions) or "FolloN" (Control or Baseline Condition, where subjects pressed one key at a time by **following** randomly generated visual targets, 1x12 random sequence). Each sequence learning condition will have different .res files and they are identified by the subject's short name along with the sequence condition (for example, WY2x6.res or WY2x12.res or WY4x6.res).
- "Hset#" is a number identifying the hyperset used in the block (21 for Sequence learning conditions and 20 to 1 for Follow or Control conditions) by the program.
- "setL" denotes the length of each set in the hyperset - 2 for 2x0 and 4 for 4x6. "HsetL" denotes the length of the hyperset (sequence) - 12 for 2x12 and 6 for 2x6.
- "HsetT" indicates the hyperset Type. For the Follow blocks it will be RAN (a random sequence) and FIX (a fixed sequence.¹) for test, or sequence learning blocks.
- "Hand" indicates the type of hand subject used. The entry R denote right, hand. However, all the subjects in our experiments are right, handed.
- "Key" & "Hset" (Hyperset) The Codes are 2 & 0 for all in this complexity experiments - No rotations or any other transformations are used.
- All the blocks are in "Mode" 1 (Fight the Sequence and Trial-and-Error key-press). Mode 2 and 3 are not supported in this complexity experiments. This mode 1 also used to reset the hyperset during the trial-and-error process.
- Block duration length (BDL) is either 18 seconds (Follow or Control blocks) or 36 seconds (Test or Sequence blocks).
- Set duration is 1.6 sec for 2x6 or 2x12 Sequence Learning blocks in complexity experiments. For 4x6 it, will be 3.2 seconds. On an average, we fixed maximum of 0.8 seconds for each key-press.

- “Trials” indicates the number of trials performed during the block.
- “Block_T” denotes the total time taken for perfect trials (where the subject completed the hyperset successfully). This value does not include the time taken for incomplete trials (where subject has committed an error).
- “Err” indicates the number of incomplete trials.
- “Corr” indicates the number of complete trials.
- “Date_&_Time” records the date and starting time of the block.

B.1.2 Running the Program

We used a modified version of Bapi et al. (2000) experimental program written in C using Metro works Code warrior compiler for Macintosh Computer (release 1.0).

B.1.3 Practice Session

In each study, the Main session in the scanner is preceded by a practice session of approximately 1 hr for the complexity experiment to ensure proper understanding of block instructions and various conditions used in the experimental session. More practice may be given, if required. The value of “Corr” can be checked by opening the corresponding practice file (and compare with corresponding total Trials).

B.2 Subject file

B.2.1 Subject file before the experiment

An example, subject file for 2x6 experiment, is given below:

```
Subject_data
First_name: Pammi
Last_name: Chandrasekhar
Reset_mode: 1 (Hyper-set)
With_text: 0 (No)
```

```

Hyper-sets: 0
Label  setL  hsetL  Hset_Data

Results_file: PC2x6.res
Number_of_blocks: 52
Current_block_number: 1
Block  Label  Hset#  setL  HsetL  HsetT  Hand  Key  Hset  Mode  BDL  Set_Dur  Trials  Block_T  Err  Corr  Date_&_Time
1      FolloN  20      1     12     Ran   R     2     0     1     18     0.8
2      TrainN  21      2     6      Fix   R     2     0     1     36     1.6
3      FolloN  19      1     12     Ran   R     2     0     1     18     0.8
4      TrainN  21      2     6      Fix   R     2     0     1     36     1.6
5      FolloN  18      1     12     Ran   R     2     0     1     18     0.8
6      TrainN  21      2     6      Fix   R     2     0     1     36     1.6
7      FolloN  17      1     12     Ran   R     2     0     1     18     0.8
8      TrainN  21      2     6      Fix   R     2     0     1     36     1.6
9      FolloN  16      1     12     Ran   R     2     0     1     18     0.8
10     TrainN  21      2     6      Fix   R     2     0     1     36     1.6
11     FolloN  15      1     12     Ran   R     2     0     1     18     0.8
12     TrainN  21      2     6      Fix   R     2     0     1     36     1.6
13     FolloN  14      1     12     Ran   R     2     0     1     18     0.8
14     FolloN  13      1     12     Ran   R     2     0     1     18     0.8
15     TrainN  21      2     6      Fix   R     2     0     1     36     1.6
16     FolloN  12      1     12     Ran   R     2     0     1     18     0.8
17     TrainN  21      2     6      Fix   R     2     0     1     36     1.6
18     FolloN  11      1     12     Ran   R     2     0     1     18     0.8
19     TrainN  21      2     6      Fix   R     2     0     1     36     1.6
20     FolloN  10      1     12     Ran   R     2     0     1     18     0.8
21     TrainN  21      2     6      Fix   R     2     0     1     36     1.6

.
.
.

40     FolloN  20      1     12     Ran   R     2     0     1     18     0.8
41     TrainN  21      2     6      Fix   R     2     0     1     36     1.6
42     FolloN  19      1     12     Ran   R     2     0     1     18     0.8
43     TrainN  21      2     6      Fix   R     2     0     1     36     1.6
44     FolloN  18      1     12     Ran   R     2     0     1     18     0.8
45     TrainN  21      2     6      Fix   R     2     0     1     36     1.6
46     FolloN  17      1     12     Ran   R     2     0     1     18     0.8
47     TrainN  21      2     6      Fix   R     2     0     1     36     1.6
48     FolloN  16      1     12     Ran   R     2     0     1     18     0.8
49     TrainN  21      2     6      Fix   R     2     0     1     36     1.6
50     FolloN  15      1     12     Ran   R     2     0     1     18     0.8
51     TrainN  21      2     6      Fix   R     2     0     1     36     1.6
52     FolloN  14      1     12     Ran   R     2     0     1     18     0.8

```

B.2.2 Subject file after the experiment

Sample file that is saved after a 2x6 sequence learning task is shown below:

```

Subject_data

First_name: Pammi
Last_name: Chandrasekhar

Reset_mode: 1 (Hyper-set)
With_text: 0 (No)

Hyper-sets: 21 Label  setL  hsetL  Hset_Data
1      1      12      8 4 7 5 2 1 6 9 3 9 5 7
2      1      12      5 7 6 9 1 8 3 2 4 4 2 2
3      1      12      1 8 7 4 9 6 2 5 3 4 4 5
4      1      12      8 3 1 2 4 9 7 6 5 9 1 2
5      1      12      5 7 6 4 3 9 8 2 1 6 6 3
6      1      12      2 5 4 9 8 7 6 1 3 2 2 6
7      1      12      1 3 9 7 4 8 5 6 2 4 6 7
8      1      12      7 2 8 4 5 9 3 6 1 2 8 7
9      1      12      4 3 1 7 6 8 2 9 5 4 2 2
10     1      12      4 8 1 2 6 7 5 3 9 9 1 4
11     1      12      1 6 9 7 5 4 2 3 8 5 7 6
12     1      12      7 3 2 9 1 8 5 4 6 9 7 9
13     1      12      5 8 1 2 7 4 3 6 9 3 1 9
14     1      12      8 3 9 6 2 7 4 5 1 3 4 1
15     1      12      5 8 1 4 9 2 3 6 7 4 6 6
16     1      12      9 5 2 8 6 4 7 3 1 6 8 4

```

```

17 1 12 9 8 4 2 5 6 3 1 7 4 3 6
18 1 12 2 8 4 7 3 5 6 9 1 1 3 2
19 1 12 7 5 2 6 4 8 1 3 9 8 6 4
20 1 12 3 4 5 6 7 1 2 8 9 1 1 8
21 2 6 8 5 9 7 7 6 1 4 9 1 3 8

Results_file: WY2x6.res
Number_of_blocks: 52
Current_block_number: 53
Block Label Hset# setL HsetL HsetT Hand Key Hset Mode BDL Set_Dur Trials Block_T Err Corr Date_&Time
1 FolloN 17 1 12 Ran R 2 0 1 18 0.800 2 5.569 1 1 2001.07.25 11:19:11
2 TrainN 21 2 6 Fix R 2 0 1 36 1.600 9 13.084 6 3 2001.07.25 11:19:29
3 FolloN 8 1 12 Ran R 2 0 1 18 0.800 2 5.037 1 1 2001.07.25 11:20:05
4 TrainN 21 2 6 Fix R 2 0 1 36 1.600 8 10.707 5 3 2001.07.25 11:20:22
5 FolloN 13 1 12 Ran R 2 0 1 18 0.800 3 0.000 3 0 2001.07.25 11:20:59
6 TrainN 21 2 6 Fix R 2 0 1 36 1.600 7 17.390 2 5 2001.07.25 11:21:16
7 FolloN 18 1 12 Ran R 2 0 1 18 0.800 2 4.838 1 1 2001.07.25 11:21:52
8 TrainN 21 2 6 Fix R 2 0 1 36 1.600 8 8.944 5 3 2001.07.25 11:22:10
9 FolloN 5 1 12 Ran R 2 0 1 18 0.800 2 0.000 2 0 2001.07.25 11:22:46
10 TrainN 21 2 6 Fix R 2 0 1 36 1.600 8 16.193 2 6 2001.07.25 11:23:04
11 FolloN 5 1 12 Ran R 2 0 1 18 0.800 2 4.904 1 1 2001.07.25 11:23:40
12 TrainN 21 2 6 Fix R 2 0 1 36 1.600 8 14.996 2 6 2001.07.25 11:23:58
13 FolloN 14 1 12 Ran R 2 0 1 18 0.800 2 4.788 1 1 2001.07.25 11:24:33
14 FolloN 14 1 12 Ran R 2 0 1 18 0.800 2 5.087 1 1 2001.07.25 11:25:34
15 TrainN 21 2 6 Fix R 2 0 1 36 1.600 8 10.707 4 4 2001.07.25 11:26:52

.
.
.

40 FolloN 8 1 12 Ran R 2 0 1 18 0.800 2 5.154 1 1 2001.07.25 11:38:22
41 TrainN 21 2 6 Fix R 2 0 1 36 1.600 9 14.032 2 7 2001.07.25 11:38:40
42 FolloN 16 1 12 Ran R 2 0 1 18 0.800 2 5.121 1 1 2001.07.25 11:39:16
43 TrainN 21 2 6 Fix R 2 0 1 36 1.600 9 12.269 3 6 2001.07.25 11:39:34
44 FolloN 15 1 12 Ran R 2 0 1 18 0.800 3 5.254 2 1 2001.07.25 11:40:10
45 TrainN 21 2 6 Fix R 2 0 1 36 1.600 9 13.500 2 7 2001.07.25 11:40:28
46 FolloN 2 1 12 Ran R 2 0 1 18 0.800 3 5.170 2 1 2001.07.25 11:41:04
47 TrainN 21 2 6 Fix R 2 0 1 36 1.600 10 13.433 2 8 2001.07.25 11:41:22
48 FolloN 6 1 12 Ran R 2 0 1 18 0.800 2 4.971 1 1 2001.07.25 11:41:58
49 TrainN 21 2 6 Fix R 2 0 1 36 1.600 10 13.200 2 8 2001.07.25 11:42:16
50 FolloN 13 1 12 Ran R 2 0 1 18 0.800 2 4.838 1 1 2001.07.25 11:42:52
51 TrainN 21 2 6 Fix R 2 0 1 36 1.600 9 11.322 3 6 2001.07.25 11:43:10
52 FolloN 8 1 12 Ran R 2 0 1 18 0.800 2 4.871 1 1 2001.07.25 11:43:45

```

B.3 Result file after the experiment

The Result file will contain details of all the trails performed in every block. A sample file (truncated) for 2x6 task is shown below:

```

Results_data

First_name: Pammi
Last_name: Chandrasekhar

Reset_mode: 1 (Hyper-set)
With_text: 0 (No)

Block: 1
Date_&Time: 2001.07.25 11:19:11
Hand: R
Hyperset_Type: Ran
Exp_mode: 1 (Trial_&Error)
Hyperset_Label: FolloN
Key-Trans: TransA
Hset-Trans: Normal
Block_Duration: 18
Set_Duration: 0.800
Number_of_Trials: 2
Hyper-set(1 x 12): 9 8 4 2 5 6 3 1 7 4 3 6

Completed
Trial HsetN Sets Items Trial_Time 0.416 0.482 0.382 0.449 0.432 0.466
1 4 12 0 5.569 0.549 0.499 0.482 0.499 0.449 0.416 0.399
2 17 5 0 2.145 0.382 0.449 0.449 0.449 0.416 0.399

```

```

Block: 2
Date_&_Time: 2001.07.25 11:19:29
Hand: R
Hyperset_Type: Fix
Exp_mode: 1 (Trial_&_Error)
Hyperset_Label: TrainN
Key-Trans: TransA
Hset-Trans: Normal
Block_Duration: 36
Set_Duration: 1.600
Number_of_Trials: 9
Hyper-set(2 x 6): 8 5 9 7 7 6 1 4 9 1 3 8
Completed
Trial HsetN Sets Items Trial_Time
1 21 0 0 0.000 0.798
2 21 2 0 1.463 0.582 0.881 0.815
3 21 6 0 4.705 0.798 0.582 0.549 0.898 0.865 1.014
4 21 6 0 4.505 1.014 0.632 0.599 0.732 0.914 0.615
5 21 0 0 0.000 0.549
6 21 6 0 3.874 0.732 0.599 0.632 0.748 0.582 0.582
7 21 2 0 1.081 0.582 0.499 0.532
8 21 0 0 0.000 0.382
9 21 0 0 0.000 0.549

Block: 3
Date_&_Time: 2001.07.25 11:20:05
Hand: R
Hyperset_Type: Ran
Exp_mode: 1 (Trial_&_Error)
Hyperset_Label: FolloN
Key-Trans: TransA
Hset-Trans: Normal
Block_Duration: 18
Set_Duration: 0.800
Number_of_Trials: 2
Hyper-set(1 x 12): 7 2 8 4 5 9 3 6 1 2 8 7
Completed
Trial HsetN Sets Items Trial_Time
1 18 12 0 5.037 0.532 0.349 0.382 0.399 0.449 0.316 0.416 0.416 0.432 0.466 0.416 0.466
2 8 5 0 1.929 0.366 0.432 0.366 0.382 0.382 0.382

Block: 4
Date_&_Time: 2001.07.25 11:20:22
Hand: R
Hyperset_Type: Fix
Exp_mode: 1 (Trial_&_Error)
Hyperset_Label: TrainN
Key-Trans: TransA
Hset-Trans: Normal
Block_Duration: 36
Set_Duration: 1.600
Number_of_Trials: 8
Hyper-set(2 x 6): 8 5 9 7 7 6 1 4 9 1 3 8
Completed
Trial HsetN Sets Items Trial_Time
1 21 6 0 3.375 0.532 0.515 0.682 0.615 0.532 0.499
2 21 2 0 1.064 0.632 0.432 0.283
3 21 6 0 3.874 0.665 0.499 0.549 0.682 1.014 0.466
4 21 6 0 3.458 0.515 0.482 0.599 0.682 0.732 0.449
5 21 2 0 1.097 0.599 0.499 0.366
6 21 3 0 1.629 0.565 0.499 0.565 0.732
7 21 2 0 1.197 0.532 0.665 0.482
8 21 2 0 1.047 0.482 0.565 0.648

Block: 5
Date_&_Time: 2001.07.25 11:20:59
Hand: R
Hyperset_Type: Ran
Exp_mode: 1 (Trial_&_Error)
Hyperset_Label: FolloN
Key-Trans: TransA
Hset-Trans: Normal
Block_Duration: 18
Set_Duration: 0.800
Number_of_Trials: 3
Hyper-set(1 x 12): 5 8 1 2 7 4 3 6 9 3 1 9
Completed
Trial HsetN Sets Items Trial_Time
1 20 0 0 0.000 0.532
2 4 10 0 4.605 0.449 0.482 0.482 0.515 0.515 0.432 0.432 0.432 0.399 0.466 0.499
3 13 2 0 0.865 0.349 0.515 0.665

```

Block: 12
 Date_&Time: 2001.07.25 11:23:58
 Hand: R
 Hyperset_Type: Fix
 Exp_mode: 1 (Trial_&Error)
 Hyperset_Label: TrainN
 Key-Trans: TransA
 Hset-Trans: Normal
 Block_Duration: 36
 Set_Duration: 1.600
 Number_of_Trials: 8
 Hyper-set(2 x 6): 8 5 9 7 7 6 1 4 9 1 3 8

Completed

Trial	HsetN	Sets	Items	Trial_Time							
1	21	6	0	2.427	0.615	0.382	0.399	0.333	0.399	0.299	
2	21	6	0	2.461	0.648	0.382	0.382	0.416	0.299	0.333	
3	21	3	0	1.347	0.565	0.349	0.432	0.083			
4	21	6	0	2.594	0.549	0.416	0.333	0.316	0.682	0.299	
5	21	6	0	2.560	0.698	0.366	0.549	0.299	0.333	0.316	
6	21	6	0	2.510	0.748	0.366	0.532	0.283	0.249	0.333	
7	21	6	0	2.444	0.648	0.333	0.466	0.349	0.316	0.333	
8	21	1	0	0.682	0.682	0.366					

Block: 13
 Date_&Time: 2001.07.25 11:24:33
 Hand: R
 Hyperset_Type: Ran
 Exp_mode: 1 (Trial_&Error)
 Hyperset_Label: FolloN
 Key-Trans: TransA
 Hset-Trans: Normal
 Block_Duration: 18
 Set_Duration: 0.800
 Number_of_Trials: 2
 Hyper-set(1 x 12): 8 3 9 6 2 7 4 5 1 3 4 1

Completed

Trial	HsetN	Sets	Items	Trial_Time												
1	11	12	0	4.788	0.482	0.399	0.399	0.399	0.349	0.416	0.432	0.466	0.349	0.333	0.399	0.366
2	14	6	0	2.477	0.366	0.382	0.349	0.565	0.449	0.366	0.399					

Block: 14
 Date_&Time: 2001.07.25 11:25:34
 Hand: R
 Hyperset_Type: Ran
 Exp_mode: 1 (Trial_&Error)
 Hyperset_Label: FolloN
 Key-Trans: TransA
 Hset-Trans: Normal
 Block_Duration: 18
 Set_Duration: 0.800
 Number_of_Trials: 2
 Hyper-set(1 x 12): 8 3 9 6 2 7 4 5 1 3 4 1

Completed

Trial	HsetN	Sets	Items	Trial_Time												
1	13	12	0	5.087	0.432	0.382	0.466	0.466	0.399	0.449	0.449	0.399	0.416	0.432	0.382	0.416
2	14	6	0	2.610	0.482	0.416	0.416	0.432	0.432	0.432	0.399					

Block: 49
 Date_&Time: 2001.07.25 11:42:16
 Hand: R
 Hyperset_Type: Fix
 Exp_mode: 1 (Trial_&Error)
 Hyperset_Label: TrainN
 Key-Trans: TransA
 Hset-Trans: Normal
 Block_Duration: 36
 Set_Duration: 1.600
 Number_of_Trials: 10
 Hyper-set(2 x 6): 8 5 9 7 7 6 1 4 9 1 3 8

Completed

Trial	HsetN	Sets	Items	Trial_Time							
1	21	6	0	1.712	0.499	0.283	0.266	0.233	0.216	0.216	
2	21	6	0	1.596	0.466	0.216	0.249	0.233	0.216	0.216	
3	21	6	0	2.028	0.466	0.216	0.266	0.632	0.249	0.200	
4	21	6	0	1.712	0.466	0.200	0.299	0.299	0.200	0.200	
5	21	6	0	1.513	0.449	0.183	0.249	0.233	0.200	0.200	
6	21	6	0	1.513	0.466	0.200	0.233	0.200	0.200	0.216	
7	21	6	0	1.546	0.515	0.183	0.216	0.249	0.183	0.200	
8	21	6	0	1.579	0.532	0.150	0.266	0.233	0.183	0.216	
9	21	3	1	0.898	0.449	0.166	0.283	0.266			
10	21	0	0	0.000	0.432						

Block: 50

```

Date_&_Time: 2001.07.25 11:42:52
Hand: R
Hyperset_Type: Ran
Exp_mode: 1 (Trial_&_Error)
Hyperset_Label: FolloN
Key-Trans: TransA
Hset-Trans: Normal
Block_Duration: 18
Set_Duration: 0.800
Number_of_Trials: 2
Hyper-set(1 x 12): 5 8 1 2 7 4 3 6 9 3 1 9
Completed
Trial HsetN Sets Items Trial_Time
1 20 12 0 4.838 0.449 0.416 0.382 0.382 0.482 0.416 0.416 0.299 0.432 0.432 0.382 0.349
2 13 5 0 2.062 0.466 0.366 0.416 0.449 0.366 0.416
Block: 51
Date_&_Time: 2001.07.25 11:43:10
Hand: R
Hyperset_Type: Fix
Exp_mode: 1 (Trial_&_Error)
Hyperset_Label: TrainN
Key-Trans: TransA
Hset-Trans: Normal
Block_Duration: 36
Set_Duration: 1.600
Number_of_Trials: 9
Hyper-set(2 x 6): 8 5 9 7 7 6 1 4 9 1 3 8
Completed
Trial HsetN Sets Items Trial_Time
1 21 6 0 1.679 0.466 0.299 0.249 0.249 0.200 0.216
2 21 6 0 1.513 0.432 0.200 0.233 0.216 0.216 0.216
3 21 6 0 1.513 0.482 0.200 0.233 0.200 0.183 0.216
4 21 4 0 1.081 0.482 0.183 0.216 0.200 0.150
5 21 6 0 1.679 0.499 0.200 0.316 0.266 0.183 0.216
6 21 6 0 3.059 0.599 0.200 0.382 0.266 1.397 0.216
7 21 3 1 0.848 0.449 0.183 0.216 0.249
8 21 6 0 1.879 0.482 0.299 0.349 0.299 0.200 0.249
9 21 4 0 1.347 0.582 0.216 0.299 0.249 0.200
Block: 52
Date_&_Time: 2001.07.25 11:43:45
Hand: R
Hyperset_Type: Ran
Exp_mode: 1 (Trial_&_Error)
Hyperset_Label: FolloN
Key-Trans: TransA
Hset-Trans: Normal
Block_Duration: 18
Set_Duration: 0.800
Number_of_Trials: 2
Hyper-set(1 x 12): 7 2 8 4 5 9 3 6 1 2 8 7
Completed
Trial HsetN Sets Items Trial_Time
1 13 12 0 4.871 0.466 0.366 0.366 0.399 0.382 0.399 0.399 0.349 0.416 0.399 0.382 0.549
2 8 6 0 2.361 0.449 0.416 0.333 0.366 0.399 0.399 0.399

```

B.4 Post processing of Behavioural Results

We developed a C program (using Turbo C Version 3.0) which automatically computed parameters of interest given a *.res* file or group of *.res* files. We generated two kinds of files *.sui* and *.avi*. The *.avi* file is computed for each experiment and it contains parameters such as total trial time, number of sets completed, non-zero trials, average key-press time, trials, success rate, successful hypersets and the number of movements, that are computed block-wise. The *.sui* file is a compressed form of result file, which we used for chunking analysis, the results of which are reported in the Chapter 6. Some of the parameters of *.avi* file were used in the behavioural analysis reported in the Chapter 5.

Appendix C

Hypersets used in the Current Study

In this appendix we list the hypersets generated by our experimental program for all the 17 subjects for each of the experimental task.

Hypersets generated for all the subjects in this study in the 2x6' experiments

FB 2x6	:	1	9	9	4	5	9	2	9	1	4	5	2
HU 2x6	:	7	5	4	8	4	3	1	2	6	8	1	7
KU 2x6	:	3	9	6	4	6	5	1	9	5	7	5	3
ST 2x6	:	3	5	7	3	6	2	4	1	2	9	7	6
TF 2x6	:	7	3	7	8	5	8	7	6	2	3	1	4
TG 2x6	:	9	6	4	5	3	7	2	3	1	8	8	9
WY 2x6	:	8	5	9	7	7	6	1	4	9	1	3	8
AS 2x6	:	3	2	2	5	3	1	8	2	9	3	8	9
BN 2x6	:	3	8	1	9	4	6	6	1	6	2	4	5
CH 2x6	:	5	6	5	1	6	4	9	3	4	7	7	3
EC 2x6	:	2	8	6	2	4	1	4	6	1	5	8	9
JC 2x6	:	9	6	7	6	1	3	5	3	6	4	8	5
NS 2x6	:	4	7	8	9	7	2	1	4	9	3	7	1
PV 2x6	:	3	8	7	2	9	1	7	3	5	6	1	8
RC 2x6	:	5	7	1	3	7	6	5	1	3	8	1	8
WP 2x6	:	2	3	5	3	7	8	1	3	7	5	8	3
YU 2x6	:	3	2	3	8	7	4	1	8	9	5	6	5

Hypersets generated for all the subjects in this study in the 2x12 experiments

```

FB 2x12 : 7 1 9 8 7 4 6 9 4 8 4 9 4 3 7 5 3 5 9 7 1 9 4 5
HU 2x12 : 5 1 3 6 7 3 6 8 1 2 9 7 9 2 3 8 6 9 6 2 1 9 1 7
KU 2x12 : 1 8 5 8 1 6 2 3 9 4 8 4 6 2 2 8 5 4 5 6 3 1 3 9
ST 2x12 : 2 3 8 6 9 6 4 5 1 6 7 2 7 4 4 2 5 8 2 5 8 9 4 1
TF 2x12 : 1 4 7 4 4 8 6 8 9 1 6 5 3 4 5 1 2 9 5 2 7 5 9 8
TG 2x12 : 8 3 3 9 6 3 8 9 6 9 5 4 7 3 2 3 8 7 2 4 4 9 1 8
WY 2x12 : 4 5 6 4 8 7 1 6 9 8 9 4 1 3 6 5 3 7 8 4 2 6 2 4
AS 2x12 : 5 4 8 1 7 6 8 3 9 3 4 8 4 7 6 5 3 2 6 1 7 5 9 2
BN 2x12 : 8 4 9 7 1 8 7 6 2 3 4 6 5 4 9 3 6 5 7 1 1 4 6 9
CH 2x12 : 5 1 2 4 8 9 1 9 2 6 8 1 1 3 9 6 6 8 5 4 7 1 4 1
EC 2x12 : 9 5 1 3 6 2 6 3 8 7 5 4 1 7 3 2 8 2 8 5 2 9 3 8
JC 2x12 : 5 3 1 4 8 9 7 4 8 7 3 7 8 6 6 2 9 1 2 3 9 6 3 8
NS 2x12 : 7 4 5 4 7 6 7 9 4 9 1 7 8 7 3 8 1 3 8 4 8 9 4 2
PV 2x12 : 8 4 4 9 8 5 7 3 9 8 3 5 6 9 1 8 4 1 4 6 3 1 2 9
RC 2x12 : 9 2 8 1 3 9 4 8 7 2 8 5 1 9 2 1 7 4 5 7 5 3 4 9
WP 2x12 : 1 6 8 9 6 5 9 6 4 2 4 7 2 7 3 2 1 4 7 8 2 5 3 7
YU 2x12 : 5 8 1 5 8 9 1 6 7 2 2 5 3 1 7 1 3 6 4 7 6 9 8 3

```

Hypersets generated for all the subjects in this study in the 4x6 experiments

FB 4x6 :	2 6 5 1	5 3 4 2	4 8 9 1	1 8 3 6	3 8 4 5	3 9 4 1
HU 4x6 :	4 9 3 6	2 4 6 9	9 1 7 8	1 7 8 3	9 7 1 4	6 7 2 9
KU 4x6 :	5 2 6 7	8 7 2 6	3 6 5 8	3 6 4 5	1 6 2 5	9 3 7 6
ST 4x6 :	1 7 6 2	5 2 8 7	1 4 2 5	9 4 2 6	4 2 6 5	5 9 4 6
TF 4x6 :	6 2 3 7	3 5 4 7	5 7 4 8	8 3 7 2	9 7 2 8	9 8 7 4
TG 4x6 :	1 8 7 3	5 3 6 4	9 7 2 8	3 9 2 1	5 3 7 1	4 7 6 9
WY 4x6 :	1 5 9 8	1 3 5 2	7 2 8 4	3 8 1 7	2 5 8 9	9 5 3 1
AS 4x6 :	7 6 9 5	9 2 5 8	8 9 1 5	4 2 3 1	1 3 7 6	3 1 5 2
BN 4x6 :	1 7 6 8	5 6 2 9	7 8 5 9	9 4 5 8	7 5 6 4	7 3 1 8
CH 4x6 :	8 3 6 2	4 1 3 5	6 5 3 9	2 7 1 4	8 7 9 6	2 4 9 8
EC 4x6 :	9 3 6 4	9 1 4 3	1 9 4 6	6 4 8 1	9 4 5 2	3 8 9 6
JC 4x6 :	7 2 9 1	8 5 6 9	4 7 1 9	8 4 7 9	2 5 9 8	3 8 7 6
NS 4x6 :	5 1 7 2	7 5 2 4	1 4 9 3	4 2 3 1	1 8 9 5	7 3 1 5
PV 4x6 :	3 7 2 4	6 3 7 1	2 8 9 7	8 7 1 5	7 2 3 6	2 6 7 8
RC 4x6 :	5 3 7 2	7 8 9 6	9 8 5 4	7 9 1 4	4 6 3 9	1 2 3 9
WP 4x6 :	7 6 3 8	6 2 7 4	1 2 9 7	4 7 1 3	7 3 9 2	3 9 8 2
YU 4x6 :	4 9 5 7	3 6 1 9	2 6 9 5	3 6 5 2	1 2 5 8	7 9 4 8

Appendix D

Data Analysis Procedure using SPM99

In this appendix, a step-by-step procedure is given for performing fMRI data analysis using the SPM package. A public domain software package, called SPM is extensively used to analyse functional neuroimaging data. SPM has an extensive website at: <http://www.fil.ion.ucl.ac.uk/spm>.

Statistical Parametric Mapping (SPM) refers to the construction and assessment of spatially extended statistical process used to test hypotheses about (neuroimaging data from SPECT, PET & fMRI). Also, SPM is a form of data reduction, condensing information (in a statistically meaningful way) from a number of individual scans into a single image volume that can be more easily viewed and interpreted.

In the following, sequence of analysis steps to be followed for image analysis is given. This description also includes a complete listing of menu options in SPM99 along with appropriate values used for our experimental analysis. We adopt a direct instructional guidance approach to present various steps here. Some of the instructions are taken verbatim from the SPM99 manual, Raima Christoff's online documentation (available at: <http://www-psych.stanford.edu/~kalina/SPM99/>) and from various web resources (references listed at the end of this Appendix).

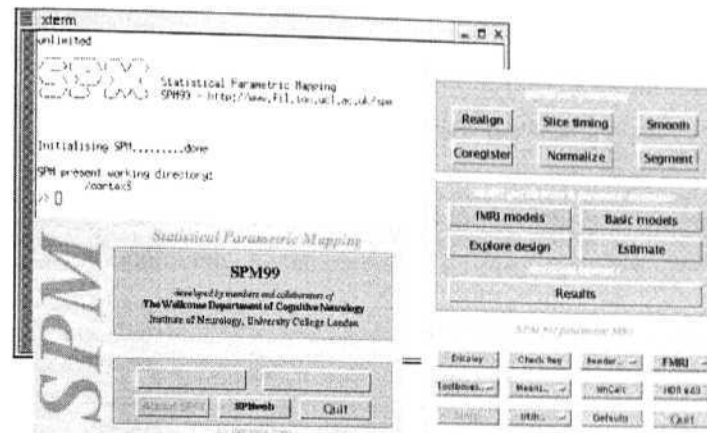


Figure D.1: SPM GUI

SPM99 requires core MATLAB (version 5.2 or higher, Maths Works, Inc.) to run. The image format used is the simple header and image file format, of ANALYZE 7.5 (Biomedical Imaging Resource, Mayo Foundation). The graphical user interface (GUI) of SPM99 is shown in the Figure: D.1. SPM99 separately examines every voxel (3-dimensional pixel) location across all images, and computes a parametric map containing a parameterized value at each voxel. Data analysis as implemented in SPM is parametric. Statistics with a known null distribution are used, such that under the null hypothesis, the probability of obtaining a statistic: greater than, or equal to, that observed can be computed. The statistical model used is a special case of the general linear model (Strange, 2000). Several preprocessing steps are required before statistical analysis. The aim of preprocessing is to reduce artifacts and noise and to perform spatial transformations.

D.1 Preprocessing

Spatial transformations are important in many aspects of functional image analysis. The first several steps put each image volume into a standardized spatial reference frame. The final preprocessing step applies a Gaussian spatial filter.

D.1.1 Setting the origin and reorientation of images

The goal of setting the origin is to set the origin of functional images to the line joining anterior commissure to the posterior commissure (AC-PC line) as shown in the Figure: D.2. The purpose of this is that during the Normalization phase performed in a later stage, the images from each subject will be warped into a standardized brain space that has the origin set for the AC. If the origin for a subject's image is not close to the AC, then the normalization process may be impeded.

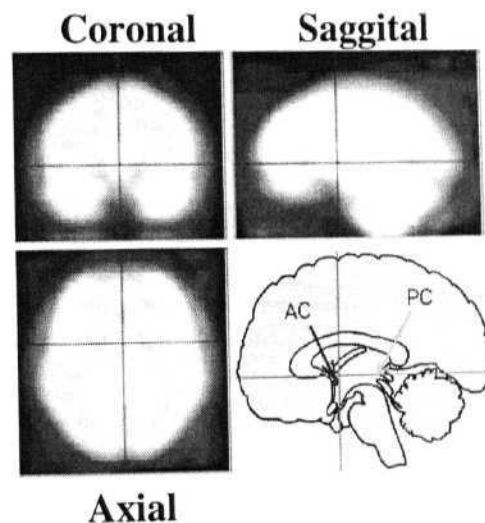


Figure D.2: EPI Template Image and Locating the Origin

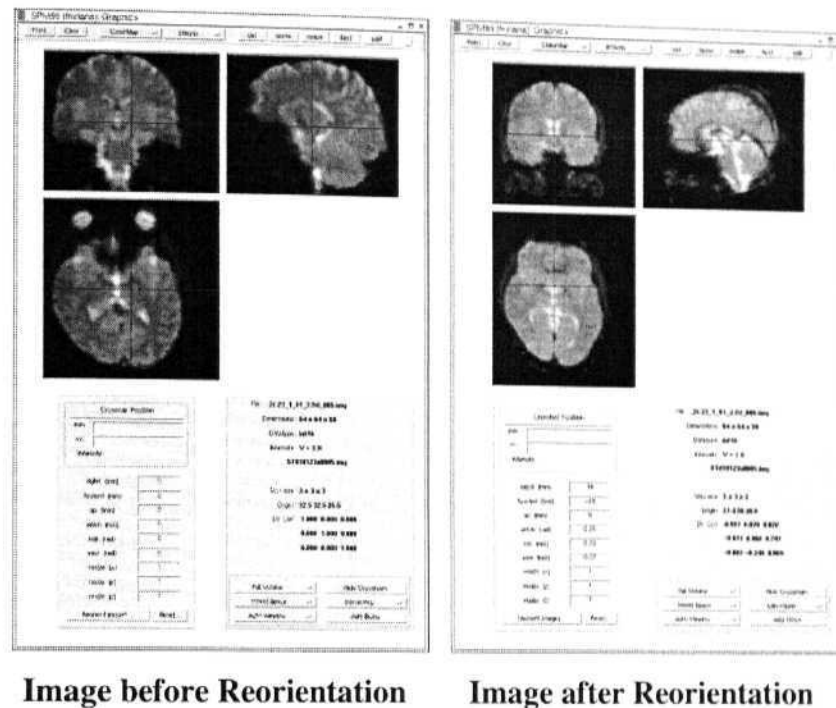


Figure D.3: Images before and after Reorientation

Select "Display" option in the SPM and then select an image to display it. In the upper part of the screen, there should be 3 boxes showing the 3 orthogonal views (coronal, axial and sagittal) of the image:

- The upper left box should look like a coronal view
- The lower left box should look like a axial (horizontal) view, with the front of the brain in the top of the box
- The top right box should display a sagittal view of the brain, with the front of the brain on the left side of the box.

Now, adjust the rotations by

- Changing the yaw, if the head is rotated in the axial plane
- Changing the pitch to set the x axis run through the AC-PC line in the sagittal plane.

- Changing the roll if the head is rotated in the coronal plane.
- Now adjust the right(x), Forward(y), and Up(z) values to set the origin

For this purpose, we can use the `spm99/templates/epi.img` as a reference. Once, everything looks okay, then click on "reorient images" at the bottom of the display box and select all the functional images to be reoriented. The results of reorientation are shown in the Figure: D.3.

D.1.2 Realignment

The next step is to realign the functional images. Although the subjects are asked to keep their heads still, movement does occur. This step will align all the functional images to a single functional image to remove any translations or rotations within the data set. This is the process used for motion correction.

Select **REALIGN**

Number of subjects: Enter the appropriate number. Most typically, you would enter 1 here.

Number of sessions for subject 1: Enter the number of sessions for the entire experiment.

Scans for subject 1, sess1: select *_1.img - DONE

Scans for subject 1, sess2: select *_2.img - DONE

... until all sessions (and subjects) are done.

Which option? Select **coregister only**.

Selecting *coregister only* will cause all files to be realigned by creating *.mat files that will contain realignment transformations that need to be applied to the corresponding image files. No new images will be produced (i.e., the image files will not be resliced).

Selecting *reslice only* will cause new r*.img files to be produced. The *.img imported will be transformed according to their corresponding *.mat files (given that they exist) and the resulting images will be written out as r*.img files. No *.mat files will be created.

Selecting *coregister & reslice* will both realign the selected files, and will produce new files.

Realignment works in two stages. First, the first files (*001.img) from each

session are realigned to the first file of the first session. Second, within each session, the second, third, etc. (2, \dots , n) images are realigned to the first image. As a consequence, after realignment, all files are realigned to the first file of the first session.

	Translation	Rotation
Blue	X	pitch
Green	Y	roll
Red	Z	yaw

Realignment produces text files with estimated motion parameters for each session. These are `realignment_params_*.txt`. They contain 6 columns and each row corresponds to a *.img file. The columns are the estimated translations in *mm* (right, forward, up) and the estimated rotations in radians (pitch, roll, yaw) that are needed to shift each image file. In *sonic*¹ experiments, the realignment parameters are used as regressors in the statistical analysis. Realignment parameters computed for a single subject are shown in the Figure: D.4. Translation and rotation parameters upto the voxel dimension (in our experiments voxel dimension is 3mm) is considered safe for the purpose of statistical analysis.

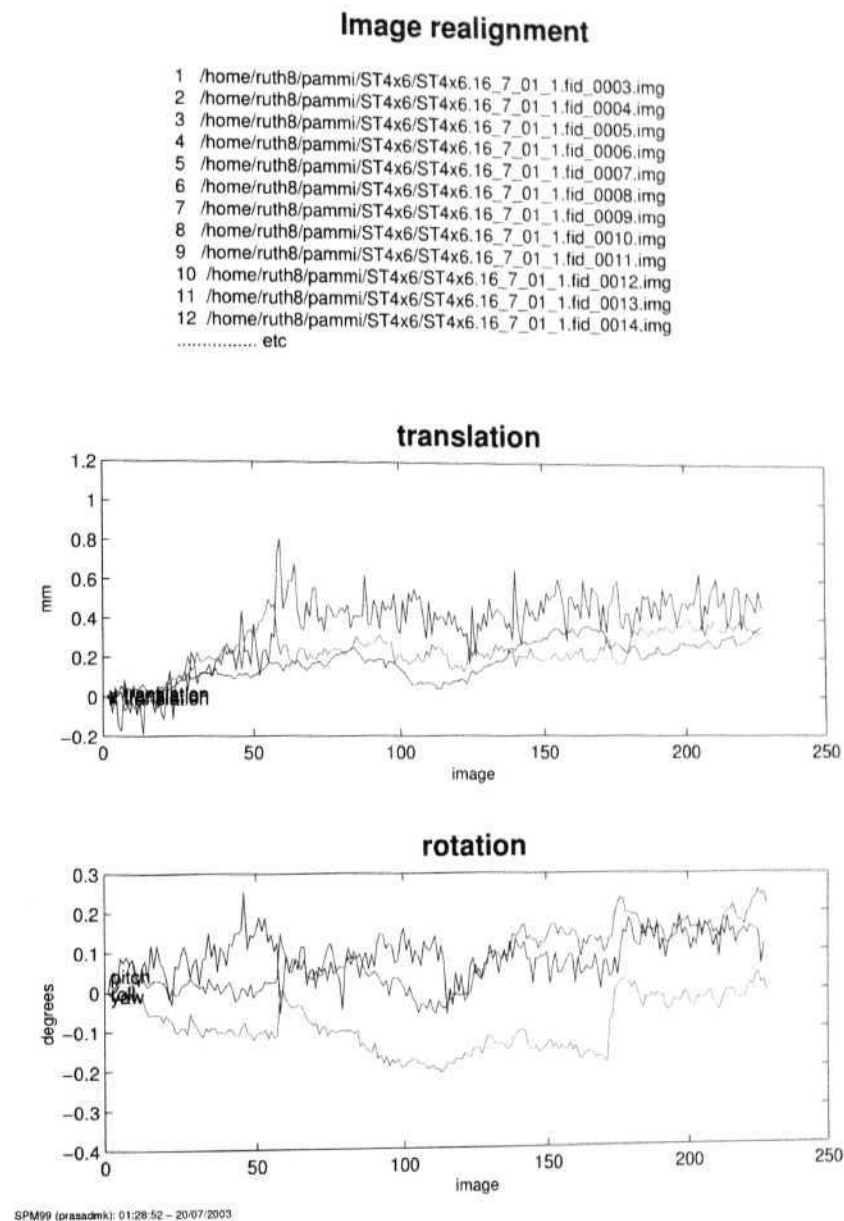


Figure D.4: Realignment Parameters

D. 1.3 Coregistration

For studies of a single subject, the sites of activation can be accurately localised by superimposing them on a high-resolution anatomical structural image of the subject. This requires the registration of the functional images with the anatomical image.

The goal of eoregistration is to enable the functional images to be overlaid onto the anatomical (or structural) image of the subject. This step finds the transformation that maps the anatomical image into the space of the functional images. A further use of this registration is that a more precise spatial normalization can be achieved by computing it with a more detailed anatomical (structural) image. A new '.mat' file is created for the anatomical image.

Select **COREGISTER**

Number of subjects : 1

Which option? coregister only.

Modality of first target image? Select EP1.

The target image is the one to which we coregister. EP1 is the generic option for functional MRI images.

Modality of first object image? Select T1 MRL

The object image is the one which is being coregistered. Select T1 MM if the structural image looks dark where gray matter should be and bright where white matter should be. If the structural image has the opposite contrast (bright where gray matter should be and dark where white matter should be, it is probably T2 MRI, so select appropriately).

Select target image for subject 1: Select the first functional (EPJ) image - DONE

Select object image for subject 1: Select the inplane anatomical 3D image : -DONE

Select other images for subject 1: - DONE (do not select any images)

If any images are selected as "other", the transformation parameters estimated to coregister the object to the target image will also be applied to the "other" images.

This step will find the transformation that maps the in plane anatomical 3D image into the space of the functional images (as defined by the first EP1 image). A new mat file will be created for the anatomical 3D image. Results of eoregistration are shown in Figure: D.5.

To check the coregistration between the functional image and the anatomical image: Select **CHECK REG** on the main menu and select the two images.

Coregistration

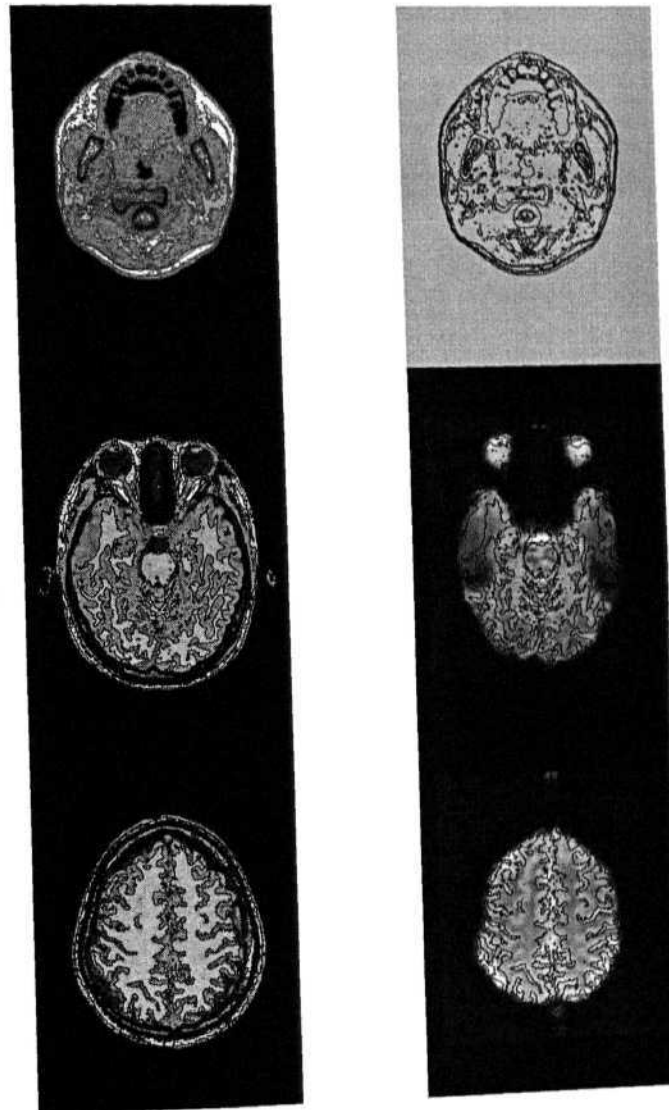
$$X1 = 0.333 \cdot X + 0.003 \cdot Y - 0.010 \cdot Z - 2.176$$

$$Y1 = -0.004 \cdot X + 0.333 \cdot Y - 0.018 \cdot Z - 7.341$$

$$Z1 = 0.010 \cdot X + 0.018 \cdot Y + 0.333 \cdot Z - 27.446$$

..h8/pammi/WY4x6/3D.img

..6_7_01_1.fid_0003.img



SPM99 (prasadm): 14:36:27 - 20/07/2003

Figure D.5: Coregistration of functional image with anatomical image

D.1.4 Normalization

Sometimes, it is desirable to warp images from a number of individuals into roughly the same standard space to allow signal averaging across subjects. A further advantage of using spatially normalized images is that activation sites can be reported according to their coordinates within a standard space. The most commonly adopted coordinate system is the one described by Talairach and Tournoux (1988).

The normalization process is used to convert the subject's brain into a common three-dimensional brain space (talairach). Normalization facilitates between-subject analysis to be performed, and allows overlays to be used for examining data across subjects.

In this process, SPM creates a 2x2x2 voxel size images by default. Also, the output images will be interpreted as "*left is left*" and "*right is right*" convention, as popularly used by neurologists. We need to specify if the images need to be flipped using the "defaults-edit" option and specifying the convention of input images (i.e. whether *Radiological* or *Neurological*).

Select **NORMALIZE**

Which Option?...: Determine Parameters Only

Number of subjects : 1

Image to determine parameters from : select anatomical 3D.img, DONE

Template to normalize to: Select the T1 image from spm99/templates as the template image. This is the brain image that is in the standardized space.

The calculated parameters will be stored in the *_sn3d.mat for the anatomical image.

Now, if the parameters seem correct, normalize all the functional images using this *_sn3d.mat in the following way.

Select **NORMALIZE**

Which Option?...: Write Normalized Only

Number of subjects : 1

Normalization parameter set : Select the *_sn3d.mat, DONE

Images to write normalized : select all functional images, DONE

Interpolation Method : *Sinc* Interpolation(9x9x9)

This step will create images with a prefix of V for all functional images.

Results of normalization are shown in the Figure: D.6.

Spatial Normalisation

Image : /tmp_mnt/home/ruth8/pammi/FB2x2/3D.img
Parameters : /tmp_mnt/home/ruth8/pammi/FB2x2/3D_sn3d

Linear (affine) component - image flipped

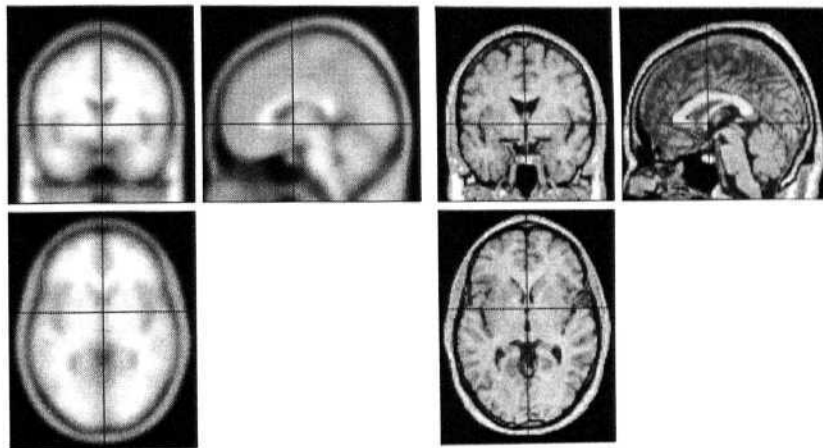
$X1 = -1.081 \cdot X + 0.007 \cdot Y + 0.029 \cdot Z - 0.641$

$Y1 = 0.000 \cdot X + 0.991 \cdot Y - 0.042 \cdot Z - 5.613$

$Z1 = 0.034 \cdot X + 0.066 \cdot Y + 1.085 \cdot Z - 0.100$

12 nonlinear iterations

7 x 8 x 7 basis functions



SPM99 (prasadmk): 14-48-13 - 20/07/2003

Figure D.6: Normalization

D.1.5 Smoothing

The idea of smoothing is to replace the intensity value within each voxel with a weighted average (as determined by a gaussian kernel centered on that particular voxel) that incorporates the intensity values of the neighboring voxels. Smoothing is performed to compensate for residual between-subject variability.

after normalization.

The matching of the brains in the Normalization step is only possible on a coarse scale, since there is not necessarily a one-to-one mapping of the cortical structures between different brains. Because of this, images are smoothed prior to the statistical analysis in a multi-subject study, so that corresponding sites of activation from the different brains can be superimposed.

Smoothing generally increases the signal relative to noise (SNR). Since, hemodynamic responses are modelled to have a gaussian shape, we need to use a gaussian kernel of size at least twice the voxel size (FWHM of about 4 or 5 mm) for smoothing the functional images. Smoothing also permits the application of Gaussian random field theory at the statistical inference stage.

Select **SMOOTH**

Smoothing FWHM in mm : 6

Select images to work on : select all normalized images i.e. n*.img, **DONE**
This step creates images with a prefix of 's' for the normalized functional images. After preprocessing the images, the data are ready for statistical analysis. This involves two steps: Firstly, statistics indicating evidence against a null hypothesis of no effect at each voxel are computed. This results in an "image" of statistics. Secondly, this statistic image must be assessed, reliably locating voxels where an effect is exhibited. The hypothesis is framed as a design matrix model. The design matrix is formed by designating a set of columns, which correspond to experimental conditions of interest (the hypothesis under test) and a set of columns which model effects of no interest.

D.2 Statistical Analysis

Statistical analysis corresponds to the computation of statistical parametric mapping using the General linear model (GLM) and theory of gaussian fields. The GLM is used to specify the conditions in the form of a design matrix, which defines the experimental design and the nature of hypothesis testing to be implemented. The design matrix has one row for each scan and one column for each effect (condition) or explanatory variable (e.g. regressor or stimulus function).

The General Linear model is an equation, which expresses the observed response variable in terms of a linear combination of explanatory variable* plus a

well-behaved error term. The general linear model is variously known as 'analysis of covariance' or 'multiple regression analysis' and subsumes simpler variants like the *t* test for a difference in means. The matrix that contains the explanatory variables (e.g. designed effects or confounds) is called the design matrix. Each column in the design matrix corresponds to some effect one has built into the experiment or that may confound the results.

D.2.1 fMRI model setup

fMRI model specification is done here:

Specify a model

Inter Scan Interval: 6 secs

Scans per session: 44 44 44 44

This specifies that there are four sessions each containing 44 scans. The actual number of fMRI volumes (scans) collected were 57. Of these, the first scan of every block was discarded as it corresponded to the instruction period.

Are sessions replicated? yes

Enter 'yes' if the sessions are exactly replicated, i.e., if there are the same condition parameters in each session. Enter 'no' if the above does not hold. For specification of user defined regressors or parametric modulation, option 'No' is be used. This enables specifying the experimental condition parameters separately for each session .

Are Timing Parameters Same? Yes

If each experimental condition has the same onset times across different sessions then select the option 'Yes'.

No. of Conditions? 2 (Follow and Sequence).

Name of Trial 1 : Follow

Name of Trial 2 : Sequence

Stochastic design? No

Stimulus onset Asynchroni (SOA) Fixed

There is a fixed sequence of occurrence of our conditions.

SOA for Follow : 7

The number of scans from the beginning of n^{th} trial to the beginning of $(n + 1)^{th}$ trial

Time to first trial : 0

The first Follow block occurs after 0 scans from the onset or the beginning of a session

SO A for Sequence : 7

Time to first trial : 2

Parametric modulation : none

Are these Trials : epochs

Events are for a shorter duration and do not occur in same sequence. Epochs occur in same sequence and for some amount of time the subjects are doing the same task, repeatedly.

Type of response : Boxcar

Convolve with hrf? yes

MRI gives us the blood flow signal, but we are interested in the neural activity. It is possible that the neural response is quicker and the changes in blood flow take place a little later. To account for these? and to find the neural activity from the MRI signal, we use the hemodynamic response function (hrf)

Add temporal derivatives : No

Epoch length (scans) for Follow : 2

Epoch length (scans) for Sequence : 5

Interactions among trials : No

user specified regressors : none

This option is used to model specific effects of behaviour with the help of *explanatory variable* obtained from the behavioural data,. These explanatory variables could be response time or accuracy or number of movements. In this complexity experiment we used response times (set completion times in 2x(i-4x(i design matrix and the hyperset completion times in 2x6-2x12 design matrix) as 'user-specified regressors'. The regressor values for each session and then subsequently for all the images are to be specified using this menu. The regressor values should correspond to the number of scans in the design matrix. Also, before entering the regressor values, the regressor values should be convolved (shifted with respect to scanner repetition time, TR) with hemodynamic response function (hrf) as the SPM will only do the implicit convolution to the conditions. In this complexity experiment as TR of the scanner is 0 seconds, we shifted the regressor values only by one scan.

This step creates `SPM_fMRIDesMtx.mat` in the current working directory

`SPM_fMRIDesMtx.mat` - a file containing the design parameters (onsets, number

of conditions, name of conditions, etc.). It can be used later on for different subjects which have the same design parameters, so that you don't have to specify them again. To use the file, select **fMRI MODELS**, and then select **estimate a specified model**.

Estimate a Specified Model

Select the fMRI design matrix `SPM_fmRIDesMtx.mat`

Select scans for session 1 – `sn_1*.img` (44 scans)

Select scans for session 2 – `sn_2*.img` (44 scans)

:

Select scans for session 4 – `sn_4*.img` (44 scans)

Remove global effects : None

If you select 'scale' the value in each voxels for a given `sn*`-file will be divided by the global brain mean value for this `sn*`-file. Global scaling can be beneficial, since it reduced intersubject variability and improves the sensitivity at the group level of analysis. However, it relies on the assumption that the global brain mean does not correlate with the task. If this assumption is violated, applying global scaling can cause large areas of the brain to appear as activated. Global scaling should be applied only with extreme caution. In our experiments, applying the Global scaling showed huge deactivations (i.e., activation in `Control>Sequence` tasks). In order to avoid these spurious deactivations, we did not perform Global Scaling in our analysis.

Temporal auto correlation options:

High Pass Filter : specify

Select 'specify' if you want to filter out the low-frequency components of the signal. High-pass filtering is usually beneficial, since the low-frequency components in the fMRI signal contain much more noise than the high-frequency components.

Session cut off period (secs) : 84

This value is computed as, $2 \times \text{period of most frequent epoch} = 2 \times 7_{\text{scans}} \times 6 \text{ seconds} = 84 \text{ seconds}$

Low-pass filter? select 'hrf'.

If 'Gaussian' or 'hrf low-pass filter' is selected, this will filter out the high-frequency components in the signal by smoothing the time-series with either Gaussian or hrf approximation. Low-pass filtering is also known as temporal smoothing. Theoretically, it is desirable, since the fMRI time-series is autocorre-

lated, and performing temporal smoothing allows the analysis to take this into account. However, in practice, temporal smoothing can make the statistical inference overly conservative, thus obscuring otherwise robust activations.

Model intrinsic correlations? none

AR(1) stands for first-order auto-regression model. Modelling intrinsic correlations has the same theoretical goal as temporal smoothing - to take into account the fact that the fMRI time-series is autocorrelated, which violates the assumption in regression analysis that the different observations are independent. Unfortunately, it also has the same practical consequence - it can make the inferences overly conservative.

Setup trial specific F contrasts : No

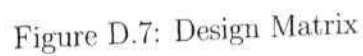
If 'yes' is selected, spm will automatically create F-contrasts for each condition within each session.

Estimate ? Now

Design matrix is shown in Figure: D.7. After estimation is done, the following important files will be saved in the "analysis" directory (among others):

Y.mad - a file containing the raw data, directly entered from the sn*-files. It is compressed, so it cannot be directly read. The Y.mad file will have the values for only those voxels that survived the upper F threshold during the analysis. This threshold is specified through the fMRLUFp variable in the spm_defaults.m files. If fMRLUFp=1 in defaults, all voxels will be present in the Y.mad file. If fMRLUFp=0, Y.mad file will not be written. We set fMRLUFp=1 in our experimental analyses. We used in this file in the brain-behaviour correlation (BBC!) analysis.

xCon.mat - file which contains the information about the contrasts, their names, values, and so forth. If these parameters are the same for two subjects, the xCon.mat file can be copied to the second subject directory, so that the parameters will only have to be entered once.



The subtractive approach assumes that brain activity scales in a linear fashion. Further, the statistical assumption in such fixed effects models is that the test

The subtractive approach assumes that brain activity scales in a linear fashion. Further, the statistical assumption in such fixed effects models is that the test

blocks are replicated and hence can be averaged and compared to the control blocks. Higher order effects can be specified by adding non-linear terms to the GLM. However, this requires that the nature of hypothesized relationship between the brain activation and an experimental variable is already known.

After the estimation is done, in order to see the results:

Select **RESULTS**

Select **SPM.mat file**: Select the SPM.mat file in the "results" directory - done.

SPM contrast manager:

Select contrasts ... T-CONTRASTS

The contrasts menu is depicted in Figure: D.8.

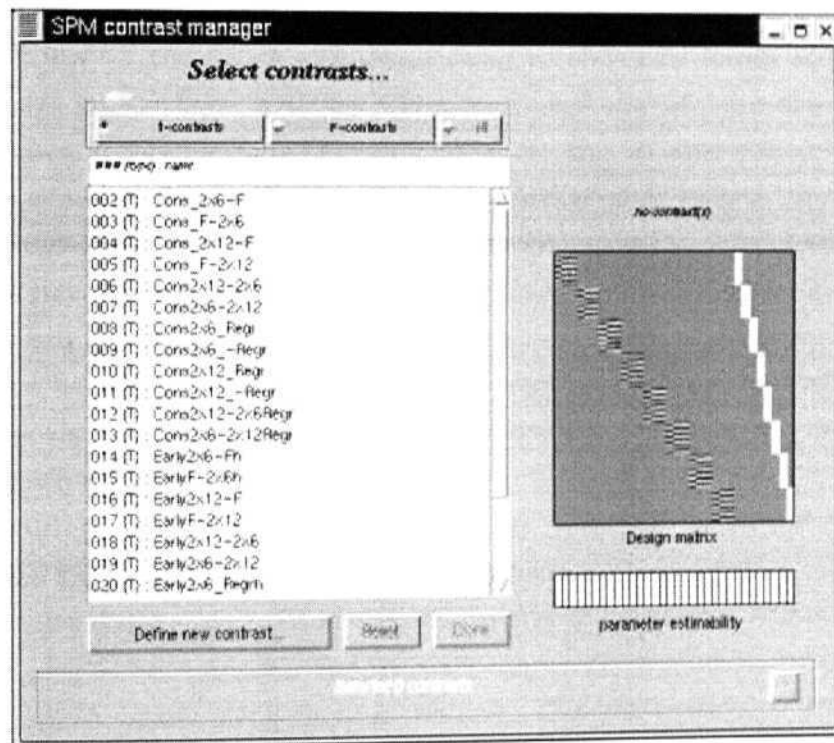


Figure D.8: Contrast Manager for selecting or creating contrasts

Define New Contrast type in name of contrast, then the contrast values. SUBMIT Check the design matrix on the right, if the entered contrast vector is correct, **Select the contrast you want to display** DONE. (if more than one contrast is selected, the conjunction between them will be computed and displayed)
Mask with other contrast(s)?no

If 'yes' is selected, user will be prompted to select another contrast from the same SPM.mat file. There are two types of masking: inclusive and exclusive. Let's say user selected contrast A first, and then chose to mask it with contrast B. Inclusive masking should display everything in contrast A plus the voxels activated by contrast B and not activated by contrast A. Exclusive masking will display those voxels activated by contrast A that are also activated by contrast B. More technically, exclusive masking is used to reject the voxels where the null hypothesis (A-B) can be rejected.

Corrected height threshold? no

If 'yes' is selected, only voxels surviving the corrected threshold value will be displayed.

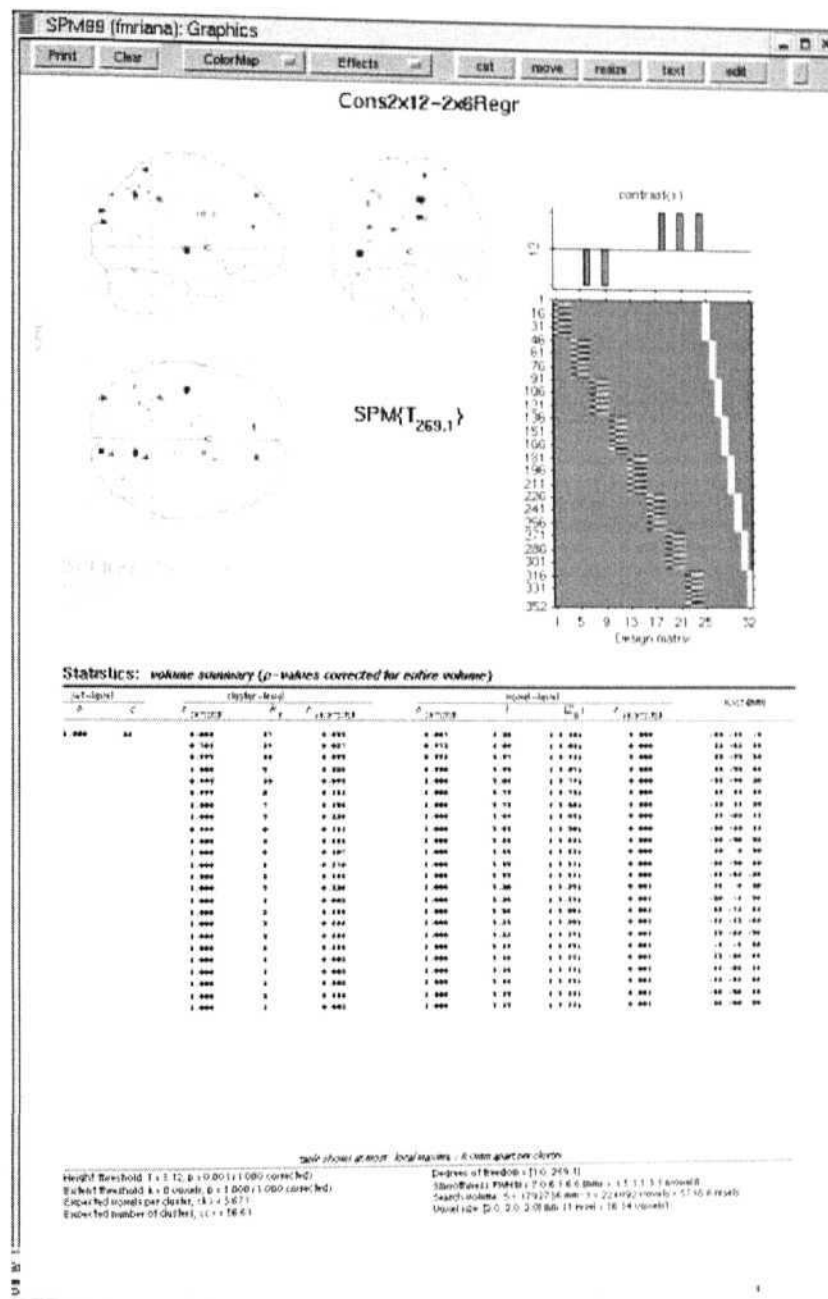
The individual voxels in most neuroimaging modalities (PET, fMRI, EEG, MEG etc.) are heavily correlated with neighboring voxels. This means a correction for multiple comparisons is needed. The traditional way of doing this is to use some version of a Bonferroni correction. However, due to large number of voxels involved, a straightforward implementation would severely reduce the estimated number of degrees of freedom. The major contribution of the SPM99 authors was to figure out a statistically valid approach. To the extent that the image data approximate a Random Gaussian Field, the theories behind Random Gaussian Fields can be used to yield valid statistical comparisons of images. This assumption is assured by applying a Gaussian smoothing filter to the image data in the pre-processing stages.

Threshold p value Enter the uncorrected p value you would like to use as threshold. Typically 0.001 for individual analysis.

Extent threshold voxels Enter the min number of voxels that a cluster should have in order to be displayed. For the least conservative estimate, enter 0.

Go through the above steps for each contrast. This will create con*.img files in the analysis directory, which are needed for the group analysis level.

Press **Volume** to show the summary of local maxima. The Figure: D.9 depicts fMRI results along with the details of activated voxels. The brain activations in three sections (sagittal, coronal and axial) will be obtained by pressing **Overlays** menu item. This option requires to choose an 'image to be rendered on'. Figure: D.10 is an example in which the brain activity is overlaid on one of our subject's normalized high resolution image.



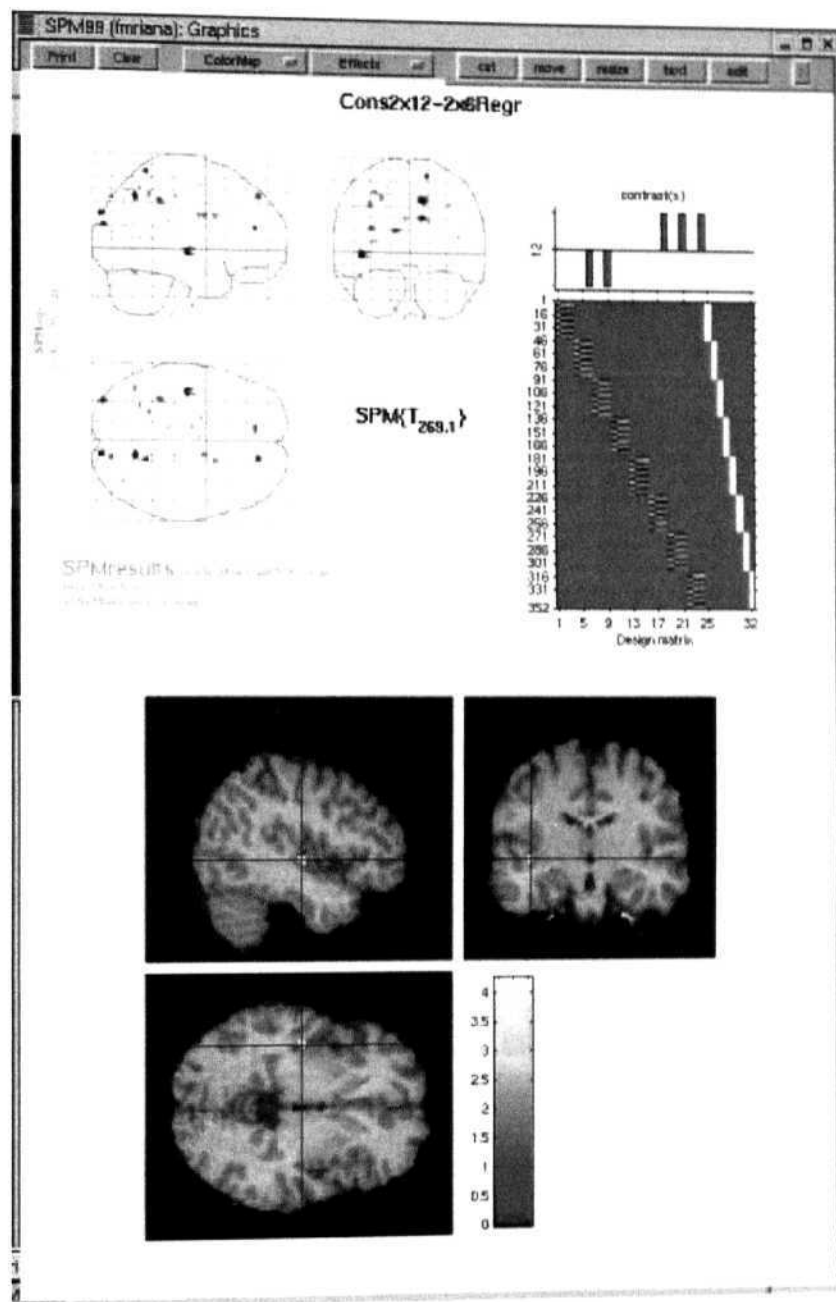


Figure D.10: Visualising activations overlaid on subject's high resolution image

D.3 Random Effects Analysis (RFX)

The purpose of the *Random Effects* analysis is to find the areas that are activated in much the same way in all subjects, as opposed to the fixed effects model which

gives the areas that are activated "on the average" across the subjects. This is really a crucial difference since a *fixed effects* analysis may yield "significant" results when one or a couple of subjects activate "a lot" even though the other subjects do not activate at all.

The *Random, Effects* analysis incorporates both within-subject variance (derived from the first level analysis), as well as between-subject/session differences (derived from the second level analysis) whose estimator is the correct mix of within and between-subject error. This allows generalization of the results to the population from which the subjects were drawn.

The implementation of RFX in SPM package involves a two-level analysis - in the first level a fixed effects analysis is done and then followed by a second level analysis. The idea is to feed a series of contrast images (con*.img) resulting from the first-level analysis of a number of individual subjects into a second level of analysis within SPM. For the second level, the con*.img's are treated exactly as if they were original image data, or possibly some sort of average image data for a particular condition.

The contrast images represent spatially distributed images of the weighted sum of the parameter estimates for a particular contrast. One contrast image for each patient and each control is required. Doing that will yield collapsing over intra-subject variability (to only one image per contrast per subject) and the image-to-image residual variability is now between subject, variance alone.

Create a new directory "group analysis"

change current working directory to this one

Create a new directory "comparison1" with the name as the contrast on which would like to perform group analysis.

Find out which con_*.img file corresponds to this contrast, e.g. con_0003.img

cd "comparison1"

Start spm99

Select BASIC MODELS

Select design type... One sample t-test

GM scale: grand mean scaling no grand Mean scaling

Explicitly mask images? no

Global calculation : omit

The Figures: D. 11, D.12 depicts the design matrix for one sample T-test at the

second level (RFX analysis) and fMRI results for an example case.

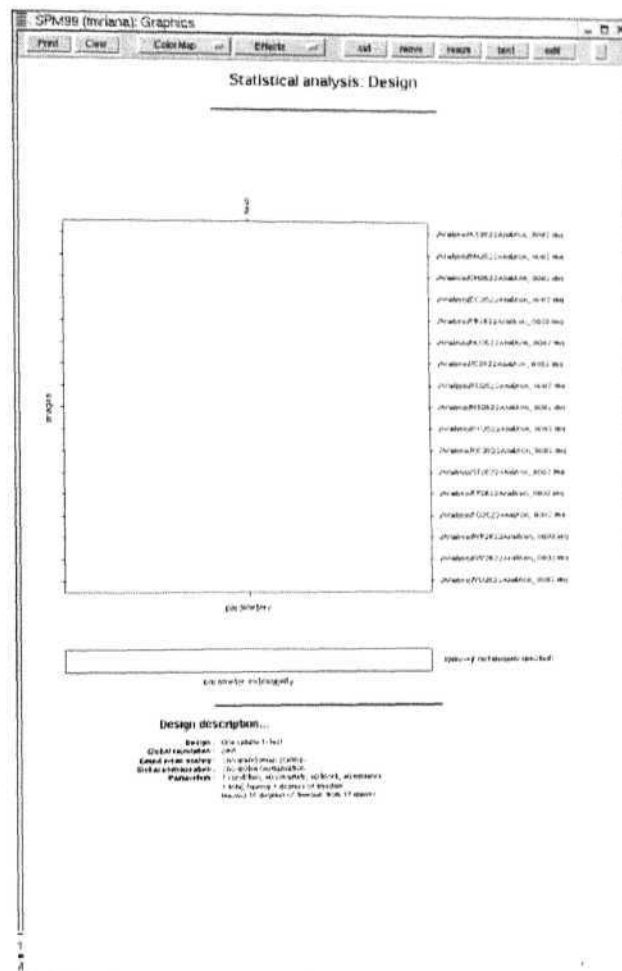


Figure D.11: Design Matrix in RFX for one Sample T-Test

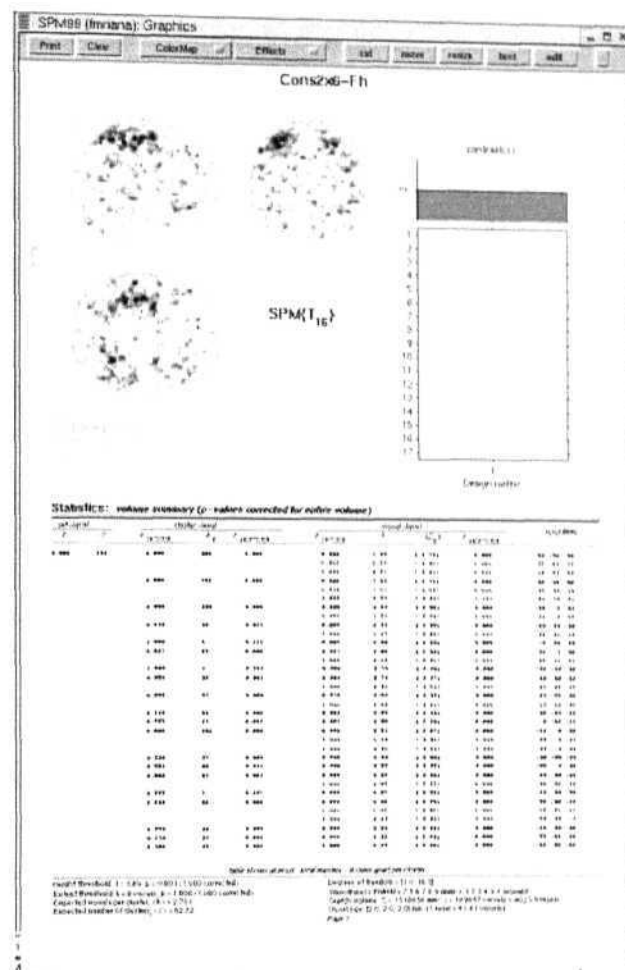


Figure D.12: Results from Random Effects (RFX) analysis for one Sample T-Test

D.4 Sources and Further Reading

The material in this appendix has been compiled from the following resources:

- SPM99: Protocols, Tools, and Documentation by Kalina Christoff, Department of Psychology, Stanford University

<http://www-psych.stanford.edu/~kalina/SPM99/>

SPM99 Preprocessing Protocol

<http://www-psych.stanford.edu/~kalina/>

SPM99/Protocols/spm99-prepros-prot.html

SPM99 Analysis Protocol

[http://www-psych.stanford.edu/~kalina/
SPM99/Protocols/spm99_analysis_prot.html](http://www-psych.stanford.edu/~kalina/SPM99/Protocols/spm99_analysis_prot.html)

- SPM Resources by Terry Oakes, W.M. Keck Laboratory for functional Brain Imaging and Behaviour, University of Wisconsin. Madison
http://www.keck.waisman.wisc.edu/~oakes/spm/spm_resources.html
SPM99 Introduction
http://www.keck.waisman.wisc.edu/~oakes/spm/SPM99_Introduction.pdf
SPM How-tos
http://www.keck.waisman.wisc.edu/~oakes/spm/spm_how_tos.html
Random Effects Analysis
http://www.keck.waisman.wisc.edu/~oakes/spm/spm_random_effects.html
- Preprocessing Steps for SPM99 by Todd Handy, Center for Cognitive Neuroscience, Dartmouth College
<http://www.dartmouth.edu/~cogneuro/ppnotes.html>
- SPM Statistics and other Tutorials by Matthew Brett, MRC Cognition and Brain Sciences Unit, University of Cambridge.
<http://www.mrc-cbu.cam.ac.uk/Imaging/Common/tutorials.shtml>

For Further Reading, the following annotated bibliography by the authors of SPM can be consulted.

Statistical Parametric Mapping: An Annotated Bibliography

W.D. Penny, J. Ashburner, S. Kiebel, R. Henson, D.E. Glaser, C. Phillips and Karl J. Friston.

Wellcome Department of Imaging Neuroscience, University College London.

<http://www.fil.ion.ucl.ac.uk/spm/bib.htm>

Appendix E

Imaging Results from Basic Comparisons

This appendix presents the basic comparison results discussed in the Chapter 7, Section 7.2.

Table E.1: Location of Stereotaxic Talairach coordinates of peak activations in the Early 2x6>Control Regressor and the Early Control>2x6 Regressor Contrasts.

Brain Area	R/L	BA	Activation				Deactivation			
			Coordinates			T-Score	Coordinates			T-Score
			X	Y	Z		X	Y	Z	
Cerebellum										
Anterior Lobule										
Culmen	R		34	-48	-25	5.29				
	L		-30	-58	-27	7.37				
Posterior Lobule										
Cerebellar Tonsil	R		14	-56	-38	5.57				
Uvula	R		12	-79	-31	4.81				
Declive	R						22	-77	-21	5.38
Basal Ganglia										
Caudate Head	R		14	10	3	5.2				
Hippocampus	L						-30	-22	-16	4.63
Amygdala	R						30	-3	-25	5.4
Occipital areas										
Middle Occipital gyrus	R	37	48	-68	-5	5.27				
	L	19	46	-79	17	4.75				
	L	37	-44	-62	-4	4.58				
	L	18	-20	-93	6	7.32				
Superior Occipital gyrus	R	19	34	-74	28	5.01				
Temporal Lobe										
Middle Temporal gyrus	L	19	-40	-82	21	4.31				
	L	21					-51	1	-22	6.6
Superior Temporal gyrus	R	39					57	-55	25	4.75

Brain Area	R/L	BA	X	Y	Z	T Score	X	Y	Z	T Score
	L	39					-53	-55	25	5.79
Parietal areas										
Superior parietal	R	7	30	-60	49	5.85				
	L	7	-26	-62	44	4.39				
Precuneus	R	7	18	-68	44	7.84				
	L	7	-18	-68	38	5.97				
Inferior parietal	R	40	36	-46	43	6.64				
	L	40	-34	-45	41	7.71				
Motor areas										
Primary Motor	L	4					-44	-15	49	5.53
Pre-SMA	L	6	-2	18	53	4.8				
Premotor (dorsal)	R	6	30	18	53	4.85				
Cingulate gyrus	L	32	-4	19	40	6.07				
Anterior Cingulate	L	32					-2	45	0	4.68
Frontal areas										
Inferior frontal	L	9	-44	9	25	6.61				
Orbitofrontal	R	11	28	46	-9	5.6				
	L	47	-38	15	-6	5.17				
	R	47					55	33	-3	6.35
	L	11/47					-34	36	-19	5.39
	L	11					-2	40	-15	4.86
Dorsolateral prefrontal	R	10/46	42	38	22	7.28				
	L	46	-42	32	19	6.4				
Superior frontal	R	9/10					8	58	27	6.48
Medial frontal	L	10					-6	63	10	7.46

Table E.2: Location of Stereotaxic Talairach coordinates of peak activations in the Early 2x12>Control Regressor and the Early Control>2x12 Regressor Contrasts.

Brain Area	R/L	BA	Activation				Deactivation			
			Coordinates			T-Score	Coordinates			T-Score
			X	Y	Z		X	Y	Z	
Cerebellum										
Posterior Lobule										
Uvula	R						30	-85	-26	4.66
Basal Ganglia										
Ventral Striatum										
Putamen	R		16	11	-7	4.53				
	L		-18	19	-3	5.44				
	L		-16	17	-8	4.62				
Substantia Nigra	R		8	-24	-11	5.08				
ParaHippocampal gyrus	R		40	-37	-12	4.83				
Amygdala	R						30	-3	-18	5.17
Occipital areas										
Middle Occipital gyrus	R	19/18	34	-81	11	5.2				
	L	19	-38	-87	14	5.29				
Inferior Occipital gyrus	R	18	38	-89	-1	5.18				
Temporal Lobule										
Middle Temporal gyrus	L	21					-61	-56	8	4.77

Brain Area	R/L	BA	X	Y	Z	T Score	X	Y	Z	T Score
Superior Temporal gyrus	R	39					50	-59	29	4.39
	L	39					-55	-61	27	5.01
Parietal areas										
Superior parietal	R	7	28	-50	45	4.37				
Precuneus	R	7	14	-66	46	6.11				
	L	7	-18	-64	38	6.22				
Inferior parietal	R	40	34	-40	48	6.07				
	L	40					-57	-45	41	4.71
	L	39					-51	-60	38	6.46
Motor areas										
Pre-SMA	R	6	-10	18	45	4.16				
Premotor (dorsal)	R	6	14	10	53	5.13				
	L	6	-28	4	48	4.36				
Cingulate gyrus	R	32/24	6	8	42	4.87				
	L	31					-6	-45	30	5.66
Anterior Cingulate	L	24	-6	21	-3	5.2				
Frontal areas										
Inferior frontal	R	9	59	7	25	4.9				
Orbitofrontal	L	11/47					-36	32	-17	4.84
Superior frontal	R	10					24	59	10	4.49
	L	9					-20	44	31	4.85
Medial frontal	R	8	4	27	39	4.63				
	R	10					2	54	-4	4.24
Middle frontal	R	9	44	13	29	5.84				
	L	8					-38	22	45	5.7

Table E.3: Location of Stereotaxic Talairach coordinates of peak activations in the Early 4x6>Control Regressor and the Early Control>4x6 Regressor Contrasts. Bold faced T-score indicates that the activation survived whole brain correction for multiple comparisons at $p < 0.05$.

Brain Area	R/L	BA	Activation				Deactivation			
			Coordinates			T-Score	Coordinates			T-Score
			X	Y	Z		X	Y	Z	
Cerebellum										
Anterior Lobule										
Culmen	R		26	-58	-24	6.63				
Posterior Lobule										
Pyramis of Vermis	R		4	-73	-27	5.59				
	L		-6	-83	-23	5.15				
Declive	R		24	-55	-11	4.27				
Cerebellar Tonsil	R		30	-43	-40	4.96				
	L		-20	-41	-38	5.41				
Inferior semi-lunar lobule	L		-14	-62	-36	5.61				
Basal Ganglia										
Ventral Striatum										
Putamen	R		18	9	-6	5.9				
	L		-18	11	-11	8.5				
Caudate Head	R		8	17	-4	5.23				

Brain Area	R/L	BA	X	Y	Z	T Score	X	Y	Z	T Score
Caudate Head	L		-8	6	0	6.1				
Caudate Body	R						14	-3	22	5.47
Caudate Tail	L						-16	-28	22	8.18
Anterior Putamen	L		-12	2	7	4.18				
Posterior Putamen	R		22	-2	0	5.0				
	R		20	-1	11	4.28				
Hippocampus	L						-28	-16	-14	5.03
	R						32	-20	-12	4.84
Amygdala	L						-28	-7	-16	8.52
Occipital areas										
Middle Occipital gyrus	R	19	36	-85	15	7.87				
	L	18/19	-28	-93	12	6.79				
Superior Occipital gyrus	R	19	38	-74	26	7.66				
	L	19	-30	-84	23	6.04				
Inferior Occipital gyrus	L	18	-46	-76	-1	5.48				
Temporal Lobule										
Middle Temporal gyrus	R	39	46	-65	22	5.35				
	R	21					65	-43	-1	5.14
	L	21					-57	-28	-9	5.89
Superior Temporal gyrus	R	39					51	-57	27	5.23
	L	39					-57	-55	29	6.33
	R	22					65	-44	13	4.6
	L	22					-50	-56	14	5.69
Parietal areas										
Superior parietal	R	7	32	-55	56	6.57				
	L	7	-18	-61	53	7.07				
Precuneus	R	7	14	-66	49	9.68				
	L	7	-8	-66	46	9.24				
Inferior parietal	R	40	34	-48	54	5.71				
	R	40					53	-58	40	5.77
	L	40	-34	-44	48	6.06				
	L	40					-57	-51	38	9.1
Motor areas										
Pre-SMA	R	6	6	16	47	5.3				
Premotor (dorsal)	R	6	26	6	51	9.68				
	L	6	-30	4	46	4.99				
Cingulate gyrus	L	31					-8	-49	28	6.74
Anterior Cingulate	R	24/32	10	23	25	4.9				
Frontal areas										
Inferior frontal	L	45	-36	24	6	4.42				
	L	45/44					-53	16	5	5.82
Orbitofrontal	R	47	34	25	-6	6.28				
	L	47					-48	25	-13	6.14
Superior frontal	L	9					-22	46	36	6.03
	R	8					20	37	48	4.38
Medial frontal	R	10					10	63	13	4.41
	L	10					-2	50	-9	6.95
Middle frontal	L	8					-38	22	43	4.75

Table E.4: Location of Stereotaxic Talairach coordinates of peak activations in the Consolidation 2x(i>Control Regressor and the Consolidation Control>2x6 Regressor Contrasts.

Brain Area	R/L	BA	Activation				Deactivation			
			Coordinates			T-Score	Coordinates			T-Score
			X	Y	Z		X	Y	Z	
Cerebellum										
Anterior Lobule	R		26	-42	-23	4.66				
Culmen										
Posterior Lobule	R						18	-79	-23	5.07
Uvula										
Tuber										
Basal Ganglia										
Anterior Putamen	L		-20	6	9	6.2				
Posterior Putamen	R		22	-2	0	5.17				
Lateral Globus Pallidus	R		20	-6	-3	5.1				
Hippocampus	L						-32	-18	-13	5.35
Amygdala	L						-22	-9	-18	4.81
Thalamus										
Pulvinar	R		20	-28	16	4.13				
	L		-12	-14	1	4.7				
Occipital areas										
Middle Occipital gyrus	L	19	-32	-85	8	4.25				
Temporal Lobule										
Middle Temporal gyrus	R	37	46	-62	5	5.17				
	R	21					50	4	-30	4.3
	L	21					-63	-25	-4	5.78
Superior Temporal gyrus	L	39					-42	-55	27	5.02
	L	22					-50	-54	17	4.57
Parietal areas										
Superior parietal	R	7	32	-62	44	5.64				
	L	7	-12	-69	53	4.35				
Precuneus	R	7	10	-62	49	7.84				
	L	7	-16	-75	44	4.6				
Inferior parietal	R	40					57	-50	39	3.73
	L	40					-51	-48	45	4.45
Supramarginal gyrus	R	40					53	-55	32	5.1
	L	40					-55	-49	30	4.74
Sensory	L	3	-30	-23	49	6.25				
Motor areas										
Primary Motor	L	4	-53	-7	45	4.67				
SMA	L	6	-4	-3	48	7.02				
Pre-SMA	R	6	4	14	45	5.71				
	R	6	8	3	51	4.87				
Premotor (dorsal)	R	6	26	8	47	7.91				
	L	6	-48	-8	32	5.18				
Cingulate gyrus	R	32	12	23	32	7.18				
Anterior Cingulate	L	32					-2	47	0	5.64
Frontal areas										
Inferior frontal	R	44	61	8	14	4.42				
Orbitofrontal	L	47					-53	25	-8	5.1

Brain Area	R/L	BA	X	Y	Z	T Score	X	Y	Z	T Score
Superior frontal	L	9					-18	39	33	5.29
	R	9					12	54	34	4.1

Table E.5: Location of Stereotaxic Talairach coordinates of peak activations in the Consolidation 2x12>Control Regressor and the Consolidation Control>2x12 Regressor Contrasts.

Brain Area	R/L	BA	Activation				Deactivation			
			Coordinates			T-Score	Coordinates			T-Score
			X	Y	Z		X	Y	Z	
Cerebellum										
Anterior Lobule										
Culmen	R		32	-56	-22	4.21				
	L		-30	-42	-26	5.5				
Posterior Lobule										
Declive	L		-30	-71	-18	4.6				
Cerebellar Tonsil	R		14	-53	-41	4.88				
Tuber	R						40	-73	-28	4.34
Inferior Semi-Lunar Lobule	R		16	-74	-35	6.35				
Basal Ganglia										
Ventral Striatum										
Putamen	R		22	11	-11	5.04				
	L		-18	13	-9	5.37				
Caudate Head	R		6	19	-1	5.3				
	L		-4	15	-2	5.91				
Caudate Body	R						12	-11	21	4.93
	R						10	1	17	5.36
	L						-16	-10	24	4.37
Anterior Putamen	R		24	6	7	5.3				
Lateral Globus Pallidus	R		22	-8	0	5.58				
Hippocampus	L						-24	-11	-20	5.79
Thalamus										
Pulvinar	R		20	-24	16	4.32				
Occipital areas										
Middle Occipital gyrus	R	19	36	-83	13	5.4				
	L	19	-36	-85	8	5.54				
Superior Occipital gyrus	L	19	-36	-78	26	4.88				
Inferior Occipital gyrus	L	18	-36	-88	-6	4.54				
	L	19	-42	-74	-5	4.19				
Temporal Lobule										
Superior Temporal gyrus	R	22	48	-27	3	5.6				
	R	39					53	-57	25	4.24
Parietal areas										
Superior parietal	R	7	32	-52	52	6.43				
	L	7	-18	-69	53	7.01				
Precuneus	R	7	14	-66	47	7.19				
	L	7	-8	-66	46	6.09				
Inferior parietal	R	40	42	-31	42	5.24				
	L	40	-36	-41	39	5.61				
Angular gyrus	L	39					-50	-66	31	4.19

Brain Area	R/L	BA	X	Y	Z	T Score	X	Y	Z	T Score
Supramarginal gyrus	L	40					-55	-53	28	4.51
Motor areas										
SMA	L/R	6	0	-5	48	4.29				
Pre-SMA	R	6	2	4	50	4.29				
Premotor (dorsal)	R	6	38	2	50	4.76				
	L	6	-24	11	60	4.22				
rCMA	R	6/32	4	27	30	4.59				
Cingulate gyrus	R	31	16	-55	27	4.91				
	L	32	-2	25	37	5.0				
Frontal areas										
Inferior frontal	R	45/9	59	15	20	4.92				
	L	9	-44	7	29	4.74				
Orbitofrontal	R	11/47					38	34	-15	4.57
	L	47	-30	23	-3	4.91				
Middle frontal	R	8	26	12	44	5.02				
	R	10	36	40	18	4.11				

Table E.6: Location of Stereotaxic Talairach coordinates of peak activations in the Consolidation 4x6>Control Regressor and the Consolidation Control>4x6 Regressor Contrasts. Bold faced T-score indicates that the activation survived whole brain correction for multiple comparisons at $p < 0.05$.

[illegible]

Brain Area	R/L	BA	X	Y	Z	T Score	X	Y	Z	T Score
Middle Temporal gyrus	L	39					-42	-61	29	4.61
	L	22					-57	-46	4	5.32
	R	21					67	-31	-5	5.08
Superior Temporal gyrus	R	39					51	-55	21	5.05
	L	22/39					-55	-57	16	7.11
Parietal areas										
Superior parietal	R	7	12	-61	55	6.37				
	L	7	-26	-54	43	5.49				
Precuneus	R	7	12	-68	46	8.91				
	L	7	-26	-68	38	9.11				
Inferior parietal	R	40	44	-31	46	5.97				
	L	40	-44	-31	40	5.25				
Angular gyrus	R	39					53	-64	33	5.37
Supramarginal gyrus	R	40					50	-53	36	6.31
Motor areas										
Primary Motor	L	4	-55	-7	45	5.51				
Pre-SMA	L	6	-4	4	50	4.55				
Premotor (dorsal)	R	6	20	10	49	9.11				
	L	6	-30	6	49	5.36				
RCMA	R	32	6	6	46	6.23				
	L	32	-6	15	32	7.55				
Cingulate gyrus	R	32	6	19	32	5.12				
	L	32	-6	15	32	7.55				
Frontal areas										
Inferior frontal	R	44/45	59	5	20	4.93				
	L	44/45					-50	16	8	5.14
Orbitofrontal	L	11/47					-44	46	-11	5.57
	L	47					-50	23	-3	4.27
Dorsal prefrontal	R	46	46	30	21	4.77				
Superior frontal	R	9					14	58	28	4.41
	L	8					-16	37	48	5.24
Medial frontal	R	10					6	61	14	5.23
Middle frontal	R	8					38	31	41	4.88

Appendix F

Imaging Results from Comparison of 2x6 with the Complex Sequence Tasks

This appendix presents the results from comparisons of 2x6 task with the complex sequence learning tasks (deactivations due to complexity) as indicated in the Chapter 7, Section 7.3.

Table F.1: Location of Stereotaxic Talairach coordinates of peak activations in the Early 2x6>4x6 Regressor and the Early 2x6>2x12 Regressor Contrasts.

Brain Area	R/L	BA	Early 2x6>4x6 R				Early 2x6>2x12 R			
			Coordinates			T-Score	Coordinates			T-Score
			X	Y	Z		X	Y	Z	
Cerebellum										
Anterior lobule (Culmen)	R						36	-48	-23	4.1
Parietal areas										
Precuneus	R	7					16	-60	47	4.0
Sensory and Motor areas										
Premotor (ventral)	L	6					-34	-4	28	4.47
Cingulate gyrus (posterior)	L	29					-12	-42	13	4.5
Frontal areas										
Orbitofrontal cortex	R	11					30	44	-11	4.97

Table F.2: Location of Stereotaxic Talairach coordinates of peak activations in the Consolidation 2x6>4x6 Regressor and the Consolidation 2x6>2x12 Regressor Contrasts.

Brain Area	R/L	BA	Consolidation 2x6>4x6 R				Consolidation 2x6>2x12 R			
			Coordinates			T-Score	Coordinates			T-Score
			X	Y	Z		X	Y	Z	
Basal ganglia										
Putamen (anterior)	L		-20	6	9	4.39				
Hippocampus	L		-22	-12	-8	3.8				
Opercular Rolandic	R		46	-3	15	4.06	46	-3	15	4.81
Occipital areas										
Middle occipital gyrus	L	18					-20	-85	10	3.98
Sensory and Motor areas										
Premotor (ventral)	L	6	-48	-8	32	4.08				
Frontal areas										
Anterior Cingulate	R	32	12	23	32	4.92				
Insula	L	45/47					-28	28	10	4.22

CURRICULUM VITAE

PAMMI V. S. CHANDRASEKHAR

Email: pvscs@yahoo.com, vscpammi@gmail.com

EDUCATION:

- Ph.D. **Computer Science**, (Thesis Submitted)
Department of Computer and Information Sciences,
University of Hyderabad, India
- M.Phil. **Computational Physics**, (August 1998 - December 1999)
School of Physics, University of Hyderabad, India
- M.Sc. **Electronics**, (August 1995 - April 1997)
School of Physics, University of Hyderabad, India
- B.Sc. **Mathematics, Physics and Electronics**, (July 1992 – April 1995)
Andhra University, Waltair, India

ACADEMIC AND INDUSTRIAL EXPERIENCE:

April 2002 - September 2003:

Research Assistant,

Indo-Japanese project titled "Sequence learning: An fMRI Investigation" funded by Kawato Dynamic Brain Project (KDB), Exploratory Research for Advance Technology (ERATO), Japan Science and Technology Agency, Japan at University of Hyderabad, India.

July 2001 – August 2001:

Visiting Researcher,

ATR International, Kyoto, Japan invited by KDB Project, ERATO, JST.

November 1998 - March 2001:

Research Fellow (Junior and Senior),

Research Centre Imarat (RCI), Defence Research and Development Organization (DRDO), Hyderabad, India

May 1997 – June 1998:

Junior Engineer (Research and Development),

Research and Development Division (R&D), APEL Radio Communication Systems (Pvt.) Ltd., Secunderabad, India.

RESEARCH ACCOMPLISHMENTS:

PUBLICATIONS:

I. Methods and Reviews

Raju S. Bapi, **V. S. Chandrasekhar Pammi**, K. P. Miyapuram, Ahmed. Investigation of Sequence Learning: A Cognitive and Computational Neuroscience Perspective. Accepted in the Current Science Journal.

V. S. Chandrasekhar Pammi, K. P. Miyapuram, Raju S. Bapi, Chakravarthy Bhagavati, T. Brahmaiah, Ch. Chandra Sekhar Rao. Investigation of Time Series Modelling to Explicate the Learning Related Activity Observed in fMRI Data. Proceedings of the International Conference on Systemics, Cybernetics and Informatics (ICSCI 2004), Hyderabad, India, pp. 667-672, 2004.

Raju S. Bapi, **V. S. Chandrasekhar Pammi**, K. P. Miyapuram. How to Characterize Learning Induced Changes in Functional MR I Data? (Abstract Submitted for a book chapter).

Raju S. Bapi, **V. S. Chandrasekhar Pammi**, K. P. Miyapuram. Methods and Approaches for Characterizing Learning Related Changes observed in functional MRI Data - A Review. Proceedings of the International Conference on Theoretical Neurobiology, India, pp. 221–229, 2003.

Raju S. Bapi, K. P. Miyapuram, **V. S. Chandrasekhar Pammi**, Ahmed. A Multi-disciplinary Approach to the Investigation of Aspects of Serial Order in Cognition. Proceedings of the National Seminar on Cognitive Science, Hyderabad, 2002. (In press)

V. S. Chandrasekhar Pammi, M. Krishna Prasad, S. Bapi Raju. Statistical Parametric Mapping For Analysis of Functional Magnetic Resonance Images - A Case Study. Proceedings of the National Conference on Recent Developments and Challenges in Physics, Hyderabad, India, 2002. (In press)

//. fMRI and Behavioural Studies

V. S. Chandrasekhar Pammi, Raju S. Bapi, Ahmed, K. P. Miyapuram, Kenji Doya. Hierarchical organization of complex visuo-motor sequences. Submitted for the book volume edited by N. Srinivasan, A. K. Gupta.

V. S. Chandrasekhar Pammi, Raju S. Bapi, Ahmed, K. P. Miyapuram, Kenji Doya. Differential Spontaneous Reorganization of Sequences during Performance of Complex Visuo-motor Skills. Proceedings of the International Conference on Cognitive Science 2004, Allahabad, India, pp. 211–215, 2004.

V. S. Chandrasekhar Pammi, Miyapuram, K. P., Bapi, R. S., Kenji Doya. Chunking Phenomenon in Complex Sequential Skill Learning in Humans. In: Pal, N.R., Kasabov, N., Mudi, R.K., Pal, S., Parui, S.K. (eds.), Lecture notes in Computer Science, Proceedings of the 11th International Conference on Neural Information Processing (ICONIP 2004), Springer-Verlag, Heidelberg, 3316, pp. 294-299, 2004.

V. S. Chandrasekhar Pammi, K. P. Miyapuram, Raju S. Bapi, K. Samejima, K. Doya. Differential roles of areas of striatum in complex sequential skill learning. International Neuroscience Conference, Hyderabad, India, pp. 67-68, 2004.

V. S. Chandrasekhar Pammi, K. P. Miyapuram, Raju S. Bapi, K. Samejima, K. Doya. Acquisition of Complex Sequential Skills: Behavioral and fMRI Investigation. NBRC International Symposium, Building the Brain, Manesar, India, 2003.

V. S. Chandrasekhar Pammi, Raju S. Bapi, K. P. Miyapuram, K. Samejima, K. Doya. The activation of Orbitofrontal Cortex reflects Trial and Error processes in a Visuomotor Sequence Learning task. NCBS International Neurobiology Symposium, Networks and Behavior, Bangalore, India, 2003.

K. P. Miyapuram, R. S. Bapi, **V. S. C. Pammi**, K. Samejima, K. Doya. fMRI Investigation of the Learning of Visuo-motor Sequences of increasing complexity. Annual Meeting of Society for Neuroscience, USA, 2001.

III Neural Network Applications

Ahmed, S. Bapi Raju, **Pammi V. S. Chandrasekhar**, M. Krishna Prasad. Application of Multilayer Perceptron Network for Tagging Parts-of-Speech. Proceedings of the Language Engineering Conference (LEC'02), IEEE Computer Society, pp. 57–63, 2002.

IV Electronics Circuit Design and Development

P. V. S. Chandrasekhar. Design and Development of band pass filter @2 GHz. Technical paper, 3rd Science meet, Research Centre Imarat (RCI), 1999.

A. Mangatayaru, Ravi, P. V. S. **Chandrasekhar**. Design and Development of Power dividers, Technical report, Research Centre Imarat, 1999.

V Journal Manuscripts in Preparation

V. S. Chandrasekhar Pammi, Raju S. Bapi. Hierarchical organization of Sequential Skills.

V. S. Chandrasekhar Pammi, K. P. Miyapuram, R.S. Bapi, K. Samejima, K. Doya. fMRI Investigation of the Learning of Visuo-motor Sequences of Increasing Complexity.

Ahmed, **V. S. Chandrasekhar Pammi**, Raju S. Bapi. Investigation of the relation between chunking and sequence learning.

Ahmed, **V. S. Chandrasekhar Pammi**, K. P. Miyapuram, Raju S. Bapi, K. Samejima, K. Doya. Neural correlates of Visuo-motor sequence learning with Trial and Error.

LECTURES / PRESENTATIONS

Presentation: titled "Differential Spontaneous Reorganization of Sequences during Performance of Complex Visuo-motor Skills", in Visual Cognition Session, International Conference on Cognitive Science 2004, Allahabad, India, December 18, 2004.

Presentation: titled "Dynamic Causal Modelling: Finding Effective Connectivity in fMRI Data", Okinawa Computational Neuroscience Course, Okinawa, Japan, November 19, 2004.

Presentation: titled "Acquisition and performance of complex sequential skills: An Experimental and Theoretical Investigation", Okinawa Computational Neuroscience Course, Okinawa, Japan, November 13, 2004.

Invited Lecture: titled "History and overview of neural networks", Institution of Electronics and Telecommunication Engineers (IETE) Vijayawada Centre, India, July 17, 2004.

Invited Lecture: titled "fMRI Investigation of Different Aspects of Serial Order in Behaviour" at Meeting on Clinical Linguistics, Central Institute of Indian Languages (CIIL), Mysore, India, March 20, 2004.

Presentation: titled "Investigation of Time Series Modelling to Explicate the Learning Related Activity Observed in fMRI Data" in the Special Session on Neural and Cognitive modeling, International Conference on Systemics, Cybernetics and Informatics (ICSCI 2004), Hyderabad, India, February 14, 2004.

Invited Lecture: titled "A Window into the Brain Function using functional MR Images – A Demonstration" at VNR Vignana Jyothi Institute of Engineering Technology, Hyderabad, India, March 7, 2003.

COURSES CONDUCTED:

Our group conducted a two-day short-course on *Functional Neuroimaging and Image Processing using Statistical Parametric Mapping*, at Indian Institute of Information Technology and Management Kerala, Trivendram, India, January 8-9, 2005.

COURSES / CONFERENCES ATTENDED:

COURSES

1. Okinawa Computational Neuroscience Course, Japan, November 9–19, 2004.
2. Short-term course on Computational Neuroscience organized jointly by Indian Institute of Technology Kanpur (IITK) and National Brain Research Centre Manesar at IITK, July 7–18, 2003.

CONFERENCES / WORKSHOPS / SYMPOSIA / MEETINGS

1. International Conference on Cognitive Science, Allahabad, December 16–18, 2004.
2. International Neuroscience Conference, Hyderabad, May 6-8, 2004.
3. Meeting on Clinical Linguistics, Central Institute of Indian Languages, March 19-20, 2004.
4. Current Trends in Software and Systems, University of Hyderabad, March 8, 12 and 13, 2004.

5. Symposium on Challenges in Mathematical and Computer Sciences, Hyderabad, February 29 and March 1, 2004.
6. International Conference on Systemics, Cybernetics and Informatics (ICSCI 2004), Hyderabad, February 12-15, 2004.
7. Building the Brain, NBRC Symposium, Manesar, India, December 14–17, 2003.
8. Tutorial on Intrusion detection and Computer Security organized by Dept. of Computer and Information Sciences, University of Hyderabad, December 5, 2003.
9. International Conference on Theoretical Neurobiology, New Delhi, February 24th –26th 2003.
10. Network and Behavior-2003, NCBS Neurobiology symposium, India, January 3rd – 6th 2003.
11. Language Engineering Conference (LEC 2002), Hyderabad, India, December 13th- 15th 2002.
12. National Conference on Recent Developments and Challenges in Physics, Hyderabad, India, December 19th - 22nd 2002.
13. Workshop on Personality development conducted by IEEE student branch at University of Hyderabad, 2001.
14. 3-G Wireless Communication Systems conducted by IEEE Hyderabad Chapter, January 2001.
15. Workshop on Hewlett-Packard - Advanced Design System tool (ADS 1.10) at Semiconductor Complex, Hyderabad. The training familiarized the ADS software, which is useful for both the Digital and Analog/RF Synthesis. June 23rd -26th 1999.

AWARDS/SCHOLARSHIPS/HONOURS/ACHIEVEMENTS

- ⇒ Selected for the Okinawa Computational Neuroscience from *worldwide competition* held in Okinawa, Japan, November 9-19, 2004.
- ⇒ *IBM Travel Grant* to attend ICONIP-2004, November 22-25, 2004 Calcutta, India.
- ⇒ *Resource Person* for the *Short Course on Computational Neuroscience* organized jointly by the Department of Computer and Information Sciences, University of Hyderabad and National Brain Research Centre, Manesar, October 11–21, 2004.
- ⇒ *Senior Research Fellowship* in engineering stream from the *Council of Scientific & Industrial Research (CSIR)*, Human Resource Development Group (HRDG), Pusa, New Delhi from July 6, 2004 - till date.
- ⇒ *University with Potential for Excellence* Doctoral Fellowship, University of Hyderabad from April 1, 2004 - July 5, 2004.
- ⇒ *Invited* to attend the Second Meeting on Clinical Linguistics, CIIL, Mysore, March 19-20, 2004, which deliberated on the concept of Clinical Linguistics in India.
- ⇒ *Session Chair* for the Cybernetics student session (SC-1) in the International Conference on Systemics, Cybernetics and Informatics, Hyderabad, India, February 13, 2004.
- ⇒ *Best poster award* in the Systems Neuroscience category at the NBRC International Symposium, Building the Brain, Manesar, December 2003.
- ⇒ *Best poster award* at the International Conference on Theoretical Neurobiology, New Delhi, February 2003.
- ⇒ *Invited* as visiting researcher to ERATO, JST, Japan, July-August 2001.